DEVELOPMENT OF GREEN HETEROGENEOUS CATALYSTS FOR SUSTAINABLE BIODIESEL PRODUCTION FROM WASTE BIOMASS

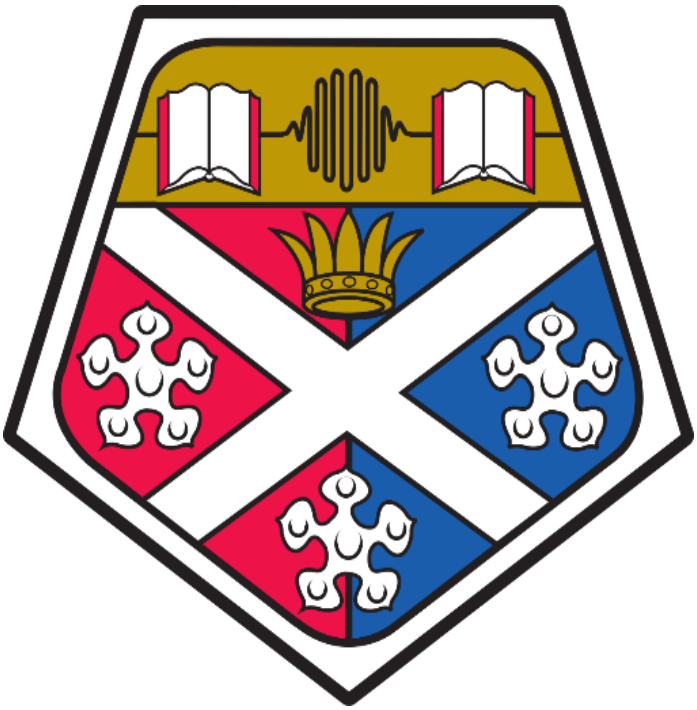

ASUQUO JACKSON ASUQUO

Department of Chemical & Process Engineering

University of Strathclyde

A Thesis Submitted to the University of Strathclyde for the Degree of Doctor of Philosophy

2025

Asuquo Jackson Asuquo

Development of Green Heterogeneous Catalysts for Sustainable Biodiesel Production from Waste Biomass

Department of Chemical & Process Engineering

University of Strathclyde

PhD Thesis

Declaration

I declare that this thesis entitled Development of Green Heterogeneous Catalysts for Sustainable Biodiesel Production from Waste Biomass has been performed and composed by the author. No part of this thesis has been previously presented for another degree or diploma at this or in any other institution, which has led to the award of a PhD degree. Under the terms of the United Kingdom Copyright Acts as certified by the University of Strathclyde Regulation 3.50, the copyright of this thesis is owned by the author and so due recognition must always be made to the use of any material contained in or extracted from this thesis.

Signed: Asuquo Jackson Asuquo

Date:29/09/25

Dedication

Dedicated to the loving memory of my father, Jackson Asuquo Akpan.

1942-2017

Acknowledgements

I would like to express my deepest appreciation to both my supervisors Dr. Jun Li and Dr. Xiaolei Zhang for their expert support throughout the period of carrying out this research. Their prudent advice, positive criticisms, encouragement and motivation were my driving force to forge ahead during the challenging times of carrying out this research.

I gratefully acknowledge the Petroleum Technology Development Fund of Nigeria for their outstanding financial and moral support through the period of doing my research, without their financial backing, this project would not have been feasible.

My love and appreciation go out to my family, mother and sister for their standing behind me through thick and thin while doing this research.

Many thanks to the Strathclyde chemical engineering department support staff for their support while this research lasted. I cannot thank enough the chemical and process engineering lab staff for their technical support.

My immense appreciation also extends to the Vice-chancellor of the university, the H.O.D and all the staff at the department of chemical engineering at the Akwa Ibom state university Ikot Akpaden, Akwa Ibom state, Nigeria for standing by me through the period of this research.

I am also very grateful to the chemical engineering laboratory team at the Ahmadu Bello University Zaria, Nigeria for their superb analytical skills.

I am grateful to my research team members and friends whose contributions to my personal and professional growth and experience would not have been complete.

Best wishes to you all.

Asuquo Jackson Asuquo

September 2025

Published work and conference presentations during current research

- **Asuquo, A. J**., Zhang, X., Lin, L., & Li, J. (2024). Green heterogeneous catalysts derived from fermented kola nut pod husks for sustainable biodiesel production. International Journal of Green Energy, 21(10), 2218–2227. https://doi.org/10.1080/15435075.2023.2297781
- **Asuquo Jackson Asuquo**, Jun Li, Xiaolei Zhang (June 6, 2023). Green heterogeneous catalysts derived from fermented kola nut pod husk for biodiesel production: the effects of pre-treatment. poster presentation: 31st European Biomass Conference & Exhibition, Bologna, Italy.
- **Asuquo Jackson Asuquo**, Jun Li, Xiaolei Zhang (September 2021). Waste *Carica Papaya* oil seeds: potential feed stock for biodiesel production to achieve net-zero. oral presentation: 28th annual SCI-CSCST conference: chemical engineering and its path to net - zero. Online, September 2021, Glasgow, UK.

Published work out with this current research

- T.F. Adepoju, O.M. Olatunji, M.A. Ibeh, K.A. Salam, B.E. Olatunbosun, **A.J. Asuquo**, Heavea brasiliensis (Rubber seed): An alternative source of renewable energy. Scientific African 8, e00339. https://doi.org/10.1016/j.sciaf.2020.e00339
- T.F. Adepoju, M.A. Ibeh, U. Ekanem, **A.J. Asuquo** (2020). Data on the derived mesoporous based catalyst for the synthesis of fatty acid methyl ester (FAME) from ternary oil blend: An optimization approach. Data in Brief 30, 105514. https://doi.org/10.1016/j.dib.2020.105514
- T. F. Adepoju, M.A. Ibeh, E.O. Babatunde, **A.J. Asuquo** (2020). Methanolysis of CaO based catalyst derived from eggshell - snail shell - wood ash mixed for fatty acid methyl ester (FAME) synthesis from a ternary mixture of Irvingia Gabonensis -

Pentaclethra Macrophylla - Elais guineensis Oil blend: an application of Simplex Lattice and Central Composite Design Optimization. Fuel, 275:117997. https://doi.org/10.1016/j.fuel.2020.117997

- T.F Adepoju, M.A. Ibeh, E.O. Babatunde, G. S. Abegunde, P.O. Adepoju, **A.J. Asuquo**, C.O. Osueke (2020). Datasets on process transesterification of binary blend of oil for fatty acid ethyl ester (FAEE) synthesized via ethanolysis of heterogeneous doped catalyst. Data in Brief, 30, 105905. https://doi.org/10.1016/j.dib.2020.105905.
- T.F. Adepoju, M.A. Ibeh, E.O. Babatunde, **A. J. Asuquo**, G.S. Abegunde, (2020). Appraisal of CaO based catalyst derived from waste fermented-unfermented kola nut pod for Fatty acid methyl ester (FAME) synthesis from Butyrospermum parkii (Shea butter) oil. South African Journal of Chemical Engineering, 33: 160-171. https://doi.org/10.1016/j.sajce.2020.07.008.
- Adepoju, T. F., Ibeh, M.A., Udoetuk, E. N., **Asuquo, A. J**. Babatunde, E. O. (2020). Quaternary blend of Carica papaya - Citrus Sinesis - Hibiscus sabdariffa - waste used oil for biodiesel synthesis using CaO-based catalyst derived from binary mix of Lattorina littorea and Mactra coralline Shell. RENE-D-2000352. Renewable Energy.
- Adepoju, T. F., Ibeh, M.A., Babatunde, E.O., **Asuquo, A.J.** (2020). A novel mesoporous CaO based catalyst derived from the mixture of Devil snare pod, beech wood husk, and walnut shell for the synthesis of biodiesel from ternary blend of Ricinus communis-Spondias dulcis-Canarium schweinfurthii Oil. EGYR-2020-517-R1.
- Adepoju, T. F; Ibeh, M. A; Babatunde, E. O; **Asuquo, A.J**; Eloboka, C. (2020) Study on the derived based catalysts from Theobroma cacao pod husks for the conversion

of beef tallow blend with waste used vegetable oil for fatty acid ethyl ester synthesis: burnt, submerged fermented, calcination, hybrid design, catalyst refining and reusability. https://doi.org/10.21203/rs.3.rs-39335%2Fv1 CorpusID:234541776

- T.F. Adepoju, M.A. Ibeh, **A.J. Asuquo** (2021). Elucidate three novel catalysts synthesized from animal bones to produce biodiesel from ternary non-edible and edible oil blend: A case of Jatropha Curcus, Hevea brasiliensis, and Elaeis guineensis oil, South African Journal of Chemical Engineering. https://doi.org/10.1016/j.sajce.2021.01.002
- T.F. Adepoju, M.A. Ibeh, U. Ekanem, **A.J. Asuquo** (2020). Data on the derived mesoporous based catalyst for the synthesized of fatty acid methyl ester (FAME) from ternary oil blend: An optimization approach, Data in Brief. https://doi.org/10.1016/j.dib.2020.105514.

ABSTRACT

The use of alternative sources of fuels such as biodiesel produced from cost effective processes and readily available waste agricultural biomass feedstocks can help to reduce the overdependence and the resulting adverse climate effects observed with the continuous usage of fossil-based fuels. In recent times, heterogeneous base-catalytic biodiesel synthesis using transesterification technology has gained significant attention because of its several advantages including increased catalytic activity, recyclability, and decreased environmental impact compared to traditional homogeneous catalysts. This research has introduced an in-depth evaluation for the transesterification of waste *Carica Papaya* Seed Oil (WCPSO) into *Carica Papaya* Oil Biodiesel (CPOB) using three green heterogeneous catalysts (Calcined Kola Nut Pod Husk Catalysts- CKNPH A, B, & C) developed from waste kola nut pod husks. The linear, two-factor interaction, and quadratic polynomial models were compared and used to fit the data obtained in this study. The quadratic model was selected as the best model due to its high f-value (162.55), low p-value (<0.0001) and had the highest adjusted R^2 value (0.9964). The yield of biodiesel was studied under different conditions which include temperature, time, methanol-oil molar ratio and quantity of catalysts. Statistical and graphical optimization have been used to optimize the process conditions to ensure maximization of synthesis of CPOB. This is observed in the yield of biodiesel as obtained from experiments, which was 96%, while the predicted yield was 95.66%. This biodiesel yield was obtained using CKNPH A catalyst quantity of 2.5g, reaction time of 70 min, methanol-oil molar ratio of 4:1, and at a flow rate of 1000 Kg/hr. The economic feasibility studies of CPOB production process were carried out using AspenPlus simulation. The Profitability index (PI) of the process was found to be relatively low (1.29). To better understand the low PI, sensitivity analysis was carried out, and it revealed that for the PI to improve, the minimum selling price per Kilogram of biodiesel must be above 0.887 $/Kg, equivalent to 0.77 $/Liter.

Table of Contents

List of figures

List of tables

List of abbreviations

AAS	Atomic Absorption Spectroscopy
AV	Acid Value
AOAC	Association of Official Analytical Chemists
ASTM	American Standards and Measurements
BBD	Box-Behnken Design
Bxx	Proportion in the volume of Petro-diesel/biodiesel mix
B2/5/20/100	Volume % biodiesel
BET	Brunauer Emmett Teller
C	Carbon
Ca	Calcium
CaO	Calcium Oxide
CH_3OH	Methanol
Cl/Cl_2	Chlorine
CN	Cetane Number
CFPP	Cold-Filter Plugging Point
CO	Carbon Monoxide
CO_2	Carbon Dioxide
CPKO	Crude Palm Kernel Oil
CPSO	*Carica Papaya* Seed Oil
CPOB	*Carica Papaya* Oil Biodiesel
DG	Di-glyceride
di-TMP	di-trimethylolpropane
DTG	Derivative Thermogravimetric
EDS	Energy Dispersive Spectroscopy
EDX	Energy Dispersive X-ray Spectroscopy
EN	European National Standard
EU	European Union

DMC	Dimethyl Carbonate
DOE	Department of Energy
DSC	Differential Scanning Calorimetry
FAEE	Fatty-Acid Ethyl Ester
FFA	Free Fatty Acid
FAME	Fatty Acid Methyl Ester
FTIR	Fourier Transform Infrared Spectroscopy
GC	Gas Chromatography
GDP	Gross Domestic Product
GHG	Green House Gases
GL	Glycerol
HC	Hydrocarbons
HCL	Hydrochloric Acid
IEA	International Energy Agency
IV	Iodine Value
K	Potassium
KOH	Potassium Hydroxide
MG	Mono-glycerides
[HMIM]HSO4	1-methylimidazolium hydrogen sulphate
M:O	Methanol Oil molar ratio
Mt/y	Million tonnes per year
MW	Molecular weight
Na	Sodium
NaOH	Sodium hydroxide
NA	Not Applicable
ND	Not Detected
NO_2	Nitrogen dioxide
NOx	Nitrous Oxide

OPEC	Organization of the Petroleum Exporting Countries
Ppm	Parts per million
RSM	Response Surface Methodology
SEM	Scanning Electron Microscopy
SPO	Sludge Palm Oil
SV	Saponification Value
TG	Triglycerides
TGA	Thermo-Gravimetric Analysis
TR	Transesterification Reaction
UN	United Nations
Wt	Weight
WCO	Waste Coking Oil
XRD	X-ray Diffraction
XRF	X-ray Fluorescence

List of nomenclatures

Ea	Activation energy
ΔH#	Activation enthalpy
ΔS#	Activation entropy
r	Rate of reaction
k	Pre-exponential factor
T	Absolute temperature
T_o	Reference temperature
n	Temperature exponent
R	Universal gas constant
N	Number of components in the reaction
Ci	Concentration of component i

Chapter 1

Introduction

1. Background

Energy consumption will continue to increase exponentially due to the rising global population, urbanization, and industrialization. The world's energy consumption from coal, oil, and renewable energy sources has increased to meet this need. For instance, Awogbemi *et al*. (2021) reported that the amount of energy from renewable sources will increase from 27 exajoules (EJ) in 2018 to 114 EJ in 2040, and this is expected to further increase to 161 EJ in 2050. A response to the increasing demand for energy sources to match the rate of consumption has necessitated the continuous exploration and use of fossil fuels. However, it is accepted globally that the current climate challenge which could be traced to increasing emissions is due to overdependence on fossil-based fuels as sources of energy. It is on this premise that the search for alternative fuel sources with low global warming potential has been carried out, and biodiesel has been investigated as a reliable alternative to fossil fuels due to the relatively low carbon footprints as compared to fossil fuel that are observed during combustion.

In the United Kingdom, the major greenhouse gas emissions include carbon dioxide, methane, nitrous oxide, and fluorinated gases (F-gases). The contribution of each of these to the overall emission is shown in Figure 1.1.

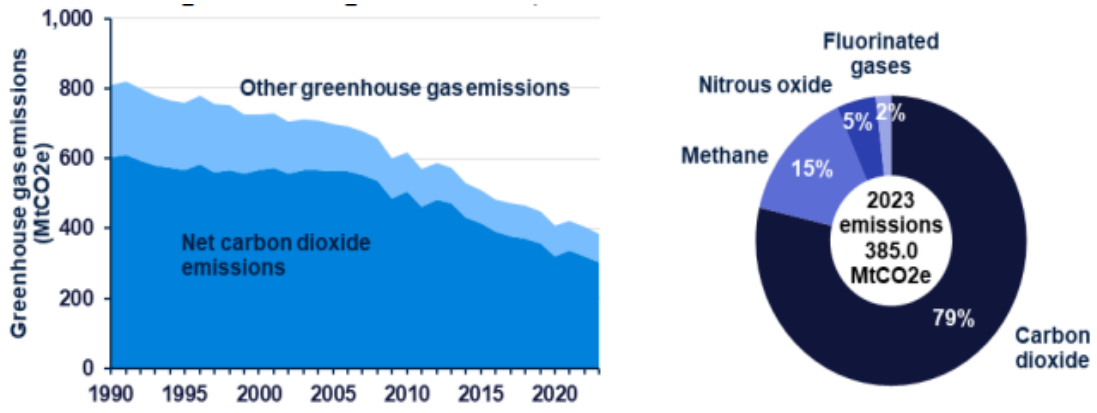

Figure 1.1: Image showing the total UK territorial greenhouse gas emissions from 1990-2023 (Source: Department for Energy Security & Net Zero 2025)

Figure 1.1 shows that 79 % of greenhouse emissions are CO_2. A significant part of CO_2 emission is from the energy sector of which the use of fossil derived fuels in internal combustion engines is one of the main culprits (Sharma and Maréchal, 2019). Global CO_2 emissions were estimated to be 35.3 billion metric tons in 2018, and if the current trend continues, it is projected that these emissions will reach 43.08 billion metric tons in 2050 (Bhowmik, 2020). Apart from CO_2 emission, carbon monoxide, Sulfur dioxide, nitrogen oxides, etc. released from combustion of fuels also contribute to the overall emissions as shown in Figure 1.1 (Rokni *et al*., 2016.; Dmitrienko *et al*., 2017). In the UK, the contribution of different sectors to the overall greenhouse emissions is shown in Figure 1.2.

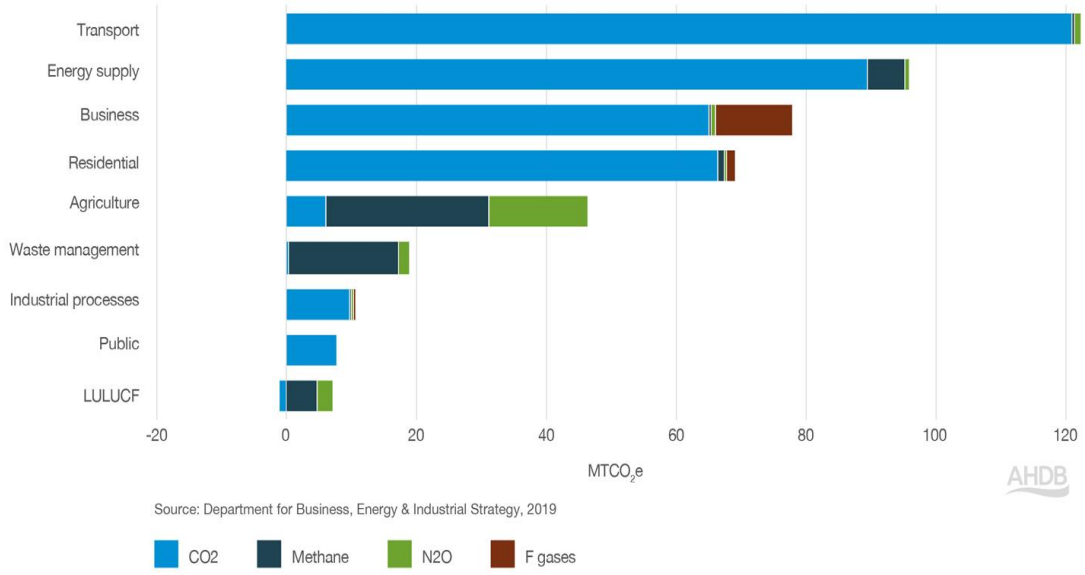

Figure 1.2: Contributions of each sector to the total greenhouse gas emissions in the United Kingdom (Source: Department for Business, Energy & Industrial Strategy, 2019) Note: LULUCF is land use, land use change and forestry

As shown in Figure 1.2, the transport and energy sectors are the major contributors to CO_2 emissions. This could be attributed to overdependence on fossil fuel as the primary source of energy. A synopsis of the world climate change conference (COP 26) held in Glasgow, United Kingdom in 2021 included the following: Recognition of the present state of the climate as an emergency, accelerating action by moving away from fossil fuels among others. The United Kingdom and indeed most countries have already set things in motion by enacting laws and legislation geared towards achieving a net zero by 2050.

The efforts of different countries in reaching this target are shown in Figure 1.3.

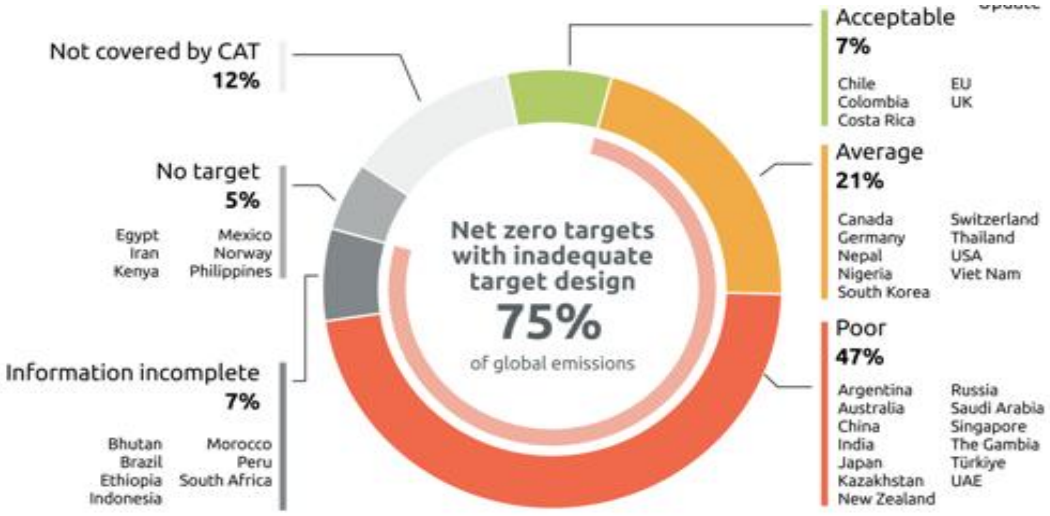

Figure 1.3: Data showing the share of global GHG emissions covered by national net zero emission targets based on data from the Net Zero Tracker (2023) and Climate Watch (2023) as of 5 October 2023 and complemented by CAT analysis.

A shift from fossils to renewable fuels has become one of the major strategies of most nations. This has been deemed essential to provide energy that satisfies performance and environmental requirements. Over the past few decades, a significant amount of financial and human resources has been dedicated to the exploration, production, and utilization of renewable fuels, such as biodiesel, bioethanol, and biogas, among others, as viable alternatives to conventional non-renewable fuels (Awogbemi *et al*., 2021).

Compared to fossil diesel, biodiesel has relatively lower GHG footprint because it is derived from biomass sources which are carbon neutral (Mathur *et al*., 2022). Regarding energy security and environmental protection, alcohol, vegetable or animal fat, is chemically reacted to produce biodiesel, an alternative fuel for diesel engines, with a significant potential to reduce carbon dioxide emissions across the whole biodiesel production cycle (Lin and Lu,

2021). Specifically, edible oil-seed crops provide more than 95% of the feedstock for biodiesel synthesis (Aransiola *et al*., 2019).

In terms of its composition, biodiesel consists of methyl esters of various fatty acids (Kaushik *et al.,* 2021). The differences in the physical and chemical properties of different biodiesel fuels have been attributed to the variations in the fatty acid profiles (Hoekman et al., 2012). In the literature, different feedstocks have been used as raw materials to produce biodiesel. These include: muster oil (Rezania *et al*., 2022), sunflower oil (Zahed *et al*., 2021), palm oil (Zabaruddin *et al*., 2019), non-edible oil (Arshad *et al*., 2023), *Jatropha curcus* (Ruatpuia *et al.,* 2023), neem oil (Dhinagaran *et al*., 2023), rubber seed oil (Ridwan *et al*., 2023), soybean oil (Sarkar *et al*., 2023), waste cooking oil (Zhang *et al*., 2023), waste fish oil (Kiehbadroudinezhad *et al*., 2023), as well as algae (Namitha *et al.,* 2021).

Transesterification is a sequence of chemical reactions that converts an alkyl ester into a new ester by the replacement of the alkoxide group of the ester used as starting material with the alkoxide group of the alcohol. A representation of this mechanism is shown in Figure 1.4 which is indicated by the presence of triglycerides, catalysts, and methanol reacting to produce glycerol as a byproduct and fatty acid methyl ester, one of the main products (Rezania *et al*., 2019; Sahani *et al*., 2020). The mechanism of the reaction can be described in two steps: The first step involves a nucleophilic attack of the alkoxide group from the alcohol on the carbonyl group of the ester to form an intermediate. This is followed by the second step, which is a rearrangement due to the instability of the intermediate to eliminate the alkoxide group of the ester.

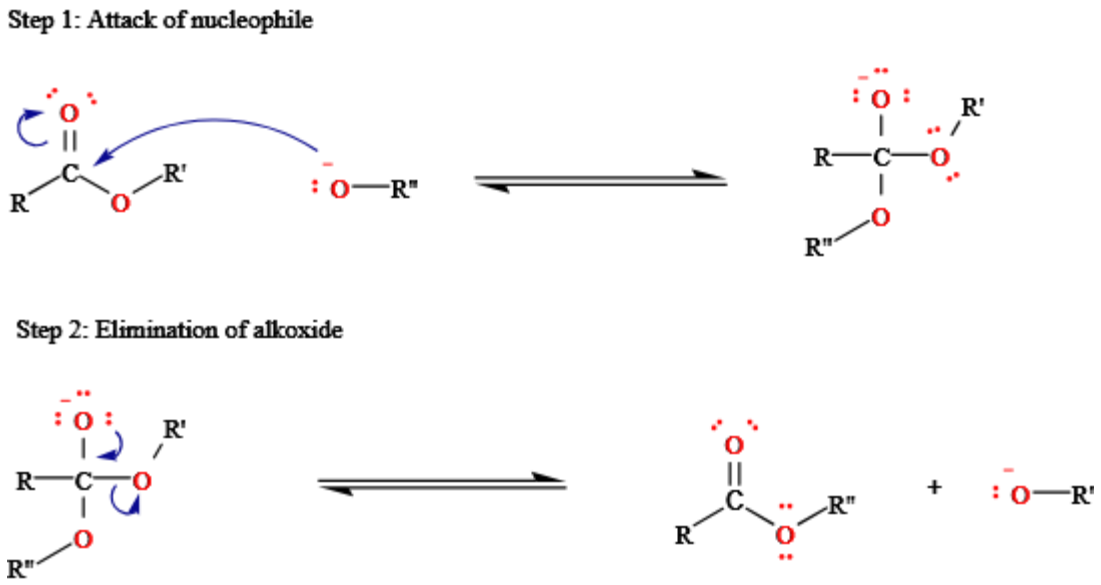

Figure 1.4: Mechanism of transesterification

In industry, it is quite beneficial to use cost efficient routes that would yield pure biodiesel in less time for this type of production (Salaheldeen *et al*., 2021). However, transesterification without a catalyst is a very slow reaction and takes a lot of time to obtain a reasonable yield which is not ideal for industries (Hajek et al 2020). Apart from the duration of the process, the cost of the reactants is also quite important. In this study, and indeed most transesterification reactions, methanol has been used as the preferred reactant over ethanol because it is less expensive (Rahimi *et al.,* 2020). Moreover, the efficiency of the reaction is also influenced by the nature of the catalyst. In the literature, the catalysts that have been explored for this type of reaction are either bio-based (Nguyen *et al*., 2021), homogeneous (Mandari and Devarai, 2021), heterogeneous (Faruque *et al.,* 2020); acidic or alkaline (Athar and Zaidi, 2020). According to Isahak *et al*. (2015), acid and base catalysts are typically divided into two categories: homogeneous acidic/basic catalysts and heterogeneous acidic/basic catalysts. A catalyst is said to be homogenous when it is in the same phase as the reactants and heterogenous when the phases are different. Homogeneous

catalysts exhibit a high yield at moderate heating, a short reaction time, and atmospheric pressure. However, emulsification, increased power consumption, catalyst removal from the blend, and the generation of excess water are some of the main disadvantages of using a homogeneous catalyst for this application (Sahu, 2021).

On the other hand, heterogeneous catalysts have been reported to be quite useful in overcoming most of the challenges reported with the homogenous catalysts (Ravi *et al*., 2020). According to Mandari and Devarai (2021), a heterogeneous catalysts have several technical advantages, including being less expensive and reusable, having a high surface area, being more accessible to separate from the product, and having less resistance to mass transfer. The heterogeneous catalysts were made using various metal and biomaterial kinds; however, their cost was higher than that of the homogeneous catalysts (Scarsella *et al*., 2020; Mukhtar *et al*., 2022).

Research is currently focused on developing biomass waste-based solid catalysts and their application in transesterification reactions to produce biodiesel (Betiku *et al.,* 2019). One of these biomasses is kola nut pod husk, derived from the tropical Kola tree, a member of the *Sterculiaceae* family that is widely distributed throughout the nations of West Africa (Ariwaodo *et al*., 2020). In Nigeria, the kola nuts known as Abata (*Cola acuminata*) and Nitida (also known as ‘‘Goro’’ or ‘‘Obi gbanja’’) hold significant social and economic importance even though there are over forty varieties of kola nuts (Betiku *et al*., 2019). The proper disposal of kola nut pod husks is a significant challenge that must be addressed due to their contribution to environmental pollution. Water purification absorbents have been made from the husk (Lateef, 2023). According to Asogwa *et al*. (2021), it has also been

utilized as a source of potash in the manufacturing of soap, which implies that it might be developed as a catalyst for the transesterification reaction (Betiku *et al*., 2019).

Carica papaya seed oil, a by-product of papaya fruit that is underutilized and frequently classified as waste. Although its properties indicate that it is a promising product, the scarcity in the number of studies assessing its usage as a potential raw material for energy applications is sufficiently evidencing that it is an underexplored feedstock. *Carica papaya*, a tropical plant primarily grown in Nigeria and other nations like Brazil, India, and Mexico, is a member of the *Carcaceae* family (Oshin *et al*., 2021). According to reports, papaya seeds can treat intestinal parasitosis (Okeniyi *et al*., 2007), act as a contraceptive in animals, and have a contraceptive effect on animals and humans (Memudu and Oluwole, 2021). It has been demonstrated that seed is a good source of oil (25.6%) and has potential uses in medicine, biofuel, and industry (Oshin *et al*., 2021). Saha and Jackson (2018) examined the fatty acid composition of oil extracted from *C. papaya*. In the report, it was observed that an oil yield of 24.01% comprises of the following acids: oleic (78.88%), palmitic (15.96%), stearic (4.7%), and arachidic (0.44%). Results indicate more unsaturated fatty acids in the seed oil than saturated ones.

According to Hasanah *et al*. (2014), the physicochemical characteristics of oil, however, dictate its quality and suitability for human consumption. According to Agunbiade and Adewole (2014), *Carica papaya* seed oil produced 31.2% of the biodiesel used in the process. The oil's characterized qualities were acceptable and on par with other oils used in biodiesel production. Therefore, Papaya seeds (*Carica papaya L*.) were chosen as the source material for sustainable biodiesel because they are categorized as non-edible waste products

(Suprianto *et al*., 2019). Hence, this study is aimed at preparing heterogeneous catalysts from kola nut pod husks to convert *Carica papaya* seed oil to biodiesel.

1.1 Motivation of the study

In the modern day, it is crucial to address the two most urgent global challenges: energy security and environmental sustainability. The prolonged dependence on fossil fuels has led to dire environmental outcomes, such as air pollution, climate change, and the depletion of limited resources. Finding sustainable and renewable energy sources has therefore become imperative for protecting the environment and diversifying the energy supply.

Considering this, using waste biomass to produce biodiesel has drawn more attention as a workable approach. As a byproduct of the papaya fruit industry, *Carica papaya* seed oil is an abundant and underutilized resource with enormous potential for biodiesel production.

Additionally, the existing method of producing biodiesel using conventional homogeneous catalysts has several disadvantages, including high energy consumption, difficult separation procedures, and environmental issues related to the use and disposal of these catalysts. To mitigate these difficulties, it is imperative to develop green heterogeneous catalysts, such as from kola nut pod husks, specifically designed for the conversion of waste *Carica papaya* seed oil to biodiesel.

Furthermore, to determine the effectiveness of the transesterification process for the conversion of oil to biodiesel for industry deployment, and to demonstrate the significance of the choice of modelling and optimization methodologies for the improvement of the process, the current study will use ASPEN PLUS modelling to assess the feasibility of converting waste *Carica papaya* oil to biodiesel and the possibilities of optimization for large scale production. Therefore, this research is inspired by the passion to convert waste

materials into highly efficient products that could serve as solutions to the ongoing climate change, and it will also address environmental concerns related to poor waste management in some underdeveloped and developing countries where these products are cultivated.

1.2 Statement of the problem

The local communities in which the kolanuts used in this study were cultivated and harvested have challenges with its sustainable disposal. As the husks of kolanut are inedible, instead of landfilling these materials, which further contribute to greenhouse gas emissions and gives poor aesthetics, the idea behind this research is to gather these materials from these locations and assess the possibilities of converting it into useful products that could facilitate the production of biodiesel.

In addition, the use of conventional homogeneous catalysts in the conversion process poses considerable problems despite the increased interest in biodiesel production as a sustainable energy option. Many of the existing techniques rely on catalysts that are complicated to separate, energy-intensive, and harmful to the environment. Also, poor waste management culminating in environmental deterioration is facilitated by the underutilization of waste biomass, such as Kola nut pod husk and Carica *papaya* seed oil.

One significant gap in the current research is the need for effective and eco-friendly heterogeneous catalysts designed for biodiesel synthesis. Such catalysts can be prepared from agricultural wastes such as Kola nut pod husk which is both economically feasible in terms of being cost effective, readily available and environmentally sustainable. Currently, there is limited literature on the conversion of waste *Carica papaya* seed oil to biodiesel. To the best of my knowledge, the use of Kola nut pod husks as heterogeneous catalysts has not been applied to waste *Carica papaya* seed oil for biodiesel production in the literature

despite being used for several other applications. Therefore, it will be interesting to explore the possibilities of converting waste *C. papaya* seed oil to biodiesel using catalyst extracted from kolanut pod husk and compare its effectiveness with other biomass that have been investigated in the literature for similar applications.

1.3 Aims and objectives of the study

This research project is aimed at solving two key issues which include: The provision of suitable material (catalysts) to facilitate the conversion of waste oil to biodiesel and the provision of an alternative energy source with low carbon footprint. These would be achieved by the following procedures:

(1) The synthesis of a green heterogenous catalyst from inedible biomaterial (Kolanut pod husk) to facilitate the transesterification of waste *C. papaya* seed oil to biodiesel, as well as investigation of its physical and chemical properties using Scanning Electron Microscopy (SEM), Fourier Transform Infrared Spectroscopy (FTIR), X-ray Diffraction Spectroscopy (XRD), Branuer-Enmett-Teller Analysis (BET) and Thermogravimetric Analysis (TGA).

(2) Investigation of the reaction conditions and physicochemical properties that would result in optimum yield and the desired characteristics required to achieve a relatively low carbon footprint when compared to fossil diesel. This study aims to produce biodiesel from *Carica papaya* (pawpaw) oil seeds using kola nut pod husk as green heterogeneous catalysts. This aim will be achieved by:

- Extraction of oil from ripened Pawpaw seeds via Soxhlet extraction, to determine the physicochemical properties of the extracted oil for suitability for biodiesel synthesis and optimize the process variables via Analysis of Variance (ANOVA) and Response Surface Methodologies (RSM).

- Development of green heterogeneous catalysts from fermented Kola nut pod husk and the characterization of the calcined kola-derived catalysts using Scanning Electron Microscopy (SEM), Fourier Transform Infrared Spectroscopy (FTIR), X-ray Diffraction Spectroscopy (XRD), Branuer-Enmett-Teller Analysis (BET) and Thermogravimetric Analysis (TGA).
- Production of biodiesel via transesterification of the extracted oil using the developed green catalysts, determine the physicochemical properties of the biodiesel to assess its suitability for use as fuel, and to optimize the process variables via ANOVA and RSM.
- Process evaluation and optimization using AspenPlus modelling.

1.4 Contribution to knowledge

The study contributes to the field of catalysis by introducing a novel green heterogeneous catalyst from waste kola nut pod husks tailored specifically for the efficient conversion of waste *Carica papaya* seed oil to biodiesel. By providing insights into the synthesis and optimization of catalysts that demonstrate increased catalytic activity, recyclability, and decreased environmental impact compared to traditional homogeneous catalysts, this research broadens the range of environmentally friendly catalysts now available. Also, for the first time, AspenPlus modelling will be used to simulate the transesterification of the waste *Carica papaya* seed oil to biodiesel.

The study emphasizes the possibility of waste valuation in the generation of sustainable energy by focusing on the conversion of underutilized *Carica papaya* seed oil into biodiesel. The work contributes to the growing debate on waste management techniques and

sustainable energy practices by highlighting the significance of using waste biomass as a significant resource for biodiesel production.

Also, this study advances the current state of knowledge of the practical implications of using green heterogeneous catalysts in large-scale biodiesel synthesis by analyzing the economic feasibility and scalability of the proposed catalytic process. The results provide insightful information about the financial implications and possible commercial uses of the developed catalysts, adding to the body of knowledge for promoting sustainable energy practices in an economical and scalable approach.

1.5 Organization & structure of the thesis

The thesis is organized into eight interrelated chapters shown in the diagram below.

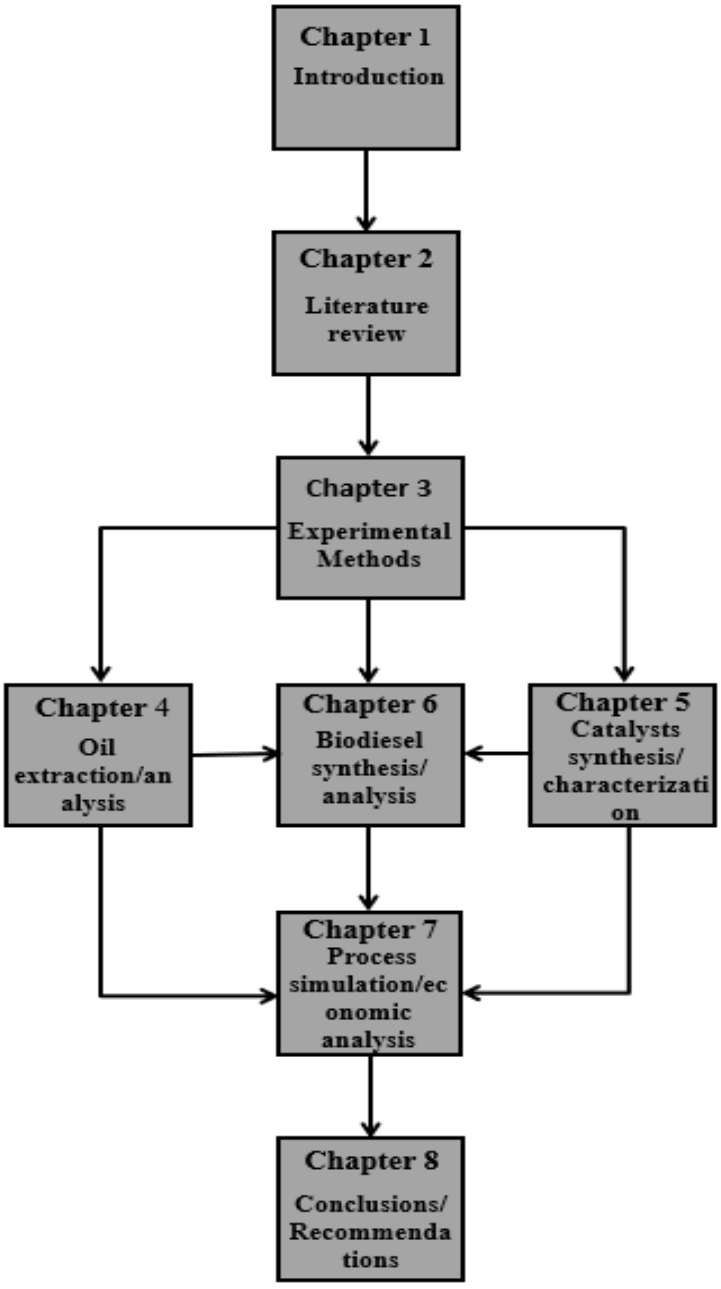

Figure 1.5: A flowchart showing layout of chapters in this thesis

Outline of the subsequent chapters

Chapter 2. This presents a review of relevant literature tailored to the study's objectives.

Chapter 3. This outlines the materials and methods section. This entails the materials used in the study and the methods applied successfully synthesizing the green heterogeneous catalyst for the conversion of waste *Carica papaya* seed oil to biodiesel.

Chapter 4. Presents the results of the analysis and discusses these results. This comprises physicochemical parameters of the *Carica Papaya* seed oil, model fitting and adequate testing, impact of reaction variables, optimization of reaction variables, validation of predicted optimum conditions, and finally, comparing the physicochemical and fuel properties of the oil with EU and US Standards for Biofuels.

Chapter 5. Entails the result and discussion segment. It comprises properties of the green heterogeneous catalysts synthesized from fermented, treated, and calcined kola nut pod husk for transesterification. Results of characterization results from BET, XRD, TGA and FTIR are also presented and discussed.

Chapter 6. Entails a development and discussion segment. It comprises experimental design and analysis of variance, modelling and optimizing results, combined process variables on *Carica papaya* oil biodiesel yield, and comparison of biodiesel quality characteristics with EU and US Standards for biofuels.

Chapter 7. Also entails a result and discussion segment comprising biodiesel process design and simulation.

Finally, chapter 8 presents conclusions and offers recommendations for further study.

Chapter 2

Literature review

2. Introduction

In this chapter, the progress that has been achieved so far in the production and usage of biodiesel as an alternative source of fuel is reported. Also, the catalysts that have been explored and the efficacy of conversion involved in the transesterification reaction are discussed. In addition, the economic feasibility of this process, which gives an indication of its application in industries, will be assessed. Firstly, the general overview of biodiesel gives an insight into its composition which varies with different blends. Secondly, it describes the various biodiesel production technologies and compares the differences between the various transesterification methods for biodiesel production. This chapter further describes the sources of feedstocks for biodiesel production such as waste kola nut pod husk for green catalyst development and *Carica papaya* oil utilization. Also in this chapter, the effects of different transesterification process variables on biodiesel production are highlighted. The physicochemical and fuel properties of biodiesel are also elaborated in this review chapter. Finally, the progress in transesterification biodiesel process design, simulation and optimization are reviewed.

2.1 Overview of biodiesel

The anticipated depletion of fossil fuels, geopolitical instability and environmental concerns prompted the quest for petroleum derivative substitutes as an alternative fuel for diesel engines. The need for biodiesel is rising annually, becoming increasingly significant in many countries' energy systems (Oyetola et al 2019). As a result, related biodiesel research,

development, and innovation (R&D&I) are likewise progressing at a comparable rate (Rezende *et al*., 2021).

In terms of production, alcohol, vegetable or animal fat is chemically reacted to produce biodiesel, the most often utilized acyl acceptors are alcohols, specifically methanol. Although they are far more expensive, other alcohols such as propanol, butanol, isopropanol, tert-butanol, branched alcohols, and octanol can also be utilized. Methanol is more affordable, more reactive, and produces fatty-acid methyl esters (FAME) that are more volatile than fatty-acid ethyl esters (FAEE) compared to ethanol. However, methanol is currently mostly made from non-renewable fossil fuels, such as natural gas. FAME and FAEE exhibit minor distinctions in their fuel properties; for instance, FAEE is somewhat more viscous and has slightly lower cloud and pour points than their comparable FAME (Yusuf et al., 2011; Tamjidi et al., 2021). FAME reaction, also known as transesterification reaction, creates new chemical compounds known as methyl esters and calls for a catalyst, typically a strong base like potassium or sodium hydroxide. These esters have become recognized as biodiesel (Elgharbawy *et al*., 2021).

According to Gbashi *et al*. (2019), biodiesel is a transparent, amber-yellow liquid with a viscosity akin to petroleum diesel. With a flash temperature of 423 K compared to 337 K for petroleum diesel, biodiesel has a higher flash point than petroleum diesel and so non-flammable and less combustible (Changmai *et al*., 2020). When burnt as a fuel, biodiesel significantly reduces harmful pollutants compared to petroleum diesel because it is non-toxic and biodegradable (Zhang *et al.,* 2022).

The Bxx nomenclature refers to biodiesel blend where xx is the proportion in the volume of the Petro-diesel/ biodiesel mix and was developed because of international practice and is

used to designate the concentration of biodiesel in blends (Soumiya and Baskar, 2017). There are four primary concentrations of biodiesel used in the fuel: pure (B100), blends (B20-B30), additive (B5), and lubricity-additive (B2). According to Cavalheiro *et al*. (2020), fuels B2, B5, B20, and B100, for instance, have a content of 2%, 5%, 20%, and 100% biodiesel, respectively. The most popular blends have volumetric proportions ranging from 5% to 20%. Engine modifications are not necessary for the B5 mix. Due to its complete miscibility and physical and chemical similarity to mineral diesel, biodiesel can be utilized in compression-ignition engines without requiring major or labor-intensive modifications (Demirbas, 2009).

The same equipment, procedures, and infrastructure typically used for conventional diesel fuel can also pump, store, and manage biodiesel (Nikolova *et al*., 2020). Transporting, handling, and storing biodiesel is safer than conventional diesel since it doesn't release explosive vapors and has a relatively high flash point (Malode *et al*., 2022).

2.2 Research progress in biodiesel production technologies

In the literature, different reaction pathways of producing biodiesel have been reported. These include homogeneous acid-catalyzed transesterification, homogeneous alkaline catalyzed transesterification and heterogeneous catalyzed transesterification. The details of these reaction mechanisms to produce biodiesel are hereby presented.

2.2.1 Homogeneous acid-catalyzed transesterification

Triglycerides can be processed using an acid catalyst to produce biodiesel. When using low-cost feedstocks, acid-catalytic transesterification of biodiesel can effectively compete with base catalytic processes utilizing virgin oil from an economic standpoint (Athar and Zaidi, 2020). As acid catalysts, hydrochloric and sulfuric acids are typically favored. To

accomplish separation and transesterification in a single step, acid-catalyzed transesterification begins by mixing the oil directly with the acidified alcohol. The alcohol serves as both an esterification reagent and a solvent in this process (Athar and Zaidi, 2020; Nisar *et al*., 2021). The homogeneous acid-catalyzed reaction's reaction time is significantly shortened when excessive alcohol is consumed. Therefore, to shorten the reaction time, a high catalyst concentration and a larger molar ratio are needed for Bronsted acid-catalyzed transesterification (Mandari and Devarai, 2021; Sahar *et al*., 2022).

Bahadi *et al*. (2021) examined the homogeneous acid-catalyzed transesterification reaction between crude palm kernel oil (CPKO) and di-trimethylolpropane (di-TMP) to generate the bio lubricant product, CPKO-di-TMPTE. Reaction surface methodology using a D-optimal design was used to optimize the reaction process based on four reaction parameters: catalyst loading, temperature, time, and reactant ratio. A CPKO/di-TMP ratio of 1.6:1 (mol: mol), a reaction period of 4.6 hours, a reaction temperature of 150 °C, and a catalyst quantity of 1.7% were the ideal reaction conditions. The ideal yield was 79%, with a tetraester selectivity of 91%. The synthetic bio lubricant exhibited a low pour point (−6 °C), a higher flash point (365 °C) that made it thermally safer, and a higher viscosity index of 140.1, which suggested its potential resistance to viscosity change at changing temperatures.

Juera-Ong (2022) used sulfuric acid and amberlyst 15 to produce homogenous catalytic reactions to study the reduction of high free fatty acid (FFA) in sludge palm oil (SPO). Therefore, this project aimed to reduce the high FFA level in SPO to less than 1wt % so that it can be suitable to produce biodiesel. To investigate FFA conversion, an esterification process using a homogeneous catalytic reaction was conducted. The ideal parameters of

16.8% sulfuric acid, 79.7 minutes of reaction time, and 58.4% methanol were fulfilled to produce the FFA concentration of 1.03 wt.%.

According to Rizwanul Fattah *et al*. (2020), homogeneous acid catalytic transesterification has a low susceptibility to the presence of FFA in the feedstock, which is an advantage over homogeneous base catalytic transesterification. Nayab *et al.* (2022) have observed that the process of homogenous acid catalytic transesterification is particularly susceptible to variations in water content. Ester yields were found to be impacted by water as low as 0.1 (wt.%) in the reaction mixture, with the reaction being nearly entirely hindered at 5 (wt.%) water concentration (Kukkohovi, 2020). Equipment corrosion (Ghedini *et al*., 2021), increased neutralization waste (Kibar *et al*., 2023), recycling difficulties (Xie and Wang, 2021), secondary product formation (Vlnieska *et al*., 2021), higher reaction temperature (Hsiao *et al*., 2020), extended reaction times (Martínez *et al*., 2019), and comparatively slow reaction rate (Rizwanul Fattah *et al*., 2020) are some of the drawbacks of homogeneous acid catalytic transesterification.

2.2.2 Homogeneous alkaline-catalyzed transesterification

The process known as alkaline catalyzed transesterification involves the reaction of an alcohol and a triglyceride (fat/oil) in the presence of alkaline catalysts, such as sodium or potassium carbonates, alkaline metal hydroxides, and esters (biodiesel) to produce glycerol and esters (Iqbal, 2021; Maheshwari *et al*., 2022; Babadi *et al*., 2022). According to Athar *et al.* (2020), alkali-catalyzed transesterification is substantially faster than acid-catalyzed transesterification. It also poses less risk to the environment and is less corrosive to industrial equipment.

Due to several factors, homogeneous alkaline catalytic catalysts are frequently utilized in industries, including modest operation conditions, high conversion can be obtained in a short amount of time, strong catalytic activity, and being readily available and reasonably priced (Kumar *et al*., 2022).

Alkaline catalytic transesterification procedures are often conducted at low catalyst concentrations (0.5–2 wt.%) and low temperatures and pressures (333–338 K and 1.4–4.2 bar) (Aderibigbe *et al*., 2021). Moderate process parameters are typical for homogeneous base catalysis: alcohol/oil molar ratio stoichiometric (or marginally higher), alcohol reflux temperature for the reaction, atmospheric pressure or minor overpressure, short reaction periods, and low catalyst concentration (Aderibigbe *et al*., 2021). The generation of soap as a byproduct and large amounts of wastewater are drawbacks of this process, which raises the permitted discharge costs even more (Gupta and Singh, 2023). The alkaline catalyst is used up in the process of making soap, which lowers catalyst efficiency because water causes the reaction to transition to saponification partially (Chanakaewsomboon *et al*., 2021). The soap increases viscosity and forms gels, which lowers the ester yield and complicates the process of separating glycerol. As a result, it is essential to minimize adverse reactions like hydrolysis and saponification (Mathew *et al*., 2021; Carlucci, 2022). As seen in Equation. 2.1, saponification converts the excess FFA in the feedstock into soap and water. Additionally, as illustrated in Equation 2. 2, a second hydrolysis step converts alkyl esters to FFA with the aid of base catalysts (Abbaszaadeh *et al.,* 2012).

$$RCOOH + NaOH \text{ or } KOH \leftrightarrow RCOONa^{+} \text{ or } RCOOK^{+} + H_20 \quad \ldots\ldots\ldots\ldots\ldots\ldots \quad (2.1)$$

$$RCOOR' + H_20 \leftrightarrow RCOOH + R'OH \quad \ldots\ldots\ldots\ldots\ldots\ldots\ldots\ldots\ldots\ldots\ldots\ldots\ldots\ldots\ldots\ldots \quad (2.2)$$

Where RCOOH is the Free Fatty Acid (FFA), NaOH or KOH is the base catalyst and $RCOONA^+$ or $RCOOK^+$ is the soap produced.

2.2.3 Heterogeneous catalyzed transesterification

The demand for wastewater treatment and the degree of difficulty in purifying the by-product glycerol is linked to the use of homogeneous catalysts, particularly base catalysts (Chong *et al*., 2020; Sahani *et al*., 2020). The benefits of using heterogeneous catalysts in both acid and alkaline forms were the ability to reuse the catalyst and the ability to separate materials quickly and inexpensively (Miceli *et al*., 2021; Jambhulhar *et al*., 2022; Mulyatun *et al*., 2022), including low reaction conditions, simple separation, high activity, and minimal contamination (Jambhulkar *et al*.,2022)

According to Faruque *et al*. (2020) and Aderibigbe *et al*. (2023), heterogeneous solid catalysts can be classified into three categories: (1) acid solids that can catalyze the esterification of free fatty acids, (2) base solids that can catalyze the transesterification of triglycerides; and (3) bifunctional solids (acid-base character) that can catalyze both esterification and transesterification reactions at the same time.

Qasemi *et al*. (2020) investigated the transesterification process of Mespilus germanica (M. germanica) kernel oil as a novel feedstock using the Taguchi technique using an Al_2O_3/CaO nanocatalyst and achieved a best transesterification yield of 96.68% under ideal circumstances (25°C, 2 hours, 12:1 methanol to oil ratio, and catalyst weight of 0.5%). Additionally, after declining with the methanol to oil ratio and catalyst concentration, the conversion yield showed an increase. Furthermore, regeneration studies demonstrated that three cycles of the present catalyst could be utilized with respectable conversion yields.

Under mild circumstances, $MnCO_3$ was found to be an effective heterogeneous catalyst for the transesterification of several alcohols with dimethyl carbonate (DMC), yielding the necessary compounds. The analysis's findings showed that $MnCO_3$ that had been calcined at 300 °C had a notably larger surface area and many weak acid sites, both of which improved the catalytic performance during transesterification (Bi *et al*., 2021).

Gogoaşă *et al*. (2023) developed a green-supported catalyst for the transesterification reaction to produce alkyl esters by employing a biodegradable superbase as a chemical component and bacterial cellulose as a catalytic support. At a temperature of 70 °C and a catalyst loading of 7.5% (1.5/20 w/w catalyst: oil), the reaction produced more than 99% of its content.

2.2.4 Feedstock pre-treatment via fermentation for green heterogeneous catalysts development for transesterification

Adepoju (2022) produced biodiesel (98.03 wt.%) from a mixture of pig and neem seed oil by using kola nut pod ash as a heterogeneous biocatalyst. It was found that fermentation had an impact on the CaO concentrations of kola nut pods, with fermented kola nut pods displaying high K and Ca amounts. With a 95.30 wt.% yield, the biocatalyst made from fermented kola nut pods generated biodiesel from shea butter oil.

2.2.5 Lipase catalyzed transesterification

At moderate reaction temperatures, enzymes such as lipases can be used to produce biodiesel with excellent purity (Cavalcante *et al*., 2021; Mathew *et al*., 2021). Nevertheless, the industrial application of lipases is limited due to their high cost, and slower reaction rates than that of acid and basic catalysis. Furthermore, the presence of methanol would cause deactivation of some enzymes. The immobilization of enzymes is an intriguing substitute

even though it is still a costly procedure (Ismail *et al*., 2021; Cavalcante *et al*., 2021; Mathew *et al*., 2021). For example, the method can be less expensive if the enzyme is immobilized in a polymer or resin and can then be used again (Wahab *et al*., 2020). Free fatty acids and the amount of water in the raw material have no effect on enzymatic processes, which results in a purer phase of glycerol and lower energy consumption. However, the procedure can only be employed on a small scale due to the high costs (Rezende *et al*., 2021). Only a few studies of the lipases have been documented in the literature Candida antarctica (Lv and Liu, 2019), Candida sp. (Kalita *et al*., 2022), C. rugosa (Najjar *et al*., 2021), Trichosporon asahii MSR54 (Pradhan *et al*., 2022), and Yarrowia lipolytica (Vasaki *et al*., 2022).

Glycerol is produced when triglycerides are transesterified using lipase enzymes. Glycerol can then bind to the lipase catalyst rather than the triglyceride molecule, inhibiting the process (Salaheldeen *et al*., 2021). To get around this, the glycerol can be bound by an acyl acceptor molecule, creating a triglyceride molecule that is unable to attach to the lipase catalyst's active site. The lipase catalyst can demonstrate a greater rate of turnover and more usefulness when an acyl acceptor is added to the reaction (Intasian *et al*., 2021; Mehmood *et al*., 2021; Karavannis *et al*., 2022).

The lipase transesterification process is superior to the chemically catalyzed transesterification method in several ways, including the production of no byproduct, ease of product removal, need for moderate process conditions, and catalyst recycling (Abdulmalek *et al*., 2022). Lipases break down triglycerides into FFA and glycerin, which are most active at the oil–water interface. The hydrolysis reaction is reversible when there is little water present (Cieh *et al*., 2023).

2.2.6 Nano catalyzed transesterification

Recent development has been made in the catalytic conversion of fats and oils to biodiesel, especially utilizing more attractive nanocatalysts and ionic liquid catalysts for the generation of biodiesel. Nanocatalysis is a process of using nanomaterials as catalysts for a range of homogeneous and heterogeneous catalysis applications. Catalytic activity is excellent in nanoscale catalysts due to their large specific surface area and surface energy. Nanocatalysts increase reaction selectivity by permitting reactions to occur at lower temperatures, decreasing the likelihood of side reactions, increasing recycling rates, and recovering energy use (Xiao *et al*., 2020).

Metal oxide, carbon, mesoporous, and magnetic materials can all be used as nanocatalysts. Graphite, carbon black, buckyball, fullerene, and inorganic nanotubes are examples of carbon-based nanocatalysts; on the other hand, metal oxide nanocatalysts include silver, aluminum, titanium oxide, cobalt, iron oxide, cerium oxide, calcium oxide, and zinc oxide (Thangaraj *et al*., 2019). There are further types of nanocatalysts, such as quantum dots and clays. Since metal oxide nanocatalysts are seen to be the most promising of the many types of nanocatalysts, they have been extensively researched to produce biodiesels from a variety of feedstocks (Mofijur *et al*., 2021). For example, Abu-Ghazala *et al*. (2023) examined the remarkable catalytic performance of $K_2CO_3/\gamma\text{-}Al_2O_3$ as a heterogeneous nanocatalyst to produce biodiesel at room temperature from waste cooking oil (WCO). The response surface methodology (RSM) is applied to optimize the catalyst loading, reaction time, and methanol: oil (M:O) molar ratio, as well as the Box-Behnken Design (BBD) approach. In comparison to similar repeating catalysts, the ideal transesterification reaction conditions for biodiesel conversion (98.7%) are 5.8 wt.% catalyst loading at 25 °C for 120 minutes with a 9:1 M:O

molar ratio. The activation energy (Ea), activation enthalpy (ΔH#), and activation entropy (ΔS#) are estimated to be 18.87 kJ mol, 16.34 kJ mol, and 217.22 J mol, respectively, for kinetic and thermodynamic parameters. For six consecutive cycles, the catalyst retains its catalytic activity.

To boost the output of palm oil biodiesel, Prabhakar *et al*. (2021) used titanium dioxide and iron oxide nanoparticles. The sol-gel and gel combustion methods were utilized to synthesize titanium dioxide and iron oxide nanoparticles, respectively. When compared to 82.14 for KOH, the improved biodiesel yield (%) for TiO_2 and Fe_2O_3 was determined to be 91.06 and 84.24, respectively.

Zhu *et al*. (2021) investigated a heterogeneous CaO/Ag nanocatalyst with aims of producing biodiesel from the transesterification of soybean oil and concluded that the silver and CaO had synergistic effects on the yield of biodiesel. During transesterification, the mass transfer resistance of triglycerides was significantly reduced, and the mass transfer constants were improved by the CaO/Ag nanocatalysts, which showed abundant strong basic sites with larger BET surface area (7.02 vs. 2.05 m^2/g), pore diameter (58.84 vs 37.08 nm), and pore volume (0.070 vs 0.016 cm^3/g). The response surface approach was used to maximize the yield of biodiesel and examine the factors influencing reaction parameters. With a methanol: oil molar ratio of 13, CaO/Ag loading of 5%, reaction time of 90 min, and reaction temperature of 72 °C, a maximum biodiesel yield of 90.95 ± 2.56% was attained. For CaO-catalyzed transesterification, the optimized biodiesel yield was 88.40 ± 3.34% with 180 min of reaction time and identical reaction conditions. Five successive reuses of both nanocatalysts were made.

High catalytic efficiency in comparison to other catalysts is one benefit of employing nanocatalysts in the transesterification process (Fattah *et al*., 2020). Nanocatalysts have higher activity than traditional catalysts due to their smaller surface areas. Moreover, they have higher reusability, an effective surface/volume ratio, and better saponification resistance, and are very stable (Rahmani Vahid *et al*., 2017). Numerous methods, such as vacuum coating, microwave burning, co-precipitation, impregnation, condensation, chemical vapor and electrochemical methods, high temperature, solvothermal, hydrothermal, solo-gel, and many more, can be used to create nanocatalysts (Quirino *et al.,* 2016; Ambat *et al*., 2018). The high cost of their synthesis and the requirement for more alcohol for an effective transesterification process are the drawbacks of nanocatalysts (Mofijur *et al*., 2021).

2.2.7 Transesterification using ionic liquids as catalysts

Ionic liquids (ILs) are becoming more well-known as effective catalysts or solvents for a range of processes (Muhammad *et al*., 2015; Zhang *et al*., 2022). Since their melting temperatures are lower than the boiling point of water, molten salts at ambient temperature are referred to as ionic liquids, a novel family of materials (Cheng *et al*., 2022). When compared with conventional chemicals, ionic liquids have several exceptional properties, including minimal vapor pressure, low combustibility, high thermostability and chemical stability, and environmental friendliness. Most ionic liquids are composed of organic cations, such as imidazolium, pyridinium, quaternary ammonium, and phosphonium, as well as organic or inorganic anions, such as halide, tetrafluoroborate, and hexafluorophosphate. Additionally, because of their tunable characteristics, ionic liquids can be coordinated by different cations and anions to satisfy specific requirements (Ong *et al*., 2021). When used

as solvents in the enzymatic production of biodiesel, ionic liquids have demonstrated exemplary performance, increasing the stability and catalytic efficiency of enzymes (He *et al*., 2022).

Furthermore, pure glycerol, which can be used in the synthesis of biodegradable polymers, medications, cosmetics, and other value-added products, can be obtained by using ionic liquids as extraction solvents to improve the quality of by-product glycerol in the production of biodiesel (Wang *et al*., 2017). Ionic liquids are used as catalysts in the biodiesel synthesis process. They are classified as acidic or alkaline ionic liquids based on the reactive sites in the liquid (Sangeetha *et al*., 2023).

Ionic liquids are room-temperature liquid organic compounds made up of anions and cations. Ionic liquids' physical characteristics, such as their density, viscosity, and melting point, are determined by the cations, whilst their chemical characteristics and reactivity are managed by the anion (Yavir *et al*., 2020). Their particular benefit is that they may be synthesized and then adjusted to the proper reaction conditions. The creation of a biphasic system at the end of the reaction is another fantastic benefit of employing Ionic Liquids, particularly to catalyze transesterification for the generation of biodiesel (Xu *et al*., 2021). According to Elgharbawy *et al*. (2020), the reason for this biphasic system is that the ionic liquid, which was insoluble in the organic phase, stays in the aqueous phase together with the catalyst that was utilized and the glycerol that was formed during the reaction. Because biodiesel makes up most of the top phase and methanol is present in tiny amounts, this makes the final products very easy to separate. Then, by simply vacuum evacuating this tiny amount of methanol, pure biodiesel can be separated (Dwivedi *et al*., 2022). Ionic liquids, glycerol, and methanol are present in the bottom phase. After three to four cycles of water rinsing, this

bottom phase can be used to extract high-purity glycerol (Wang *et al*., 2022). Alternatively, pure glycerol can be produced by distillation, leaving the pure Ionic Liquid behind for direct use in another procedure (Ahmad *et al*., 2012).

Ionic liquids containing the 1-n-butyl-3-methylimidazolium cation are the most researched compounds among the several kinds of ionic liquids that could be used to catalyze the transesterification reaction for the manufacture of biodiesel (Ahmad *et al*., 2012).

According to Roman *et al*. (2019), 1-methylimidazolium hydrogen sulphate, or [HMIM]HSO4, is an ionic liquid that can be successfully used as a catalyst in the esterification reaction between oleic acid and methanol to produce biodiesel. Twenty-seven trials were used in a Box-Behnken Design (BBD) to optimize the critical experimental conditions. The goal of the optimization was to increase the amount of Fatty Acid Methyl Esters (FAME) and oleic acid conversion in the biodiesel samples that were produced. The molar ratio of oleic acid to methanol and the dosage of the catalyst were found to be the two crucial parameters that affected both conversion and FAME content. The model indicated that 8 hours of reaction time, 110 ± 2 °C, a methanol/oleic acid molar ratio of 15:1, and a catalyst dosage of 15 wt.% would result in a 95% conversion as the ideal circumstances for reaching maximal conversion. Similarly, 8 hours of reaction time, 110 ± 2 °C, a methanol/oleic acid molar ratio of 14:1, and a catalyst dosage of 14 wt.% were ideal for obtaining the maximum FAME content, which resulted in a FAME content of 90%.

Panchal *et al.* (2020) also reported the synthesis of Fatty Acid Methyl Esters (FAME) by transesterification of soybean oil with methanol and the use of an ionic liquid as a catalyst. The ionic liquid used in the transesterification of soybean oil for the manufacture of biodiesel was 3- (N, N-dimethyl dodecyl ammonium) propane sulfonic acid p-toluene sulfonate

([DDPA] [Tos]), which was synthesized, characterized, and used. The ratio of soybean oil to methanol (1:2 v/v), the concentration of the ionic liquid catalyst (8.0%w/v), the reaction period (4 hours), the agitation speed (325 rpm), and the constant refluxing reaction temperature were among the factors that were optimized in the study. In ideal circumstances, 75% biodiesel output was attained. In addition, the biodiesel's characteristics were described, including its density at 25 ºC and kinematic viscosity at 40 ºC.

Amino acids (AAs) were used as anions by Wang *et al*. (2022) in the synthesis of eleven ionic liquids. Tetraethylammonium (N2222) served as the cation in these ionic liquids, which were referred to as [N2222] [AA]s. The study found that a methanol/oil ratio of 10:1 mol/mol, a reaction temperature of 100 °C, a catalyst dosage of 20 wt.% (based on the oil weight), and a reaction time of 60 minutes were the ideal parameters for the transesterification reaction of soybean oil, which produced a biodiesel conversion rate of 98.4%.

2.2.8 Supercritical transesterification

A potential remedy for catalytic transesterification is the creation of supercritical biodiesel. Unlike other biodiesel generation systems, this process does not require the use of catalysts. Supercritical processing can handle a variety of feedstocks with continuity and is tolerant to FFA and water. Methanol has a critical temperature of 239.2 °C and a critical pressure of 8.09 MPa. Triglycerides and methanol are frequently used as input materials in supercritical processes. In the supercritical technique, the methanol density rises, and its dielectric constant falls. The intensification of density causes a slight decrease in the polarity of methanol (Qadeer *et al*., 2021). Under supercritical circumstances, a homogenous phase forms because nonpolar triglycerides dissolve more readily in methanol (Ortiz, 2020). High

methanol-to-oil ratios, which can raise production costs, and high pressure and temperature requirements are just a couple of the difficulties associated with using supercritical technologies to produce biodiesel (Sakdasri *et al*, 2018).

The possibility of producing biodiesel by supercritical transesterification has been investigated in a few existing studies. Singh *et al*. (2021) highlights the method's high conversion rate, rapidity, and environmental friendliness but also stresses the need for more research and development. Additionally, compared to other catalytic processes, this technique has been demonstrated to be more sustainable and efficient (Andreo-Martínez *et al*., 2020). Son *et al*. (2018) presented a novel method of producing biodiesel from wet spent coffee grounds (SCGs) without the need for pre-drying by supercritical methanol. The process made use of subcritical water and supercritical methanol to enable in situ transesterification, which produced biodiesel. This procedure increased the porosity of SCG, which improved lipid extraction and conversion. An optimal biodiesel yield of 10.17 wt.% of dry SCG mass (86.33 w/w% of esterifiable lipids in SCG) was achieved under reaction conditions of 270 °C, 90 bars, methanol to wet SCG ratio of 5:1, space loading of 58.4 ml/g, and reaction time of 20 min. The study identified space loading as a critical factor for biodiesel production. The typical drying procedure and the requirement for a catalyst were removed by using wet SCG waste as feedstock directly, which also lessened the environmental problems associated with landfill accumulation.

Tobar *et al*. (2018) studied the non-catalytic supercritical transesterification of spirulina oil with alcohol (methanol and ethanol) to produce biodiesel. They investigated the effects of temperature (200 and 300 °C) and co-solvent amount (0.0005–0.003 g CO_2/g methanol and 0.0003–0.001 g CO2/g ethanol) on the reaction yield using a factorial experimental design.

The results of the investigation showed that adding more CO_2 as a co-solvent enhanced the reaction yield, which reached 72% at 300°C and 65% at 200°C. Reducing the reaction mixture's critical point with the use of CO_2 as a co-solvent increased the reaction yield overall.

In the study of Ahmed *et al*. (2023), supercritical transesterification with no catalyst was optimized and simulated to produce biodiesel from used cooking oil. With the added benefit of lower pretreatment costs, the study chose a catalyst-free technique, acknowledging the possible detrimental effects of catalysts when water is present in used frying oil. The study involved two stages: response surface methodology optimization and the creation and verification of a process simulation program. The temperature was found to be the most significant process parameter after statistical analysis, including analysis of variance, was conducted using a face-centered central composite design of experiments for matrix creation. The optimization study yielded a maximum biodiesel output of 94.16% at an optimal temperature of 274.8 °C, pressure of 7.02 bar, oil to methanol molar ratio of 12.43.

2.2.9 Microwave assisted transesterification

In general, producing biodiesel using conventional heating methods utilizes a lot of energy. The primary issue with the conventional approach is that it only applies heat to the material's surface (Khedri et al., 2019). Due to this, the reactants' internal molecules can directly receive thermal energy from the microwave systems (Wang *et al*., 2021). Microwave radiation can shorten the reaction time from several hours to several minutes while maintaining other parameters such as alcohol-oil molar ratio, and dosage of catalyst concentration. Microwave heat is more effective than conventional heating at accelerating

the transesterification reaction (Buasri and Loryuenyong, 2017). Nevertheless, using microwaves as a heating source is more expensive (Agu *et al*., 2017).

Microwave methods have been reported to be useful in the production of biodiesel. The primary goal is to maximize product yield while maintaining the lowest possible total cost of production. In the biodiesel manufacturing process, triglycerides are chemically broken down into smaller, straight-chain alkyl ester molecules. One mole of triglycerides reacts with three molar equivalents of methanol to create glycerol and fatty acid ester molecules (Mohamad Aziz *et al*., 2021).

According to Mohamad Aziz *et al*. (2021), the microwave technique of biodiesel production has the potential to increase product yield and energy efficiency, especially when paired with other technologies such as: ultrasound assisted technologies, microemulsion and supercritical methods. Optimization models for this process have been presented by Silitonga *et al.* (2020) and Qadariyah *et al*. (2021), who focused on the production of *Ceiba pentandra* biodiesel and *Chlorella sp.* biodiesel, respectively. The energy efficiency and high yield potential with microwave-assisted transesterification were highlighted in both investigations. The benefits of combining microwave technology with heterogeneous catalysts-which can drastically shorten reaction durations while preserving or enhancing catalytic activity-are further highlighted by Khan et al. (2021).

To produce olive oil methyl esters, Dehghan *et al.* (2019) used microwave-assisted transesterification (MAT) of olive oil. The effect of a variety of reaction parameters on the yield, purity, and physicochemical characteristics of methyl esters was examined. These variables included microwave power level (100-900 W), methanol to oil molar ratio (3-15), catalyst concentration (0.4-2.0%), and reaction time (3-15 min). The best response

conditions attained with MAT were compared to those attained with the conventional heating system in the study. The methanol-to-oil molar ratio, power level, reaction time, and catalyst amount all increased the methyl ester production and purity proportionately. MAT effectively enhanced the yield of methyl ester while consuming less energy and reaction time than the traditional magnetic stirrer transesterification process.

In their study, Falowo et al. (2019) investigated the possibility of using a combination of neem-rubber seed oil and calcined elephant-ear tree pod husk as a catalyst for the transesterification process that yields biodiesel with the help of microwave radiation. The study employed response surface methods in conjunction with a central composite rotatable design to optimize key process parameters. With a 60:40 ratio of neem to rubber seed oils, a 25:1 methanol/oil blend ratio,10 wt.% catalysts ($Fe_2(SO_4)_3$), a 120-minute reaction period, and a 65°C reaction temperature, the free fatty acid content was successfully lowered from 17.76 to 0.67%. High catalytic activity was shown by the calcined ash of *E. cyclocarpum* pod husk, which was rich in K, Mg, Ca, and Fe. Microwave-assisted transesterification of ferric sulphate ($Fe_2(SO_4)_3$) - pretreated oil blend worked best when the molar ratio of methanol to oil was 11.44:1, the catalyst dose was 2.96 wt.%, and the reaction time was 5.88 min. The microwave heating power was 150 W, and a biodiesel yield of 98.77 ± 0.16 wt.% was obtained.

2.2.10 Ultrasound assisted transesterification

Recent studies have focused on ultrasound-assisted transesterification for biodiesel synthesis, showing that it can improve mixing and use less energy (Tan *et al*., 2019). This procedure falls under the larger category of transesterification, which also includes lipase-mediated transesterification and reactions that are catalyzed by bases, acids, and acid-bases

(Kulkarni *et al.,* 2019). Transesterification using ultrasound is just one of the cutting-edge methods being investigated along with others such as microemulsion and pyrolysis.

Ultrasonic radiation in the transesterification reaction produces many microbubbles by creating bubble cavitations close to the alcohol-oil phase boundary. Certain bubbles remain stable for the subsequent cycle, while the remaining ones will undergo dramatic collapse when they reach a crucial size. The phase boundary is disrupted by micro-turbulence created by the asymmetric collapse of the cavitation bubbles. The immiscible reactants are intimately mixed along the phase boundary by the microjets produced by the liquid impingement, which can reach speeds of up to 200 m/s and cause emulsification. The development of emulsion results in an increase in the mass transfer and interfacial region between the oil and alcohol phases, which accelerates the reaction kinetics (Tan *et al*., 2019). The total reaction rate increased because of the microbubbles that were created and burst by ultrasonic cavitation, which also energized the molecules of the reactant and increased local energy transfer (Fallah *et al*., 2023).

By creating microjets and raising the localized temperature, the use of ultrasound in the biodiesel synthesis process eliminates the need for external agitation and heating. According to Xuan (2019), the chemical effect of ultrasound can be accelerated by the production of highly reactive species such as OH*, HO_2*, and H* radicals from the dissociation of solvent vapor trapped in the bubble during a transient implosive collapse of bubbles.

2.3 Comparison between transesterification technologies

There are benefits and drawbacks to each of the various transesterification methods (Mumtaz *et al.,* 2017). The costs of input materials, the amount of trash generated, the cost of production, the purity of the product, the yield percentage, and the risks to the environment

and human health are just a few of the factors that impact these benefits and drawbacks. The advantages and disadvantages of these main transesterification procedures are summarized in Table 2.1, together with the characteristics of appropriate feedstock that are needed for each approach (Gebremariam and Marchetti, 2018).

Table 2.1: Comparison of different methods for transesterification of oil and/or fat for biodiesel production (Gebremariam and Marchetti, 2018).

Transesterification method	Suitable feedstock character	Advantages	Disadvantages
Homogeneous Acid catalyzed	Any type of oil/fat feedstock including those with high free fatty acid	Gives relatively high yield. Insensitive to FFA content in feedstock, thus preferred method if low-grade feedstock is used Esterification and transesterification occur simultaneously Less energy intensive	Corrosiveness of acids damage equipment. More amount of free glycerol in the biodiesel. Requires higher temperature operation but less than supercritical. It is relatively difficult to separate catalyst from product. Has slower rate of production (relatively takes longer time)
Homogeneous Base catalyzed	Oil/fat feedstock with FFA content is less than 0.5% by weight of the oil	Faster reaction rate than acid catalyzed transesterification Reaction can occur at mild reaction conditions and less energy intensive Common catalysts such as NaOH and KOH are relatively cheap and widely available less corrosive	Sensitive to FFA content in the oil Saponification of oil is the main problem due to the quality of feedstock Recovery of glycerol is difficult, Alkaline wastewater generated requires treatment
Heterogeneous Base Catalysis	Oil/fat feedstock with	Improved selectivity Easy to separate catalyst from reaction mixture	Catalysts might be poisoned when

	FFA content is less than 0.5% by weight of the oil	Reduced process stages and wastes Enable to regenerate and reuse the catalyst Reaction can occur at mild reaction conditions and less energy intensive	exposed to ambient air. Sensitive to FFA content in the oil so selective to feedstock type. Soap will be formed if there is high FFA content. Soap formation is associated with reduced biodiesel yield and problem in product purification. Leaching of catalyst active sites may result in product contamination
Heterogeneous Acid Catalysis	Any type of oil/fat feedstock including those with high free fatty acid.	Catalyst separation from reaction mixture is easy. It has reduced process stages and waste. Insensitive to feedstocks' FFA content. Preferred method if low-grade oil is used. Esterification and transesterification occur simultaneously. Solid acid catalysts can be easily removed and recycled	Complicated catalyst synthesis procedures lead to higher cost Requires high reaction temperature, high alcohol to oil molar ratio and long reaction time. Relatively energy intensive.
Lipase catalyzed transesterification	Any type of oil/fat feedstock including those with high free fatty acid and water content.	Insensitive to FFA and water content in the oil, thus preferred when low grade feedstock is used. It is carried out at low reaction temperature. Purification requires simple steps, by enabling easy separation from the byproduct, glycerol. It gives high purity products (esters).	The cost of enzymes is usually very high. Gives relatively low yield. It takes high reaction time. The problem of lipases inactivation caused by methanol and glycerol.

		Enables to reuse immobilized enzyme	
Nano catalyzed transesterification	Any type of oil/fat feedstock including those with high free fatty acid and water content	Relatively with shorter reaction time. Less amount of catalyst can be enough since it has a high specific surface area. Catalyst can be reused many times. Wide range of catalyst choice.	Requires relatively more alcohol for effective yield In some cases, preparation of appropriate catalysts costs more.
Ionic liquid catalyzed transesterification	Any type of oil/fat feedstock including those with high free fatty acid and water content but dependent on which type of ionic liquid is used (Acidic/basic)	Easy to separate final products due to formation of biphasic. Efficient and time saving while preparing catalysts their properties can be designed to suit a particular need. Catalyst can be easily separated and reused many times. High catalytic activity, excellent stability	High cost of ionic liquid production. Requires relatively more alcohol for effective yield
Supercritical transesterification	Any oil and fat with greater range and water content and high FFA content (in particular, used cooking oil)	It takes very little time to complete. Insensitive to greater water content of the feedstocks. Produces more than a kilo of fuel per kilo of feedstock. No need to wash the product as there is no catalyst used. It is easier to design as a continuous process.	Requires higher temperature and pressure. It is not an economic alternative due to its high operating cost, due to high pressures and high temperatures. Relatively there is high methanol consumption (high methanol/crude-oil molar ratio of 40/1)

2.3.1 The mechanism of transesterification

The most widely used method for producing biodiesel is transesterification, which involves treating oils (triglycerides) with alcohol to produce biodiesel (known as fatty acid alkyl esters, or FAAE) as the primary product and glycerin as a byproduct. Triglycerides are initially converted to diglycerides, which are then converted to monoglycerides and finally to glycerol. At each stage, one methyl ester molecule is produced from each glyceride (Ma and Hanna, 1999; Abbaszaadeh *et al*., 2012). Transesterification, also known as alcoholysis, is the process of replacing one ester's alcohol with another alcohol. It is comparable to hydrolysis but uses alcohol instead of water (Mandari and Devarai, 2021). According to Günay *et al*. (2019), the most critical operational factors influencing the transesterification process are reaction temperature, time, pressure, alcohol-to-oil ratio, concentration and nature of the catalyst, mixing intensity, and feedstock type.

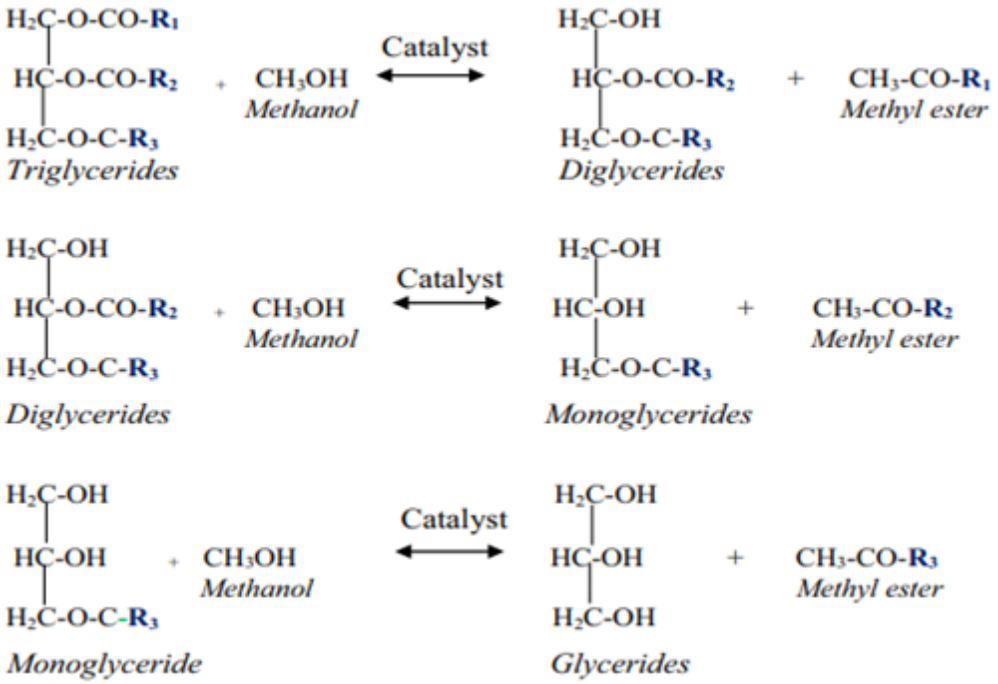

Figure 2.1: The overall transesterification reaction and the stepwise process (Figueiredo *et al* 2022).

2.4 Availability and current usage of Kola nut

Kola is a member of the Sterculiaceae family and are mostly cultivated in Africa largely in Nigeria. It is also known to grow in Ivory coast, Ghana, Brazil and the West Indian Islands (Eijnatten, *et al* 1973, Opeke 1982, Oludemokun 1983). The total annual production of Kola nut from these countries is over 250,000 tons compared to total world production of about 300,000 tons. Nigeria alone accounts for about 70% of the total world production of kola nuts (Quarcoo 1973, Pala 1976, Oluokun *et al* 1999). The two main kola species that are of economic importance are Cola nitida (Vent) Schott and Endl and C. acuminata (P. Beav) Schott and Endl. (Oladokun 1982). Cola nitida is also referred to as "the true kola of trade" has featured in the internal trade of West Africa since the 19th century (Nzekwe1961, Eijnatten *et al* 1969).

Kola nuts are chief economic cash crops to a large resident of Nigerian farmers who are involved in the cultivation, trading and industrial utilization (Asogwa *et al* 2012). The nut is used as a masticatory and stimulant and has social and traditional importance in many traditional ceremonies in Nigeria. It is widely used industrially in the production of soft drinks and beverages, pharmaceuticals, wines and confectioneries (Beattie 1970, Ogutuga 1975). Kola nut pod husks which are waste products from processing the nut, are commonly used for animal feeds as it has great nutritional value. It is believed that broilers fed with kola husk meal diets had a tremendous growth accomplishment (Babatunde *et al* 2005).

2.5 Waste Kola nut pod husk for catalyst development

Several studies have explored the possibility of using waste kola nut pod husk as a catalyst in numerous biodiesel production processes. Although kolanut pod husk is used as an ingredient in animal feeds, there are several other alternatives such as cocoa pod husks, cassava peels, palm kernel cake, among others that can also be used as ingredient in animal feeds, which reduces the likelihood of competition for biodiesel production. In the literature, Osakwe *et al*. (2018) developed kola nut pod as a bio-based catalyst for biodiesel production from yellow oleander seed oil. At a reaction temperature of 60 °C for 90 minutes, a maximum yield of 84.50% was obtained using 1.5 wt.% kola nut pod ash.

Betiku *et al*. (2019) catalyzed Kariya seed oil using a heterogeneous catalyst made from kola nut pods, producing a 98.67 wt.% biodiesel output. Due to the considerable K and Ca present, the catalyst, which was made by burning dry pod powder to ash and then calcifying it further, demonstrated catalytic activity.

In related work, Falowo *et al*. (2020) reported using kola nut pod ash as a catalyst to produce 98.45 wt.% biodiesel from a combination of honne, rubber, and neem oil. The components

of the calcined pod ash were heterogeneous, containing 4.21% magnesium, 5.56 % calcium, and 47.67% potassium.

Betiku and Ishola (2020) reported a biodiesel production of > 99.0 wt.% using C. nitida calcined pod ash as a heterogeneous catalyst in an optimized system using a neural-fuzzy-genetic algorithm instead of a neuro-fuzzy-genetic algorithm. Similarly, Oladipo and Betiku (2020) used the Taguchi optimization technique to create a biocatalyst from kola nut pods on rubber seed oil for transesterification, resulting in the production of biodiesel (96.97 wt.%).

A unique biocatalyst was presented by Falowo and Betiku (2022), which was made of a blend of calcined ashes from pumpkin, cocoa, and kola nut pods (1:1:1). This biocatalyst produced biodiesel with a 95.02 wt.% yield by catalyzing the transesterification of a 50:50 combination of yellow oleander and rubber oil.

The production of green heterogeneous biocatalysts by the valorization of readily available kola nut waste was highlighted by Lateef (2023). It was discovered that these biocatalysts were efficient, providing a lengthy catalyst life as well as a wide range of catalysts for the generation of biodiesel from different kinds of oils with microbial, plant, and animal origins.

Ajewole *et al*. (2022) employed a combination of cocoa and kola nut pods to hydrolyze acid and then ferment the resulting bioethanol with yeast. Promising energy generation was shown by the 10% bioethanol-fuel blend, which produced 13.1 Nm torque and 2953 W power, more than gasoline's 12.4 Nm torque and 2574 W power.

Figure 2.2: Kolanut (*cola nitida*) inside its protective pod (Sanders, 2008)

2.6 Sources of oil feedstock for biodiesel synthesis

A variety of feedstocks, including vegetables, algal, microbial, and animal fats, can be used to produce biodiesel. Biodiesel derived from diverse feedstocks exhibits variations in both composition and purity. The important stage in the production of biodiesel is choosing the feedstock, which affects several variables, including yield, composition, cost, and purity of the fuel. The feedstock for biodiesel production can be obtained from edible, non-edible, and waste materials (Singh *et al*., 2020). Regions also play a role in the feedstock selection process for biodiesel manufacturing. When choosing feedstock, availability and cost are the primary factors that should be taken into consideration (Avagyan and Singh, 2019).

In Canada, canola oil is used as feedstock, while soybean oil is used in Brazil and the United States. Rapeseed oil is utilized as a biodiesel feedstock in Italy, Germany, Finland, and the United Kingdom, whereas coconut and palm oils are used as biodiesel feedstock in Indonesia and Malaysia. In India, karanja and jatropha have been proposed as potential future feedstocks for biodiesel. Among these, sunflower oil, rapeseed oil, soybean oil, and mustard

oil have all been utilized as feedstocks for biodiesel in the past; however, their use has slowed down because of adverse effects on food production (Garg *et al*., 2023; Ghosh *et al*., 2023). Because it directly affects the food chain, using edible oils as feedstocks for biodiesel is a significant problem (Gebremariam, 2021). It has been determined that using non-edible oil as a feedstock for biodiesel offers numerous advantages, including being biodegradable, having low Sulphur content, not affecting the food chain, and having low aromatic content and availability (Shaah *et al*., 2021; Devarajan *et al*., 2022). Biodiesel can also be produced from a variety of feedstocks, including fish oil, tallow oil, animal fats, and microalgae (Singh *et al*., 2020).

2.7 Waste *Carica papaya* seed oil a prospective feedstock

Papaya seeds were reported to be extracted into oil using soxhlation and distillation techniques by Sarianto *et al.* (2019). Papaya seed oil was shown to contain oleic acid according to GCMS analysis. *Strombus canarium* shells have been used as a source of CaO catalyst for biodiesel transesterification. The papaya oil to methanol molar ratio was 1:6, the catalyst was present at 5 wt.% to the oil, and the reaction was run for two hours at 65 °C. The results of the GC/MS analysis revealed that the content of methyl esters is 50.35%, with 10-octadecenoic acid having the highest abundance and 9-octadecenoic acid having the lowest abundance.

Carica papaya L. seed oil was studied by Suprianto and Gunawan (2019) as a potential renewable energy source to replace petroleum diesel fuel. The oil was extracted from papaya seeds using the Soxhlet method and n-hexane solvent. This was followed by transesterification reaction using 1wt.% NaOH as the catalyst and 20 wt.% methanol at 400 rpm for one hour. The fuel qualities of CPSB-10, a blend of 10% C. papaya seed biodiesel

and 90% petroleum diesel fuel, satisfy the required specifications. According to the results of the performance test conducted in a diesel test engine, the highest brake thermal efficiency is 32%, the lowest sfc is 268 g kW–1 h–1, and the maximum brake power and thermal are 30.6 kW and 140.23 N m, respectively.

The extraction of Carica papaya seed oil (CPSO) using a solvent technique was described by Abubakar and Uthman (2020). The oil's physicochemical properties were examined. With a 31.60% oil output, the seed is commercially sustainable. The following parameters were measured using conventional procedures: specific gravity (0.94), viscosity at 40 0C (49.20 cp), iodine value (53.80 g/100g), saponification value (158.60 mg/g), peroxide value (6.70 m mol/kg), calorific value (44.37 MJ/kg), and free fatty acid (0.34). The oil's fatty acid profile revealed that it is highly unsaturated (67.4%), which suggests that the seed oil contains more unsaturated fatty acids than saturated ones. This implies that when oil is added to engines, it will flow as oil rather than fat and not readily solidified. Therefore, the seed can be used to extract oil, which can then be used as a feedstock to produce biofuel.

According to Sultana *et al*. (2020), papaya seed waste has the potential to be used as a feedstock due to its high lipid content and inedibility, which makes it ideal for making biodiesel. The papaya fruit is year-round. In tropical nations, it is always available, and the glove produces over 75% of the total papaya. Therefore, oil yields from wasted papaya seeds can be predicted using a variety of soft computing or data mining techniques, including Response Surface Methodology (RSM), Artificial Neural Networks (ANNs), and Support Vector Regression (SVR). The experiments used in this study to get the oil yield data were based on a central composite design. The suggested models were then developed, contrasted, and compared with the experimental data. According to several performance-measuring

metrics, the SVR model outperformed the ANN and RSM models in predicting oil yields (i.e., relative error, correlation coefficient, mean absolute error, and root mean squared error). It has been noted that oil yields rise with longer extraction times but fall with larger particle sizes. An interface based on the SVR and crow search algorithms was developed to determine the global optimal set. With a particle size of 0.85 mm and a maximum oil production of 28.55%, the extraction process took 6.5 hours. With an error rate of less than 5%, the expected oil output was confirmed through experimental validation.

Adepoju *et al.* (2021) developed an effective CaO-based catalyst by synthesizing it from a binary mixture of seashells, Mactra coralline, periwinkles, Lattorina littorea and using it to transesterify a quaternary mixture of waste, *Carica papaya*, *Citrus Sinensis*, and *Hibiscus sabdariffa*. Process parameters for the transesterification process were optimized to find the best yield of biodiesel from the oil blend. After drying, Lattorina littorea and Mactra coralline were ground into a powder and combined in an identical ratio to create a produced catalyst that was then subjected to characterization. Oil was recovered from the powdered seeds of *Carica papaya*, *Citrus sinesis*, and *Hibiscus sabdariffa* by using a solvent extraction method. The extracted oil was combined with waste-used oil in a quaternary ratio, and its qualities were assessed prior to transesterification with ethanol. Response Surface Methodology (RSM), in conjunction with Central Composite Design (CCD), was used to optimize the process while considering four independent variables: reaction time, temperature, reaction temperature, and EtOH/OMR. The catalyst recyclability test was run, and the physicochemical parameters of the biodiesel were used to assess its quality. The 25:25:25:25 quaternary combination produced oil with low viscosity and significant volatility, according to the results. The generated catalyst was utilized for base

transesterification for a maximum of three cycles. The statistical optimization predicted a biodiesel yield of 99.8044 (wt.%); however, the most significant experimental yield of 99.95 (wt.%) was attained at a reaction period of 60 min, DCCP amount of 3.0 (g), reaction temperature of 70 °C, and EtOH/OMR of 6:1 (ml/ml). This yield was confirmed in triplicate, and an average biodiesel yield of 99.7800 (wt.%) was produced at a reaction duration of 57.72 min, DCCP amount of 3.0 (g), reaction temperature of 69.54 °C, and EtOH/OMR of 6:1 (ml/ml). The chosen variable factors were highly significant, according to the analysis of variance and p-value (p-value<0.0001). The coefficient of determination (R squared) was found to be 99.84%, with the adjusted R^2 of 99.68 and the expected R^2 of 99.06 showing reasonable agreement based on fit statistics and model comparison statistics. The quality of the produced biodiesel fell within the biodiesel standard's specified bounds.

Oshin *et al*. (2021) studied the physiochemical characterization of C. papaya seed oil extract for the generation of biodiesel. The physical characteristics of Carica papaya seed oil yielded the following results: oil yield (30.31±2.38%), color (golden yellow), specific gravity (0.9162±0.012), viscosity (22.45±2.00 mms-1), melting point (42.30±3.0°C), smoke point (212.13±9.0°C), and flash point (274.74±12°C). Acid value (2.848±0.28%), free fatty acid (1.29±0.16%), saponification value (mg KOH/g) (192.06±1.62), iodine value (70.78±1.69 gI2/100 g), and peroxide value (5.079±0.079 meq/kg) are all present according to the chemical properties. The seed oil's fatty acid profile reveals that it comprises the following: stearic acid (5.09±0.5%), linoleic acid (4.56±0.20%), oleic acid (73.36±1.07%), and palmitic acid (14.36±0.96%). The seed oil's overall percentage of unsaturated and saturated fatty acids was 20.48% and 79.52, respectively. The oil demonstrated feasible prospects as a feedstock for biodiesel, as indicated by the outcomes of the physicochemical characteristics.

The transesterification method of using *Carica papaya* (pawpaw) and *Citrullus lanatus* (watermelon) seed oil to create biodiesel was reported by Nkeiru *et al.* (2023). To evaluate the differences in reaction circumstances between the homogeneous (KOH) catalyst and the heterogeneous (alumina-chitosan nanocomposite biocatalyst), experiments were conducted to determine the % yield of biodiesel in relation to reaction parameters, molar ratio, and catalyst dose. To enhance the performance of biodiesel, a novel and cost-effective environmentally friendly catalyst was developed. The production of biodiesel using a homogenous catalyst, potassium hydroxide (KOH), was compared to the production of biodiesel using a heterogeneous catalyst, alumina-chitosan nanocomposite. Using conventional techniques reported by Nkeiru *et al.* (2023), the hard shell of *Rhynchophorus phoenicis* was used to create the alumina-chitosan nanocomposite. The ethyl ester yield of the biodiesels for 1g, 2g, 3g, 4g, 5g, and 6g ranges from 53.40 ± 0.55 - 72.36 ± 0.17%, 64.70 ± 0.40 - 86.40 ± 1.10%, 80.10 ± 0.40 - 97.00 ± 0.50%, 79.60 ± 0.55 - 97.10 ± 1.05%, 74.70 ± 0.45 - 95.40 ± 1.55.%, and 77.40 ± 0.88 - 96.40 ± 0.95%, respectively. Citrullus lanatus seed oil with KOH catalyst had the lowest measured temperature, whereas Carica papaya seed oil with nanocomposite catalyst had the highest. A 4g dosage of catalyst and a 12:01 molar ratio of ethanol to extracted oil were the ideal parameters for the transesterification process.

The potential of *Carica papaya* seeds as a feedstock for the generation of bio-oil was examined by Tagarda *et al.* (2023). Pentane was utilized as the solvent in the extraction process, which was optimized by applying the central composite design of the response surface technique. Examined were the effects of extraction time and the biomass-to-heptane ratio on oil yield. An ideal oil yield of 45.77±0.057% was obtained under the optimized

conditions of 1:11 biomass to heptane ratio (g: mL) and 4-hour extraction time. The chemical composition analysis demonstrated that the material had a high heating value of 37.52 MJ/Kg, indicating its potential for energy, and a kinematic viscosity of 12.58 mm^2/S at 40°C, indicating favorable flow qualities. Alkanes and carbonyl functional groups were found by Fourier transform infrared (FTIR) analysis, suggesting that *Carica papaya* seed oil is suitable for the generation of biodiesel. The results demonstrated the potential of *Carica papaya* seeds as a sustainable feedstock for bio-oil and supported the advancement of sustainable energy.

2.8 Effects of different transesterification variables on biodiesel production

2.8.1 Effect of reaction temperature

The reaction temperature is one of the critical factors that influence the rate of transesterification reaction. It has been observed that raising the temperature accelerates the reaction and increases yield. This could be because of the oil's reduced viscosity, which improves oil-alcohol mixing and speeds up the process of separating glycerol from biodiesel. Nevertheless, a considerable decrease in biodiesel yield was seen with each rise in temperature. This may be because the transesterification reaction proceeds more slowly at higher temperatures than the side reactions, which, for instance, hydrolyze fatty acid methyl esters into corresponding acid and alcohol, producing a lower yield of biodiesel (Verma and Sharma, 2016).

The rate of reaction rises with increasing reaction temperature, according to reaction kinetics, even though the reaction can be carried out successfully at room temperature (Yang *et al*., 2018). Additionally, higher temperatures during the transesterification of oils result in a decrease in the oil's viscosity and improved reactant mixing (Takase *et al*., 2014). There

is, however, a temperature threshold that must be reached to prevent increased saponification (in the case of alkaline-type homogenous catalysts) and rapid evaporation of the alcohol used (methanol boils at 64.6 °C at 1 atm pressure) from reducing the yield of biodiesel (Abbah *et al*., 2016). As a result, the reaction temperature is typically maintained below the alcohol's boiling point. At the same time, reflux conditions allow for the reaction to be carried out at a higher temperature (Abbah *et al*., 2016) or under subcritical conditions such as high pressures up to 2.5 MPa and temperatures up to 200 °C (Jiang et al., 2010).

2.8.2 Effect of time

Higher biodiesel yields are generally associated with longer reaction times. The type of feedstock, the concentration of the catalyst, and other variables all affect the completion time of the transesterification reaction. All these factors work together to determine the ideal time required for a successful biodiesel production process. Base catalysts significantly increase the pace at which biodiesel is produced, almost 4000 times quicker than acid catalysts (Suzihaque *et al*., 2022). Acid catalysts are frequently used as pretreatment prior to the transesterification process. Even though acid catalysts help to speed up the transesterification reaction, alcohol and raw materials still need to be sufficiently mixed or dispersed in situations where the reaction time is insufficient. Early in the process, this reaction time deficit results in a meagre yield of biodiesel. The feedstock first changes to monoglycerides and diglycerides, the two primary triglycerides. This change makes it easier to synthesize biodiesel. As soon as a suitable concentration of mono and diglycerides is obtained, the manufacturing reaction picks up speed and eventually reaches equilibrium at the ideal reaction time. However, when the reaction time is longer than the ideal amount of time, two unfavorable outcomes occur. The saponification process follows the hydrolysis of the ester.

Reduced biodiesel yields are the result of these two processes happening during extended reaction durations (Suzihaque *et al*., 2022).

2.8.3 Effect of alcohol to oil molar ratio

One crucial factor impacting the output of biodiesel is the molar ratio. While a larger molar ratio may reduce the yield, a lower alcohol-to-oil molar ratio will impact on the ability of triglycerides to be converted into methyl esters. The polar hydroxyl group in methanol causes the glycerol and the biodiesel produced during the process to emulsify. This promotes the reverse reaction, which reduces the output of biodiesel by recombining glycerol and esters. It is essential to keep in mind that the transesterification process is reversible, necessitating the use of a significant amount of alcohol to enhance the forward reaction (Verma and Sharma, 2016).

Alcohols such as methanol, ethanol, propanol, butanol, pentanol, and amyl alcohol are frequently utilized in transesterification reactions (Romero *et al*., 2011). Among alcohols, methanol is the most utilized due to its short chain and high polarity, with ethanol being the next. Both methanol and ethanol have benefits and drawbacks. According to Meneghetti *et al*. (2006), the methanol reaction is faster at a lower optimal temperature than the ethanol reaction. Additionally, the methanol reaction may result in a higher biodiesel yield, as in the case of transesterification of sunflower oil (Sankaranarayanan *et al*., 2011). However, according to Demirbas *et al.* (2005), ethanol produced using renewable resources is less harmful than methanol, and in some circumstances—like the transesterification of soybean oil—it may even react more quickly than methanol (Ghesti *et al*., 2009).

According to Romero *et al*. (2011), the alcohol-to-oil ratio has virtually no upper limit; however, raising it above a certain degree is ineffective. According to Wen *et al.* (2010), an

alcohol-to-oil ratio of more than 15 complicates the heating and post-separation processes during the transesterification of soybean oil by methanol over a Li-doped MgO catalyst. In the literature, the complication has been reported during the separation of the by-product (glycerol) from the biodiesel. Hence, the researchers found that the ideal ratio falls between 12 and 15. Furthermore, Xie *et al*. (2013) discovered that because of the increased solubility of the glycerin product in the reaction mixture, an alcohol-to-oil ratio higher than 30 was even more harmful. Higher alcohol-to-oil ratios, however, were shown to be advantageous when transesterification reactions were conducted in high-temperature and pressure autoclaves, as demonstrated by the transesterification of rapeseed oil by methanol using Zn/Al catalyst (Jiang *et al.,* 2010).

2.9 Physicochemical and fuel properties of biodiesel

2.9.1 Acid number

Acid number is defined by the quantity of free fatty acids in the fuel sample (AN). The acid number is expressed in mg KOH/g. A high acid number, which is caused by a high free fatty acid content, causes corrosion in the engine's fuel delivery channel (Singh *et al*., 2019; Bothon *et al*., 2020). In addition, the acid number can serve as a signal for lubricants in the fuel channel. For biodiesel fuel, acid number (AN) is empirically evaluated using ASTM D664, EN 14,104, and P1. The highest allowable amount of acid number, according to current regulations, is 0.5 mg KOH/g (Singh *et al*., 2019).

2.9.2 Boiling point

A substance reaches its boiling point (BP) at the temperature at which its vapor pressure matches the ambient pressure. The typical boiling point may also function as an indicator of an element's overall volatility. Any substance with a higher boiling point indicates that the

element is less volatile, whereas one with a lower boiling point indicates that the element is more volatile. The type of bond between an element's molecules determines its boiling point (BP). With the aid of the ASTM-D7398 standard, gas chromatography is utilized to determine the boiling point range. According to ASTM-D7398 standards, the BP point ranges from 100 to 615 °C (Singh *et al*., 2019).

2.9.3 Calorific value

The amount of energy released when a unit amount of fuel burns is known as the fuel's heating value or calorific value (CV). Fuel with a higher calorific value is preferable for internal combustion engines (Bukkarapu *et al.,* 2022). Diesel fuel has a larger calorific value than biodiesel fuel. Compared to petroleum diesel, biodiesel fuel has a lower energy content (approximately 10%) due to its high oxygen concentration. Accordingly, the amount of energy decreases as the blend level of the biodiesel mixture increases (Pullagura *et al*., 2021). At a constant degree of unsaturation, the mass fraction of oxygen decreases as the length of the fatty acid carbon chain increases, and the calorific value rises (Kalsoom *et al*., 2017; Niyas and Shaija, 2022). The degree of unsaturation in biodiesel has a significant impact on heating values (Kumbhar *et al.,* 2022). Compared to saturated esters, unsaturated esters have a more incredible volumetric energy amount (MJ/gal.) and a lower mass energy amount (MJ/kg) (Zhang *et al.,* 2020). According to Paul *et al*. (2020), the minimum calorific value for biodiesel intended for heating purposes is 35 MJ/kg, as stated in EN 14213.

2.9.4 Cetane number

The primary factor influencing the fuel's ignition delay phase is its cetane number. An ignition delay is the amount of time between when fuel is released into the cylinder or combustion chamber and when ignition starts. A high cetane number indicates that the fuel

can ignite rapidly once it is introduced into the combustion chamber (Ge *et al*., 2020; Thiruselvam *et al*., 2023). According to Kamaruddin *et al.* (2020), a low Cetane level signifies more engine exhaust emissions, more deposits from incomplete combustion, and a rise in knocking. With respect to biodiesel, cetane number increases with fatty acid chain length and saturation level. Due to its higher oxygen content and improved combustion efficiency, biodiesel has a higher cetane number (Yesilyurt, 2020). The guidelines provided by ASTM D613, EN ISO 5165, and ISO 5156/P9 specify the cetane number of biodiesels. The European standard for Cetane number is 51; however, the ASTM standard states that it must be at least 47 (Singh *et al*., 2021).

2.9.5 Density

Density is a measure of how much fuel the injector supplies to the combustion process (Sakthivel *et al*., 2018). The energy content and the air-fuel (A/F) ratio in the combustion chamber are influenced by the fuel density. The methyl ester profile, feedstock type, and method of biodiesel synthesis all affect the density of the fuel (Neupane *et al*., 2021). The ASTM D1298, ISO 3675/P32, and EN ISO 3675/12185 test procedures can be used to evaluate the density of biodiesel. Biodiesel derived from different feedstock generations has a density ranging from 832 to 982 kg/m^3. According to Singh *et al*. (2019), biodiesel derived from neem seed pyrolysis oil has the highest density (982 kg/m^3), whereas biodiesel derived from beef tallow oil has the lowest density (832 kg/m^3).

2.9.6 Viscosity

The fuel's viscosity indicates how well it flows. Compared to conventional fossil fuel, biodiesel has a higher viscosity because of its larger molecular mass and chemical structure (Singh *et al*., 2019; Neupane et al., 2021; Hassan *et al*., 2022). While lower viscosity makes

it easier to transport fuel to the combustion chamber, a higher viscosity decreases thermal efficiency (Dehhaghi *et al*., 2021; Padmanabhan *et al*., 2022). The ASTM D445, ISO 3104/P25, and EN ISO 3104 guidelines are followed to calculate the biodiesel kinematic viscosity. The range of kinematic viscosity for biodiesel fuel, as per ASTM standards, is 1.9 mm^2/S to 6 mm^2/S, whereas the range for EN standards is 3.5 mm^2/s to 5 mm^2/S (Singh et *al*., 2019).

2.9.7 Water (moisture) and sediment content

The amount of moisture and sediment present in the biodiesel fuel indicates the fuel's purity (Brahma *et al*., 2022). Biodiesel may contain water in the form of suspended or dissolved droplets (Johnson *et al*., 2022). The presence of water in fuel reduces the calorific value of biodiesel and causes the corrosion of the components of the engine, which in turn reduces the efficiency of the engine (Hosseinzadeh-Bandbafha *et al*., 2019; Hoang *et al*., 2020). Also, dirt particles in the sediment found in biodiesel fuel have the potential to choke fuel lines (Micic, 2020). The hydrolysis reaction of the fatty acids in biodiesel is enhanced by high water content (Lin and Ma, 2020). The ASTM D2709, EN ISO 12,937, and D2709/P40 standards specify the methodology to determine the amount of water and sediment present in biodiesel (Singh *et al*., 2019).

2.9.8 Iodine number

The amount of iodine absorbed by the double bonds of FAME molecules in a 100 g fuel quantity is indicated by the iodine number (Huang *et al*., 2022). When fuel reacts with air, its degree of unsaturation and propensity to oxidize are measured using the iodine number (Folayan *et al*., 2019; Cavalheiro *et al*., 2020; Varghese *et al*., 2022). The location of the double bonds that are accessible for oxidation is irrelevant to the iodine number. Further

research revealed a connection between the iodine number and the viscosity of biodiesel, cetane number, and cold filter plugging point. While ASTM D6751 does not provide an iodine number, EN 14111 states that the maximum iodine value is 120 (Singh *et al*., 2019; Bukkarapu and Krishnasamy, 2022).

2.9.9 Flash point

The lowest temperature at which fuel would ignite when they are exposed to an ignition source is known as the flashpoint (FP) (Lefebvre *et al* 2010). Most biodiesel fuels have a flashpoint of over 150 °C, while regular diesel has a flashpoint of 55–65 °C. The procedures for flash point evaluation are described using ASTM D93, P21, and EN ISO 3679 standards. The biodiesel made from linseed has been found to have a maximum FP value of 241 °C, while the biodiesel made from neem seed pyrolysis oil has a minimum FP value of 55 °C (Alagu and Sundaram, 2018; Neupane *et al*., 2021).

Biodiesel derived fuels possess better safety characteristics, especially for storage and transport from one place to another. Due to their reduced volatility, methyl ester straight vegetable oils have a higher flash point than petroleum diesel (Mulula and Manoka, 2021). The flash point has an inverse relationship with fuel volatility (Jamil *et al*., 2021). The flash point criteria are primarily used to ensure that the generated FAME has been sufficiently purified by eliminating highly volatile undesirable products, primarily excess methanol left over after product stripping techniques (Singh *et al*., 2019).

2.9.10 Lubricity

The frictional force existing between two machine parts that are moving relative to one another is known as lubricity (Hsieh *et al*., 2015). Biodiesel Fuels derived from various feedstocks have been reported to possess good lubricating properties (Fevzi 2020). Through

mixing, they can be utilized to increase the lubricity of ultra-low sulphur diesel. Due to its high lubricity, biodiesel (B100) is exempt from US and European standard lubricity specifications. The ester of FAME components and contaminants is responsible for this. The lubricity of biodiesel fuel is found to diminish when impurities are eliminated by a distillation process, where the biodiesel is heated under reflux to boiling point and the vapour is collected using a cooling system (Singh *et al*., 2019).

2.9.11 Pour point

The pour point (PP) is the lowest temperature at which liquid fuel flow properties are lost (Sakthivel *et al*., 2018). Compared to biodiesel fuels, diesel fuel often has a lower pour point and cloud point. The pour point value for biodiesel fuel is calculated using the ASTM D97 standard. The European Union has not specified any requirements for pour point (Singh *et al.*, 2019).

2.9.12 Cloud point

The lowest temperature at which the fuel's wax crystallizes to give the appearance of clouds is known as the cloud point (CP) (Sakthivel *et al*., 2018). The manufacturing of biodiesel involves the use of many feedstocks, each of which has unique fatty acid content. As a result, the cloud point of the biodiesel generated varies depending on the feedstock used (Singh *et al*., 2019). The quantity and kind of saturated fatty acids affect the cloud point. Due to the higher melting temperatures of saturated fatty acids compared to unsaturated fatty acids, biodiesel has higher cloud points (Neupane *et al*., 2021). ASTM D2500 describes the standard process for determining the CP for biodiesel at temperatures ranging from 3 to 12 degrees Celsius (Singh *et al*., 2019).

2.9.13 Oxidative stability

Oxidative stability is a crucial component that greatly affects the length and state of storage (Fattah *et al.,* 2014). It refers to the fuel's resistance against oxidation. The higher oxygen content in biodiesel makes it more prone to oxidative deterioration (Hosseinzadeh-Bandbafha *et al*., 2022). The level of oxidation in biodiesels varies according to the type of fatty acids they contain. Polyunsaturated FAME has a significant impact on the stability of fuel oxidation (Neupane *et al*., 2021).

The stability of oxidation of biodiesel is influenced by the quantity of bis-allylic sites found in its unsaturated constituents. This is illustrated in the organic moiety shown in Figure 2.2 where the bis-allylic site is represented by the methylene group sandwiched between two double bonds. Fuel oxidation is determined by factors such as storage conditions, FAME content, and biodiesel age. The presence of antioxidants such as pyrogallol and butylated hydroxytoluene in biodiesel fuel has been reported to increase its stability. The state of the double bond determines whether unsaturated FA can self-oxidize, and more unsaturation results in less stability. To verify that biodiesel is stable during oxidation, the oxidative degradation method can be employed. According to the British Standard (BS EN 14112:2020), the induction time of biodiesel is the period from the start of the test where a refined dry air is bubbled through biodiesel to the formation of volatile secondary products. The lowest permitted induction time for biodiesel fuel is three hours, according to BS EN 14112, while ASTM D6751 does not specify a minimum induction time (Singh *et al*., 2019).

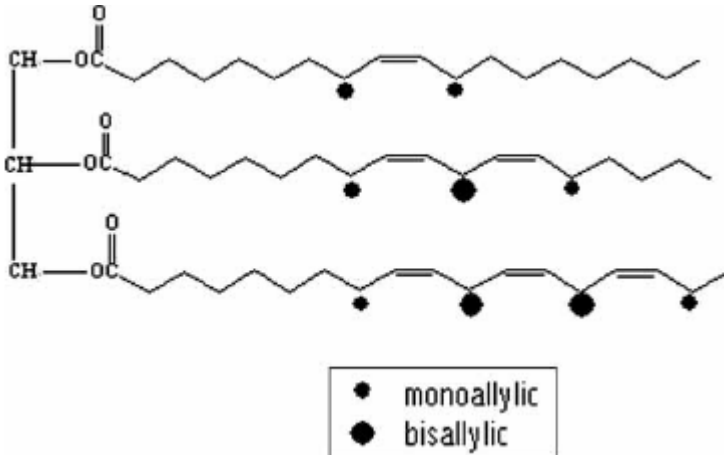

Figure 2.3: The location of mono and bis-allylic sites in unsaturated hydrocarbons (Petrovic, 2008).

The location of double bonds influences fuel oxidation; for example, a cis arrangement is less stable than a trans arrangement. Most natural oils have a cis configuration. Blending two biodiesels made from different feedstocks might increase the stability of the biodiesel since their oxidation stability values vary. A further option for improving biodiesel's stability is to include antioxidant compounds (Singh *et al*., 2019).

2.9.14 Cold filter plugging point

The lowest temperature at which sample fuel is discharged via a typical precision filter is known as the cold filter plugging point (CFPP) (Sakthivel *et al*., 2018; Neupane *et al*., 2021). To evaluate a fuel's capacity to flow under cold conditions, the CFPP is utilized. The highest value of filterability is described by the terms CP and CFPP. Compared to the CP, the sample fuel's CFPP value is less. The CFPP of biodiesels is described in different standards such as ASTM D6371 and EN 14,214 standards (Singh *et al*., 2019). Poor cold flow characteristics are a problem for biodiesel containing long-chain fatty acids and saturated fatty acid esters (Sia *et al*., 2020; Hazrat *et al*., 2020). The pour point and cloud point are improved when

diesel fuel is combined with saturated methyl esters longer than C-12. Longer carbon chains generally raise melting points and decrease performance at low temperatures (Singh *et al*., 2019).

Since the PP, CP, and CFPP are all intimately related, any one of these points can be used to calculate other parameters (Gomez-Rodriguez *et al*., 2021). The average chain length does not distinguish between the saturated and unsaturated portions of fatty acids. In the study of FAME, it is difficult to establish a relationship between temperature and chain length. The degree of unsaturation is directly correlated with the low-temperature properties of FAME. Many variables affect the quality of fuel; hence a more complex procedure is needed to determine the effect. As the blend proportion of biodiesel fuel improves, the low-temperature performance decreases. The mixture of different components causes non-linear variations in low-temperature characteristics (Singh *et al*., 2019).

2.10 Biodiesel standards

Every biodiesel fuel must meet the standard established by the European Union (EN) and the American Society of Testing and Materials (ASTM). These guidelines define acceptable levels for several chemical and physical properties of oil that should be used in the engine sequentially, as well as providing principles for testing fuels. These specifications cover a number of important chemical and physical properties of the fuel, including density (kg/m^3), heating value (MJ/kg), kinematic viscosity (mm^2/S), oxidation, glycerin (% m/m), cetane number, Sulphur content, copper strip corrosion, pour point, acid number (mg KOH/g), boiling point (°C), cloud point (°C), flash point (°C), and many more. Notable standards include ASTM D6751, EN 14,214, and IS 15,607 for biodiesel (B100) and ASTM D975 for diesel fuel (Singh *et al*., 2019).

2.11 Research progress in transesterification biodiesel process design and simulation

Despite the advancements in research and the marketing of high-quality biodiesel as drop-in biofuel in accordance with standard specifications (EN14214 or ASTM6751), the production of biodiesel and the effort to optimise its prospect for real life application is still a complicated process; thus, there is need for both empirical study and modelling approach. The production of biodiesel as reported in different literatures has involved the use of a wide variety of catalysts, reaction and separation conditions, and feedstock, including edible and inedible oil crops and waste oils. To address the complexity of biodiesel production, several modelling tools have been used, such as process design and simulation, sustainability evaluation, and optimization (Pasha *et al*., 2021).

A model-based representation of technical processes and unit operations in software, such as chemical, biological, and physical ones, is called process simulation. The production processes of biodiesel can be designed, developed, analysed, and optimized with its help. Process simulation has two benefits: (a) it speeds up plant design by enabling designers to test different plant configurations quickly, and (b) it helps to improve existing processes by providing answers to "what if" questions, identifying ideal process conditions, and guiding the identification of process constraints (Pasha *et al.,* 2021).

Choosing an appropriate thermodynamic model and determining the chemical components are typically the first steps in process simulations. Next, it is necessary to specify plant capacity, input conditions, operating conditions, and unit operations. The software library contains most of the component property data (Nasir *et al*., 2013; Gmehling *et al*., 2019).

Real-time optimization, online performance monitoring, and quicker troubleshooting are the ultimate goals of process simulation. Researchers and engineers can model, simulate, and

design their processes using a range of modelling tools, including Aspen Plus, Aspen HYSYS, and SuperPro Designer (Mahmud *et al*., 2021; Kasani *et al*., 2022).

There are multiple challenges when utilizing these modelling systems. Determining and choosing the proper chemical species involved in the entire process is typically the first difficulty faced by researchers (Pasha *et al*., 2021). Yun *et al.* (2013) included one triglyceride (tri-olein) and three distinct free fatty acids (oleic acid, stearic acid, and palmitic acid) as model components to simulate the process of producing biodiesel from leftover vegetable oil. Abdulrahman *et al.* (2018) used five different triglycerides (tri-palmitin, tri-stearin, tri-olein, tri-linolein, tri-linolenic) and five FFA (linoleic acid, oleic acid, palmitic acid, stearic acid, linolenic acid) as model components to compile a more thorough representation of the waste vegetable oil. Research has demonstrated that using actual feed compositions and accounting for compositional changes is crucial for producing a more accurate assessment of large-scale plants (Abdurakhman *et al*., 2018). The integration of all the components in a process simulator is another complex problem because of the changeable composition of biodiesel feedstock. The Aspen Plus databanks contain several triglycerides with different fatty acid chains, but the physical property data for these triglycerides is poorly characterized. Furthermore, some components—like enzymes—remain non-databank components. It is still difficult to incorporate these components into process simulators because they typically have vague structures and are hard to characterize (Pasha *et al*., 2021).

Finding the chemical and physical properties that are available in the database presents the second difficulty when utilizing modelling platforms. The polar chemicals (glycerol, methanol, and water) and the non-ideal nature of the transesterification reaction system

typically led to the use of either the NRTL or UNIQUAC thermodynamic models for modelling the biodiesel synthesis system in these simulators. Zong *et al.* (2010) estimated the thermo-physical characteristics of triglycerides using the chemical ingredient fragment technique. Then, individual mono- and diglycerides were included in this manner (Zong et al., 2010). NRTL coefficients of the triolein-methanol and triolein-glycerol binary systems were reliably predicted using the UNIFAC method, which was used in most simulation studies for biodiesel production (Sotoft *et al*., 2010; West et al., 2008; Yun *et al.,* 2013; Pasha *et al*., 2021).

Integrating solids, batch, and custom processing unit modelling presents another difficulty when utilizing modelling systems (Pasha *et al*., 2019). The membrane is one tool that can be used to achieve the required product purity and recovery of recyclable materials (such as methanol, water, and liquid lipase) in the synthesis of biodiesel, for instance, which requires many separation and FAME purification phases (Hobden, 2013; Kumar *et al*., 2020). In addition to these difficulties, several crucial variables must be obtained before designing and simulating a process flowsheet. These include the kind of reactor and catalyst, the rate of reaction or conversion, the stoichiometry of the reaction, the process conditions, the production capacity, and the mode of operation, among many other factors. Reactor selection is the starting point of the method that is frequently used in the process design and simulation of production facilities. Separation and recycling systems are incorporated later (Smith *et al*., 2005; Nasir *et al*., 2013; Pasha *et al*., 2021). The transesterification process and the kind of catalysts used are two of the most critical steps in determining the purity of the final product and the separation and purification processes (Glisic *et al.*, 2014).

2.11.1 Process design and simulation of bio-catalyzed biodiesel production processes

There are numerous studies available on process design and simulation for the manufacture of biodiesel (Pasha *et al*., 2021). Salehi *et al*. (2019) designed and simulated five continuous biodiesel production processes using the Aspen Plus v8.6 software in their study. The first three processes used both alkali- and acid-catalyzed methods to convert virgin vegetable oil (VVO) and waste cooking oil (WCO) into biodiesel. Hexane extraction was used in the fourth and fifth processes to convert WCO into biodiesel using the two-step supercritical method (noncatalytic) and the acid-catalyzed procedure. The two-step supercritical methanol process had the fewest operational units (98.47%) but the lowest FAME purity (98.47%), per the technical assessment. Processes 3 and 1 have the purest glycerol (99.98%) and FAME (99.7%), respectively. Consequently, of all the processes that were examined, the two-step supercritical methanol process and the homogeneous acid catalytic process of WCO are the best options in terms of technical evaluation.

Ihoeghian and Usman (2020) used exergy analysis to determine the location, magnitude, and sources of thermodynamic inefficiencies in a heterogeneously catalyzed rice bran oil biodiesel production plant. The study compared how the exothermic energy of the transesterification reaction may drive the system and showed how inappropriate utility placement can result in energy losses in a heterogeneously catalyzed rice bran oil biodiesel production facility. Aspen HYSYS was used to simulate two rice bran oil biodiesel production facilities designated as schemes 1 and 2. The difference in both production lines is that scheme 1 has hot utility supplies to the reactor, while the second scheme does not. Energy efficiency for scheme 1 was 63.92%, with 94.2% of the total energy destruction occurring in the reactor, according to the overall analysis. In contrast, scheme 2's efficiency

was seen to improve to 75.15%, with 1.63% of the energy consumption occurring in the reactor.

The whole process of biodiesel fuel production using solid acid catalysts has been simulated by Gebremariam and Marchetti (2021) using the commercially known software SuperPro Designer, and the effects of some selected market variables on the economic feasibility of the whole process have been investigated. The price of oil, biodiesel, alcohol, labor, maintenance, tax variance, catalyst, oil, and glycerol were among the market variables considered. The metrics used to assess how changes in these market variables affect the process's economic viability are net present value and project payback period. The feasibility of the production process is significantly impacted by potential market fluctuations in the price of biodiesel and oil, whereas labor and equipment maintenance costs may have less impact.

Im-Orb *et al*. (2021) studied the design of the biodiesel production from palm fatty acid distillate (PFAD) using process intensification approach. To select the best intensifying unit, a transport phenomenon investigation was carried out. This involves the application of reactive distillation step to the hydrolysis-esterification and esterification-transesterification processes. Aspen plus V 8.4 was used to construct the models for producing biodiesel through the esterification-transesterification and hydrolysis-esterification reactions using both standard and enhanced procedures. The optimal conditions for reactive distillation in esterification and transesterification were reached when the liquid holdup was kept at $6m^3$, and the methanol was fed at the third stage of the 4-stage column. In comparison to the intensified hydrolysis-esterification process, the intensified esterification-transesterification method yields more biodiesel while using less energy. The enhanced esterification-

transesterification process is determined to be economically feasible, according to the economic analysis. Lastly, life cycle analysis (LCA)-based environment evaluation revealed that both procedures have comparable environmental effects.

In their investigation, Liu *et al*. (2021) produced biodiesel using waste cooking oil (WCO) as a feedstock. The financial viability of WCO biodiesel production was examined using the Life Cycle Cost (LCC) approach. They were successful in proving that the price of manufacturing one tonne of WCO biodiesel is 6291.56 RMB, which is 65.28% more expensive than diesel. Further analysis was done on the variables affecting the cost of producing WCO biodiesel. While WCO is inexpensive for commercial applications, it must undergo pretreatment, which adds to processing costs because WCO cannot be utilized directly for transesterification to make biodiesel. Pretreatment costs make up 15.60% of the total cost, which is significant. A two-step strategy was employed to model the production process of biodiesel from WCO using Aspen Plus software. For creating a trustworthy benchmark for the industrial production of biodiesel from WCO, the processing parameters of the methanol and biodiesel rectification towers were optimized in the simulation.

The techno-economic feasibility, optimization, and predictive modeling with uncertainty analysis of bio-catalyzed biodiesel production from *Azidirica Indica* oil (BCBPAIO) were studied by Oke *et al*. (2021). Design Expert software was used to build the BCBPAIO optimal conditions and the Central Composite Design (CCD) predictive model. Monte Carlo simulation was used for the model uncertainty analysis. The economic analysis and simulation were carried out using ASPEN Batch Process Developer V10. The CCD model yielded an adjusted R^2 value of 0.9780 and a correlation coefficient (R^2) of 0.9922. The oil transesterification optimum circumstances yielded 87.04% conversion with 3.62 wt.% of

catalysts methanol to oil molar ratio of 8:1 at 59 °C for 4 hours, while the CCD model certainly gave 73.51% with 100,000 trials. The internal rate of return, payback period, total capital investment, and yearly production cost are 43%, 2.67 years, $5,243,784, and $3,537,105, respectively. This analysis demonstrates that production is viable from a financial standpoint.

The simulation and multi-objective optimization (MOO) of a dry microalgae-based in-situ biodiesel plant using the Aspen Plus V11 was investigated by Ahmed *et al*. (2022). Considering the non-dominated genetic algorithm-II (NSGA-II), the process optimization was completed using Excel-based multi-objective optimization (EMOO). For a limited multi-objective optimization (MOO), total annualized cost (TAC), organic waste, and CO_2 emissions were the goals. Economic and environmental factors were also considered. The effects of the choice variables on the selected objectives were evaluated to analyze the statistical trade-offs. Investigations were conducted on tri-objective and bi-objective optimization scenarios. When the production of organic waste and CO_2 emissions decline, the TAC rises. In the created Pareto-optimal front, the net flow method (NFM) selected the first-rank solution. Scenarios A, B, and C produced an optimal plant operation with a TAC of 62.64 million USD, 61.52 million USD, and 60.23 million USD, respectively, with savings of 6.67 million USD, 7.79 million USD, and 9.08 million USD in comparison to the base case study with a TAC of 69.31 million USD. Concurrent optimization of the three contrasting objectives resulted in notable decreases in TAC (13.1%), organic waste (55%), and CO_2 emissions (41%), in that order.

Techno-economic prediction models, multi-objective optimum profitability scenarios, and optimal laboratory experimental data were used by Oke *et al.* (2022) to examine ASPEN

Base Case Simulation (BCS) of biodiesel synthesis from palm kernel oil. The ASPEN Batch Process Developer V10 environment was used to design the BCS. In Historical Data Design of Design Expert, predictive models were developed for forecasting and optimizing techno-economic parameters, such as production capacity (PC), ROI, payback time (PBT), and Net Present Value (NPV). The sensitivity and model uncertainty of the Monte Carlo Simulation (MCS) were verified using the Oracle Crystal Ball. Batch size, production rate, production batch number, and BCS results for 3,000,000 kg/year were 13,482.48 kg, 5.72 kg/min, and 223 batches/year, respectively. ROI, PBT, NPV, and PC predictive models have correlation values of 0.969, 0.982, 0.987, and 0.987, respectively. The techno-economic models' MCS certainly provided a negligible uncertain value (confidence = 100%). As for ROI, PBT, NPV, and PC, the optimal values were 39.9%, 2.48 years, $1,001,320, and 3,000,690 kg, respectively. Techno-economic and sensitivity evaluations for the manufacture of palm kernel biodiesel can, therefore, be carried out using ASPEN Batch Process Developer and Monte Carlo Simulation.

Trirahayu *et al*. (2022) modeled and simulated the production process of biodiesel from RSO via transesterification reaction by employing methanol and a heterogeneous catalyst. ASPEN HYSYS v11 was used to carry out the simulation. The use of acid-based catalyzed esterification was made to prevent soap production, which could drastically reduce the output of biodiesel. They found that producing biodiesel at an RSO inlet rate of 1100 L/h and a methanol-to-oil molar ratio of 1:6 could yield about 1146 L/h. Approximately 95% of the extra methanol could be recovered after methanol recovery was carried out. The results of the simulation showed that the characteristics of the generated biodiesel are suitable for use with contemporary diesel engines. The economic study demonstrates the potential of this

technology and significant investment criteria such as reduced Capital Expenditure (CAPEX), reduced Operating Expenditure (OPEX), improved Return on Investment (ROI) and safety and sustainability.

Elavazhagan *et al*. (2023) examined the process simulation of biodiesel production on a large scale using the ASPEN process simulator. To identify the most effective mode of transesterification under various initial feedstock raw material conditions, simulations of catalytic transesterification and non-catalytic supercritical methods of transesterification were conducted using experimental data. Supercritical processing (280℃; 276.4 atm; 42:1 alcohol to oil ratio) is a cost-effective and high-quality product technology for feedstocks containing a high percentage of free fatty acids (FFAs). Alkali-catalyzed homogeneous transesterification (60–65°C; 4 atm; 6:1 alcohol: oil ratio) was effective for feedstocks with very little FFA, but it was more expensive than the supercritical method of transesterification. However, it produced products with better quality and yield. The ASPEN simulation was used to investigate pre-treatment procedures such as simple esterification and glycerolysis for feedstocks with high levels of FFA. The Cantera combustion chamber, which is scripted in Python, was used to study the combustion characteristics of the biodiesel blend and n-heptane, a substitute for Petro-diesel. The results showed that the combustion process was complete and efficient because there was very little soot and carbon monoxide emission. The DWSIM simulation program was used to conduct simulation investigations.

The technical competence and economic viability of producing biodiesel on an industrial scale using two different catalysts: CaO and sulphonated carbon were evaluated by Qian and Huey (2023). ASPEN HYSYS was used in the process simulation of the efficiency of the acid and base catalysts including the computation of the material and energy balances for

both process configurations. The equipment sizing and costs were completed before beginning the economic analysis. For every process, the following important performance metrics were determined: total capital investment, total production cost, payback time, breakeven point, and net profit after tax rate. The computed Return On Investment (ROI), which has a short payback period of 0.94 years to recover its initial investment, is 105.36%, according to the economic study. According to the Discounted Cumulative Profit (NPV) analysis, which represents the total sum of cash inflow and outflow, the third year's breakeven point was reached. However, for the plant that uses sulfonated carbon in the transesterification procedure, the breakeven point was reached in the ninth year, and the calculated ROI was 14.02% with a payback duration of 7.13 years. Therefore, the most promising route in terms of both technology and economics seems to be the transesterification reaction manufacturing plant that is catalyzed by CaO catalyst.

2.11.2 Process optimization

With consideration for the interplay between subsystems and economic trade-offs, mathematical programming has been widely used to optimize the biodiesel process synthesis problem. Heat exchanger network synthesis, separation sequences, and superstructure optimization for various technologies are by far the most methodically studied synthesis challenges in biodiesel production (Plesu *et al*., 2015; Kianimanesh *et al*., 2017; Pasha *et al*., 2021).

To meet the highest performance standards, it is imperative to optimize the biodiesel production process by identifying the values of critical variables. Better personnel utilization, lower energy usage, lower maintenance costs, less equipment wear, and increased plant performance were all beneficial to plant operations (Cardoso *et al*., 2021).

To achieve the goal of maximum profit, a critical analysis of the process design is quite crucial (Nasir *et al*., 2013). In fact, the kinds of systems used also influence how well a biodiesel plant is optimized. Cost minimization and the maximization of economic potential, or the "objective function," are commonly considered in optimization. For instance, the best conversion is significantly impacted by heat integration, heat exchanger network costs, and utility costs. Moreover, reactor conversion may be impacted by the separator system's order if there are two separators (Nasir *et al*., 2013; Gonçalves *et al*., 2020).

The variables involved in the process itself determine how the optimization process is carried out during the design stage (Osaba *et al*., 2021). After identifying the objective function, a one-dimensional search is used for a single variable. Newton's method and region elimination are techniques for searching in a single variable. There are two types of search methods utilized in multivariable optimization: deterministic and stochastic. Stochastic search techniques include evolutionary algorithms and simulated annealing, while deterministic search techniques include direct and indirect search techniques. According to the literature, most process optimization are composed of three fundamental components: objective function, equality, and equality restrictions. The objective function is the mathematical expression that defines the targeted profit, the equality relates to the function that yields the targeted value, while the mandatory conditions that the mathematical function must satisfy are the equality restrictions. Linear programming is used to design search strategies for situations when all the elements are linear. However, optimization turns into a nonlinear programming problem if the objective function, equality, or inequality constraints are nonlinear (Smith, 2005).

The techno-economic potential of ultrasonic cavitation was evaluated by Gholami *et al*. (2021). Aspen HYSYS V8.4 was used to build two plants based on the traditional mechanical stirring and ultrasonic cavitation processes. The net present value, internal rate of return, total investment, and product costs were all used to compare the two procedures together. The ultrasonic cavitation procedure required a total expenditure of about 20.8% less than the mechanical stirring method. The expenses of the products decreased by 5.2% when ultrasonic reactors were used instead of the traditional method. It was better to use the ultrasonic cavitation technique since it had an internal rate of return of 18.3% and a positive net present value. Furthermore, there was a noticeable drop in the amount of energy used and waste generated because of ultrasonic cavitation. Using ultrasonic cavitation resulted in a 6.9% reduction in total energy consumption. One-fifth of the waste generated by the mechanical stirring process was generated by the ultrasound-assisted method.

Chapter 3

Materials and methods

3. Introduction

This chapter contains the overall experimental plan, analytical analyses and process design and simulation for biodiesel synthesis. The materials, standard operating protocol, and the characterization methods employed in achieving the research objectives are described in this chapter. This chapter is comprised of three major parts which includes: (i) The experimental procedures for the extraction and characterization of oil from *Carica papaya* seeds (ii) Catalysts preparation and characterization (iii) Experimental steps for biodiesel synthesis via transesterification using final products from (i) and (ii) above, and (iv) AspenPlus process design and simulation of the extraction steps and feasibility of the synthesized biodiesel.

3.1 An overview of the experimental plan

This section contains a detailed presentation of the methods of oil extraction, catalyst preparation, biodiesel synthesis, characterization of both the extracted oil and the prepared catalyst, as well as quality control tests of the prepared biodiesel. Standard methods reported in ASTM D6751 were used for oil extraction, EN14241were used for catalyst preparation and quality control tests. The sequence and plan for this chapter are as follows:

i. *C. papaya* seed oil extraction and physicochemical analysis, as well as assessment of the fatty acid composition using GCMS analysis. The results are compared to US and EU quality standards EN 14214 and ASTM D 6751 specifications respectively.

ii. Catalysts preparation and development from waste kola nut pod husks to calcined catalysts CKNPH A, B, C. Catalysts characterization using Powder X-ray Diffraction (PXRD), X-Ray Fluorescence (XRF), Scanning Electron Microscopy - Energy Dispersive

Spectroscopy (SEM-EDX), Fourier Transform Infrared Spectroscopy (FTIR), BET surface area and porosity analysis, as well as TGA-DSC analysis

iii. Transesterification reactions involving the reaction between the extracted oil, synthesized green heterogeneous catalysts and methanol under different reaction conditions. The produced FAME was analyzed to determine the physicochemical properties, the conversion, yield and purity of the methyl esters synthesized from the transesterification from the different produced catalysts. The biodiesel synthesized are also compared to US and EU quality standards EN 14214 and ASTM D 6751 specifications respectively

iv. Process design and simulation of the bio-catalyzed biodiesel production system to study the feasibility of the transesterification process for industrial application. The feasibility and economic analysis of the process will also be determined via AspenPlus modelling.

3.2 Materials

Waste kola nut pod husks and Maradol *Carica papaya L* cultivars were collected from a nearby farm at Mkpat Enin, Southern Nigeria. These were used as the starting materials for oil extraction and green heterogeneous catalysts development.

List of the feedstock utilized in this present study are presented in Table 3.1.

Table 3.1: List of feedstocks

Materials	Purity/specification	Supplier
Waste *Carica Papaya L* oil seeds	Pure and meets ASTM and EU biodiesel standards	Local farm in Nigeria
Waste Kola nut pod husk	Waste biomass	Local farm in Nigeria

3.3 Experimental methods

3.3.1 Oil seed preparation and extraction

The steps involved in the extraction of oils from *C. papaya* seeds are shown in Figure 3.1. Fresh *C. papaya* fruits were obtained from the local stores and cut into halves to reveal the seeds which were collected and washed with distilled water to remove any adhering fruit particles.

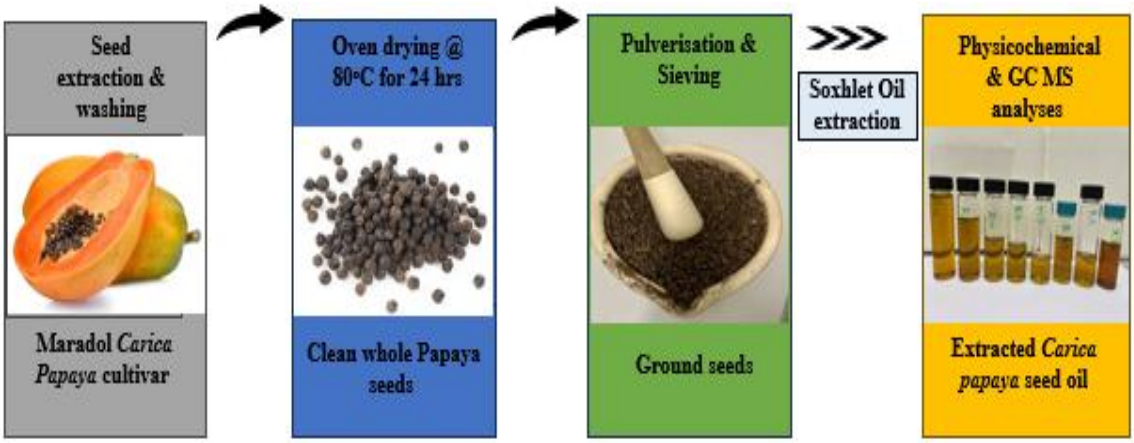

Figure 3.1: Oil extraction processes and steps

The seeds were then dried in a hot air oven at 80 °C for 24 hours and weighed repeatedly until a constant weight was obtained. The dry seeds were then pulverized using a mortar and pestle before being passed through a sieve shaker with a 0.4-0.5 mm mesh size. The powder was kept in an airtight plastic bag for oil extraction.

3.3.2 Solvent - aided oil extraction

The extraction process was carried out using Soxhlet apparatus as shown in Figure 3.2. Soxhlet extraction was chosen because it offers a closed system where the oil can be continuously extracted in a reflux pattern with no loss of material to the environment. Also, a non-polar organic solvent (n-hexane) was chosen as the solvent because of its properties

such as solubility in oils without reacting with it (inertness). Also, its relatively low boiling point (68.7 ºC) is quite ideal for extraction without decomposing the oils and so aid rapid recovery of the solvent.

The prepared papaya seeds powder was weighed and placed in the extraction muslin thimble. 250 mL n-hexane was measured into the reaction flask and placed on a heating mantle. The temperature for the oil extraction was set within the range of 68-70 ^{0}C. As the temperature reaches the target extraction temperature, isolation of oil from the seed sample was achieved. After successful oil extraction, the oil is rotary evaporated to remove n-hexane, after which it was then filtered and centrifuged to remove any remaining seed particles and moisture. The oil yield was calculated using Equation 3.1.

$$y_{oil\left(\frac{v}{v}\right)} = \frac{\text{m extracted oil}}{\text{m seeds sample}} \text{ x } 100 \ldots\ldots\ldots\ldots\ldots\ldots\ldots\ldots\ldots\ldots\ldots\ldots\ldots\ldots\ldots\ldots. (\text{Eq. } 3.1)$$

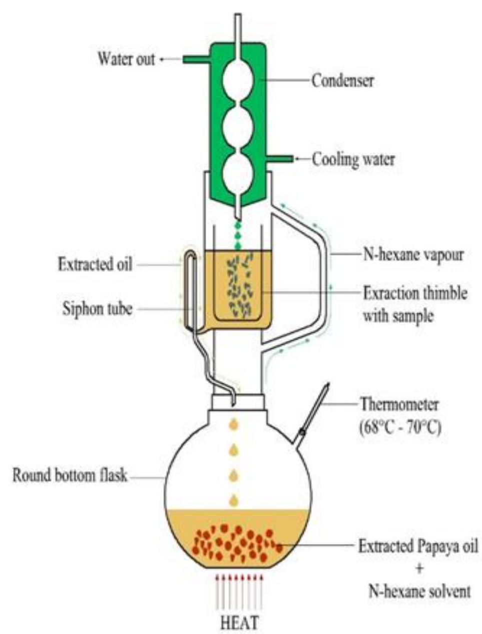

Figure 3.2: Soxhlet oil extraction lab set-up (left); schematic diagram (right)

3.3.3 Design of experiment for seed oil extraction

Experimental treatments for oil extraction were designed using JMP software (version 16). The Design of Experiment (DOE) was conducted with three core components, namely sample weight, extraction time, and solvent volume. The full factorial randomized design resulted in 27 experimental scenarios as shown in Table 3.3. Minitab version 20 was used for data analysis to assess the effects of the three variables' interactions: sample weight, solvent volume, extraction time, and temperature, on the final response, which was the oil yield. The independent process parameters and their coded levels are shown in Table 3.2.

Table 3.2: Factor information and their coded levels

Factor	Code	Levels	Values
Sample weight (g)	X_1	3	50, 60, 70
Solvent volume(ml)	X_2	3	250, 300, 350
Extraction time(min)	X_3	3	55, 65, 75

3.3.4 Linear regression model

A linear first-order regression model was used to analyse the experimental data for oil yield. In theory, it is expected that the oil yield will increase as the quantity of the starting material increases. For this reason, the linear regression model was used to assess the relationship between oil yield and sample weight, solvent volume and the extraction time. Equation 3.2 provides the general regression equation for this model:

$$y = b_0 + b_1x_1 + b_2x_2 + b_3x_3 + b_{12}x_1x_2 + b_{13}x_1x_3 + b_{23}x_2x_3 + b_{123}x_1x_2x_3 \ldots \text{(Eq.3.2)}$$

Where y (oil yield v/v%) is the response (dependent variable), b_0 is the constant regression coefficient, b_1 is the linear regression coefficient, b_{ij} and b_{ijk} $(ijk = 1, 2, 3)$ are the

regression coefficients of 2- and 3-factor interactions, respectively and x_1, x_2 and x_3 are the factors (independent variables). A positive value of the regression coefficients indicates a synergistic effect, while a negative sign indicates an antagonistic effect. The coefficients in the regression equation were for analyzing the relevance of each term relative to others.

Table 3.3: Matrix for oil extraction experiments

Run Order	Variables		
	Sample weight (g)	Solvent volume (ml)	Extraction time (min)
1	70	300	55
2	60	250	75
3	50	250	75
4	70	300	65
5	50	300	65
6	50	250	55
7	70	350	65
8	70	250	55
9	60	250	55
10	50	300	55
11	50	350	75
12	70	250	75
13	60	350	75
14	70	300	75
15	60	300	55
16	70	250	65
17	60	350	65
18	60	350	55
19	50	250	65
20	70	350	55
21	60	300	65
22	70	350	75
23	60	300	75
24	60	250	65
25	50	300	75
26	50	350	55
27	50	350	65

3.4 Evaluation of the physicochemical properties of the extracted oil

Physicochemical characterization of the extracted oil was carried out to assess the suitability of the extracted oil for use as a biodiesel. This is to assess key properties such as the pour point, moisture content, acid value, iodine value, saponification value, peroxide value, saponification value, cetane number, heating value, among others, which are crucial variables expected to attain a certain value to be suitable for use as a biodiesel. The physicochemical properties were assessed based on the AOAC (1997) standard and Wijs method reported by Adepoju *et al*. (2018). The fuel properties such as Higher Heating Value (HHV), Cetane number (CN), Diesel Index (DI), and Aniline Point (AP) were also determined.

3.4.1 Pour Point (PP)

In this method, a cylindrical test tube was filled with the sample to a specific level (5 cm^3) and clamped with a wooden clamp bearing a thermometer the sample was then allowed to cool below 0 $^{\circ}C$ in an ice/salt bath. At this point it was removed and tilted on a clamp and was observed at intervals. The lowest temperature at which the sample was observed to flow was recorded as the pour point.

3.4.2 Moisture content (MC)

A small portion of the oil sample was placed in a dried and weighed crucible and then placed in a griffin temperature adjustable oven at 105℃. Heating and weighing were recorded at hourly intervals until the weight of the sample remained constant. The crucible was then cooled, and the moisture content determined.

3.4.3 Acid Value (AV)

The British Standards Institute (BSI 684) was employed for the determination of acid value. 1 g of the sample was placed in a 250 cm^3 conical flask and warmed. 25 cm^3 of propan-2-ol was then added with thorough stirring followed by 2 drops of phenolphthalein indicator. The contents were then titrated with 0.1 M KOH solution until a light pink colour which persisted for 1 minute was observed. The endpoint was recorded and used to calculate the acid value using the equation below:

$$\text{Acid Value} = \frac{\text{Molarity of KOH} \times \text{Molar mass of KOH} \times \text{titre Value})}{\text{Mass of sample}} \ldots\ldots (\text{Eq. } 3.3)$$

3.4.4 Iodine Value (IV)

The iodine value was determined using Wijs method as described in IUPAC (1979). Exactly 1g of oil sample was weighed into a conical flask and 25 cm^3 Wijs reagent was added, then shaken and placed in the dark for 1 hour. After the set time, it was titrated against 0.1M sodium thiosulphate using 2 cm^3 starch solution as indicator. A blank test was carried out simultaneously under the same condition. The Iodine value was calculated as:

$$\text{Iodine value} = \frac{12.69\text{T}(\text{V1} - \text{V2})}{\text{M}} \ldots\ldots\ldots\ldots\ldots\ldots\ldots\ldots\ldots\ldots\ldots\ldots\ldots\ldots\ldots\ldots\ldots\ldots\ldots\ldots\ldots\ldots (\text{Eq. } 3.4)$$

Were

T = Molarity of sodium thiosulphate solution

V_1 = volume of thiosulphate solution used for the blank

V_2 = volume of the thiosulphate solution used for the sample

M = Mass of sample (g)

3.4.5 Saponification value (SV)

The saponification value was determined using the method described by IUPAC (1979). 2g of the oil sample was weighed into a conical flask, and 25 cm^3 of 0.5 M ethanolic KOH was

added. Antidumping was added and the mixture was boiled for one hour in a reflux condenser. After 60 minutes, 0.5 cm^3 of phenolphthalein was added and titrated with 0.5M HCL solution. A blank test excluding the oil was carried simultaneously. The saponification value was calculated using the equation below:

$$\text{Saponification Value} = \frac{\text{V1} - \text{V2 T 0.5}}{\text{M}} \ldots\ldots\ldots\ldots\ldots\ldots\ldots\ldots\ldots\ldots\ldots\ldots\ldots\ldots\ldots\ldots \text{(Eq. 3.5)}$$

Were

T = Concentration (Molarity) of HCl used

V_1 = Volume of HCl used for the blank

V_2 = Volume of HCl used for the sample

M = Mass of test sample (g)

3.4.6 Peroxide Value (PV)

The peroxide value was determined using IUPAC (1979) method. 4g of the sample was weighed in a conical flask and 10 cm^3 of chloroform was added to dissolve the sample. This was followed by the addition of 15 cm^3 of acetic acid and 1cm^3 of 15% of potassium iodide solution. The mixture was shaken and kept in the dark for 5 minutes. Thereafter, 25 cm^3 water was added and titrated with 0.002 M sodium thiosulphate. The peroxide value was calculated using the following expression:

$$\text{Peroxide value} = \frac{\text{V T100}}{\text{M}} \ldots\ldots\ldots\ldots\ldots\ldots\ldots\ldots\ldots\ldots\ldots\ldots\ldots\ldots\ldots\ldots\ldots\ldots\ldots\ldots \text{(Eq. 3.6)}$$

Were

T = Concentration (molarity) of thiosulphate used

V = Volume of thiosulphate solution used

M = Mass in gram of test sample

3.4.7 Cetane Number (CN)

The expression reported by Eevera *et al.* (2009) was employed to calculate the cetane number:

$$\mathrm{CN} = 46.3 + 5458\ (\mathrm{SV}) + 0.225\ (\mathrm{IV}) \quad \text{(Eq. 3.7)}$$

3.4.8 Higher Heating Value (HHV)

The higher heating value was calculated using equation 3.8 as reported by Ababu *et al*. (2021) as:

$$\mathrm{HHV} = 49.43 - 0.041\ (\mathrm{SV}) + 0.015\ (\mathrm{IV}) \quad \text{(Eq. 3.8)}$$

3.4.9 Diesel Index (DI)

The diesel index (DI) was calculated according to the following expression:

$$\mathrm{DI} = \frac{\mathrm{CN}-10}{0.72} \quad \text{(Eq.3.9)}$$

3.5 GC-MS analysis for fatty acid composition of *Carica Papaya* Oil (CPO)

The GC-MS analysis was carried out using a combined 7977A gas chromatograph instrument (Agilent, U.S.) and mass spectrophotometer. The spectrophotometer was equipped with a 5977B MSD detector and an HP-5 MS Ultra inert column (30.0m × 250 µm x 0.25 µm). Helium gas was employed as the carrier gas, and the column velocity flow was set at 0.53 mL/min. At an injection temperature of 250 °C, the sample (1 µL) was introduced in a split mode with a 5:1 split ratio. The column temperature began at 120 °C for 4 minutes and gradually increased to 170 °C at a rate of 6.5 °C/min. With a rate of 2.75 °C/min, the temperature was increased to 250 °C and maintained for 5 minutes. The entire elution time was 30 minutes. The relative percent amount of each component was determined by comparing the average peak area of each component to the total areas. The data acquisition and system control were both accomplished using Mass Hunter (Agilent) software.

Based on their retention indices, the components present in the seed oil were identified, and the National Institute of Standards and Technology (NIST) database was used to interpret the mass spectrum.

Figure 3.3 Agilent GC-MS analyser used for this study

3.6 Green heterogeneous catalysts synthesis and characterization

3.6.1 Feedstock preparation and pre-treatment via fermentation

The fresh kola pods were washed with distilled water to remove wax and any unwanted materials. 5 kg of the clean pods were placed in a bucket, soaked, and completely submerged in distilled water. Fermentation of the Pods was carried out for 10 days following the procedure as reported by Adepoju *et al*. (2020). The fermented product at the end of 10 days was rinsed thoroughly in distilled water and oven dried at 85 ^{0}C to a constant weight. The

dried pods were ground using a blender and sieved to particle size of 0.5 mm. The sieved powder was divided into 3 equal portions of 10 g each before pre-treatment with methanol and calcination (Adepoju *et al*. (2018); Udoetuk *et al*. (2018); Balajii and Niju (2019). Figure 3.4 presents the workflow for catalysts synthesis and characterization.

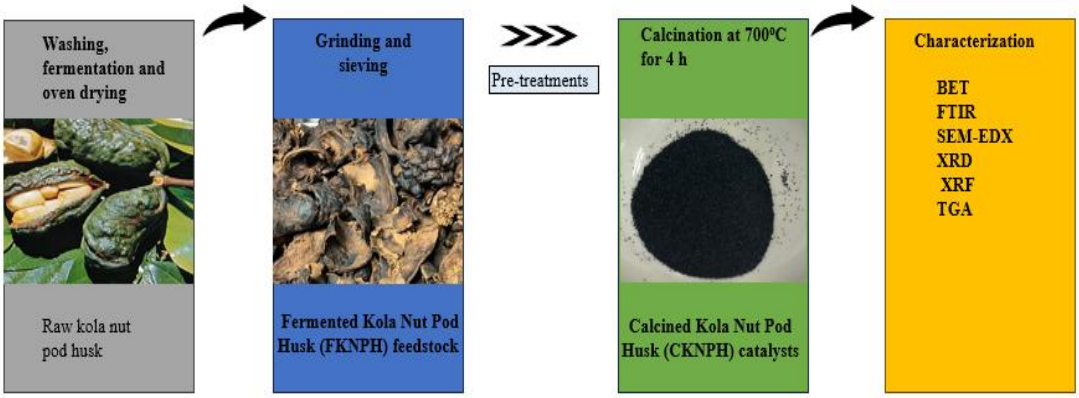

Figure 3.4 Catalysts preparation workflow

3.6.2 Catalyst calcination

Catalyst calcination was performed to investigate the impact on the surface areas and elemental compositions of the three generated catalysts. The catalysts were subjected to a distinct calcining process for four hours at a temperature of 700 ºC using a Thermoconcept KLS 10/12/WS furnace (Adepoju *et al*. (2018); Udoetuk *et al*. (2018); Balajii and Niju, (2019). Following calcination, the biocatalysts were placed in sealed glass vials and stored in a desiccator for further processing. The three calcined catalysts were utilized as renewable heterogeneous catalysts without any further treatment.

Figure 3.5: Calcination furnace-balance system

Three catalysts were produced: Calcined Kola Nut Pod husk Catalysts (CKNPH) A, B and C. The Calcined catalyst A was not pre-treated with MeOH and so no drying was required, and the ash content after calcination was not removed. Catalyst B was pre-treated with MeOH, it was therefore dried before and after calcination, and the ash content was shaken off. Catalyst C was not pre-treated with MeOH, therefore drying was not required and the ash content was shaken off. All three catalysts were calcined at 700°C for 4 hr. The catalysts were labelled CKNPH-A, CKNPH-B and CKNPH-C while the raw sample was labelled FKNPH. Table 3.4 presents the treatment matrix for catalysts preparation.

Table 3.4: Types of treatment methods for catalysts development

CKNPH Catalyst	Pre-treatment with MeOH	Drying	Ash removal
A	NA	NA	NA
B	YES	YES	YES
C	NA	NA	YES

3.6.3 Catalysts' yield

The equation which was used to calculate the yield is shown in equation 3.10.

$$\%\ \text{Catalyst yield} = \frac{(\text{W2})}{(\text{W1})} \times 100 \ldots\ldots\ldots\ldots\ldots\ldots\ldots\ldots\ldots\ldots\ldots\ldots\ldots\ldots\ldots. (\text{Eq. } 3.10)$$

Where W_2 represents the mass of the produced catalysts. W_1 is the mass of the starting material utilized in the production of the catalysts.

3.6.4 Catalysts characterization techniques

The catalyst analysis equipment used in this study is shown in Figure 3.6.

3.6.4.1 Powder x-ray diffractometer

Powder x-ray diffraction patterns of the synthesized catalysts were recorded at room temperature using a Rikagu MiniFlex 600 analyzer x-ray diffractometer with Cu-Ka radiation (λ = 0.154060 nm). The diffractometer was operated at 40 kV and 44 MA, scanned with a step size of 0.02 ° and a count time of 1°/min in the 2q range 2° to 70°. The Scherrer formula (Equation 3.10) was used in determining the crystallite sizes of the catalysts.

$$D = \frac{k\lambda}{\beta COS\Theta} \ldots\ldots\ldots\ldots\ldots\ldots\ldots\ldots\ldots\ldots\ldots\ldots\ldots\ldots\ldots\ldots\ldots\ldots\ldots\ldots\ldots\ldots. (Eq\ 3.11)$$

Where λ (nm) is the wavelength characteristic of the Cu-Kα radiation, k is a constant (0.9) β is the full width at half maximum (in radians) and Θ is the Bragg angle.

Rikagu MiniFlex 600 XRD analyzer

ABB Spectra MB 3000 FTIR analyser

Xenemetrix Genius IF XRF analyser

BET Micrometrics ASAP 2420

Figure 3.6: Key catalysts characterization analysis equipment used in this study

3.6.4.2 Brunaer-Emmett-Teller (BET) surface area and pore size determination

A BET Micrometrics ASAP 2420 Surface area and porosity was used to analyse the surface area, pore-volume, and pore size distributions of the synthesized catalysts using N_2 sorption isotherm. The surface area of the synthesized materials was calculated using the Brunaer-Emmett-Teller (BET) equation at 0.07-0.28 relative pressure P/P_o. The pore volume was calculated from the amount of nitrogen adsorbed at the highest relative pressure $P/P_o = 0.99$

diameter, and pore size distribution plots were generated by fitting the isotherm to the Barrett-Joyner Halenda (BJH) model.

3.6.4.3 Scanning Electron Microscopy – Energy Dispersive X-ray spectroscopy (SEM-EDX)

A Field Emission Scanning Electron Microscope coupled with EDX was used to examine the surface morphology of the catalysts (PhenomProX). The catalyst was placed on a clean carbon strap attached to a sample holder that fits into the SEM chamber, and some allowance was made to prevent charge build up and the sample from contacting the detector. The secondary electron mode was activated for imaging, and a homogeneous region on the catalyst was identified. The microscope was operated with a high electron tension of 15 kV for both imaging and EDX.

3.6.4.4 X-ray fluorescence analyser

A Xenemetrix Genius IF X-Ray Fluorescence analyser was used to ascertain the elemental and metal oxide compositions of the FKNPH raw material and the produced CKNPH catalysts.

3.6.4.5 Fourier-Transform Infra-Red (FTIR) spectroscopy

The FTIR spectrum was recorded on an ABB Spectra FTIR Spectrophotometer MB 3000.

3.6.4.6 Thermogravimetric Analysis-Differential Scanning Calorimetry (TGA-DSC)

The thermal and energy profiles of the catalysts were investigated using TGA-DSC. To determine the thermal properties of the nanoparticles, a NETZSCH STA 449F3 Simultaneous Thermal Analyzer with a heating rate of 10 K/min in Nitrogen (N_2) atmosphere was used. Thermal analysis detects interatomic and inter-/intra-molecular

interactions caused by an external temperature change. The inert gas was nitrogen, and the oxidative gas was oxygen. The catalysts were then placed in the specimen holder and heated from 30°C to 900°C. Before starting the heating program, the initial weight was set to 100%.

Figure 3.7 Thermal analyser

3.7 Biodiesel synthesis via transesterification

3.7.1 Acid value test

The Acid value is a major determining factor for successful transesterification of triglycerides from seed oil to biodiesel. This is because it is an indicator of the quantity of free fatty acids (FFAs) present in the extracted oil. An idea of the FFAs content of oils would determine the choice of other parameters such as choice of catalyst and reaction conditions

which must be controlled to reduce the likelihood of soap formation (saponification) which adversely affects the yield of biodiesel. In this study, the acid value test was carried out using standard methods reported by Adepoju *et al.* (2018a). Prior to the transesterification reaction, the free fatty acid content was determined to check whether a single step base-catalysed process was appropriate, or an acid pre-treatment step would be necessary. The formation of soap through the saponification reaction that occurs when excess FFAs react with the base heterogeneous catalyst results in lower biodiesel yield. The FFA content of the *Carica papaya* oil (CPO) to be used for the transesterification was determined by calculating the acid value. 1g of the sample was placed in a 250 cm^3 conical flask and warmed. 25 cm^3 of propan-2-ol was added with thorough stirring followed by 2 drops of phenolphthalein indicator. The contents were then titrated with 0.1M KOH solution until a light pink colour, which persisted for 1 minute was observed. The endpoint was recorded and used to calculate the acid value according to Equation.3.4. The %FFA was simply calculated as follows:

$$\%\text{FFA} = \frac{\text{Acid Number}}{2} \quad \text{(Eq. 3.12)}$$

Acid and FFA values for CPO used in this research were obtained as 0.56 mgKOH/g and 0.28% respectively. These values are compliant with EN14214 and ASTM D6751 standards that specifies that the acid value should not exceed 0.5 and 0.8 respectively. In addition, the fact that the FFA values are below 1 wt. %, implies that a single-step alkali transesterification was considered suitable.

3.7.2 Transesterification reaction

Figure 3.8 shows the biodiesel production process. This section describes the transesterification reactions involving the extracted and characterized *Carica papaya* seed oil, the calcined kola nut pod husk catalysts without pretreatment with alcohol designated as

CKNPH A, and the calcined catalyst following pretreatment with methanol designated as CKNPH B. For CKNPH C catalyst, due to funding constraints, the transesterification results were only assessed for CKNPH A and CKNPH B. This decision was necessary because the properties of CKNPH C was quite similar to CKNPH B; moreover, the focus of the research was on preparation of biodiesel rather than catalyst.

The reaction is a stepwise process based on stoichiometry a 3:1 ratio and can be increased to ensure maximum biodiesel conversion. Biodiesel was synthesized by a single alkali transesterification process using the produced catalysts. The reaction was carried out as a batch process in a glass reactor following the conditions set out on Table 3.6. The biodiesel yields were calculated as follows:

$$\text{Biodiesel Yield (\%)} = \frac{\text{Volume of biodiesel produced (ml)}}{\text{Volume of oil used (ml)}} \times 100 \ldots\ldots\ldots\ldots \text{(Eq. 3.13)}$$

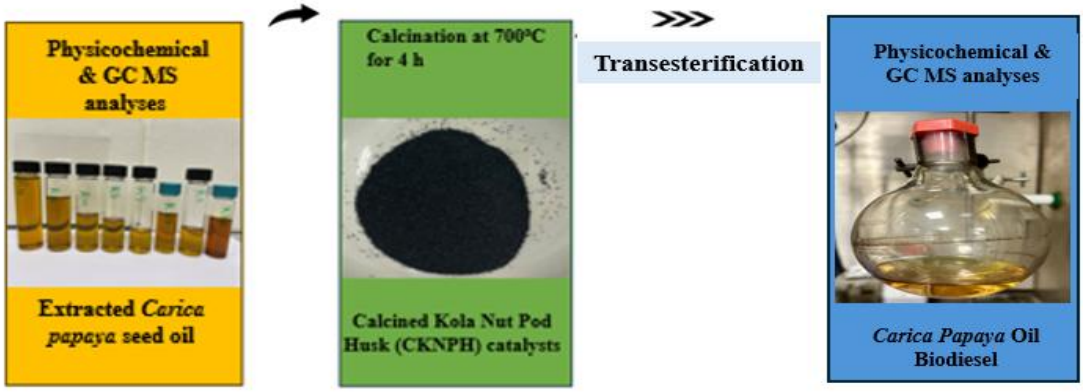

Figure 3.8: Biodiesel production process

3.8 Procedures for the transesterification reaction batch experiments

A similar procedure was employed (Omotola 2011) for the transesterification of sunflower oil to biodiesel. Similarly, in this current study, the transesterification reactions under the laboratory batch experiments were done in a fume cupboard using 100g of the *Carica*

papaya oil samples which were weighed and introduced into a 500ml three necked Pyrex flask as the reactor. The produced green kola catalysts were weighed accordingly between 1.5 – 3.5g and then suspended in the specified amount of methanol after which the mixtures were introduced to the oil in the 500ml reactor reflux flask. To maintain the reaction temperatures between 60 - 80°C, the oil samples were heated on a hot plate fixed with a mechanical stirrer operating at speed of 600rpm. Immediately upon introduction of the catalysts and methanol mixtures into the reactor, the reaction time range of 60 – 80 min was monitored using a timer. After the reaction time had elapsed, the reaction was stopped and allowed to cool under ambient temperature after which the mixture was collected using a suction flask. The mixture was then introduced into a separating funnel and left to stand for 24hrs to ensure proper separation of the biodiesel phase from glycerol. After 24hrs, two clear phases where visible, the methyl esters formed the upper phase while glycerol formed the bottom phase, and these were separated by decanting the biodiesel phase into a flask. To ascertain that the final biodiesel product is devoid of any remaining methanol, glycerol and catalysts, it was washed thoroughly with three volumes of water until it was clear. Lastly, the *Carica papaya* oil biodiesel (CPOB) samples were dried by heating on a heating mantle. These batch processes were carried in duplicate using catalysts CKNPH A and B for comparison and ensure accuracy of the results.

3.8.1 Purification and drying of product

The reaction mixture, which included the catalysts, methanol, and glycerol, were separated by gravity settling with a separating funnel and allowed overnight to allow the biodiesel (polar) and glycerol to separate. The glycerol was extracted from the bottom of the separating

funnel by opening the tap. The final biodiesel products were washed with water to eliminate any contaminants and physically dried with constant heating to 150 ^{0}C.

3.9 Experiment design for biodiesel production

The transesterification experiments were performed using different conditions of reaction time, quantity of catalyst, reaction temperature and methanol/oil molar ratio. Considering the synthesis conditions reported in the literature for an enhanced biodiesel yield, five levels of reaction time (60, 65, 70, 75 and 80 min), quantity of catalyst (1.5, 2.0, 2.5, 3.0 and 3.5g), reaction temperature (60, 65, 70, 75 and 80 ^{o}C) and meth/OMR (4:1, 5:1, 6:1, 7:1 and 8:1) were selected for the study. The responses chosen are active value and percentage biodiesel yield, as reported by Danbaba *et al*. (2015).

Initially, a full factorial design involving 625 experimental runs (5^4 design) with no replication was proposed. However, this number will be too cumbersome and expensive. Therefore, a fractional factorial design (FFD) was adopted for the biodiesel production experiments.

The coded and actual levels of the 5^4 fractional factorial design are presented in Table 3.5, while the experimental matrix of the level combinations of the biodiesel production process conditions for 20 experimental runs of FFD are presented in Table 3.6.

Table 3.5: Five level- four variable- factors experimental design

Variables	Units	Code	Levels				
			1	2	3	4	5
Reaction time	(min)	X_1	60	65	70	75	80
Quantity of Cat.	(g)	X_2	1.5	2.0	2.5	3.0	3.5
Reaction temp.	(°C)	X_3	60	65	70	75	80
MeOH/OMR	-	X_4	4	5	6	7	8

3.9.1 Linear regression model

Table 3.6 shows the coded and actual levels of experimental variables and the resulting responses, which are biodiesel yield and acid values, respectively. The experimental data of mineral yield was analyzed with a linear first-order regression model. The general regression equation of this model is given in Equation 3.2.

The significant changes in oil yield and biodiesel yield content in relation to the changes in the independent variables (x_1, x_2, x_3) are presented in Table 3.6.

Table 3.6: Experimental design matrix for biodiesel production from *C. Papaya* oil

Runs Order	Variables: Reaction time(min)	Catalyst quantity(g)	Reaction temp(°C)	Meth/OMR
1	60	3	60	7:1
2	65	2	70	6:1
3	75	2.5	75	5:1
4	80	2.5	65	8:1
5	80	2	60	4:1
6	80	1.5	75	7:1
7	80	3	80	5:1
8	60	3.5	75	4:1
9	65	3.5	80	7:1
10	75	1.5	60	6:1
11	70	3.5	60	5:1
12	65	3	75	8:1
13	60	1.5	70	5:1
14	70	2.5	70	4:1
15	75	3.5	70	8:1
16	65	1.5	65	4:1
17	75	2	65	7:1
18	60	2.5	80	6:1
19	70	2	80	8:1
20	70	3	65	6:1

3.9.2 Analysis of Variance (ANOVA)

The biodiesel data was statistically analysed using SPSS software (version 26.0).Various procedures, including preparation, transformation, and description of data, hypothesis testing, t-tests, one-way/ two-way ANOVA, cross tabulations, correlation analysis, ordinary least squares regression, discriminant analysis, logistic regression, cluster analysis, factor analysis, reliability analysis, nonparametric tests, general linear models with ANOVA, nested effects, repeated measures and split plot designs, profile analysis, will be done using SPSS.

3.10 Physicochemical and fuel property analysis of the produced biodiesel

The physical, chemical and fuel properties of the produced biodiesel were determined using the same procedures and calculations using Equations 3.3 – 3.9 above.

3.11 GC-MS analysis for FAME profile of *Carica Papaya* Oil Biodiesel (CPOB)

Fatty Acid Methyl Esters (FAME) found in biodiesel derived from *Carica papaya oil* (CPO) were analyzed using the same chromatographic instrument employed for CPO GC-MS analysis for fatty acid composition. Helium gas was chosen as the carrier gas, and the column velocity flow was set to 0.73781 mL/min. The National Institute of Standards and Technology (NSIT) database was used to interpret the mass spectra and identify FAMEs based on their retention indices.

3.12 Biodiesel process simulation and optimization

This section presents the methodology involved in the simulation of biodiesel production from *Carica papaya* seeds oil in the presence of an heterogenous catalyst. AspenPLUS V12 software package was used to simulate the process. Figure 3.9 depicts the process steps in execution of the biodiesel production process in AspenPLUS.

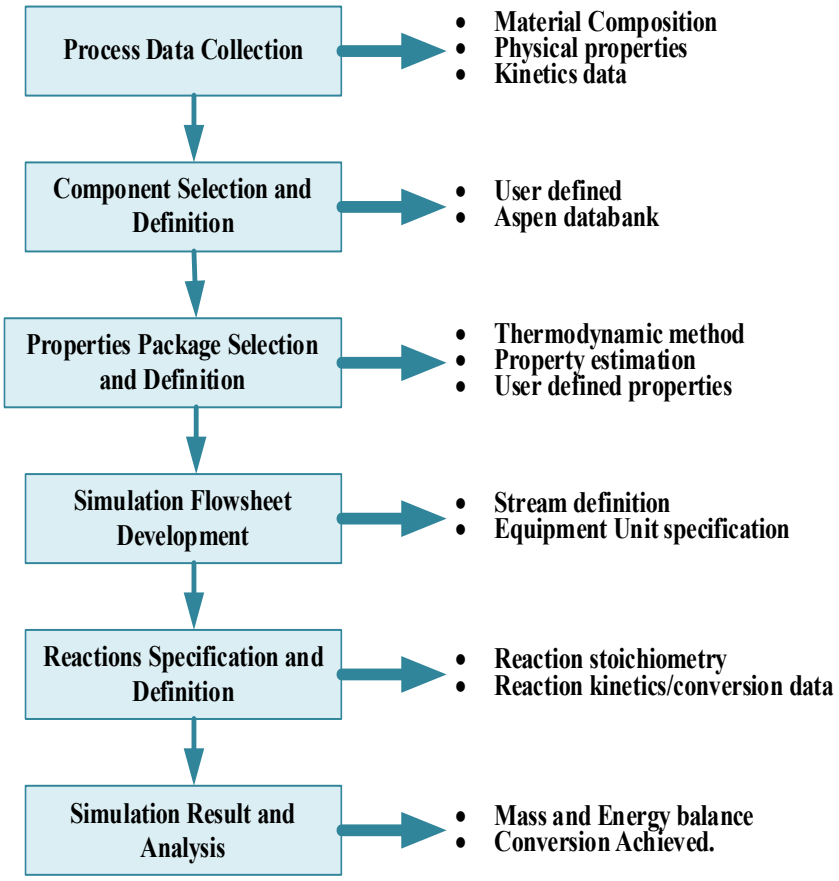

Figure 3.9: AspenPlus simulation process steps

3.12.1 Process data

Process data used in this study are the constituent components of vegetable (*Carica papaya* seeds) oils. The simulation model utilizes the new biodiesel databank which offers physical properties of triglycerides, diglycerides and monoglycerides with kinetic model for transesterification. Table 3.7 presents the reported fatty acid components from GCMS analysis of *Carica papaya* seed oil from this present study.

Since fatty acid of an oil reflects the triglycerides present in the oil, the fatty acid constituents in Table 3.7 are represented in the simulation model by their corresponding triglycerides while the corresponding esters (biodiesel) products are represented as Methyl-Oleate,

Methyl-Palmitate, Methyl-Myristate, Methyl-Linoleate, etc. as major products, with glycerol as a by-product. Table 3.8 presents the components representing the chemical species present in the simulation model.

Table 3.7: Fatty acid profile of CPO

Fatty Acid	% Composition
Palmitic acid	0.27
Oleic acid	64.11
cis-Vaccenic acid	23.35
9-Eicosenoic acid	7.44
Myristoleic acid	4.31
cis-5-Dodecenoic acid	0.52
Saturated Fatty Acid	0.27
Unsaturated Fatty Acid	99.73

Table 3.8: Components used in biodiesel simulation model

Component ID	Component name	Formula
TRIPALM	TRIPALMITIN	$C_{51}H_{98}O_6$
TRIOLEIN	TRIOLEIN	$C_{57}H_{104}O_6$
TRILINOL	TRILINOLEIN	$C_{57}H_{98}O_6$
TRIEICOS	TRIEICOSENIN	$C_{63}H_{122}O_6$
TRILAURA	TRILAURIN	$C_{39}H_{74}O_6$
TRIMYRIS	TRIMYRISTIN	$C_{45}H_{86}O_6$
M-PALMIT	METHYL-PALMITATE	$C_{17}H_{34}O_2$
M-OLEATE	METHYL-OLEATE	$C_{19}H_{36}O_2$
M-LINOLE	METHYL-LINOLEATE	$C_{19}H_{34}O_2$

M-EICOS	METHYL-ARACHIDATE	$C_{21}H_{42}O_2$
M-MYRIST	METHYL-MYRISTATE	$C_{15}H_{30}O_2$
M-DODECA	METHYL-DODECANOATE	$C_{13}H_{26}O_2$
METHANOL	METHANOL	CH4O
GLYCEROL	GLYCEROL	C3H8O3
CATALYST		
WATER	WATER	H2O

The power expression was used for the rate-controlled transesterification reactions in the simulation model according to the Equation 3.14.

$$r = k\left(\frac{T}{T_O}\right)^n exp\left(\frac{E}{RT}\right)\prod_{i=1}^{N} C_i{}^{ai}\left(\frac{1}{T}-\frac{1}{T_o}\right) \quad \text{(Eq.3.14)}$$

Where:

r = Rate of reaction k = Pre-exponential factor

T = Absolute temperature T_o = Reference temperature

n = Temperature exponent E = Activation energy

R = Universal gas constant N = Number of components in the reaction

Ci = Concentration of component i

ai = The stoichiometric coefficient of component i in the reaction equation

In Equation 3.14, the concentration basis is Molarity, the factor n is zero, and k and E are given in Table 3.9, adopted from Narvaez *et al*. (2007). Narvaez *et al.* (2007) just proposed the transesterification kinetics of the oil instead of the individual triglycerides that make up the oil. Hence, it is assumed that the kinetics of all the constituent triglycerides are the same as that for the triglyceride mixture (oil).

Table 3.9: Kinetic parameters

Reaction	k (T_o = 303.15K)	E_a (kcal/mol)
TG → Esters (FAME): Example: TRIPALMITIN + 3 METHANOL + 0 CATALYST → 3 METHYL-PALMITATE + GLYCEROL	0.05754	6.2
Esters (FAME) → TG: Example: 3 METHYL-PALMITATE + GLYCEROL + 0 CATALYST → TRIPALMITIN + 3 METHANOL	0.000267	11.9

Source: Narvaez *et al*. (2007)

3.12.2 Process description

The process simulation model covers the set of chemical species and property parameters used for this process, as well as transesterification, methanol recovery, water washing, FAME purification, catalyst removal, glycerol purification, feed stock recovery and the streams connecting these units. It also covers the reaction kinetics of transesterification, and key process control specifications such as pure methanol to oil flow ratio, phosphoric acid flow rate, and specifications for distillation columns.

The property method used in this biodiesel simulation model is NRTL (Non-Random Two Liquid), because NRTL give more accurate results, though, requires estimation of some NRTL binary interaction parameters (Zong *et al*., 2010). Thermophysical property model parameters of tri-, di-, and even mono-glycerides are currently available in the new biodiesel databank in version 12 and above. It includes vapor pressure, heat of vaporization, ideal gas

heat of formation, ideal gas heat capacity, liquid heat capacity, liquid molar volume and liquid viscosity. The study considers a flow basis of 1000 kg/hr oil flow rate.

CPO at 25 ^{o}C and 1 atm is pumped via PUMP-1 to deliver a discharge pressure of 3 bar, prior to heating to 60 ^{o}C at constant pressure in HEATER-1. Similar, equivalent methanol flow rate at a methanol to oil molar ratio of 4:1 (optimum determined experimentally) and a CKNPH-A catalyst equivalent of 2.5% oil weight were mixed and then pumped via PUMP-2 into the transesterification reactor, REACTOR, alongside the CPO from HEATER-1. The reactor utilized is a CSTR reactor and operates at the optimum condition experimentally determined. The reactor operates at 70 ^{o}C, with a constant pressure of 3 bars and a reaction residence time of 70 min. The reactor product (R-PROD) is sent into a filter, FILTER, where the heterogenous CKNPH-A catalyst is filtered out at constant pressure of 3 bar and separated from the reactor product as R-PROD1. The filtrate (R-PROD1) from the filter is then sent into the methanol recovery column, MEOHCOL, where excess unconverted methanol is vaporized and separated from the heavier component (esters, glycerol and residual CPO) under vacuum operation.

The heavier component (ester, glycerol and residual CPO) from the bottom of MEOHCOL is then pumped via PUMP-3 to give an outlet pressure of 2 bar and then enters through cooler, COOLER-1, where the temperature is reduced to 60 ^{o}C prior to entering the settling column, SET-TK. The catalyst free mixture is separated into two layers, one rich in biodiesel (esters) at the top and heavy glycerol layer at the bottom at constant inlet operating condition to give a high purity glycerol product of 99.99wt.%. The esters rich layer from the settling column, SET-TK enters a distillation column, ESTE-COL, where unconverted CPO is separated from the biodiesel product to obtain high purity biodiesel product of 99.97 wt.%.

Figure 7.1 presents the process simulation flow diagram of the heterogenous base-catalyzed transesterification process of biodiesel production from CPO.

The CPO conversion and biodiesel yield were estimated from the equation below:

$$\text{Conversion} = \frac{\sum \text{Mole of Triglycerides}_{\text{feed}} - \sum \text{Mole of Triglycerides}_{\text{product}}}{\sum \text{Mole of Triglycerides}_{\text{feed}}} \quad \text{(Eq.3.15)}$$

$$\text{Yield} = \frac{\sum \text{Mass of Esters}_{\text{product}}}{\sum \text{Mass of Triglycerides}_{\text{feed}}} \text{ x } 100 \quad \text{(Eq.3.16)}$$

3.12.3 Cost estimation and economic analysis

The biodiesel capital investment (CAPEX) and operating cost (OPEX) were estimated using Aspen Process Economic Analyzer (APEA) while raw material, revenue and project cash flow and economic analysis were performed in Microsoft Excel (2019). The profitability of the biodiesel production process was determined based on the payback period (PBP), return on investment (ROI), Internal Rate of Return (IRR), Profitability Index (PI) and Net Positive Value (NPV).

Chapter 4

Carica Papaya Oil (CPO) properties, fatty acid composition and optimization of reaction variables

4. Introduction

This chapter presents and discusses the fatty acid composition and physicochemical characteristics results of the extracted *Carica papaya* seed oil which was used for the synthesis of biodiesel in this research. This chapter also focuses on the impacts, validation and optimization of reaction variables on CPO oil yield. Finally, the physicochemical and fuel properties of the extracted oil are discussed and compared to EU and US standards for biodiesel to determine the oil's suitability for transesterification.

4.1 Fatty acid composition of *Carica papaya* oil sample

The fatty acid profile of the extracted *Carica Papaya* seed oil was analyzed, and the quantified values are detailed in Table 4.1.

Table 4.1: Fatty acid composition of *Carica Papaya* seed oil

Fatty Acid	Lipid Number	% Composition
Palmitic acid	C16:0	0.27
Oleic acid	C18:1	64.11
cis-Vaccenic acid	C18:1	23.35
9-Eicosenoic acid	C20:1	7.44
Myristoleic acid	C14:1	4.31
cis-5-Dodecenoic acid	C12:1	0.52
Saturated Fatty Acid	-	0.27
Unsaturated Fatty Acid	-	93.88

Table 4.1 revealed that the oil is predominantly composed of unsaturated fatty acids, comprising 93.88% of the total composition, while saturated fatty acids, represented as palmitic acids constitute 0.27%.

Specifically, the dominant fatty acid identified was in order as: oleic acid at 58.26%, followed by cis-Vaccenic acid (23.35%), 9-Eicosenoic acid (7.44%), Myristoleic acid (4.31%), and cis-5-Dodecenoic acid (0.52%). These results align with established patterns of fatty acid distribution as reported in literature references (Babatunde *et al*., 2019; Devi and Khanam, 2019).

The notable prevalence of unsaturated fatty acids over saturated ones indicates that the oil is less prone to solidification, making it conducive potentially for applications in engines, where a liquid state is preferable (Agunbiade and Adewole, 2014). To produce high-quality biodiesel or bio lubricants, the number of fatty acids, especially oleic acid present in oil, is quite important (Hossain *et al*., 2020). High levels of oleic acid make the oil more resistant to oxidation and hence suitable for processes requiring high oxidative stability at high temperatures as in biodiesel and bio lubricants applications (Balat, 2011).

4.2 Physicochemical and fuel properties of extracted *Carica papaya* seed oil

To evaluate its suitability for the synthesis of biodiesel, it is critical to identify *Carica papaya* oil's physical, chemical, and other fuel qualities. Table 4.2 displays the physical and chemical characteristics of *Carica papaya* seed oil as determined by standard methods (AOAC 1997) and Wij's method (Adepoju *et al*., 2020).

The extracted oil was liquid at room temperature and had a yellowish hue. According to Sim *et al*. (2020), colour plays a significant role in handling and processing applications and can

provide an initial insight into the oil's purity and processing conditions. Figure 4.1 show some samples of the Waste carica Papaya Oil (WCPO) extracted in this current research.

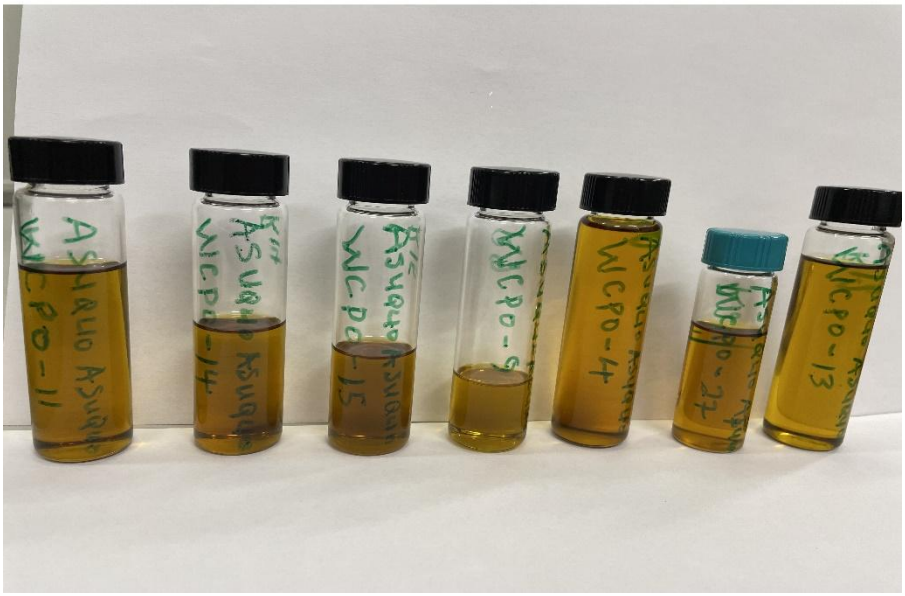

Figure 4.1: Some samples of waste CPO lab extractions

Table 4.2: Physical, Chemical and fuel properties of Carica papaya oil extracted

Parameters	CPO
Physical properties:	
Physical state at 25°C	Yellowish in colour
Moisture content (wt.%)	0.0012
Specific gravity at 25°C	0.86
Density (g/cm^3)	0.85
Dynamic viscosity (mPaS)	9.9
Kinematic viscosity (mm^2s^{-1})	11.56
pH	5 – 5.5
Chemical properties	
%FFA (Oleic acid)	0.2869
Acid value (mg KOH/g oil)	0.57
Saponification value (mg KOH/g oil)	61.71

Iodine value (gI_2/100g oil)	59.39
Peroxide value (meq O_2/kg oil)	Not detected
Calorific value (MJ/kg)	47.85
Fuel properties	
Cetane Number	121.38
API	33.61
Diesel Index	154.69
Aniline point℃	237.92

4.2.1 Iodine value

The degree of unsaturation of oils can be inferred from their iodine value (Nduka *et al.,* 2021). According to Maliki and Ifijen (2020), higher unsaturation levels are associated with higher iodine values. The Iodine value was determined to be 59.3892 gI2/100g. This value is higher than that reported by Abubakar *et al*. (2020), Oyelaran *et al*. (2020) and Adeleke *et al*. (2023) for *Carica papaya* seed oil. This finding reveals that the oil is highly unsaturated, non-drying, and has a high oleic acid content (Gbonjubola *et al*., 2023).

4.2.2 Acid value

The acid value, which is a measure of free fatty acid content due to enzymatic activity, was found to be 0.57%. The oil has a comparatively low acid value. Oil with low acidity is safe to consume (Jimenez-Lopez *et al*., 2020). Acidity levels of less than 0.1mgKOH/g are typically ideal. Due to its strong acidity, the oil extracted from *Carica papaya* seeds is unfit for human consumption. It can, however, be used as a feedstock for vegetable oil-based chemicals like biodiesel (Evwierhoma and Ekop, 2016). This acid value indicates a high resistance to hydrolysis, which is required for successful transesterification to biodiesel (Senrayan and Venkatachalam 2020; Asuquo *et al*., 2021). The acid value found in this study

is lower than that reported in the literature for *Carica papaya* seed oil (Oshin *et al*., 2021; Oguntoye *et al*., 2023).

4.2.3 Moisture content

The moisture content of the *Carica papaya* seed oil was determined to be 0.0012 wt. % (Table 4.2). Compared to the moisture content of *Carica papaya* seeds reported in the literature (Oshin *et al*., 2021; Tagarda *et al*., 2023; Salsabila and Broto, 2023), this moisture content is comparatively low. During transesterification, a high moisture content in the vegetable oil feedstock might cause soap formation (Chanakaewsomboon *et al*., 2021; Ahmed Elgharbawy, 2021). Moisture content affects oil yield, viscosity, specific gravity and iodine value as revealed in Table 4.2. Viscosity will decrease with increase in moisture content. The specific gravity which is the density of substance to that of water will also increase with increase in moisture content. The higher the moisture content the lower the iodine value (Adejumo *et al*., 2013). The oil's low moisture content will improve biodiesel production due to increased oil yield that gives higher conversion possibilities to biodiesel (Adepoju *et al*., 2018; Udoetuk *et al*., 2018; Adepoju *et al*., 2018a; Adepoju *et al*., 2020).

4.2.4 Saponification value

Saponification value is a measure of oxidation during storage and shows oil deterioration (Zhang *et al*., 2021). An increase in saponification value in oil enhances its volatility. It improves the oil's quality since it demonstrates that 1 g of the oil contains lower molecular weight components, which when burned, will provide more energy (Aremu *et al*. 2015). On the other hand, a lower saponification value suggests that the glycerol backbone of a sample contains long-chain fatty acids (Ivanova *et al*., 2022). Table 4.2 reveals a high saponification

value of 61.71 mg KOH/g. Notably, triacylglycerols with substantial unsaturation are indicated by a high saponification value (Ivanova *et al*., 2022).

4.3 Physicochemical and fuel properties of oil compared with EU and US standards for biofuels

The physicochemical and fuel properties were obtained and compared with the US and EU biofuel standards as presented in Table 4.3. The oil extracted was liquid and yellowish in colour with moisture content of 0.0012 wt. %. It is widely acknowledged that a low moisture content of the oil will give a better conversion to biodiesel (Adepoju *et al*., 2018) The results show that the value obtained for moisture content is similar and better than that obtained by Adepoju *et al* 2018, who reported a moisture content of 0.013 wt. %. The moisture content of the waste *Carica papaya* oil **(**WCPO) is within the range specified by ASTM D6751 and EN 14214, which recommends a value less than 0.03% and 0.02% respectively. The specific gravity of WCPO (0.857) falls within the range specified by ASTM D751, and the density of 0.854 g/cm^3 agrees with EN 14214 specification. The percentage FFA and acid values of the oil were observed to be 0.2 wt. % and 0.5 mg KOH/g respectively. These results indicate high resistance to hydrolysis which is desirable for the successful transesterification of oil to biodiesel (Adepoju *et al.,* 2018). The peroxide value which is an indication of the presence of hydroperoxides in the oil was not detected and this is a good sign that the oil has a high resistance to oxidation. A high saponification value of 61.71 mg KOH/g and high Iodine value of 59.39 gI_2/100g, shows a bare minimum percentage of triglycerides of oil with significant level of unsaturation. The high HHV of 47.852 (MJ/Kg) is close to 47.312 (MJ/Kg) calculated for *Thevetia Peruviana* oil for biodiesel production (Adepoju *et al* 2018). The higher the HHV of the oil, the more suitable the oil is for use as a biofuel. The value of

47.852 (MJ/kg) obtained from this study indicates that the WCPO is a good raw material for biodiesel production. The cetane number of 121.38 of WCPO was computed which is much higher than the biofuel standard with a minimum value of 40, indicating its fuel ignition delay and combustion quality. The API, aniline point, and diesel index of WCPO were computed (Adepoju *et al* 2018).

Table 4.3: Physicochemical properties of Carica papaya oil as compared with literature on other seed oils

Parameters	Present study	Senrayan & Venkatachlam (2020)	DeMelo & Sousa (2016)	Yanty *et* al. (2014)	Adepoju *et al*. (2020)	Adepoju *et al*. (2018)	Adepoju et al.(2018a)	Adepoju *et al*. (2018)	Adepoju *et al*. (2018)
Density(g/cm^3)	0.85411	0.45	n. d	n. d	n. d	0.9804	-	0.84	0.86-0.90
Specific gravity	0.857	0.879	0.900	n. d	0.9190	n. d	0.8984	0.85	0.913
Moisture content (%)	0.0012	-	-	-	2.6	0.0011	0.0131	Less than 0.03	0.02
Dynamic viscosity (mPaS)	9.9	-	-	-	n. d	-	-	-	-
Kinematic viscosity (mm^{2}s^{-1})	11.56	-	-	-	4.2	-	-	-	-
%FFA (as oleic acid)	0.2869	1.29	n.d*	1.4	7.64	2.3175	1.9024	Less than 0.40	0.25 max
Acid value (mg KOH/g oil)	0.56555	2.52	1.03	n. d	15.28	4.6350	3.8048	Less than 0.8	0.5 max
Saponification value (mg KOH/g oil)	61.71	187.30	189.98	193.5	198.60	75.2500	57.5025	-	-

Iodine value (g I_2/100g oil)	59.3892	70.90	70.45	76.8	124.80	87.6000	97.600	-	120 max
Peroxide value (meq O_2/kg oil)	Not detected	-	-	-	20.00	33.6000	23.800	-	-
Higher Heating Value (MJ/kg)	47.85	-	-	-	39.44	45.3588	47.056	-	-
Cetane Number	121.38	-	-	-	45.70	99.1216	140.998	-	-
API	33.61	-	-	-	22.47	12.8289	26.00	36.95	-
Diesel Index	154.69	-	-	-	49.58	123.78	181.94	50.4	-
Aniline Point (^{0}F)	460.25	-	-	-	220.64	964.8566	699.77	331	-

4.4 Optimization of reaction variables

StatEase Design Expert software (version 13) was used to analyse the experimental design matrix. Table 4.4 shows the optimization process results obtained from Response Surface Methodology (RSM) model.

Table 4.4: Experimental and predicted oil yield using RSM custom factorial design

Run	Sample weight (g)	Solvent volume (ml)	Extraction time (min)	Experimental oil yield (%)	Predicted oil yield (%)
1	70	300	55	25.04	24.73
2	60	250	75	18.39	18.45

3	50	250	75	23.47	23.04
4	70	300	65	29.13	28.69
5	50	300	65	28.9	28.98
6	50	250	55	18.06	17.90
7	70	350	65	25.33	25.53
8	70	250	55	18.72	18.83
9	60	250	55	14.21	14.53
10	50	300	55	23.73	23.80
11	50	350	75	25.45	25.78
12	70	250	75	21.52	21.53
13	60	350	75	21.58	21.19
14	70	300	75	27.23	27.43
15	60	300	55	20.47	20.43
16	70	250	65	22.7	22.79
17	60	350	65	21.79	21.84
18	60	350	55	17.55	17.27

19	50	250	65	23.06	23.08
20	70	350	55	21.33	21.57
21	60	300	65	24.89	25.00
22	70	350	75	24.36	24.27
23	60	300	75	24.18	24.35
24	60	250	65	19.1	19.10
25	50	300	75	28.8	28.94
26	50	350	55	20.59	20.64
27	50	350	65	25.91	25.82

The oil yield ranged from 14.21% to 29.13 %. The optimum yield within the range was observed to be 29.13%, which was achieved at a sample weight of 70 g, solvent volume of 300 ml and at an extraction time of 65 minutes.

The model estimated response (predicted oil yield) was close to the experimental data for the system. Meanwhile, the residual values which depicted the difference between the predicted and the actual experimental yields was negligible, indicating a good fit of the model adopted for the design.

4.5 Model fitting and adequacy testing

Linear, two-factor interaction and quadratic polynomial model equations were used to fit the response of the experiment to select the best model. This is shown in Table 4.5.

Table 4.5: Model evaluation for best fit

Source	Sum of Squares	df	Mean Square	F-value	p-value	Adjusted R^2
Linear Model	103.31	3	34.44	3.07	0.0480	0.1928
2FI *Model	4.53	3	1.51	0.1190	0.9478	0.0880
Quadratic Model	252.36	3	84.12	1257.94	< 0.0001	0.9952

*2FI means Two factor Interaction

The Linear, two-factor interaction, and quadratic polynomial equations were used to fit the response of the experiment. When the fit for each model was compared, the quadratic model was selected as the best model. It was selected due to its highest order polynomial with highest F value, lowest P-value and highest adjusted R^2 value as shown in Table 4.5. Table 4.6 shows the result of a statistical analysis of variance (ANOVA). It determines the significant fitness of the quadratic model as well as the effect of individual terms and their interaction on the *Carica papaya* oil yield. The level of significance and adequacy of the generated model was assessed by ANOVA, considering the p-value. Generally, the model terms with p-value less than 0.05 are significant. The larger the magnitude of F-value and smaller the magnitude of p-value, the higher will be the significance of the corresponding coefficient (Obika *et al*.,2020; Singh and Tirkey, 2022). The F-value for the model was high ($F = 815.67$) with a very low probability ($p < 0.0001$), which indicates the very high significance of the model. The significance of each term was investigated by their respective p-values. In the model, all the linear terms (sample weight (A), solvent volume (B) and extraction time (C), two-way interactions (AC) and all the quadratic terms (A^2, B^2 and C^2) were statistically significant and considerably affected the extraction yield to determine the

fitness of the model, the value of regression coefficient R^2 for the model is 0.9967. The high value of R^2 indicates the capability of the model to satisfactorily describe the system within the range of parameters that were investigated (Sulaiman *et al.,* 2024). The model exhibited a high adjusted and predicted R^2 values of 0.9955 and 0.9932 respectively as shown in Table 4.6. The predicted R^2 value shows that this model performs well on new data. Also, it is worthy to note that the higher the value of the adjusted coefficient of determination, the more the significant the fitted model (Rahman *et al*., 2020). In this study, the coefficient of determination (R^2) is higher than the adjusted coefficient (adjusted R^2) which shows that the fitted model is significant. The predicted sum of squares (PRESS) is 2.46. This low value of PRESS suggests that the model has good predictive accuracy.

Table 4.6: Test of significance and Analysis of Variance (ANOVA) for all regression coefficient terms for oil extraction from Carica papaya seed

Source	Sum of Squares	df	Mean Square	F-value	p-value	
Model	360.14	7	51.45	815.67	<0.0001	significant
A-Sample Weight	0.3785	1	0.3785	6.00	0.0242	
B-Solvent Volume	33.78	1	33.78	535.62	<0.0001	
C-Extraction Time	69.15	1	69.15	1096.29	<0.0001	
AC	4.47	1	4.47	70.79	<0.0001	
A^2	88.19	1	88.19	1398.21	<0.0001	
B^2	123.37	1	123.37	1955.87	<0.0001	
C^2	40.80	1	40.80	646.89	<0.0001	
Residual	1.20	19	0.0631			

Cor Total	361.34	26
Fits Statistics		
R^2	0.9967	
Adjusted R^2	0.9955	
Predicted R^2	0.9932	
Adeq Precision	105.7082	
PRESS	2.46	
BIC	18.89	
AICc	16.52	

4.6 Impact of reaction variables on oil yield

The surface and contour plots were used to establish the interactions between the parameters and their effect on oil yield. Figure 4.2 shows the yield intensity guide for the extracted CPO and produced biodiesel from this research. The interaction of extraction time and sample weight on *Carica papaya* oil yield is presented in Figure 4.3 and Figure 4.4 for surface and contour plots respectively.

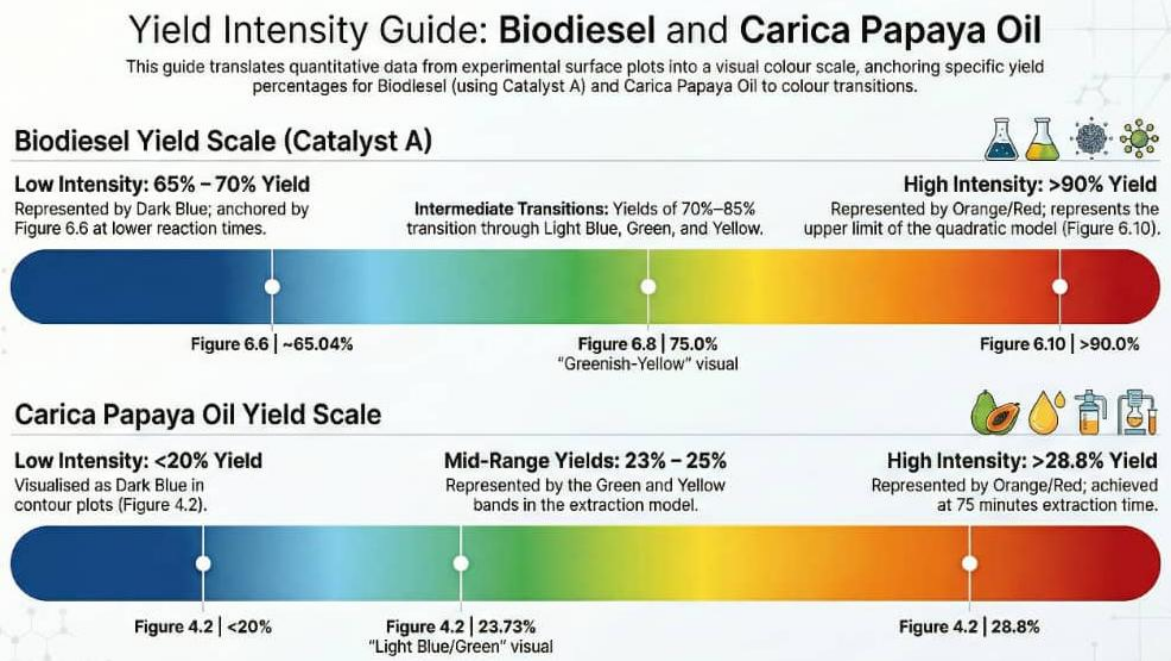

Figure 4.2: Yield intensity guide for biodiesel and CPO

Figure 4.3 shows the interactive effect of sample weight and time of extraction on oil yield. The oil yield increases as extraction times increases. As extraction time increased from 55 minutes to 75 minutes, the oil yield also increased from 23.73% to 28.8 %. Maximum yield was achieved at 75 minutes (28.8%). This trend agrees with the contour plot (Figure 4.4) whereas extraction time increased from 55 minutes to 75 minutes, there was a corresponding increase in the oil yield.

Also, it can be observed that as sample weight increased from 50 g to 60 g, there was initial decrease in oil yield 23.73% to 20.47%. Increasing the sample weight beyond 60 g resulted in a corresponding increase in oil yield from 23.73% to 25.04%. Maximum yield was achieved at 25.04% (70 g). The initial decrease in the oil yield as the sample weight increases may be due to random errors. However, the overall increase of the extracted oil with sample weight is due to the increase of the starting material (C. papaya seeds) as would be expected.

The contour plot (Figure 4.4) also corroborates this trend where increase in sample weight resulted in a corresponding increase in oil yield.

Its worthy to note that the contour plot reveals elliptical curves which signify that the interaction between the extraction time and sample weight is significant ($p < 0.0001$) as shown in the ANOVA quadratic model (Table 4.6), hence will have effect on the response (oil yield).

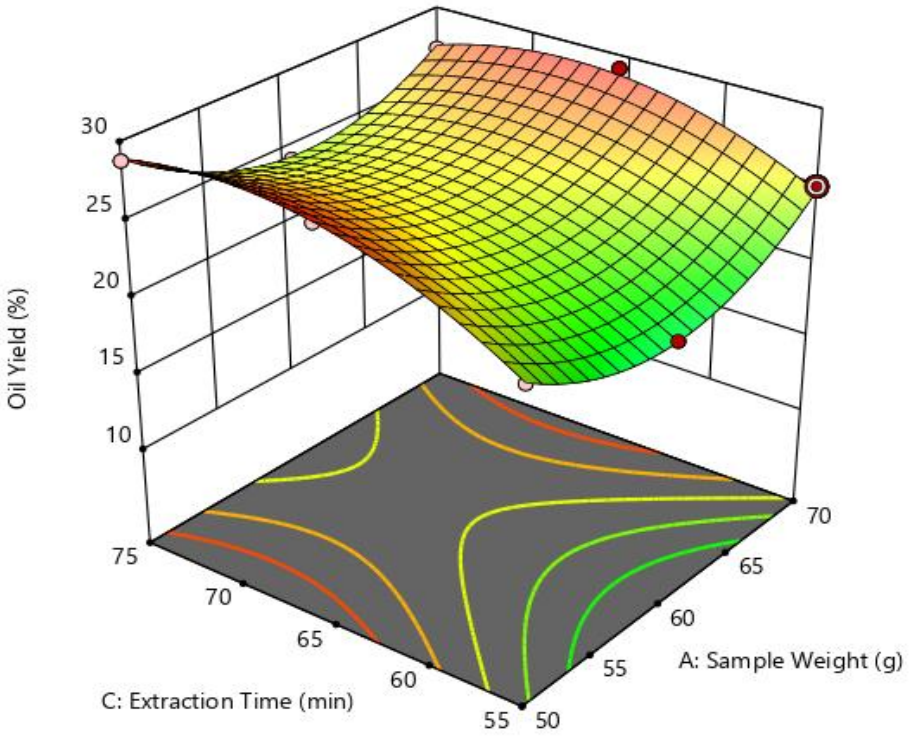

Figure 4.3: 3-D surface plot showing combined effect of extraction time and sample weight on *Carica papaya* oil yield

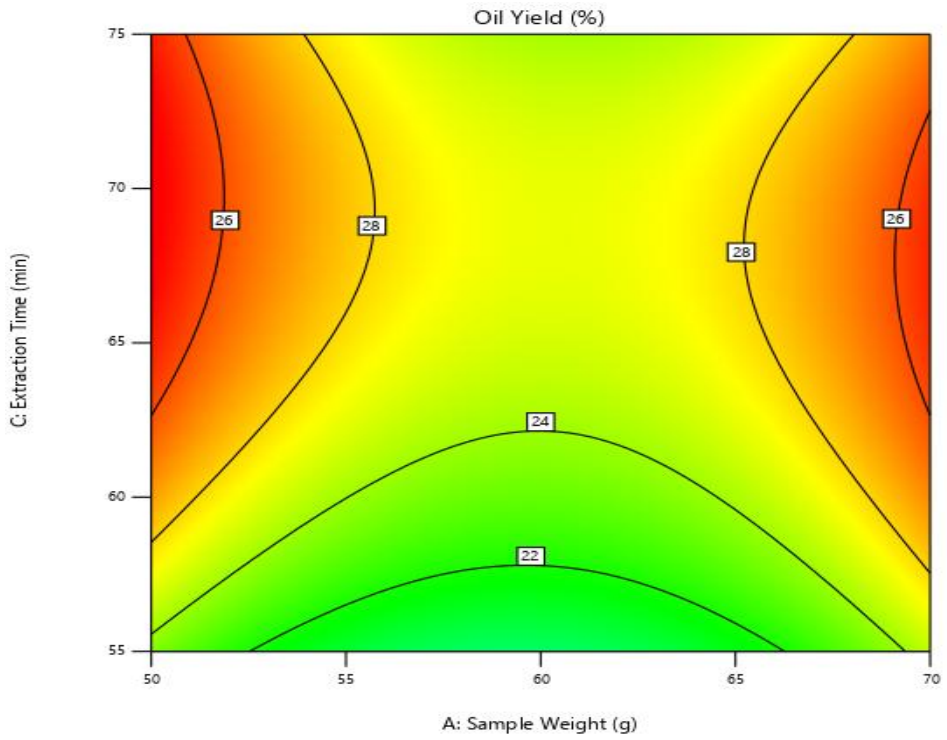

Figure 4.4: Contour plot showing combined effect of extraction time and sample weight on *Carica papaya* oil yield

Figure 4.4 shows the interactive effect of sample weight and time of extraction on oil yield. The oil yield increases as extraction times increases. As extraction time increased from 55 minutes to 75 minutes, the oil yield also increased from 23.73% to 28.8 %. Maximum yield was achieved at 75 minutes (28.8%). This trend agrees with the contour plot (Figure 4.3) whereas extraction time increased from 55 minutes to 75 minutes, there was a corresponding increase in the oil yield.

Also, it can be observed that as sample weight increased from 50 g to 60 g, there was initial decrease in oil yield 23.73% to 20.47%. Increasing the sample weight beyond 60 g resulted in a corresponding increase in oil yield from 23.73% to 25.04%. Maximum yield was achieved at 25.04% (70 g). The contour plot (Figure 4.3) also corroborates this trend where increase in sample weight resulted in a corresponding increase in oil yield.

Its worthy to note that the contour plot reveals elliptical curves which signify that the interaction between the extraction time and sample weight is significant ($p < 0.0001$) as shown in the ANOVA quadratic model (Table 4.6), hence will have effect on the response (oil yield).

4.7 Regression Equation

The regression equation that defines the experimental correlation is demonstrated by the quadratic equation (Equation 4.1).

$$\text{Oil Yield} = 25 - 0.1450\,\text{A} + 1.37\,\text{B} + 1.96\,\text{C} - 0.6100\,\text{AC} + 3.83\,A^2 - 4.53\,B^2 - 2.61C^2 \quad \ldots\ldots (4.1)$$

Where the term A is the sample weight, B is the solvent volume and C is the time of extraction.

The equation shows the coefficient of the full regression, numerical significance and the exact impact of each model expression on the *Carica papaya* oil yield.

The positive and negative sign before each term shows synergistic or antagonistic effect respectively. The solvent volume, time of extraction and square of sample weight has synergistic effect on the oil yield. This suggests that an increase in solvent volume and time of extraction will improve oil yield. Also, the synergistic effect of the sample weight itself (A^2) shows that when the sample weight is increased to a certain (higher) level, it will improve the oil yield.

On the other hand, sample weight, interaction between sample weight and time of extraction, square of solvent volume and square of extraction have antagonistic effects on the oil yield (Matthew *et al*., 2015). This implies that when the sample weight (A) is increased, it will lead to a decrease in the oil yield. Also, when both sample weight and time of extraction are

increased together (AC), the resulting effect will be a decrease in the oil yield than when they are increased independently. Also, at higher levels of solvent volume (B^2) and extraction time (C^2), there will be a decrease in the yield of the oil.

4.8 Validation of predicted optimum conditions

Figure 4.5 and 4.6 shows the normal plot of residuals and the predicted vs actual plots which were used confirm the validity of the model predicted by regression analyses.

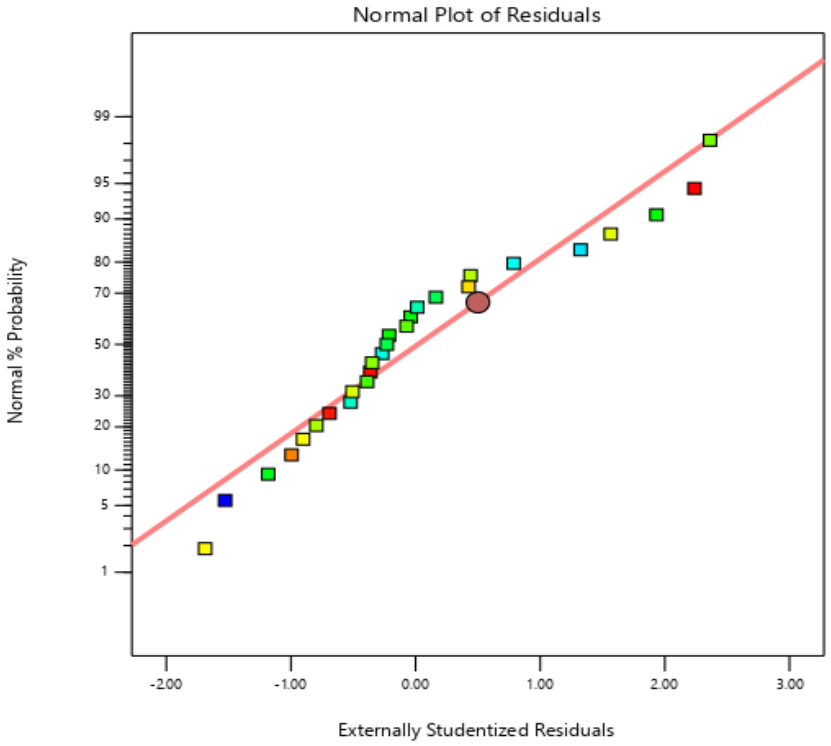

Figure 4.5: Normal probability plot of residuals of *Carica papaya* oil

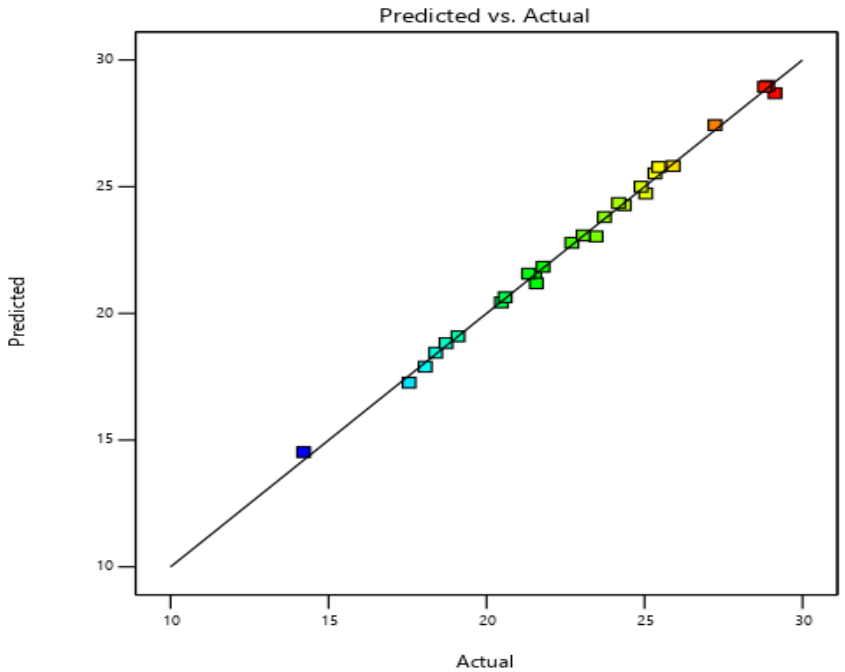

Figure 4.6: Plot of experimental oil yield versus predicted oil yield

A straight line was observed that passed through the origin with nearly all points indicating that the residual values known as an error, are so small to be neglected (Figure 4.5). The close distributions of the points along the straight lines indicate the excellent relationship between the experimental and predicted values of the response (Figure 4.6). These plots validate that the chosen model was sufficient for prediction of the response variables in the experimental values.

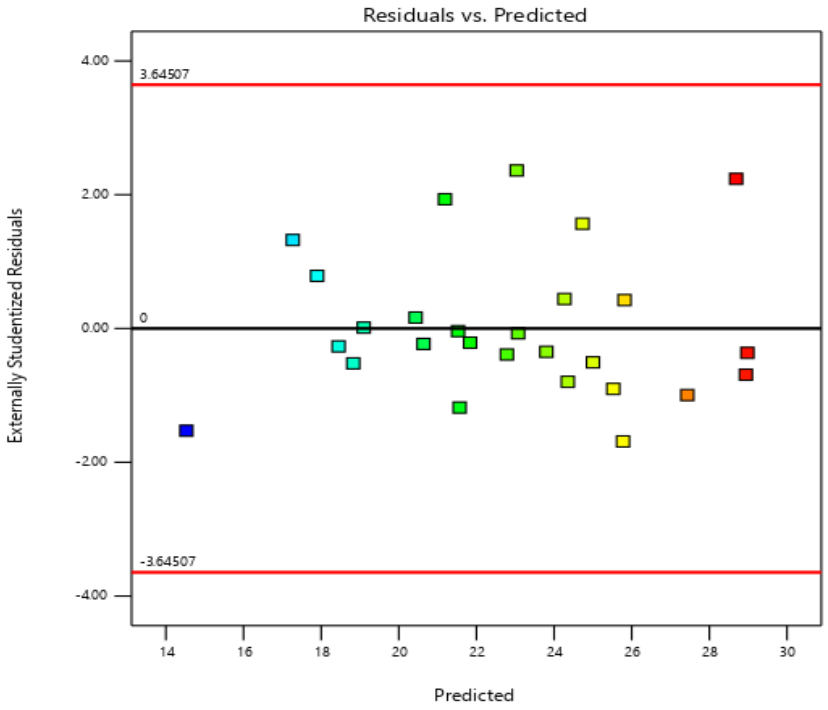

Figure 4.7: Plot of residuals versus predicted response

Figure 4.7 shows the plot of residuals versus predicted response. The scatter plot suggests the minimum value of residual for predicted data. Most of the standard residuals should lie in the interval of ± 3.65. Any observation outside this interval renders an operational error in the experimental data or a potential error in the model (Nayak and Viyas, 2018). The plot shows that all the standard residuals lie within the interval of ± 3.65 thereby validating the selected model.

4.9 Chapter summary

The results of the physicochemical characterization of the extracted *C. papaya* oil have been reported. The oil was observed to be predominated by unsaturated fatty acids with a value of 93.88 %. The dominance of unsaturated fatty acids implies that the oil is less prone to solidification which is highly desirable for this process. Also, this result was confirmed by the iodine value of 59.38 $gI_2/100g$ which is indicative of a high level of unsaturation. Among the different unsaturated fatty acids (UFAs), oleic acid was observed to be the predominant UFA in the oil. Also, the oil showed high acidity values which suggests that it is inedible.

It is important that the feedstock that would be employed for transesterification be unsuitable for consumption so that there will be no competition between its usage as a raw material for biodiesel production and its usage as a food ingredient. Besides, the low moisture content when compared to other reports in the literature is suggestive of a reduced possibility of soap formation which will result in improved yield of biodiesel. The cetane values, specific gravity and other physicochemical parameters were within the specified limits according to ASTM D6751 and EN 14214 standards which indicates compliance with regulations.

Statistical analysis of the effects of the parameters with respect to the oil yield indicates that all the studied parameters have some effects on the final yield of the oil. The quadratic model showed the highest correlation coefficient of 0.99 compared to the linear and the two factor interaction models. This suggests a multiple parametric effects on the oil yield rather than a single linear relationship between each parameter and the yield of oil.

Chapter 5

The Synthesis and properties of catalysts for biodiesel production

5. Preamble

The yield of catalysts as well as its physicochemical properties such as elemental composition, presence of relevant functional groups, crystallinity, porosity, surface area, among others, are important parameters that determine the effectiveness of the catalysts for its intended application. In this chapter, the yield of catalysts, as well as the results obtained from the investigation of these physical, chemical, and thermal characteristics are presented and discussed. The objective is to assess how these catalysts could be deployed for the conversion of waste *C. papaya* oil to biodiesel as well as what modifications could be made to enhance the efficiency of this conversion. The key characterization techniques and equipment used in this study for the characterization of the fermented kola nut pod husk (FKNPH) feedstock and the calcined kola nut pod husk catalysts (CKNPH A, B and C) were carried out using BET analysis, Fourier transform infrared spectroscopy (FTIR), Powder X-ray diffraction (PXRD), scanning electron microscopy-energy dispersive X-ray (SEM-EDX) and Thermogravimetric Analysis/ Differential Scanning Calorimetry (TGA/DSC) analyses. These results will help to establish the suitability of the catalysts for biodiesel production.

5.1 Catalysts' yield

The yield of a catalyst is a measure of the quantity of a catalyst that can be obtained from a certain quantity of feedstock. In this study, the feedstock used was kolanut pod husk and the entire process of converting the feedstock to the desired product has already been provided in the previous chapter. The results showing the catalyst yield in relation to the quantity of feed stock used are presented in Table 5.1. Figure 5.1 shows the pictures of the Calcined Kola Nut Pod Husk Catalysts (CKNPH) A, B and C.

Figure 5.1: Calcined Kola nut pod husk catalysts A, B and C produced in this current research.

Table 5.1: Catalysts' yield

CKNPH catalyst	(W_1) Wt. of sample before calcination (g)	(W_2) Wt. of catalysts after calcination (g)	Yield (%)
A	10	0.9558	11.95
B	10	0.5825	7.28
C	10	0.6847	6.85

Prior to discussing the yield of the catalysts, it is important to be reminded of the key modifications that were carried out which were labelled as CKNPH-A, B and C as shown in Table 5.1. CKNPH-A refers to the calcined kolanut pod husk. There was no further treatment on this sample apart from calcination of the raw material which was carried out at 700 ^{o}C. Also, CKNPH-B refers to the calcined kolanut pod husk with further treatment with methanol to wash off organic impurities, while CKNPH-C refers to the calcined material which was sieved to remove the ash using a sieve with aperture size of 212 µm.

The results indicate that CKNPH-A has the highest yield of 11.95%. This is as expected as no additional treatment that reduces its composition was carried out. On the other hand, CKNPH-B and CKNPH-C showed relatively lower yields of 6.85% and 7.28% respectively. The reduction in the yield is suggestive of the fact that organic impurities were washed off when treatment with methanol was carried out for CKNPH B and the reduction in the ash content in the case of CKNPH-C. To assess the composition of the calcined materials, an in-depth analysis was necessary which is presented and discussed in the subsequent sections.

5.2 X-ray fluorescence analysis

X-ray fluorescence (XRF) spectroscopy is an analytical technique that is employed to reveal the elemental composition of materials. This is achieved when x-rays are incident on a sample of unknown composition, and the resulting emitted rays are analyzed. Each emission at specific energy is characteristic of an element, and the intensity of the emitted rays is related to the concentration of the element responsible for the emission. Therefore, this allows for both identification and quantification of the elements. In this study, x-ray fluorescence spectroscopy was employed to assess both the elemental composition and its concentration in the three different forms of the calcined catalysts (CKNPH: A-C) and the results were compared with the fermented kola nut pods feedstock (FKNPH) as a control. The results of these investigations are shown in Figure 5.2.

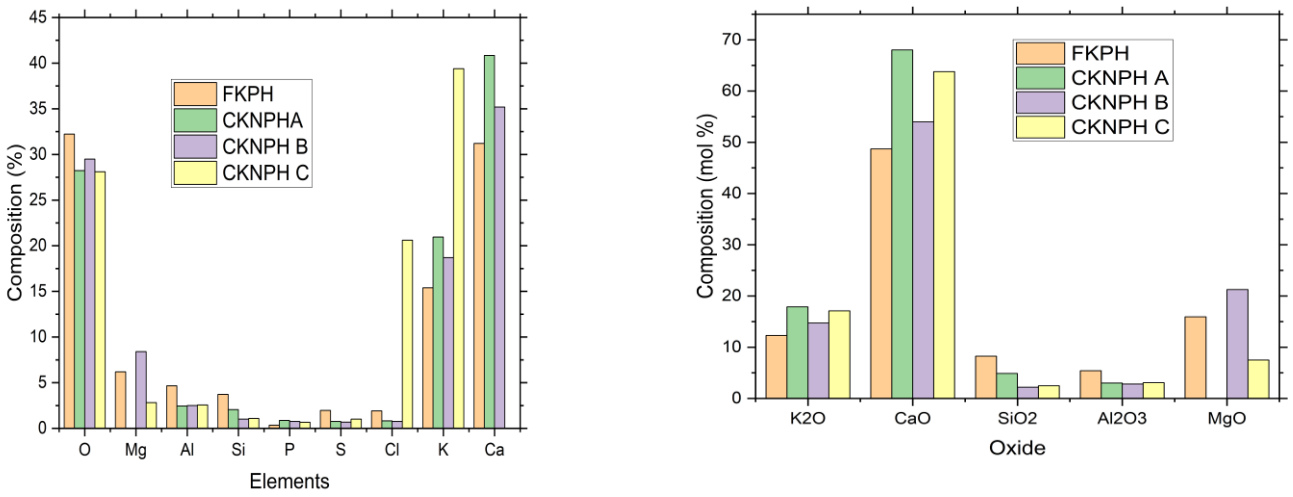

Figure 5.2: XRF of feedstock and calcined catalysts (a) Elemental composition (b) metal oxide composition

The results in Figure 5.2a revealed that the catalysts were significantly enriched in elements like potassium, calcium, magnesium, and oxygen, even though trace levels of silicon, aluminum, and Sulphur were also detected. When the elemental compositions of the FKNPH and CKNPH catalysts A, B, and C were compared, it was evident that the elemental compositions of all the catalysts that were calcined (A, B, and C) were significantly higher than those of the feedstock (FKPH). In particular, the CKNPH-A sample showed the largest mole fraction of calcium (40.84 mole%) at 700°C, followed by CKNPH-C (39.39 mole%) and CKNPH-B (35.18 mole%), respectively. Similar patterns were observed for potassium, where CKNPH-A had the largest mole fraction (20.95 mole%), followed by CKNPH-C (20.60 mole%) and CKNPH-B (18.70 mole%). The increase in the elemental composition of the calcined catalysts compared to the raw material (uncalcined feedstock) is suggestive of a decomposition reaction and the high calcination temperature also encourages the existence of free elements within the sample matrix. It was observed that the CKNPH B catalyst had the highest magnesium content, On the other hand, magnesium was not detected

in the CKNPH-A catalyst; however, it was detected in the CKNPH-C sample with a mole fraction of 2.81 mole%. As shown in Figure 5.2b, the calcium compositions of catalysts A, B, and C were higher than the feedstock. The effectiveness of the MeOH pre-treatment and calcination processes is demonstrated by the slight increase in elemental quantities in the CKNPH catalysts samples when compared to the FKPH sample. The lignin-carbohydrate matrix has been broken down by these processes, which has made it easier to extract and enrich the minerals found in the FKPH sample (Adepoju *et al*., 2020: Krishnan *et al*., 2023). Table 5.2 presents a comparison between the results of this study and information from the literature regarding the composition of metals and oxides. Single base metal oxides, including CaO, MgO, and K_2O, which are the main constituents of solid base heterogeneous catalysts, were found to provide similar results at low temperatures and within reduced reaction durations (Maroa and Inambao, 2021). Interestingly, CaO catalysts are widely used in the manufacture of biodiesel because they are cost effective and highly reactive in low-free fatty acid environments (Santos *et al*., 2019; Ooi *et al*., 2021).

In this study, the main difference between CKNPH-A and B is the treatment with methanol to remove the organic impurities. Based on the like dissolve like principle, the washing of the sample (CKNPH-B) with methanol should only remove organics; hence, it would be expected that the difference in the elemental compositions of both samples would be insignificant. However, sample B had a higher magnesium content than sample A and the slight difference in other elemental compositions of both samples is suggestive of the need for a confirmatory characterization using another spectroscopic technique, which is presented and discussed in the next section.

Table 5.2: Effect of biomass pre-treatment on elemental composition of various heterogeneous catalysts

Bio - catalysts	Treatment Methods	Calcination conditions		Key metallic content (%)	References
		Heat (^{0}C)	Time (h)		
Musa acuminata (Red banana) peduncle	Oven dried at 650C for 4 days	700	4	K (42.23), Ca (1.70)	(Adepoju *et al*., 2020)
Carica papaya peels	Sun-dried for 2 weeks	700	4	K (30.74) Cl (10.3) P (3.64) S (4.31)	(Domingos *et al*., 2008)
Kola nut pod husk	Burnt to ash in open air	500	4	K (47.14) Ca (7.59) Mg (5.32)	(Rakopoulos et al., 2006)
Kola nut husk	Sun drying for 30 days	600	3	K (33.91) Ca (25.38) Mg (12.39)	(Haldar et al., 2009)
Cocoa pod husk, plantain peel	Open combustion in air	500	4	K (47.6) Ca (5.56) Mg (4.21)	(Senrayan and Venkatachalam, 2018).
Calcined kola nut pod husk A	Fermentation	700	4	K (20.95) Ca (40.84) Al (2.44) Mg (0.00)	This study
Calcined kola nut pod husk B	Fermentation, pre-treatment with MeOH	700	4	K (18.70) Ca (35.18) Al (2.48) Mg (8.40)	This study
Calcined kola nut pod husk C	Fermentation, ash removal after calcination	700	4	K (20.60) Ca (39.39) Al (2.55) Mg (2.81)	This study

5.3 Energy dispersive x-ray analysis

Energy Dispersive X-ray spectroscopy (EDX) is another analytical technique that is used in investigating the elemental composition of a sample. Unlike x-ray fluorescence spectroscopy, EDX uses an electron beam to excite the target analyte, and the emitted beam is collected and analyzed. This technique is more useful for the investigation of elemental composition at the microstructural level. The elemental composition of the feedstock (FKNPH) and the catalysts CKNPH-A, CKNPH-B, and CKNPH-C were confirmed using energy-dispersive X-ray spectroscopy, and the results are shown in Figures 5.3a-d for each catalyst. Additionally, Tables 5.3–5.6 provide an overview of the elemental compositions (atomic concentration) of all catalysts and feedstock.

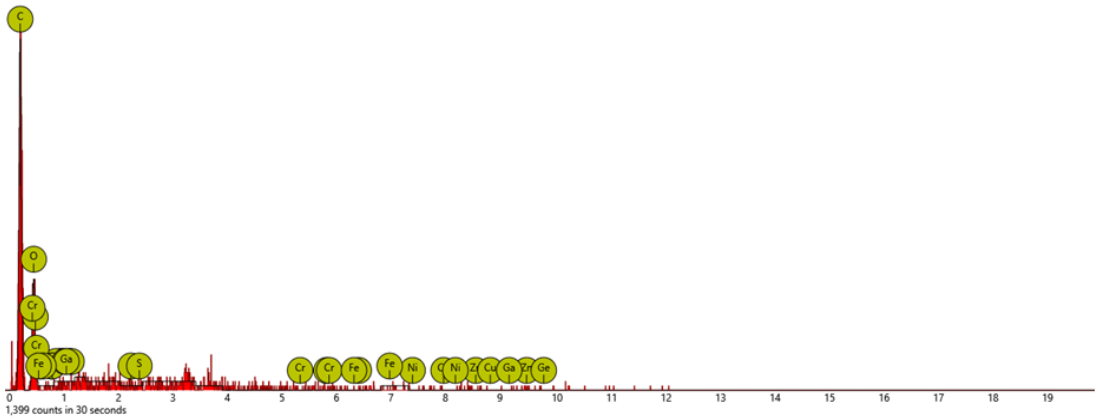

Figure 5.3a: EDX spectra of FKPH feedstock

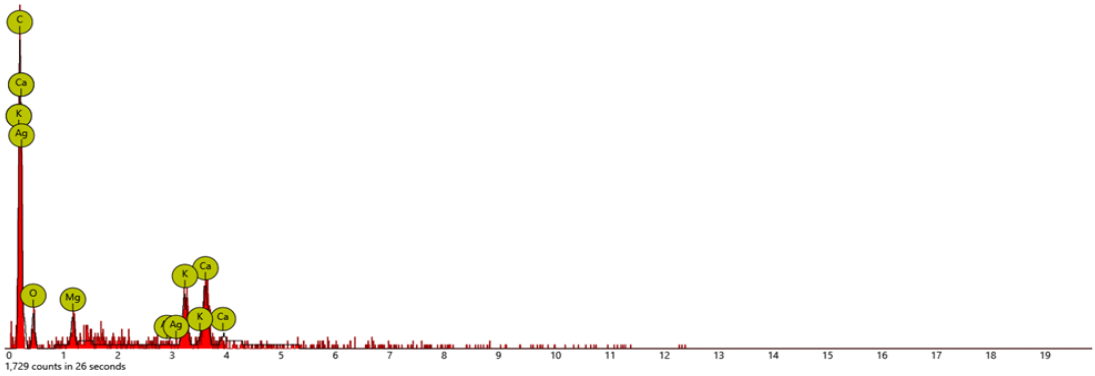

Figure 5.3b: EDX spectra of CKNPH A

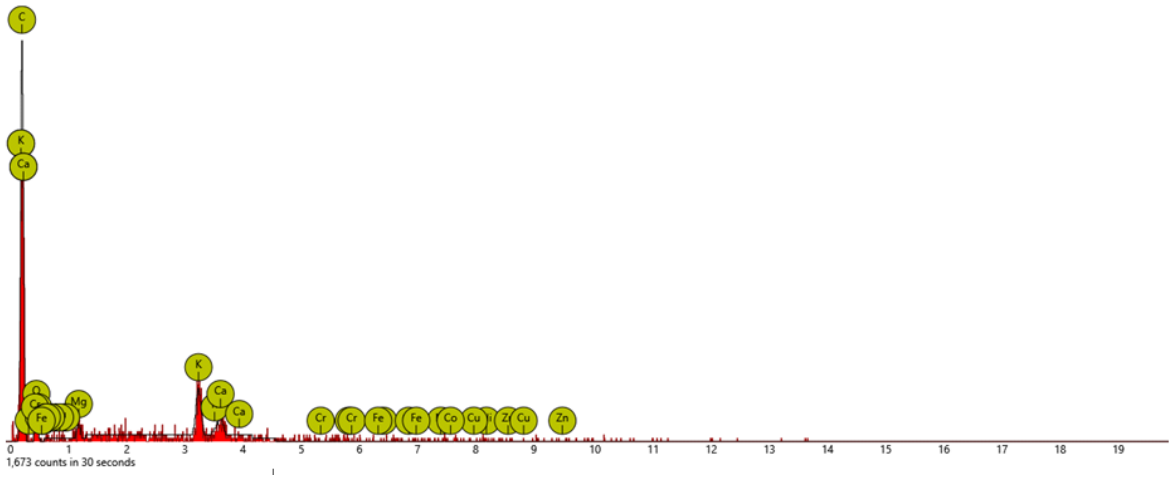

Figure 5.3c: EDX spectra of CKNPH B

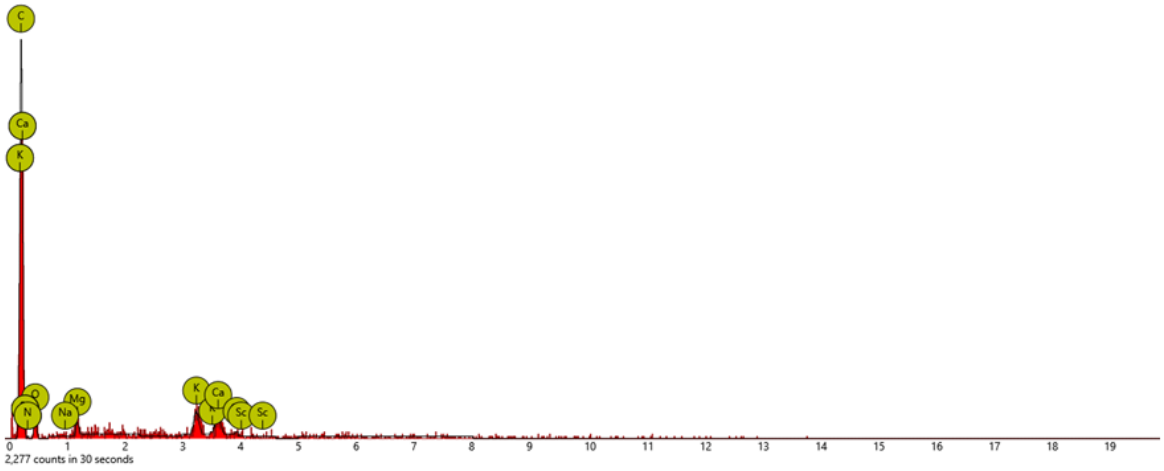

Figure 5.3d: EDX spectra of CKNPH C

The spectrum of the feedstock, FKNPH (Figure 5.2a), revealed the presence of carbon (72.86 atomic conc.) and oxygen (24.59 atomic conc.). The trace levels of additional elements, including iron, Sulphur, gallium, chromium, germanium, zinc, copper, manganese, nickel, and sulfur indicate the complexity of the feedstock and may be caused by contaminants. The spectra of the catalysts for CKNPH-A (Figure 5.2b), CKNPH-B (Figure 5.2c), and CKNPH-C (Figure 5.2d) also revealed the presence of carbon (73.13 wt. %; 79.01 wt. %; 78.35 wt. %;) and oxygen (17.09 wt. %; 11.07 wt. %; 11.53 wt. %;). In addition, potassium, calcium, and magnesium were also detected in all the catalysts. This could be attributed to the

effectiveness of the calcination and MeOH pre-treatment processes. The atomic concentrations of potassium, calcium, and magnesium were estimated to be 3.17, 4.83, and 1.65, respectively, for the CKNPH-A catalyst (Table 5.4), while the atomic concentrations of potassium, calcium, and magnesium were estimated to be 2.76, 1.37 and 0.72 respectively for CKNPH-B catalyst (Table 5.5). The CKNPH-C catalyst (Table 5.6) showed atomic concentrations of 1.61, 1.53, and 0.86 for potassium, calcium, and magnesium, respectively. The presence of potassium and calcium were confirmed using EDX which is consistent with previous results obtained using XRF spectroscopy. However, EDX showed the presence of magnesium in all the catalysts which differs from the result obtained from XRF for CKNPH-B. It is evident that elemental compositions vary (increase or decrease) in the EDX analysis conducted before (FKNPH) and after (CKNPH) catalysts calcination. However, the calcination process improves the concentration of some elements like potassium, calcium, and magnesium, which are essential for the transesterification process (Kolakoti *et al*., 2022). Due to crystalline and lattice rearrangement, some elements may have improved (Aleman-Ramirez *et al*., 2021). These findings are consistent with earlier research that has been published in the literature (Balajii and Niju, 2020; Aleman-Ramirez *et al*., 2021; Kolakoti *et al*., 2022). Consequently, because CKNPH catalysts have important elemental compositions that enhance catalytic activity during the manufacture of biodiesel, it may be used as an effective heterogeneous catalyst.

Table 5.3: EDX elemental composition of FKPH feedstock

Element	Atomic concentration	Weight concentration
Carbon	72.86	61.16
Oxygen	24.59	27.49
Germanium	0.63	3.22
Zinc	0.59	2.68
Copper	0.33	1.45
Manganese	0.28	1.08
Nickel	0.25	1.03
Gallium	0.21	1.03
Chromium	0.12	0.44
Iron	0.06	0.22
Sulfur	0.09	0.19

Table 5.4: EDX elemental composition of CKNPH-A catalyst

Element	Atomic concentration	Weight concentration
Carbon	73.13	57.66
Oxygen	17.09	17.95
Calcium	4.83	12.72
Potassium	3.17	8.14
Magnesium	1.65	2.63
Silver	0.13	0.90

Table 5.5: EDX elemental composition of CKNPH-B catalyst

Element name	Atomic concentration	Weight concentration
Carbon	79.01	63.93
Oxygen	11.07	11.93
Potassium	2.76	7.28
Calcium	1.37	3.69
Nickel	0.70	2.78
Zinc	0.61	2.71
Nitrogen	2.65	2.50
Copper	0.34	1.47
Magnesium	0.86	1.40
Manganese	0.34	1.25
Cobalt	0.14	0.55
Chromium	0.08	0.29
Iron	0.06	0.21

Table 5.6: EDX elemental composition of CKNPH-C catalyst

Element	Atomic concentration	Weight concentration
Carbon	78.35	69.20
Oxygen	11.53	13.56
Nitrogen	6.00	6.18
Potassium	1.61	4.63
Calcium	1.53	4.52
Magnesium	0.72	1.29
Scandium	0.12	0.40
Sodium	0.13	0.22

5.4 Scanning electron microscope analysis

Scanning Electron Microscopy (SEM) is an analytical technique that uses a beam of electrons to create topographic images at the micro and nano structural levels. The results

obtained from an SEM analysis primarily reveal the shape as well as porosity of the material under investigation. In catalysis, the shape of a catalyst as well as its porosity influences three important parameters, namely: selectivity, availability of active site and mass transport. These parameters determine the efficacy of catalysts for synthetic applications. The ability to influence these parameters depends on the extent to which the morphology of the catalytic material and its pore size distribution can be controlled during synthesis.

In this study, the surface morphology of the fermented feedstock and the calcined kola nut pod husk catalysts were examined using micrographs obtained from scanning electron microscopes. These micrographs are depicted by Figures 5.4 a-d. These results indicate the porosity of the catalysts, and the effect of the calcination process on the prepared samples.

Figure 5.4a shows the micrograph for the FKNPH feedstock. FKNPH is characterized by a flat surface, a flake particle structure that is irregular and rough, and particles at the pore position that are relatively loose (Gao *et al*., 2020). There are fewer pores on the surface of the FKNPH. The carbohydrate-lignin matrix during calcination could be responsible for the rough surface of the FKPH catalyst.

The micrographs for CKNPH-A, CKNPH-B, and CKNPH-C are displayed on figures 5.4b, c and d, respectively. The CKNPH catalysts exhibited pores and an uneven, honeycomb-like structure (Santana et al., 2022). As can be seen, the CKNPH-C catalyst exhibited more pores than the CKNPH-A and CKNPH-B catalysts.

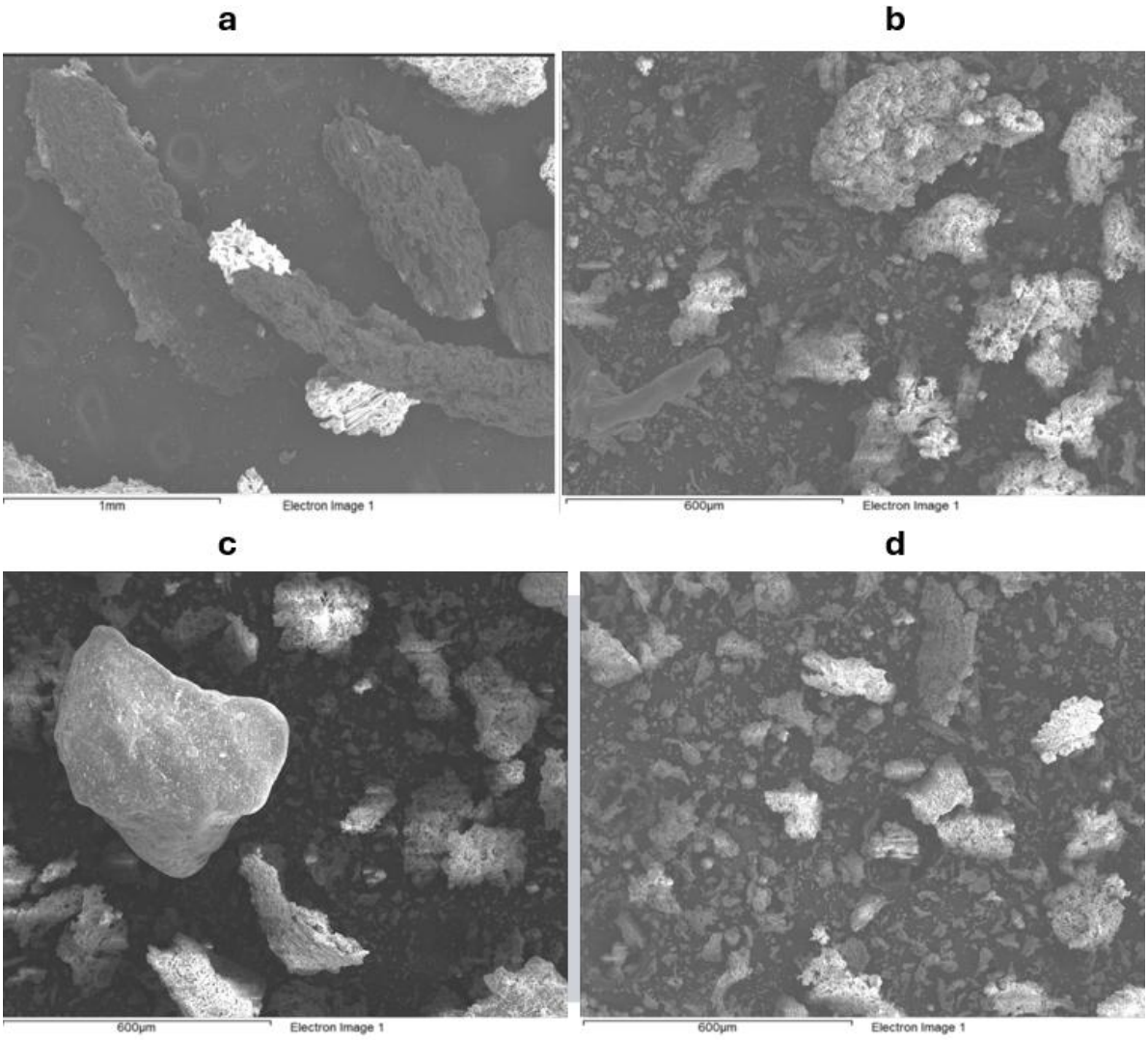

Figure 5.4: scanning electron micrographs of (a) FKNPH feedstock (b) CKNPH-A catalyst (c) CKNPH-B catalyst (d) CKNPH-C catalyst

According to previous studies, calcined biomass ash can be used as a solid heterogeneous base catalyst for the synthesis of fatty acid methyl esters, since it exhibits little mineral aggregate caused by the sintering of metal oxides (Balajii and Niju, 2020). Sequel to the enlarged surface area as corroborated by BET analysis and ordered, smooth, and flat surfaces with many pores and perforations, the biocatalysts CKNPH-A, CKNPH-B, and CKNPH-C that were generated is expected to enhance the conversion of biodiesel (Oloyede *et al*., 2023).

The micro changes in the morphology of the calcined catalysts indicate that the calcination temperature and the MeOH pre-treatment have a substantial effect on the morphology of the FKNPH feedstock. The development of pores because of thermally cracked organic compounds and successful treatment is suggested by the SEM micrographs of CKNPH-A, CKNPH-B, and CKNPH-C (Wang L *et al*., 2022). It is evident from the XRF data that K and Ca are the main constituents. Furthermore, trace amounts of Mg, Mn, Zn, Cu, N, Cr, Fe, and Ni were also discovered in the CKNPH-B catalyst sample. Notably, S and Cl were absent in the catalysts. The particles are clear and bright, mostly made of inorganic materials, primarily iron, alkali and alkaline earth metals. The SEM micrographs also highlight the catalytic function of minerals and their oxides at the micro-level by showing the release of a more significant number of pores in tiny spots or points during thermal cracking influenced by the presence of mineral oxides like CaO and K_2O (Wang L *et al*., 2022).

5.5 BET surface area analysis (N_2 adsorption)

Brunnaeur-Emmett-Teller (BET) analysis is a characterization technique that is used to assess the surface area as well as the pore size distribution of materials. The surface area is an indication of the degree of active sites where intended reactions take place. In this study, the pore size distribution is demonstrated using the nitrogen adsorption-desorption isotherms as shown in Figures 5.5 (a-c), which describes the nature of the catalyst when an inert gas nitrogen is passed through it. The corresponding pore size distribution of the material is plotted and shown in Figures 5.6 (a-c). A summary of the surface area, pore-volume, and pore sizes of the calcined catalysts is presented in Table 5.7.

In this study, the relative pressure (P/Po) covering a range of 0.05 to 0.1 were used to compute the BET surface area using the multipoint BET technique. The nitrogen adsorption

volume at P/Po = 0.99 was used to calculate the average pore size and pore volume. According to the IUPAC classification, it was found that all the calcined catalysts showed type-IV physisorption isotherms, with a H_3-type hysteresis loop indicating that these materials are mesoporous. Also, in literature, slit-shaped pores and well-ordered porous materials have been linked to this hysteresis (de Oliveira *et al*., 2022). The isotherm of the calcined kola nut pod husk catalyst that had previously been documented in the literature showed no discernible differences (Betiku *et al*., 2019).

The presence of large pores in the catalysts is indicated by a rapid spike in the adsorption curve at P/Po ratios approaches unity. This is corroborated by the pore size distribution, which ranges from 2 to 50 nm (López *et al*., 2019; Saputra) (Betiku *et al*., 2019), as shown in Figures 5.5a-c.

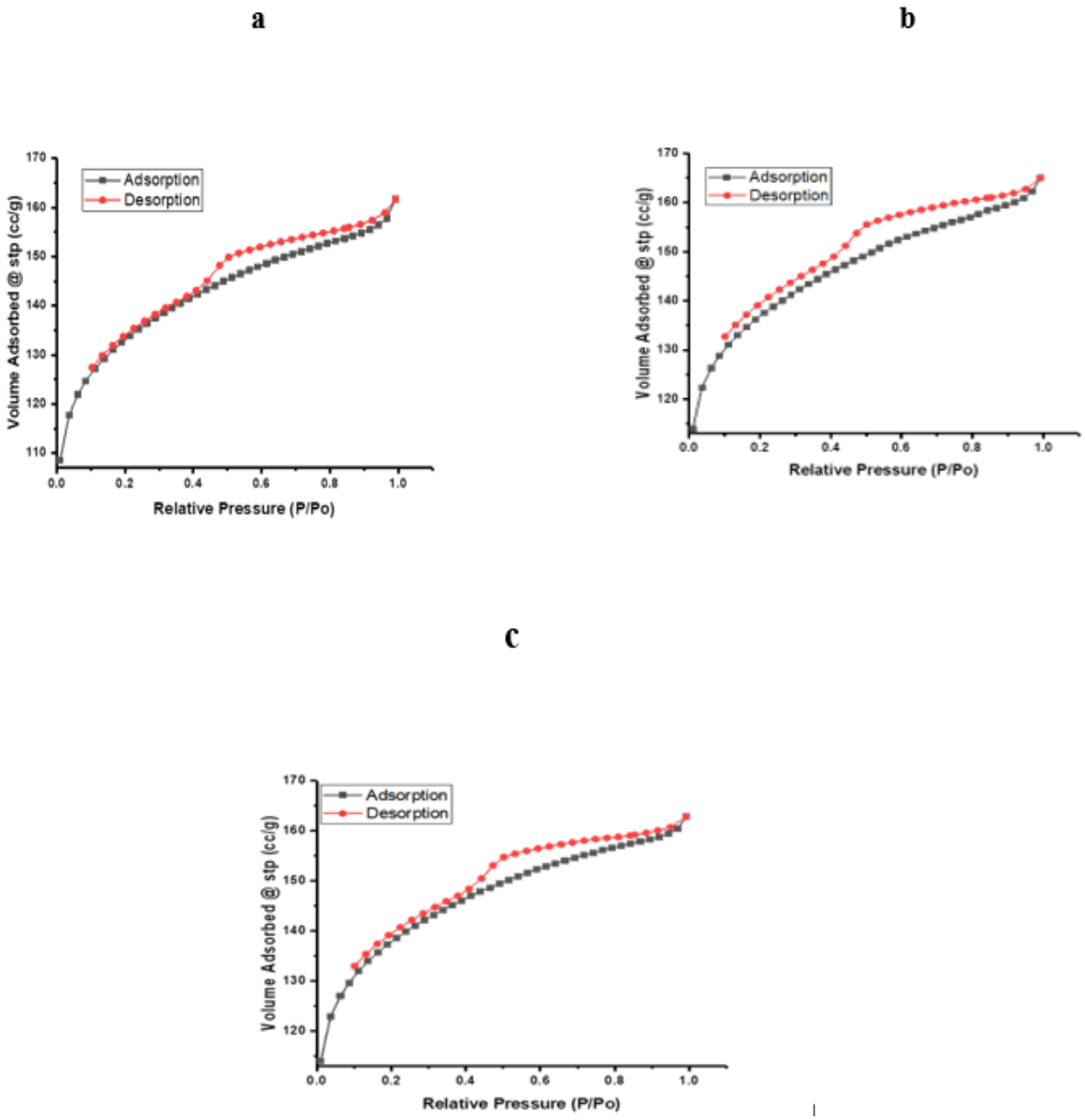

Figure 5.5: Nitrogen Adsorption-Desorption isotherm of catalysts (a) CKNPH-A, (b) CKNPH-B and (c) CKNPH-C

The pores of a material serve as conduits through which the active sites could be accessed (Leofanti *et al* 1998). The active sites are specific areas within a catalyst surface where the intended chemical reactions take place. The porosity of materials occurs in different sizes, which have been grouped into microporous for sizes less than or equal to 2 nm, mesoporous

for sizes between 2 nm and 50 nm, and macroporous for sizes greater than 50 nm according to IUPAC classifications. Pore size distribution shows the occurrence of these various sizes, which gives an idea of the predominant size range. The activity of catalysts during chemical reactions is also influenced by the pore size distribution. In this study, the Barrett–Joyner–Halenda (BJH) method was utilized to compute the pore size distribution as shown in Figure 5.6a-c. For each catalyst, the distribution curve shows a narrow unimodal pattern. While CKNPH-A indicated a pore diameter of 3.53 nm, the pore size distribution of all the catalysts reveals a peak value of 3.48 nm for CKNPH-B and 3.32nm CKNPH-C.

The pore size distribution plot shown in Figure 5.6a-c is not and average value but a range of pore volumes relative to the pore diameter across the sample. It is possible that there might be variation in the porosity distribution of different batches if repeated. In this study only a single measurement was carried out as the focus of the work was on the conversion of *C. Papaya* oil to biodiesel.

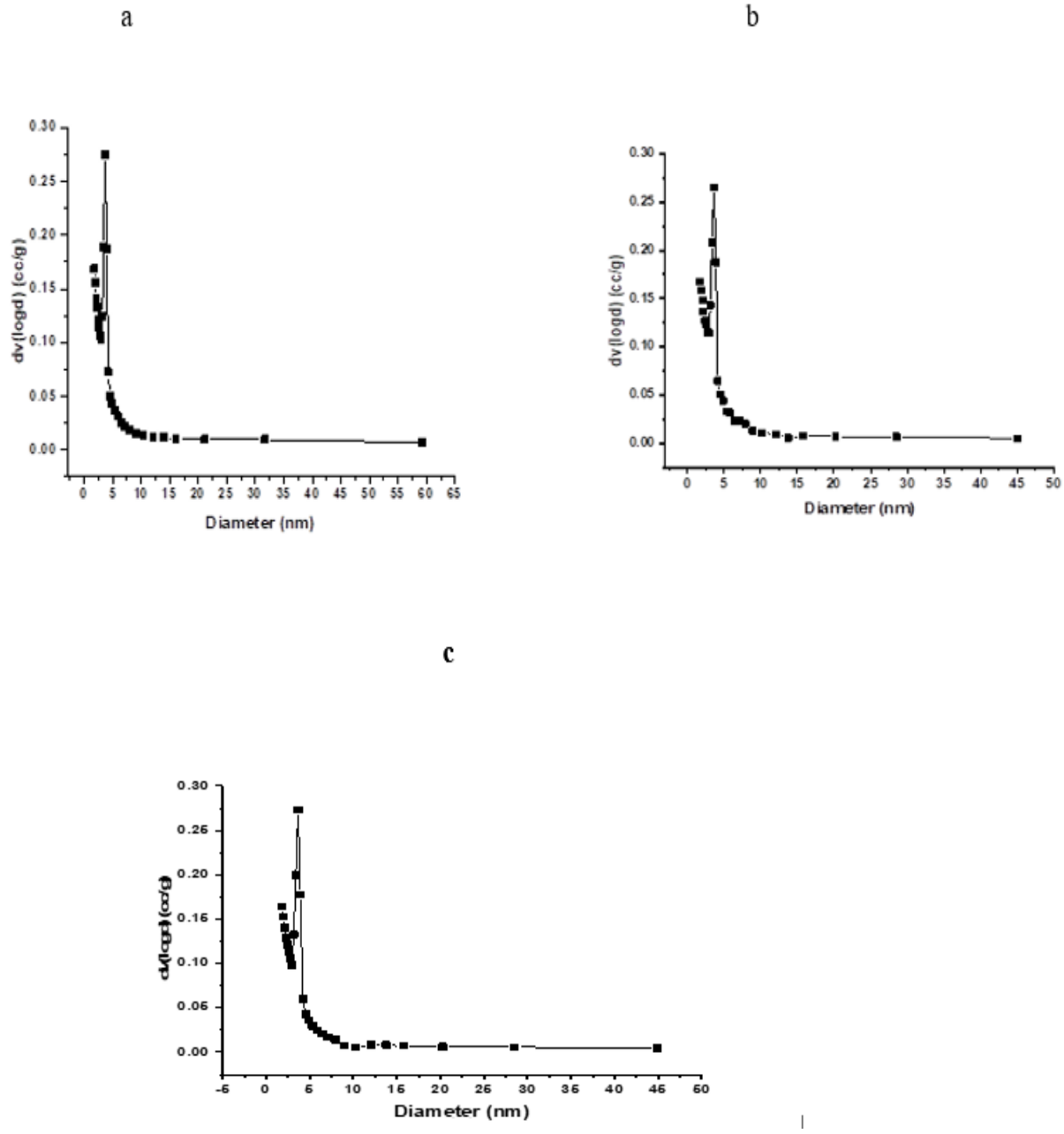

Figure 5.6: Pore size distribution of catalysts (a) CKNPH-A, (b) CKNPH–B and (c) CKNPH-C

Table 5.7: Summary of BET analysis results of CKNPH Catalysts

Catalyst	BET Surface Area (m^2/g)	Pore Volume (cm^3/g)	Pore diameter (nm)
CKNPH-A	420	0.25	3.53
CKNPH-B	430.5	0.26	3.48
CKNPH-C	432.6	0.25	3.32

The pore size distribution of all the catalysts appears to be within the mesoporous range (between 2–50 nm), as shown in Figure 5.6 except for CKNPH-A that was only calcined at 700 ^oC with no further treatment. The catalyst (CKNPH-A), unlike others, shows pore size distribution that spans across the microporous, mesoporous and macroporous ranges. This unique feature is typical of hierarchical porous architectures. The uniform pore characteristics observed between CKNPH-B and CKNPH-C may be attributed to the treatment with methanol and sieving respectively. During the preparation of a catalyst, the use of methanol to wash the catalyst have been reported to block micropores due to carbonaceous deposits especially when they are reduced to olefins (Zapater et al., 2024). The consequence of this would be variation in the pore volume. In this study, there was no significant change in the pore volume across the three catalysts as presented in Table 5.7, which suggests little or no formation of carbon deposits that would culminate in pore constriction or blockage.

An overview of the BET results is provided in Table 5.7. It was discovered that the BET surface areas of CKNPH-A, CKNPH-B, and CKNPH-C were 419.9049 m^2/g, 430.5414 m^2/g and 432.5738 m^2/g, respectively. There was a noticeable increase in the values of the BET

surface area, pore volume, and pore size. This demonstrates the effectiveness of the methanol pre-treatment and calcination method on the calcined kola nut pod husk catalysts. Furthermore, the catalysts all had large surface areas ranging from 420-432.6 m^2/g which are expected to possess sufficient active sites to facilitate the conversion of the extracted oil to biodiesel. In addition, higher levels of unburnt carbon which may be attributed to the porous nature of the ash particles, could also contribute to the observed high specific areas (Pathak *et al*., 2018).

Furthermore, the results obtained in this study were compared with other catalysts reported in the literature. A summary of the BET results obtained on several biomass catalysts is presented in Table 5.8. Comparing the generated CKNPH-A, CKNPH-B, and CKNPH-C catalysts to other ash-contained solid catalysts reported by Adepoju *et al*. (2020), they have higher surface areas. It was noted that CKNPH-A had the lowest surface area, as shown in Table 5.7. This might be explained by the glycerol, esters, and biomass ash content clogging the pores (Adepoju *et al*., 2020). The enhanced surface area of CKNPH-B may have resulted from pre-treatment with methanol and sieving to remove ash content. The sample with the largest surface area was CKNPH-C. This increased surface area can be the consequence of the ash content being removed from the catalyst surface that was created during the calcination process. According to reports, the high surface area of the biomass solid catalysts produced could be aided by size reduction, screening, and calcination temperature (700°C for 4 hours) processes (Adepoju *et al*., 2018; Udoetuk *et al*., 2018; Adepoju *et al*., 2020; Balajii and Niju, 2020).

Table 5.8: Summary of BET analysis reported on different biomass catalysts

Catalyst Source/Catalyst/Catalyst Support	Surface area (m^2/ g)	Pore volume (cc g−1)	Pore diameter or radius (nm)	Biodiesel yield or conversion (%)	References
Calcined Kola Nut Pod husk catalyst A	420	0.25	3.53	96	This study
Calcined Kola Nut Pod husk catalyst B	430.5	0.26	3.48	96	This study
Calcined Kola Nut Pod husk catalyst C	432.6	0.25	3.32	-	This study
Mesua ferrea Linn seed derived char	23.419	7.5206	-	-	(Gohain *et al*., 2017)
Mesua ferrea Linn seed derived AC	333.833	115.63	-	-	(Gohain *et al*., 2017)
Mesua ferrea Linn seed derived sulfonated carbon	150.326	55.32	-	-	(Gohain *et al*., 2017)
Date pits powder	432	0.22^{C}	6.62^{D}	-	(Betiku *et al*., 2019)
Date pits derived carbon catalyst (C3)	211	0.14^{C}	5.98^{D}	91.6	(Betiku *et al*., 2019)
Flamboyant pods derived carbon catalyst	820	0.3534^{C}	-	89.81	(Chin et al., 2009)
Char	354	0.34^{C}	3.8^{R}	-	[35]
Wood char catalyst	337	0.24^{C}	2.7^{R}	96	[35]
Pomelo peel bio char catalyst	6.7	24.4^{M}M	-	98	(Adepoju, 2020)
Wood ash	9.38	-	25	40.2	(Rasoulinezhad *et al*., 2020)
Calcined wood ash catalyst (CWC_{800})	3.72	-	26	98.7	(Rasoulinezhad *et al.,* 2020)
Activated wood ash catalyst (A_KWC_1)	0.65	-	53	99	(Rasoulinezhad et al., 2020)
Lemna perpusilla Torrey ash	9.622	$2.170 \times 10^{-8\ M}$	$4.512 \times 10^{-9\ R,\ M}$	89.43	(Betiku *et al*., 2017)
Musa 'Gross Michel' peel ash	4.442	0.020C	17.86^{D}	98.5	(Chinyere *et al*., 2017)
Tucuma peel ash	1.0	-	-	97.3	(Ogunsua and Badifu,1989)
Musa balbisiana Colla peel	10.176	0.065	1.60^{R}	-	(Barnwal and Sharma, 2005)
Musa balbisiana Colla peel ash	14.036	0.074	2.603^{R}	100	(Barnwal and Sharma, 2005)
Uncalcined red banana Peduncle	24.466	0.083	11.754	-	(Danbaba *et al*., 2015)

Calcined red banana Peduncle	45.992	0.145	9.770[D]	98.73 ± 0.50	(Danbaba *et al*., 2015)

[R]Pore radius, [R, M]pore radius expressed in m, [D]pore diameter, [S]particle size expressed in μm, [C]pore volume expressed in $cm^3\ g^{-1}$, [M]pore volume expressed in $m^3\ g^{-1}$, [MM] pore volume expressed in $mm^3\ g^{-1}$.

5.6 Powder X-ray Diffraction (PXRD) analysis

Powder X-ray crystallography is an analytical technique that produces diffraction patterns when x-rays interact with the material under investigation. These results can reveal the crystallinity as well as the phases in which the intended materials occur. In principle, catalysts with less crystallinity are known to possess higher surface areas with more defects compared to catalysts with more crystalline structures (Arghaei and Haghighi, 2014). Moreover, increased crystallinity of catalytic materials enhances the predictability of active sites as well as increased stability and performance (Arghaei and Haghighi, 2014). In this study, powder x-ray diffraction study was carried out to identify the crystalline phases of the catalysts, and the results are shown in Figures 5.7(a-d). The diffractogram revealed the phases that were present in the catalysts. The Joint Committee on Powder Diffraction Standards (JCPDS) data was used to match the diffraction patterns and the average crystallite size for the predominant phase was calculated using the Scherrer model as presented in Table 5.9. Figure 5.7a displays the diffraction patterns of the FKNPH catalyst, with distinct peaks at $2\theta = 20.98°$ (100), 25.86° (101), 36.87° (110), 39.86° (102), 40.40° (111), 49.64° (112), 54.53° (103), 60.10° (211), and 66.76° (300) which indicate a hexagonal quartz phase as verified by the ICDD file number 00-002-0458.

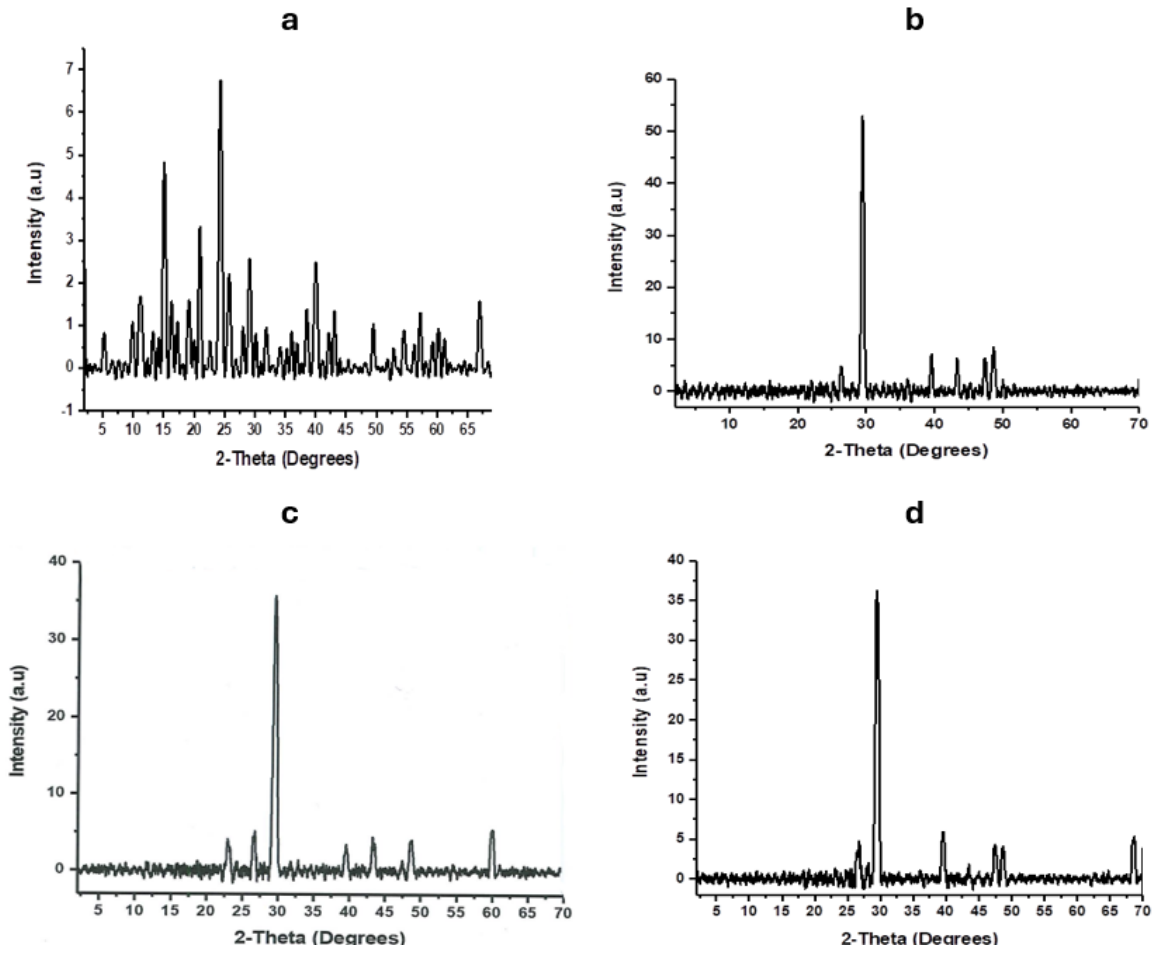

Figure 5.7: Powder x-ray diffraction pattern of (a) FKNPH feedstock (b) CKNPH-A (c) CKNPH-B (d) CKNPH -C

The X-ray diffraction patterns for the CKNPH-A catalyst are displayed in Figure 5.7b. Peaks at 29.57 ^{0}, 39.58^{0}, 43.32^{0}, 48.68^{0}, which correspond to the (104), (113), (202) (116) planes (ICDD: 01-086-4274), clearly demonstrated the calcite phase in the diffraction patterns. This suggests that the catalyst's diffraction patterns differ from those of FKNPH, which indicates that the material's structural integrity was lost during pretreatment and calcination. Additionally, it was found that the quartz phase's average crystallite size was 24 nm.

Figure 5.7c displays the diffraction pattern of the CKNPH-B catalyst. The pattern has distinct peaks at 2θ = 29.58º, 39.55º, 43.33º, and 68.54º. ICDD reference number 00-002-

0623 confirms that these peak positions correspond to the calcite quartz phase. The diffraction patterns also deviate from those of FKNPH, indicating that pretreatment and calcination were successful in generating phase transitions from the quartz to the calcite phase. The Scherrer equation was used to estimate the crystallite size to be 18 nm.

The diffraction pattern for the catalyst CKNPH-C is displayed in Figure 5.7d. The diffraction patterns predominantly showed calcite phase with peaks at 29.58°, 39.55º, 43.33º and 68.54º with peaks corresponding to the (202), (116), (104), and (113) planes. The patterns matched the ICDD reference card number 00-002-0623, which indicates a rhombohedral crystalline structure. The catalyst's diffraction patterns, like those of CKNPH-A and CKNPH-B catalysts, do not match those of FKNPH. This suggests that the material's structural integrity was lost during pretreatment and calcination. The average crystallite size was determined to be 26 nm as well.

When the XRD patterns of FKNPH and CKNPH-A, CKNPH-B, and CKNPH-C were compared, it was observed that most of the peaks recorded for the CKNPH catalysts were absent in the FKNPH catalyst. This could be attributed to the presence of the carbohydrates and lignin matrices (Balajii and Niju, 2019). Furthermore, it was observed that all the CKNPH catalysts, except for FKNPH, showed a strong similarity to the natural mineral calcite, a calcium carbonate compound (Ogunkunle and Laseinde, 2023).

Also, the transesterification reaction is significantly influenced by the crystallite size (Sulaiman *et al*., 2023). The surface area of the catalyst increases when the size of the crystallites decreases (Somvanshi *et al*., 2020). Also, the surface area increases because of smaller crystallites exposing a larger percentage of their atoms or molecules on the surface (Seal *et al*., 2020). It has been reported that a small crystallite size can lead to increased

reactivity, since they have more surface area accessible for interactions with other materials (Mazari *et al*., 2021). The calcined kola nut pod husk - B catalyst exhibited the smallest crystallite (18 nm). This is an indication that pretreatment with MeOH and calcination reduces the crystallite size and enhances the surface area, pore volume and pore diameter as confirmed by the BET results.

Table 5.9: Crystallite sizes of feedstock and Catalysts

Catalyst	Crystallite Size (nm)	Crystal Phase	Crystal System
FKNPH	-	Quartz	Hexagonal
CKNPH-A	24	Calcite	Rhombohedral
CKNPH-B	18	Calcite	Rhombohedral
CKNPH-C	26	Calcite	Rhombohedral

5.7 Thermogravimetric Analysis-Differential Thermal Analysis (TGA-DTA)

TGA-DTA was used to study the thermal degradation of the CKNPH-A catalyst. This was accomplished by placing 30.697 mg of the catalyst in an alumina pan and heating it at a rate of 10 K/min under a nitrogen atmosphere over a temperature range of 30°C - 900°C. TGA curve, which is supported by DSC, was used to observe structural transformations. The TGA-DTA curve is shown in Figure 5.8.

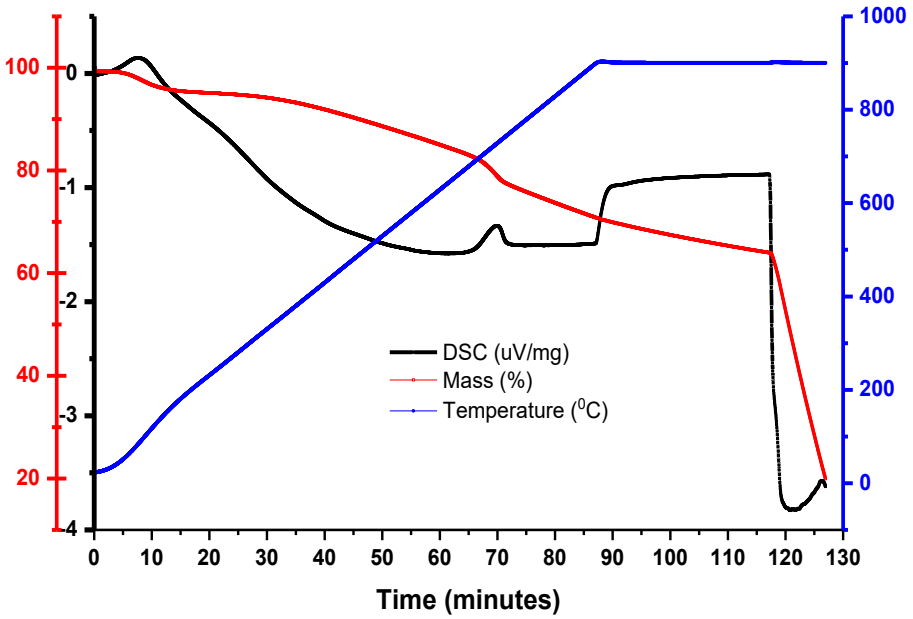

Figure 5.8: TGA-DTA thermogram for CKNPH-A Catalyst

The TGA curve revealed four distinct weight-loss stages. The first stage showed a weight loss of 3.68 % in the temperature range of 30 °C - 150 °C, which might be attributable to the removal of moisture adsorbed on the surface of the catalyst and the crystal lattice (Roy *et al*., 2020). This is consistent with FTIR data, which showed that water (O-H group) was removed during pretreatment and calcination. The second stage showed a weight loss of 18.28 % in the temperature range 160 °C - 718 °C. This loss could be attributed to the degradation of organic matter, which may be required for the formation of active sites on the catalyst. In the third step, a 14.34 % weight loss was recorded at temperatures ranging from 725 °C to 890 °C, indicating the breakdown of complex organic structures and the creation of a more porous and active catalyst structure. The last stage showed a weight loss of 43.78 % at the temperature range of 895 °C - 900 °C. This suggests that a phase transition or

structural rearrangement has occurred. The notable reduction in weight observed in this phase may be attributed to the removal of any residual organic matter, resulting in the development of a more stable catalyst structure. This agrees with the XRD data that showed a phase change from quartz (SiO_2) to calcite ($CaCO_3$).

On the other hand, the DSC curve showed a broad endothermic peak, with a maximum point observed at 80 °C for a temperature range of 19 °C to 122 °C, which indicates a slow process. This process, like the TGA which involves the elimination of water that is bonded to the catalyst's surface. There was also a sharp endothermic peak at a temperature range of 675 °C - 742 °C, with a maximum around 729 °C, indicating that the process was fast. This could be due to structural alterations or phase transitions. This demonstrates the catalyst's thermal stability and resistance to high temperatures, which are essential for its possible application in high-temperature reaction-based biodiesel manufacturing processes.

Furthermore, it was important to note that the TGA data indicated that organic impurities were efficiently removed during the calcination process at 700 ºC, which yielded a catalyst with a stable inorganic framework. The organic components are expected to decompose at this temperature without causing the catalyst particles to agglomerate or sinter excessively.

5.8 Fourier Transform Infra-Red (FTIR) analysis

An FTIR examination is a characterization technique that reveals the presence of functional groups within a substance. Identification of the functional groups is particularly important for this study because the intended chemical reaction (transesterification) is expected to occur at specific sites (active sites). The type and number of these active sites represented by the presence of the functional groups in the substrate is directly related to the efficiency of the intended reaction. Therefore, the transesterification process is anticipated to be significantly aided by these important functional groups on the catalysts. In addition to

increasing the surface area and porosity, these functional groups improve selectivity and provide binding sites. They facilitate significant chemical interactions, which improves the catalysts' capacity for adsorption even further (Idowu *et al*., 2023). The FTIR spectra of the CKNPH and FKNPH catalysts are displayed in Figures 5.9a-d. Figure 5.9a shows the FTIR spectra of FKNPH feedstock. FTIR spectra consists of two distinct sections: (1) The region where chemical bonds are observed to undergo bending vibrations are indicated by frequencies below 1500 cm^{-1}, and (2) the region where functional groups undergo stretching vibrations are indicated by frequencies greater than 1500 cm^{-1}. In this study, an absorption band observed at 3313.54 cm^{-1} is indicative of the O-H stretching vibration of water molecules, which is visible in the FKNPH sample (Betiku *et al*., 2019). Also, the band observed at 1604.48 cm^{-1} is indicative of the stretching vibration of the carbonyl group C=O that is present in the fresh sample. The peak at 1051.74 cm^{-1} corresponds to C-O stretching. Similar peaks are shown by the CKNPH-A, CKNPH-B, and CKNPH-C catalysts (figures 5.9b-d). The band at 1420.86 cm^{-1} could be linked to alcohol O-H bending vibrations. The absorption peak at 1051.55 cm^{-1} is attributed to the presence of C-O stretching vibration, which is like the FKNPH catalyst. This suggests that the C-O functional group which is recorded in the spectra of all the catalysts plays an important role in the transesterification reaction. Adsorption of ambient CO_2 on metal oxide surfaces can result in the formation of metal carbonates. This suggested that the catalysts contained Ca, K, and other metal carbonates (Pathak *et al*., 2018). It was noted that after pretreatment and calcination, the peak at 3313.54 cm^{-1} in the FKNPH catalyst disappeared. The reason for this is the elimination of water molecules that adheres to the surface of the catalysts (Santos *et al*., 2020). The peak at 860.85 cm^{-1} is assigned to O-C-O in-plane bending vibration, which is

sufficient evidence for the presence of carbonate (CO_3^{2-}) moiety, as validated by the XRD analysis (Roy *et al*., 2020).

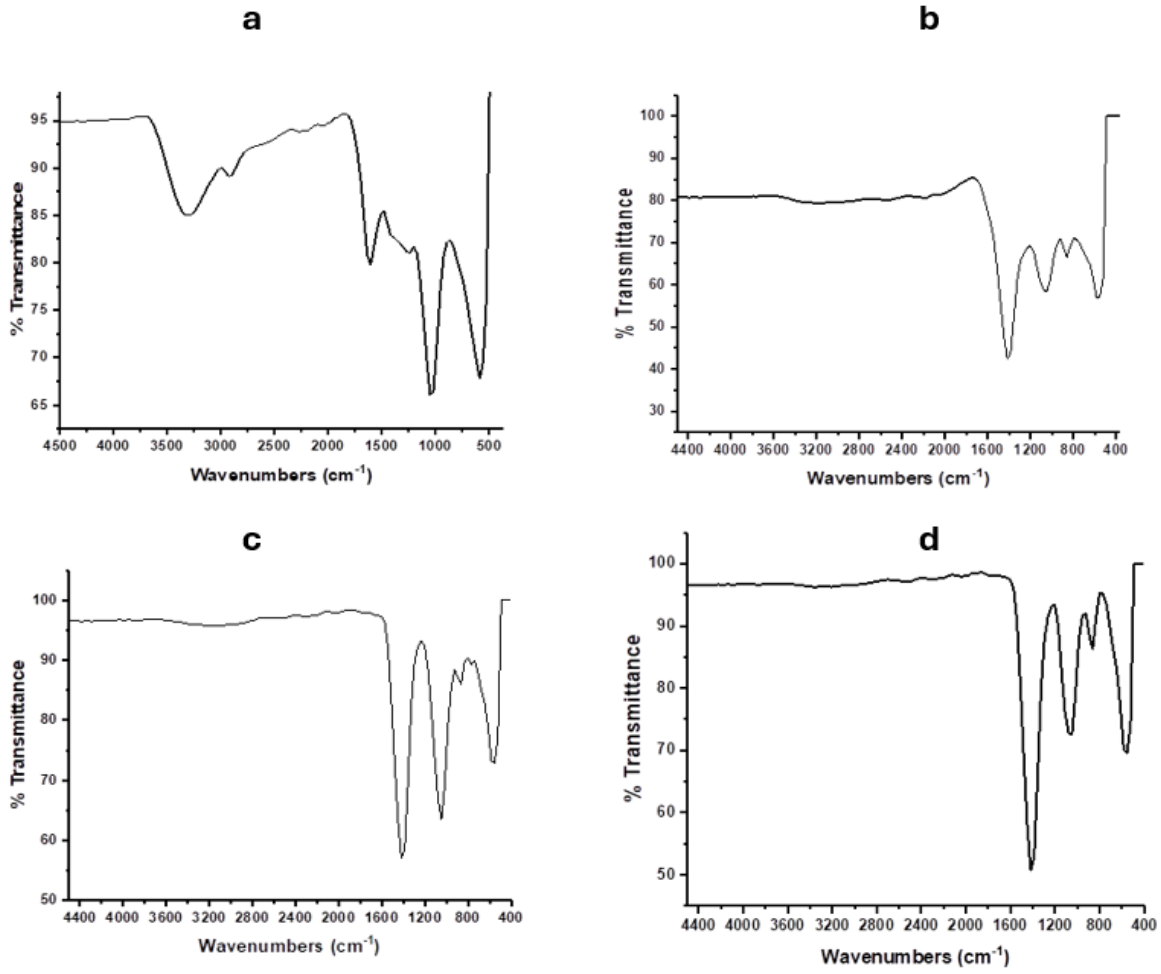

Fig.5.9: FTIR Spectra of (a) FKNPH (b) CKNPH A (c) CKNPH B (d) CKNPH C

5.9 Chapter summary

In this chapter, the yield obtained from the preparation of the catalyst as well as the properties of the catalysts were assessed using different characterization techniques such as X-ray fluorescence spectroscopy and Energy dispersive x-ray spectroscopy for elemental analysis, powder x-ray diffraction for crystallinity, FTIR for surface functionalities, BET for surface

area and porosity analysis, SEM for morphological assessment and TGA for thermal stability evaluation.

The yield of the catalysts was obtained as 11.95% after calcination at 700 °C but reduced to 7.28 % after treatment with methanol which is believed to have washed off organic impurities and a further decrease to 6.85 % after sieving. The elemental composition of the catalysts was evaluated using both X-ray fluorescence spectroscopy and energy dispersive x-ray spectroscopy. Both results indicated that the catalyst was rich in magnesium, potassium, calcium and oxygen when compared to the feedstock. However, XRF, Magnesium was not detected in the sample that was treated with methanol, but it was detected with EDX.

The results obtained from the scanning electron microscope, showed small pores with honeycomb-like structures were observed. This observation agreed with similar reports in the literature. The tiny pores were believed to be formed during the thermal cracking steps which is believed to be influenced by the presence of mineral oxides such as calcium oxide and potassium oxide. These were also confirmed by the BET results as the predominant pores that were observed within the mesoporous range of 2nm – 50 nm. In addition, the nitrogen adsorption isotherm showed a type IV physisorption isotherm according to IUPAC classifications which is characteristic of slit shaped pores and well-ordered materials. Moreover, the surface area of the catalysts was observed to range between 420-432.6 m^2/g, pore volume ranged between 0.25-0.26 cm^3/g and pore diameters were between 3.32-3.53 nm.

Furthermore, the FTIR results indicated the presence of O-H and C-O groups with their characteristic stretching bands. The thermal stability of the catalyst was investigated from

30 °C to 900 °C. The loss in materials was observed in stages; the first stage was observed from 30 °C to 150 °C with a loss of 3.68 % representing the removal of moisture. The second stage was from 160 °C- 718 °C representing the degradation of organic matter giving a loss of 18.28 %. The breakdown of complex organic materials was believed to occur between 725 °C-890 °C resulting in a loss of 14.34%. After this stage, a loss of 43.78% was observed between 895 °C – 900 °C which could be attributed to phase transition or structural rearrangement as confirmed a change from the quartz phase to the calcite phase when assessed using powder x-ray diffraction spectroscopy.

Chapter 6

Biodiesel synthesis using developed green heterogeneous catalysts

6. Introduction

Sequel to the extraction of oil from *C. papaya* seeds and subsequent preparation of catalysts from kolanut pod husks, the results obtained when the prepared catalysts were deployed through transesterification reaction to produce biodiesel is presented and discussed in this chapter. In addition, the results obtained for different process variables for the three developed catalysts in this study: CKNPH A, B, and C, which serve as the basis for optimization are also discussed. Biodiesel is comprised of fatty acid methyl esters (FAME); therefore, in this study, the technical name (FAME) reveals its chemical composition would be used where necessary. The process parameters optimization was also carried out to study the FAMEs production by changing the quantity of catalysts, methanol-oil ratio, and the reaction times. Figure 6.1 show sample of *Carica Papaya* Oil Biodiesel (CPOB) produced in this current research.

Figure 6.1: *Carica Papaya* Oil Biodiesel (CPOB) sample produced in this study

6.1 Statistical significance of the input parameters with respect to biodiesel yield.

In this section, statistical analyses of the results were carried out to assess the importance of each parameter to the overall biodiesel yield. To achieve this, a linear, two-factor interaction and quadratic polynomial models were used to fit the response of the experiment to select the best model. In addition, a one-way analysis of variance (ANOVA) was used to evaluate the significance of multiple parameters on the yield of biodiesel. The input parameters used for analysis included: temperature, quantity of catalyst, methanol-oil molar ratio and the reaction time, while the output variable was the biodiesel yield. The results showing the outcome of the linear, two factor interactions and quadratic models are presented in Table 6.1, while the results obtained for the Anova is presented in Table 6.2.

Table 6.1: Model evaluation for best fit

Source	Sum of Squares	df	Mean Square	F-value	p-value	Adjusted R^2
Linear Model	201.87	4	50.47	0.5956	0.6713	-0.0931
2FI Model	1088.98	6	181.50	8.98	0.0022	0.7392
Quadratic Model	180.54	4	45.13	162.55	< 0.0001	0.9964

2FI represents a two-factor interaction model.

The linear, two-factor interaction, and quadratic polynomial models were used to fit the data obtained in this study. When the fit for each model was compared, the quadratic model was selected as the best model due to its high f-value (162.55), low p-value (<0.0001) and has the highest adjusted R^2 (0.9964) value. Also, it is interesting to note that there is a significant

improvement in the values of the correlation coefficients as the model is changed from linear to quadratic models. This improvements in the correlation coefficients suggest that the observed biodiesel yield is a consequence of a multiple effects of the input parameters. Table 6.2 shows the result of the ANOVA. It determines the significance fitness of the quadratic model, the interactions of the parameters as well as the contributions of each parameter to the biodiesel yield using catalyst A.

The level of significance and adequacy of the generated model was assessed by ANOVA, using the p-values. Generally, the model terms with p-value less than 0.05 are significant. In the literature, the larger the magnitude of the f-value and the smaller the p-value, the higher will be the significance of the corresponding coefficient (Obika *et al*.,2020; Singh and Tirkey, 2022). In this study, the f-value for the model was high (f= 499.95) with a very low probability ($p < 0.0001$), which indicates a very high significance of the model. The significance of each term was investigated by their respective p-values. In the model, the linear terms (reaction time (A), catalyst amount (B) and Meth/OMR (D)), two-way interactions (AD, BC and BD) and the quadratic terms (B^2 and D^2) were statistically significant and considerably affected the biodiesel yield.

To determine the fitness of the model, the value of regression coefficient R^2 for the model is 0.9982 which implies that 99.82 % of the variability in the response can be explained by the model. In fact, this high value of R^2 indicates the capability of the model to satisfactorily describe the system within the range of parameters that were investigated (Sulaiman *et al.,* 2024). The model exhibited a high adjusted and predicted R^2 values of 0.9962 and 0.9871 respectively as shown in Table 6.2. The predicted R^2 value shows that this model performs well on new data. Also, it is worthy to note that the higher the value of the adjusted

coefficient of determination, the greater the significance the fitted model (Rahman *et al*., 2020). The coefficient of determination (R^2) is higher than the adjusted coefficient (adjusted R^2) which shows that the fitted model is more significant. Also, the predicted sum of squares (PRESS) was obtained as 18.95, which suggests that the model has good predictability.

Table 6.2: Test of Significance and ANOVA for all regression coefficient terms for biodiesel yield for catalyst A

Source	Sum of Squares	df	Mean Square	f-value	p-value	
Model	1470.12	10	147.01	499.95	< 0.0001	significant
A-Reaction Time	6.73	1	6.73	22.89	0.0010	
B-Catalyst Amount	20.13	1	20.13	68.46	< 0.0001	
C-Reaction Temperature	0.0728	1	0.0728	0.2477	0.6306	
D-Meth/OMR	20.56	1	20.56	69.93	< 0.0001	
AB	1.04	1	1.04	3.52	0.0932	
AD	3.02	1	3.02	10.26	0.0108	
BC	104.87	1	104.87	356.65	< 0.0001	
BD	132.63	1	132.63	451.03	< 0.0001	
B^2	478.14	1	478.14	1626.03	< 0.0001	
D^2	99.03	1	99.03	336.78	< 0.0001	
Residual	2.65	9	0.2941			
Cor Total	1472.77	19				
Fits Statistics						
R^2	0.9982					
Adjusted R^2	0.9962					
Predicted R^2	0.9871					
Adeq. Precision			105.7082			
PRESS			18.95			
BIC			49.26			
AICc			71.31			

6.2 Effects of process parameters on biodiesel yield

In this study, the yield of biodiesel was studied under different conditions which include temperature, methanol-oil ratio and quantity of catalysts. By varying the parameter of interest, while ensuring that other variables are kept constant, the resulting yield of biodiesel under these conditions were assessed. The results showing the effects of temperature of reaction, quantity of catalyst used, and the methanol-oil ratio are presented and discussed. At the end of this section, a comparative analysis is carried out to determine the strength of the effect of each parameter on biodiesel yield. These results are expected to provide insight into the various combinations that could be useful for process optimization as well as measures of improving the yield of biodiesel for real life applications.

6.2.1 Effects of temperature on biodiesel yield

Temperature plays a crucial role in transesterification reactions. In theory, an increase in temperature is expected to result in a corresponding increase in the yield of fatty acid methyl esters. However, there is a threshold beyond which further increase in temperature may culminate in undesired reactions resulting in the formation of unwanted side products or even enhancing the evaporation of the alcohol resulting in lower yield of biodiesel (Istiningrum et al., 2017). In this study, the effect of the temperature of reaction on the yield of biodiesel was assessed between the temperature range of 60°C - 80°C, for both the calcined catalyst (CKNPH-A) and the catalyst with treatment with methanol following calcination (CKNPH-B), while maintaining other parameters and the result is shown in Figure 6.2.

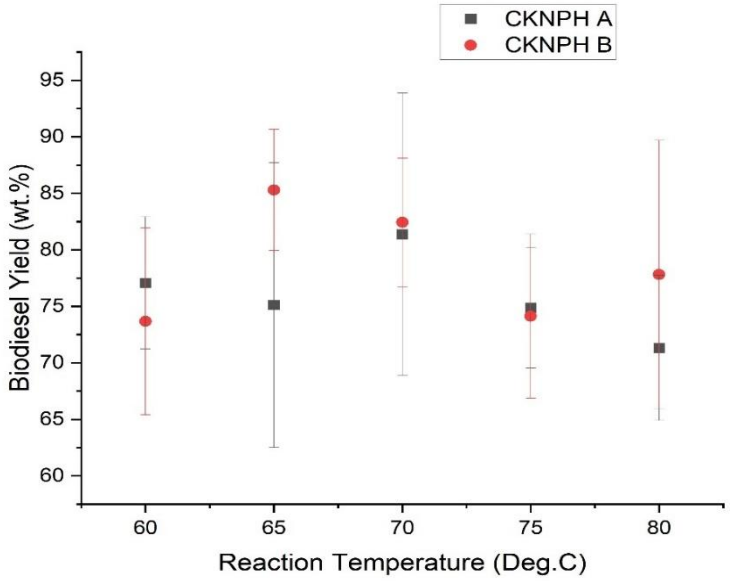

Figure 6.2: The effects of temperature on biodiesel yield for CKNPH A and B (reaction time: 70 min., quantity of catalyst: 2.5g, methanol-oil ratio: 4:1, flow rate: 1000 Kg/hr). Error bars indicate the standard deviation of four replicate measurements.

The results shown in Figure 6.2 indicates an initial increase in biodiesel yield from 77 wt.% to 83 wt.% as the temperature is increased from 60 °C to 70 °C as expected. This increase in the biodiesel yield when the temperature is increased is fundamentally attributed to the increased kinetic energy of the reactants as the temperature is increased which results in effective collision resulting in an increased conversion to the desired products. In this study, the optimum biodiesel yield is observed at 70 °C, which indicates the climax of these molecular interactions devoid of any significant interfering reactions. However, when the temperature is further increased beyond 70 °C, the yield of biodiesel decreases significantly to 74 %. The fact that there is a significant increase in the yield of biodiesel across 65 °C to 70 °C is suggestive of the fact that the evaporation of methanol has little or no effect on the observed results as methanol has a boiling point of 64.7 °C. Besides, the closed nature of the

reacting system suggests a continuous mixing of the alcohol in both the liquid and gaseous phases with little or no loss of methanol in the process. The main reason for the decrease in the biodiesel yield at temperatures exceeding 70 °C may be due to the formation of undesirable side products. To convert esters to biodiesel through transesterification, a major limitation has been the co-formation of saponified products, predominantly soap (Istiningrum et al. 2017).

Furthermore, there are several options that could be explored to resolve the issues of co-formation of side products to produce biodiesel from natural oils. The first option would be to carry out the reaction over different temperature ranges to assess the optimum temperature at which little or no side products are formed. The second option would be to use an enzyme that suppresses soap formation even at elevated temperatures. In the literature, some researchers have employed different enzymes such as lipase to suppress saponification reactions during biodiesel production (Andrade et al., 2017; Istiningrum et al., 2017). However, this is an expensive option as the cost of enzyme in addition to more stringent reaction conditions to prevent enzyme denaturation are major limitations. In this study, the first option was followed and the optimum temperature requirements required to obtain the maximum biodiesel yield was observed at 70 °C.

A comparative assessment of the yield of biodiesel at different temperatures obtained in this study with the published reports in the literature was carried out and the outcome is shown in Figure 6.3. The conditions under which each study was carried out is also reported. Istiningrum et al (2017) studied the effects of temperature on biodiesel production in the presence of lipase as a biocatalyst. The results also indicated a similar initial increase in the yield of biodiesel as temperature was increased from 45 °C up to 55 °C resulting in a yield

of 64.89 wt. % and 81.19 wt.% respectively. A further increase in temperature beyond 55 °C resulted in a decrease in the yield of biodiesel. According to the authors, the denaturation of lipase is expected at 60 °C; however, they suspected some initial inactivation of the enzyme as the temperature approaches its denaturation point which explains why the decrease in the biodiesel yield was observed.

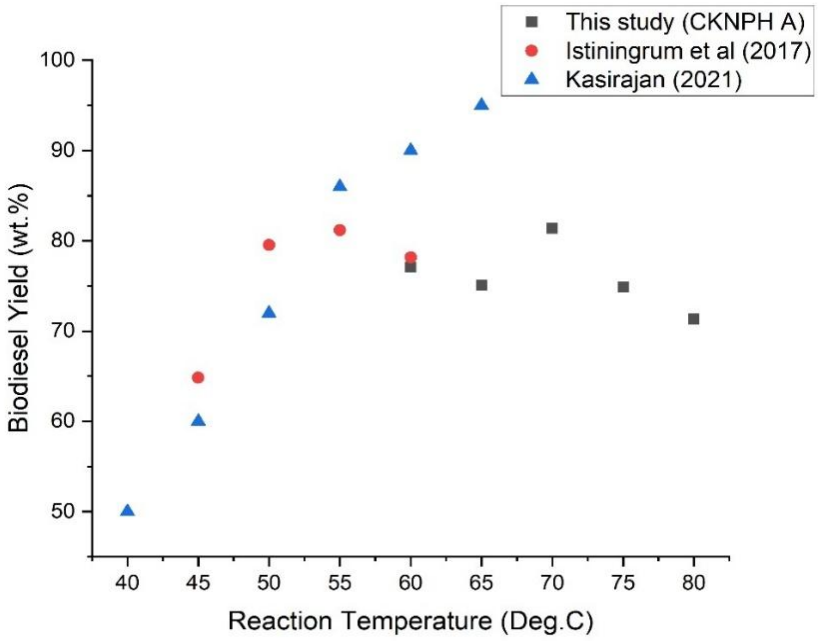

Figure 6.3: A comparative assessment of the yield of biodiesel as reported in the literature with this study

In another study, a chemical catalyst (sulphuric acid) was used in the conversion of *Chrysophyllum albidum* seed oil to biodiesel. The result of this study is also shown in Figure 6.3. In this report, a similar increase in the yield of biodiesel was observed as the temperature was increased from 40 °C to 65 °C. This corresponded to an increase in the yield of biodiesel from 51 wt.% to 96 wt.%. However, the authors did not report what should be expected if the temperature is further increased beyond 65°C. Most of the results of the yield of biodiesel reported in the literature are similar to the results of this study. The existing differences could be attributed to the differences in other parameters such as the type and quantity of catalyst

used, reaction times, among others. A different temperature range was used in this study to accommodate the specific feedstock properties, catalyst behavior, and reactor design, and to optimize reaction efficiency while minimizing side reactions and improving energy efficiency.

6.2.2 Effects of methanol-oil ratio on biodiesel yield

The alcohol-oil molar ratio is another important process parameter that affects the yield of biodiesel. This is based on the reversibility of transesterification reaction which implies that as the alcohol and oil reacts in the presence of a catalyst to produce biodiesel, there is a possibility of the products (biodiesel) reacting or dissolving in solution to form the reactants again. The implication of this is that the overall yield of the intended products will be reduced. For transesterification, the reversibility of the reactions is mostly observed in the dissolution of the glycerol products in the presence of excess alcohol, which shifts the chemical equilibrium in the opposite direction favouring reactant formation (Musa, 2016). To prevent this, a definite methanol-oil ratio is required to ensure that only the forward reaction is favoured resulting in the yield of biodiesel. In this study, the results obtained for four replicate measurements for the effects of methanol-oil ratio is shown in Figure 6.4.

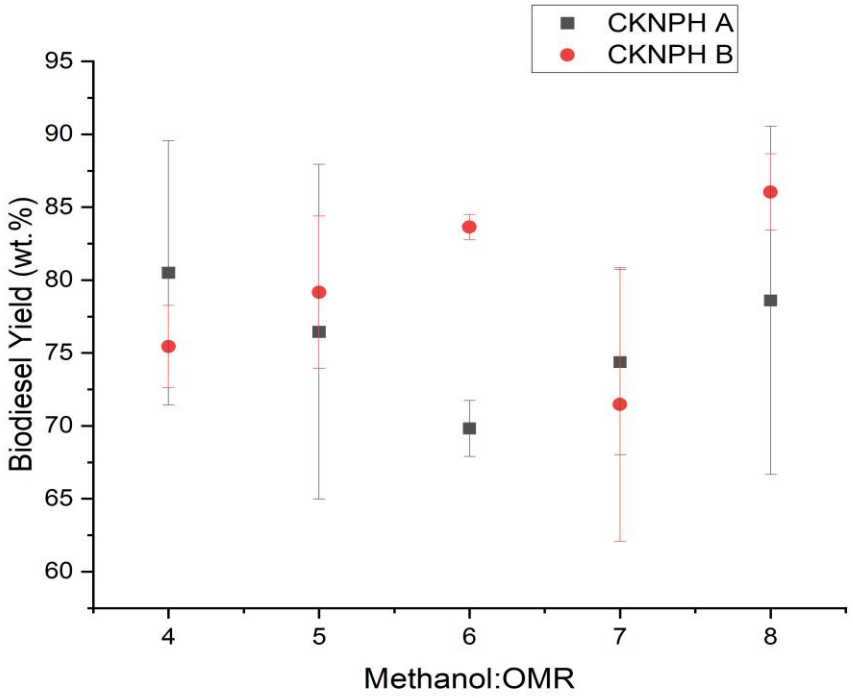

Figure 6.4: Effects of methanol-oil ratio on the yield of biodiesel

In Figure 6.4, the methanol/oil ratio tends to increase with the yield of biodiesel. However, the observed variability may be attributed to the fact that the biodiesel yield is also affected by other factors such as the sample weight and the reaction time. The observed increase indicates that the chemical equilibrium of the reaction is shifted to the right favouring the formation of biodiesel. This enhanced yield is possible due to the conversion of the esters in the oil to biodiesel with little or no side reactions. A similar increase in the yield of biodiesel as the methanol-oil molar ratio was increased was reported by Kasirajan et al (2021). This increase was observed from an initial methanol-oil ratio of 3 to 9 which corresponded to a yield increment from 42 wt.% to 81 wt.%. However, on further increase in the methanol-oil molar ratio beyond 9, a decrease in the yield of biodiesel was observed. The reduction may be attributed to the presence of excess alcohol resulting in the dissolution of the products to give the reactants, thereby shifting the equilibrium in the reverse direction.

6.2.3 Effects of the quantity of catalyst on biodiesel yield

The quantity of catalyst used is another important factor that influences the degree of conversion of oils to biodiesel. The ability of catalysts to influence biodiesel yield lies in the degree of available active sites that promote transesterification reactions. In fact, the more the number of active sites on the surface of the reaction substrate, the higher the conversion from oils to biodiesel would be possible. Moreover, the quantity of catalyst required to convert natural oils to biodiesel also contributes to the overall cost of production. Therefore, this section aims to assess the minimum quantity of catalyst required to obtain the maximum biodiesel yield. In real life applications, the lower this value, the more feasible the production would be which is quite desirable in industry. The results for four replicate measurements showing the effect of the quantity of catalyst for both CKNPH A and B are shown in Figure 6.5.

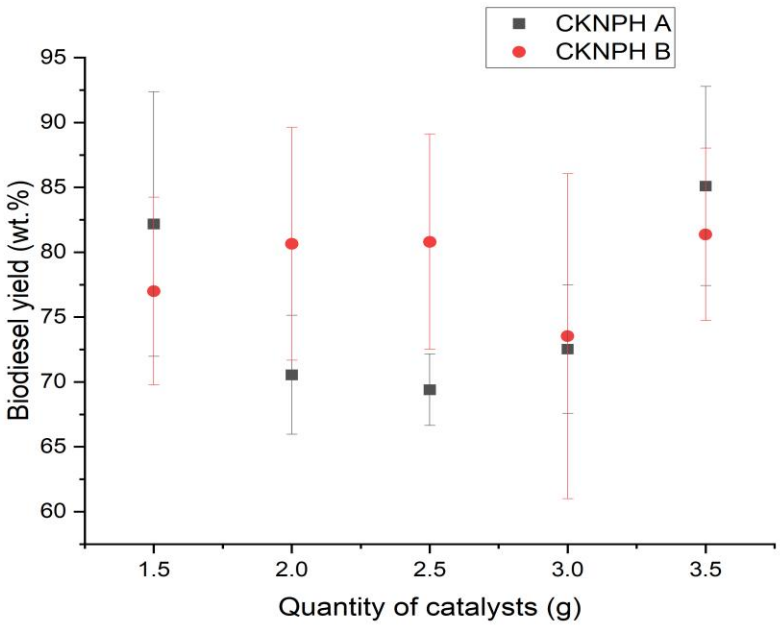

Figure 6.5: Effects of the quantity of catalyst on biodiesel yield for both CKNPH A and B.

The results shown in Figure 6.5 indicates an initial decrease in the yield of biodiesel when the quantity of catalyst was increased from 1.5 g to 2.5 g. However, as the quantity of catalyst is further increased up to 3.5g, the oil yield is observed to increase. This variability in the oil yield with respect to the quantity of catalyst used is suggestive of the fact that there are other factors that may have stronger influence on biodiesel yield. The degree of conversion of esters to biodiesel during transesterification is determined by several factors, such as reaction time, temperature, nature of catalyst, stirring speed, alcohol/oil ratio, among others. Moreover, there is a possibility that these parameters may exert a cumulative effect that determines the overall yield that could be obtained. Based on this insight, it will be interesting to assess the combined effects of these parameters on the yield of biodiesel as well as analyse the results statistically to evaluate the significance of each input parameter to the overall biodiesel yield. To achieve this, the results of two randomly selected

parameters and the oil yield will be analysed in a three-dimensional space to assess the interactions between the parameters and the resulting effects on the overall biodiesel yield.

6.3 The synergistic effects of process variables on biodiesel yield

In this section, the results showing the combined effects that temperature, reaction time, methanol-oil ratio and quantity of catalyst have on biodiesel yield are presented and discussed. The surface and contour plots were used to establish the interactions between the parameters and their effect on biodiesel yield. As the model has four variables, the plots were formed each with two targeted variables, while two variables were held constant at zeros in their coded values. The interaction of reaction time and Meth/OMR on biodiesel yield using catalyst A is presented in Figure 6.6 and Figure 6.7 for surface and contour plots respectively.

Figure 6.6 shows the interactive effect of Meth/OMR and reaction time on biodiesel yield. The biodiesel yield increases as the reaction time increases. As the reaction time increased from 60 minutes to 80 minutes, the biodiesel yields also increased from 69.8 % to 73.1 %. The maximum yield was achieved at 70 minutes (73.1 %), which agrees with the contour plot (Figure 6.7), whereas when the reaction time was increased from 60 minutes to 80 minutes, there was a corresponding increase in the biodiesel yield.

Also, it can be observed that as Meth/OMR increased from 4 to 8, there was a corresponding increase in the biodiesel yield from 69.8 % to 73.1 %. The maximum yield was achieved at 4 ml/ml (73.1%). The contour plot (Figure 6.7) also corroborates this trend where an increase in the Meth/OMR from 4 to 8 resulted in a corresponding increase in biodiesel yield.

It is important to note that the contour plot showed elliptical curves which indicates that the interaction between the Meth/OMR and reaction time is significant ($p = 0.0108$) as shown

in the ANOVA quadratic model (Table 6.2), hence, this will have effect on the response (biodiesel yield).

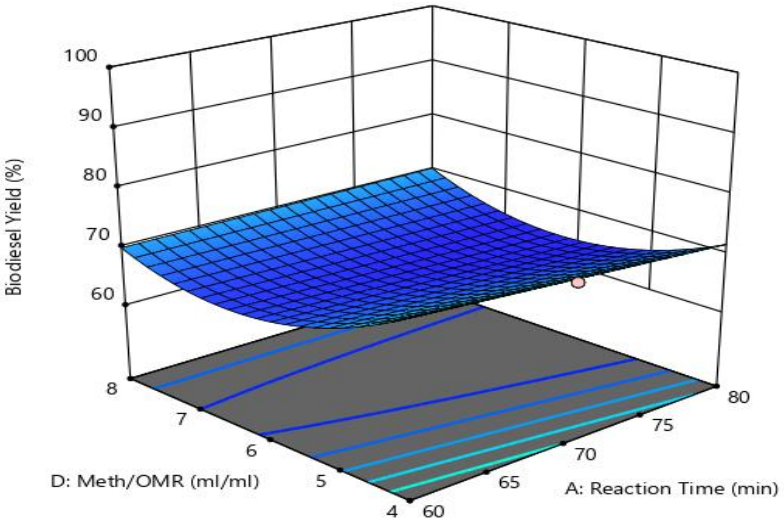

Figure 6.6: 3-D Surface plot showing the combined effect of reaction time and Meth/OMR on biodiesel yield using catalyst A

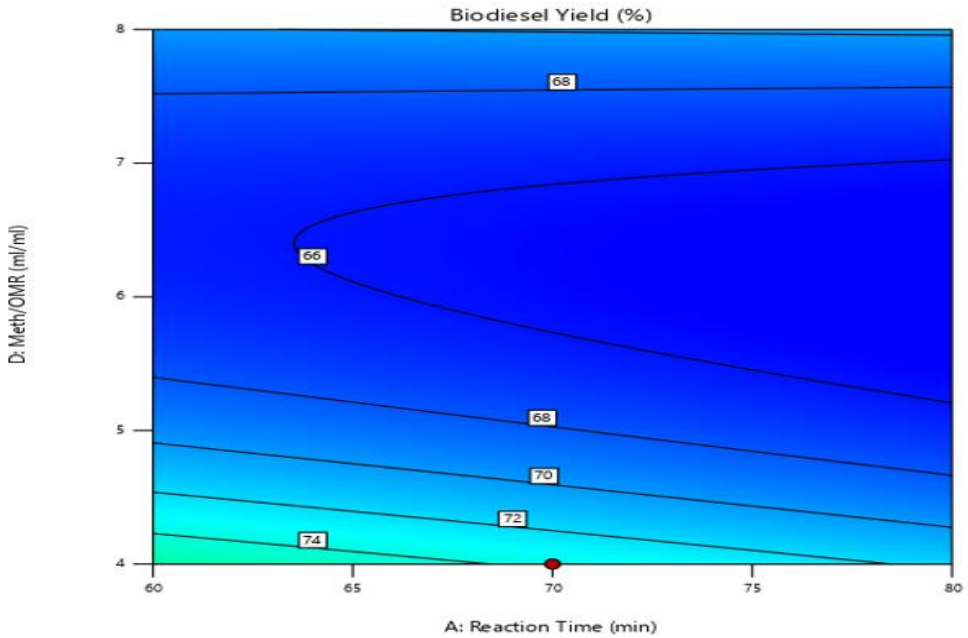

Figure 6.7: Contour plot showing the combined effect of reaction time and Meth/OMR on biodiesel yield using catalyst A

Figure 6.8 shows the interactive effect of the quantity of the catalyst and the reaction temperature on biodiesel yield. The biodiesel yield increases as the reaction temperature increases. As the reaction temperature increased from 60 ºC to 80 ºC, the biodiesel yields also increased from 65.04 % to 83.9 %. The maximum yield was also achieved at 80 ºC (83.9 %). While this trend agrees with the contour plot shown in Figure 6.7, as the reaction time was increased from 60 ºC to 80 ºC, there was also a corresponding increase in the biodiesel yield.

Also, it can be observed that as the quantity of the catalyst was increased from 1.5 wt.% to 3.5 wt.%, there was a corresponding increase in the biodiesel yield from 71.5 % to 75.5%. In this case, the optimum yield was achieved at 3.5wt.% (75.5%). The contour plot (Figure 6.9) also corroborates this trend where an increase in the catalyst amount from 1.5g to 3.5g resulted in a corresponding increase in the biodiesel yield.

It is crucial to note that the contour plot reveals elliptical curves which suggests that the relationship existing between the catalyst amount and reaction temperature is significant ($p < 0.0001$) as shown in the ANOVA quadratic model (Table 6.1), hence, this will have effect on the response (biodiesel yield).

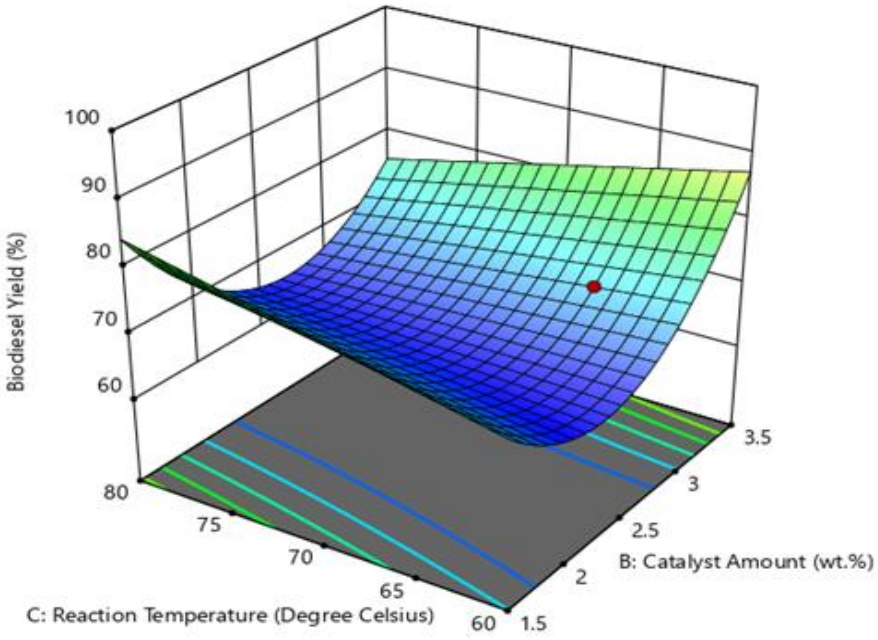

Figure 6.8: A 3-D surface plot showing the combined effect of the reaction temperature and the quantity of catalyst on biodiesel yield using catalyst A

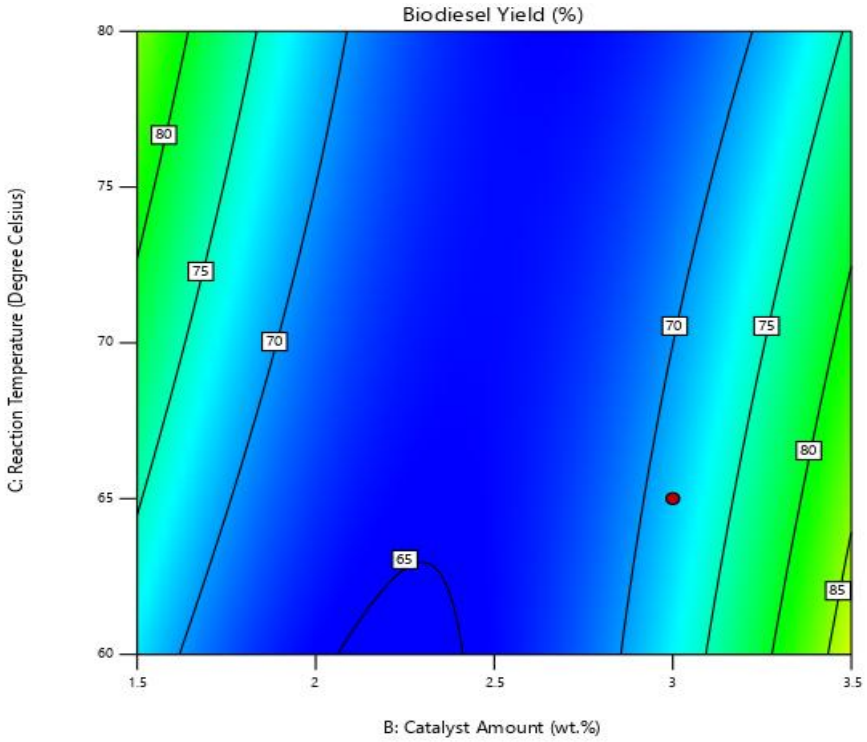

Figure 6.9: A contour plot showing the combined effect of the reaction temperature and the quantity of catalyst on biodiesel yield using catalyst A

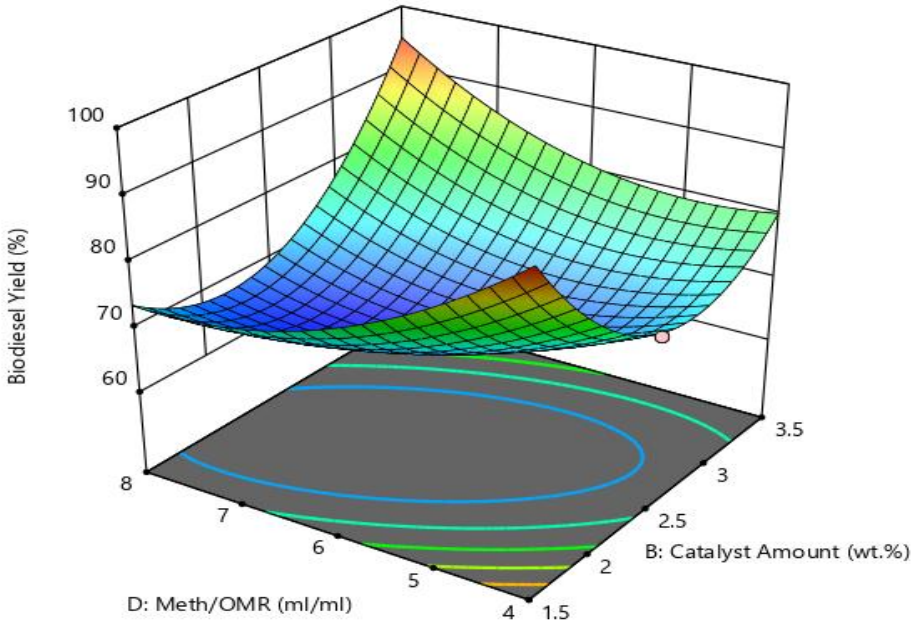

Figure 6.10: A 3-D surface plot showing a combined effect of Methanol/OMR and catalyst amount on biodiesel yield using catalyst A

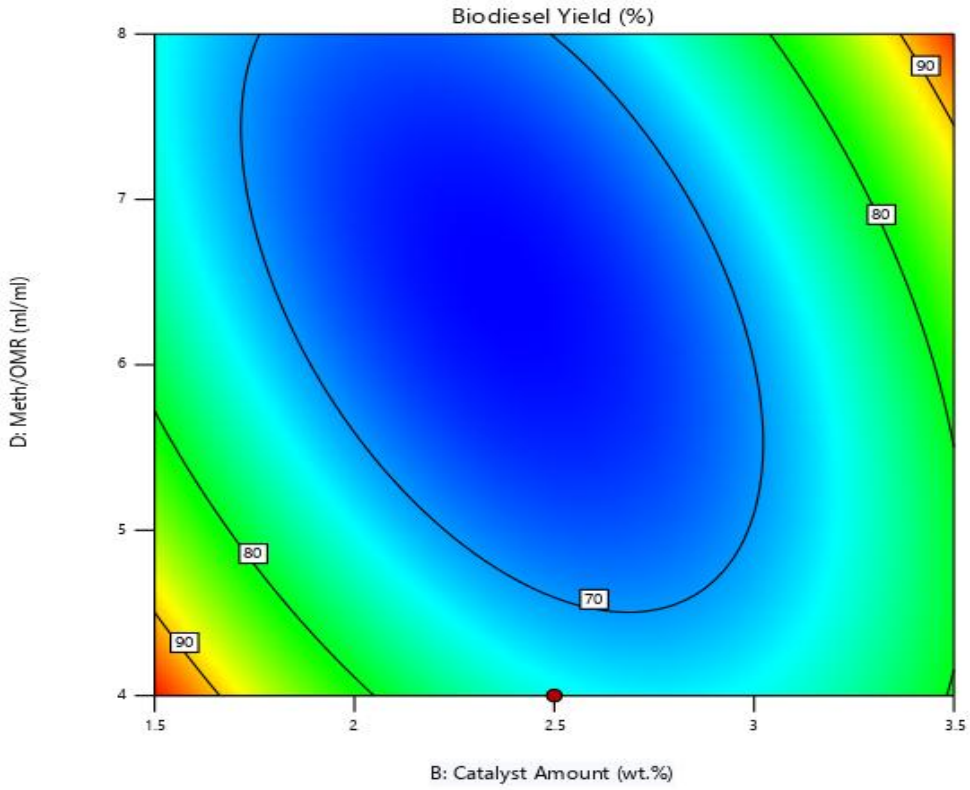

Figure 6.11: A contour plot showing combined effect of Meth/OMR and the quantity of catalyst on biodiesel yield using catalyst A

6.4 Chapter Summary

In this chapter, the yield of biodiesel as well as the effects of different process parameters such as temperature, methanol-oil molar ratio and the quantity of catalyst on biodiesel yield. The results showed that as the reaction temperature increased from 60 °C to 70 °C, there was a corresponding increase in the biodiesel yield from 77 wt.% to 83 wt.%. However, when the reaction temperature was further increased to 80 °C, the yield of biodiesel was observed to decrease significantly to 74 °C. This significant reduction in the yield of biodiesel could be attributed to the shift in the equilibrium of the reaction in which the reverse reaction is favoured culminating in the formation of side products (saponification). This has also been reported by other researchers at different reaction temperatures. However, a major limitation with the use of enzymes was the likelihood of denaturation, where the enzymes are deactivated because of the increased temperature of reaction culminating in reduced biodiesel yield.

In addition, the effect of the methanol-oil ratio on biodiesel yield was assessed in this study. The results indicate an increase in the biodiesel yield as the methanol-oil ratio was increased which suggests that the forward reaction was favoured. Other researchers, especially those with enzyme-based catalysts have reported a decline at some threshold, beyond which the reversible reaction predominates culminating in soap formation which significantly reduced the yield of biodiesel (Istiningrum *et al.,* 2017; Kasirajan *et al.,* 2021). Also, the effects of the quantity of catalyst on biodiesel yield was observed to be variable, which may be because of the influence of other contributing variables. This was confirmed by statistical analysis using linear, two-factor interactions and quadratic models. The coefficient of determination as derived from the plot of these models significantly favoured the quadratic model compared to the other models, suggesting the dependence of the yield of biodiesel on

multiparameter rather than a single parameter. These observations were also confirmed by the results of the one-way ANOVA which indicates an increase in the statistical significance values (p-values) as the models were changed from linear to quadratic.

Chapter 7

AspenPlus biodiesel process design and simulation

7. Introduction

This chapter presents the results obtained from Aspen Plus simulation of heterogeneous catalyzed biodiesel production from *Carica papaya* oil (CPO) using calcined kolanut pod husk catalyst A (CKNPH-A). The result of the Techno-Economics Analysis (TEA) of the biodiesel production is presented to demonstrate the economic feasibility of the process. The Profitability Analysis results are also presented to show the profits that could be derived from the biodiesel production plant. Finally, the sensitivity analysis results are presented to show the potential for improvement of the profitability indices of the biodiesel production process.

7.1 Process design and simulation

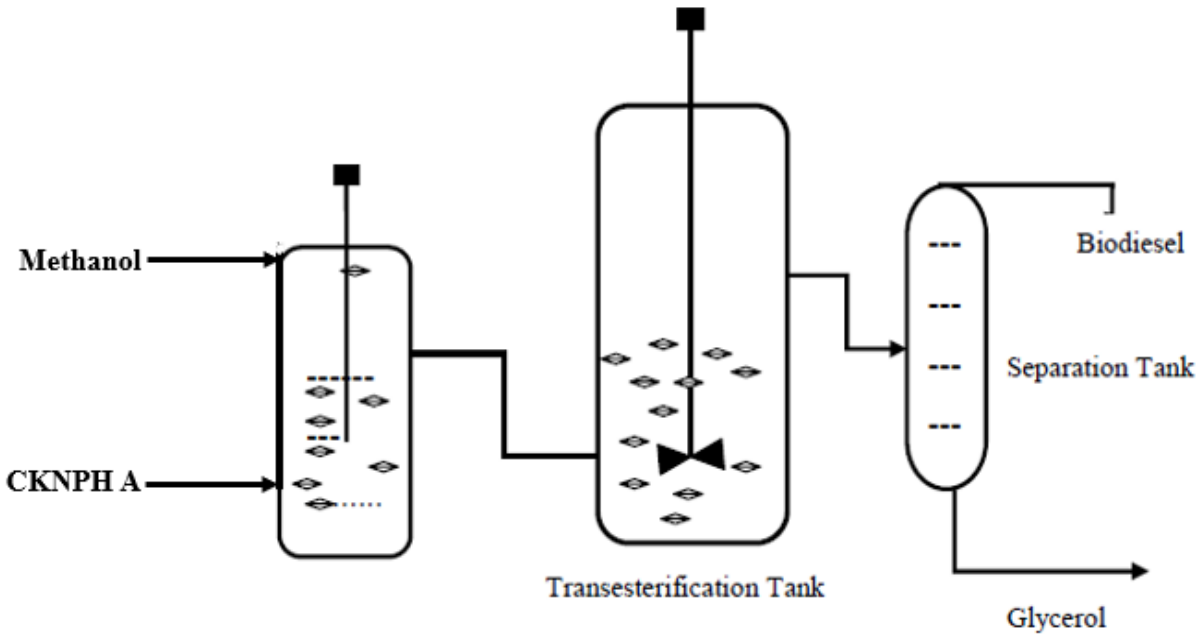

Figure 7.1: Process flow diagram of the heterogenous base-catalyzed transesterification process (Adapted from Omotola 2011)

Details of the Aspen PLUS simulation models and the results obtained are presented in the appendix section, simulation results are presented in Table 7.1.

Table 7.1: Process simulation results

Parameters	Value
Plant Capacity, kg/hr biodiesel	956.865
CPO Feed, kg/hr	1000
Methanol Feed (4:1 molar ratio), kg/hr	145.715
Catalyst Feed (2.5wt.%), kg/hr	25.000
Transesterification Reactor Biodiesel	81.709
Composition, wt.%	
Transesterification Reaction Time, min	70
Transesterification Reaction Temperature, ^{o}C	70
Transesterification Reactor Size, m^3	1.696
Transesterification Reactor Heat Duty, kJ/hr	59188.792
Glycerol purity (wt.%)	99.989
Biodiesel purity (wt.%)	99.970

Table 7.2 presents the fuel properties of the biodiesel produced experimentally in comparison to that of the simulation.

Table 7.2: Biodiesel fuel quality using catalyst CKNPH A

Fuel quality	Experimental-This study	Simulation results
Moisture Content (%)	0.0137	–
Density (g/cm^3) @ 25 ^oC	886	868.408
Kinematic Viscosity (mm^2s^{-1})	3.71	3.796
Iodine Value ($gI_2/100g$)	91.2	–
Acid Value (mg KOH/g)	0.48	–
Calorific Value (MJ/kg)	38.26	39.982
Saponification Value (mg KOH/g)	0.43	–
Cetane Number	57.63	56.830

From Table 7.2, the biodiesel density obtained from the simulation is 868.408 kg/m^3 at 25 ^oC which is close to that obtained experimentally with an absolute error of 1.99%. Also, the obtained biodiesel density from the simulation agrees with EN14214 standard quality specification required for biodiesel density which range from 860 – 900 kg/m^3. Indicating that the simulation model results agree with those obtained experimentally.

The conversion and yield obtained from the Continuous Stirred Tank Reactor (CSTR) for the simulation process are presented in Table 7.3.

Table 7.3: Transesterification and biodiesel yield

Parameters	Simulation value	Experimental value
Conversion	0.952	-
Yield (%)	95.66	96.00

Also, Table 7.3 shows that the biodiesel yield obtained from the simulation results (95.66%) is in close agreement with 96.00% obtained experimentally, suggesting that simulation model agrees with the experimental results and adequately describes the experimental process.

7.2 Techno-economics analysis

This study also carried out the Techno-Economic Analysis (TEA) of the biodiesel production process to assess the economic feasibility of the process. AspenPLUS process economic analyzer was used for the estimation of the capital investment cost while utilities and operating cost were estimated from material and energy balance from the biodiesel process flowsheet. The economic analysis of the biodiesel production process was assessed using profitability indicators such as net present value (NPV), internal rate of return (IRR), return on investment (ROI), payback period (PBP) and profitability index (PI). The TEA study was based on the economic parameters and assumption presented in Table 7.4, like those obtainable in previous studies.

Table 7.4: Economic parameters and assumptions

Parameters	Value
Operating life of plant	15 years
Operating days per year	345 days
Engineering, procurement and construction (EPC) period (40% first year and the remaining 60% second year)	2 years
Depreciation type	Straight line depreciation method
Depreciation period	13 years zero (0) salvage value
Income tax rate	35%
Production volume in first year of operation	70%
Production volume in second year of operation	90%
Ramp up production to 100%	3rd year of operation
Interest rate	10%
Unit prices of papaya oil	$0.5/kg
Unit prices of methanol (99.9%)	$0.51/kg
Unit prices of catalyst	$0.2/kg
Unit prices of glycerol	$0.7/kg
Unit prices of biodiesel	$0.8/kg

The total capital investment (CAPEX) and the operating/production cost (OPEX) of the biodiesel production plant are presented in Table 7.5. The capital investment requirement of the plant is $9,798,540 and the operating/production cost requirement is $5,216,078. The raw material cost accounted for about 85% of the operating/production of the biodiesel plant. This is consistent with the fact that the raw material cost has been reported to exceed 50% of the total production cost (Peters and Timmerhau, 1991).

Table 7.5: Total capital and operating/production cost of the biodiesel plant (Peters and Timmerhau, 1991)

Items	Value
Purchase Equipment Cost [$]	535,200
Total Installed Cost [$]	1,836,200
Total Capital Cost [$]	9,798,540
Total Raw Materials Cost [$/yr]	4,422,220
Total Utilities Cost [$/yr]	59,457
Total Operating Cost [$/yr]	5,216,078

Figure 7.2 presents the contribution of the different items that make up the operating/production. The raw material cost which comprises of papaya oil, methanol and catalyst contributes the largest cost of the operating/production cost while utilities contribute the least. This is consistent with

report from previous studies where raw material cost accounted for over 80% of biodiesel production cost (Wood *et al*., 2014; Tibesigwa *et al*., 2023).

The low utilities contribution could be attributed to low operating condition requirement and less waste generation of the heterogenous catalyzed transesterification process of the biodiesel production.

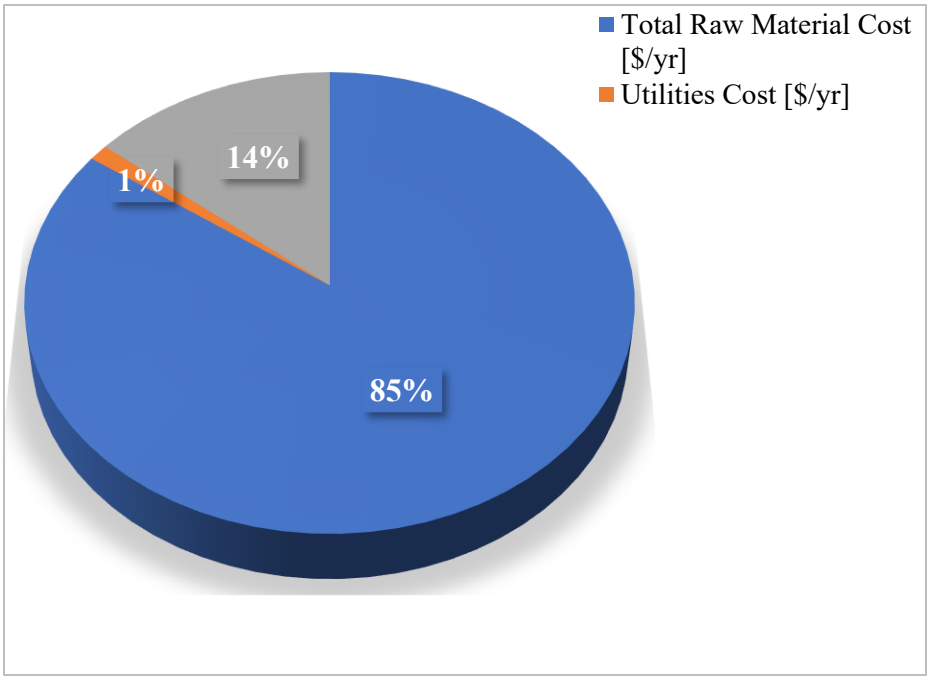

Figure 7.2: Contribution to operating/production cost

An economic analysis of the biodiesel process was conducted utilizing a 15-year operating life of the plant and 345 operating days per year (94.50 stream factor). Also, the economic assessment considers engineering, procurement and construction period of 2 years with 40% of total capital investment expended in the first year while the remaining 60% in the second year. Details of the economic analysis is presented in the Appendix while Table 7.6 present a summary of the income and expenses.

Table 7.6: Summary of income and expenses

Year	Total Production Cost [$/yr]	Revenue [$/yr]	Depreciation [$]	Profit Before Tax [$]	Tax 35% [$]	Net Income [$]	Cash Flow, CF [$]	Discounted Cash Flow [$]
1	-	-	-	-	-	-	- 3,919,415	- 3,563,105
2	-	-	-	-	-	-	- 5,879,123	- 4,858,779
3	3,651,255	5,527,404	753,734	1,122,415	392,845	729,570	1,483,304	1,114,428
4	4,694,471	7,106,662	753,734	1,658,458	580,460	1,077,998	1,831,731	1,251,097
5	5,216,078	7,896,291	753,734	1,926,479	674,268	1,252,212	2,005,945	1,245,534
6	5,216,078	7,896,291	753,734	1,926,479	674,268	1,252,212	2,005,945	1,132,304
7	5,216,078	7,896,291	753,734	1,926,479	674,268	1,252,212	2,005,945	1,029,367
8	5,216,078	7,896,291	753,734	1,926,479	674,268	1,252,212	2,005,945	935,788
9	5,216,078	7,896,291	753,734	1,926,479	674,268	1,252,212	2,005,945	850,717
10	5,216,078	7,896,291	753,734	1,926,479	674,268	1,252,212	2,005,945	773,379
11	5,216,078	7,896,291	753,734	1,926,479	674,268	1,252,212	2,005,945	703,072
12	5,216,078	7,896,291	753,734	1,926,479	674,268	1,252,212	2,005,945	639,156
13	5,216,078	7,896,291	753,734	1,926,479	674,268	1,252,212	2,005,945	581,051
14	5,216,078	7,896,291	753,734	1,926,479	674,268	1,252,212	2,005,945	528,228
15	5,216,078	7,896,291	753,734	1,926,479	674,268	1,252,212	2,005,945	480,207

Table 7.7: Profitability indicators

Profitability Indicators	Value
NPV	2,842,444
IRR	15%
ROI	10.60%
PBP [yr]	7.25
Profitability Index	1.29

7.3 Profitability analysis

To assess the profitability of investment in the biodiesel production plant, key economic indices such as NPV, IRR, ROI and PBP and profitability index were used to assess the viability of the investment. Table 7.7 presents the profitability performance of the biodiesel production process. The NPV, a key economic performance indicator of an investment that considers the time value of money and its effect on project profitability was used to assess the investment, which is the algebraic sum of the discounted values of the cash flows of each year during the life of a project (Winston, 1995). A NPV > 0 implies that the project will return more than opportunity cost of investment while a NPV < 0 implies that the project is not profitable (Ward, 1994; Couper, 2003; Anderson and Fennell, 2013). From Table 7.7, the NPV of the biodiesel production process is positive, indicating that the project is viable and profitable. Also, IRR, which is the discounted rate when NPV equals zero, was used to assess the profitability of the investment. An IRR value of 15% and ROI of 10.60% were obtained for the biodiesel production process. This implies that biodiesel production process will break even at IRR of 15%, resulting in a return on invest after tax of 10.60%. However, the ROI value for biodiesel production process is low compared to 15 - 30%, commonly considered as reasonable for investment in production processes.

Similarly, the profitability of the biodiesel production process was analyzed using payback period (PBP), which is the time required for a project to return the initial investment (Couper, 2003; Anderson and Fennell, 2013). The PBP of the biodiesel production process was found to be 7.25 years while the profitability index for the biodiesel production process is 1.29. This implies that the process is relatively profitable and that it will take 7.25 years to recover the total initial investment in the biodiesel production process. The relatively low profitability indices obtained in this study could be attributed to the low unit selling price of biodiesel and the relatively high unit price of raw material considered in this study.

7.4 Sensitivity Analysis

To assess the potential for improvement of the profitable indices of the biodiesel production process, sensitivity analysis was performed on the economic indicators. The effect of variation in biodiesel selling price and papaya oil price on the profitability indicator were analyzed. Figure 7.3 shows the effect of biodiesel selling price and papaya oil price on the profitability indices.

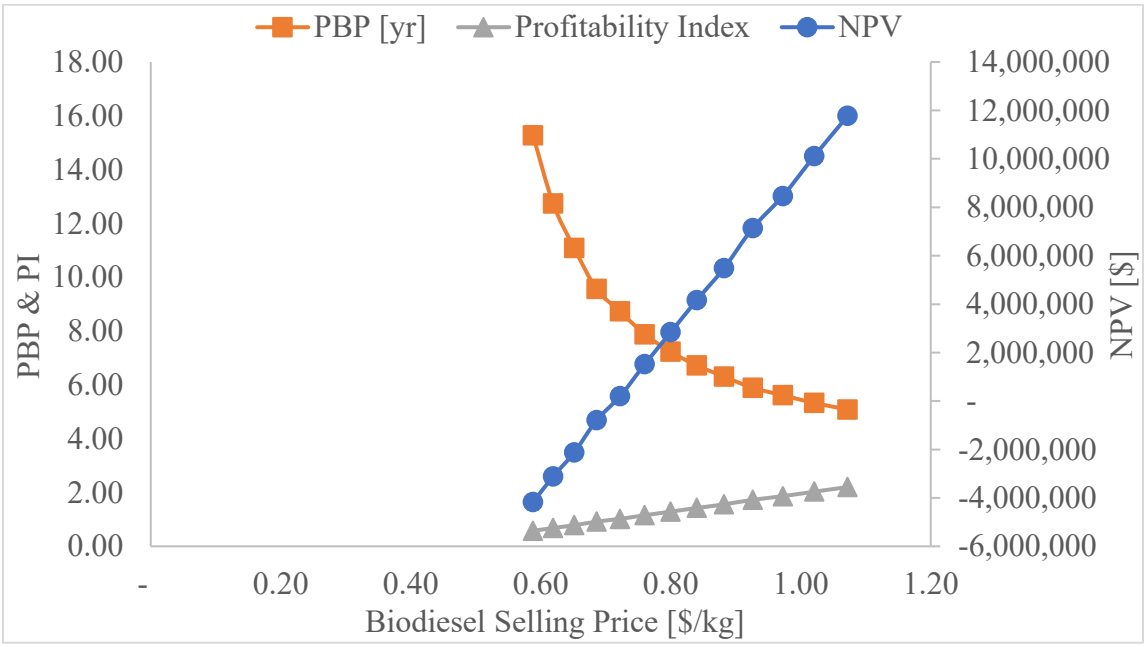

Figure 7.3: Effect of variation in selling price on NPV, PBP and Profitability Index

Figure 7.3 shows the effect of variation in biodiesel selling price from 0.59 – 1.07 $/kg on NPV, PBP and Profitability Index (PI). Decrease in biodiesel selling price below 0.8 $/kg resulted in a more unfavorable profitability indices which resulted in a negative NPV of –$795,464 and PI of 0.92 with a PBP of 9.56 years at a biodiesel selling price of 0.69 $/kg. The negative NPV and PI < 1 indicating that the project is not profitable (Ward, 1994; Couper, 2003; Anderson and Fennell, 2013).

A comparison of this estimated cost with the commercial biodiesel also known as hydrogenated vegetable oil indicates that it is less expensive compared to the commercial biodiesel which cost about 1.62-1.95 $/kg. The difference in cost might be attributed to further purification processes with the commercial biodiesel.

The Internal Rate of Return (IRR) is a valuable indicator of probability. A positive IRR indicates that the return on investment outweighs the investment cost. In this study, the IRR is observed to increase with the selling price. The value of the IRR at the basic selling price of 0.8 $/kg indicates a value of 10%. This positive value indicates that the return on investment outweighs its capital cost.

Similarly, Figure 7.4 presents the effect of variation in biodiesel selling price from 0.59 – 1.07 $/kg on internal rate of return (IRR) and return on investment (ROI). A decrease in the biodiesel selling price below 0.8 $/kg also indicates a more unfavorable profitability indices which resulted in an IRR and ROI of 8.31% and 5.01% respectively at a biodiesel selling price of 0.69 $/kg. The lower IRR and ROI demonstrate that the project is less profitable (Ward, 1994; Couper, 2003; Anderson and Fennell, 2013).

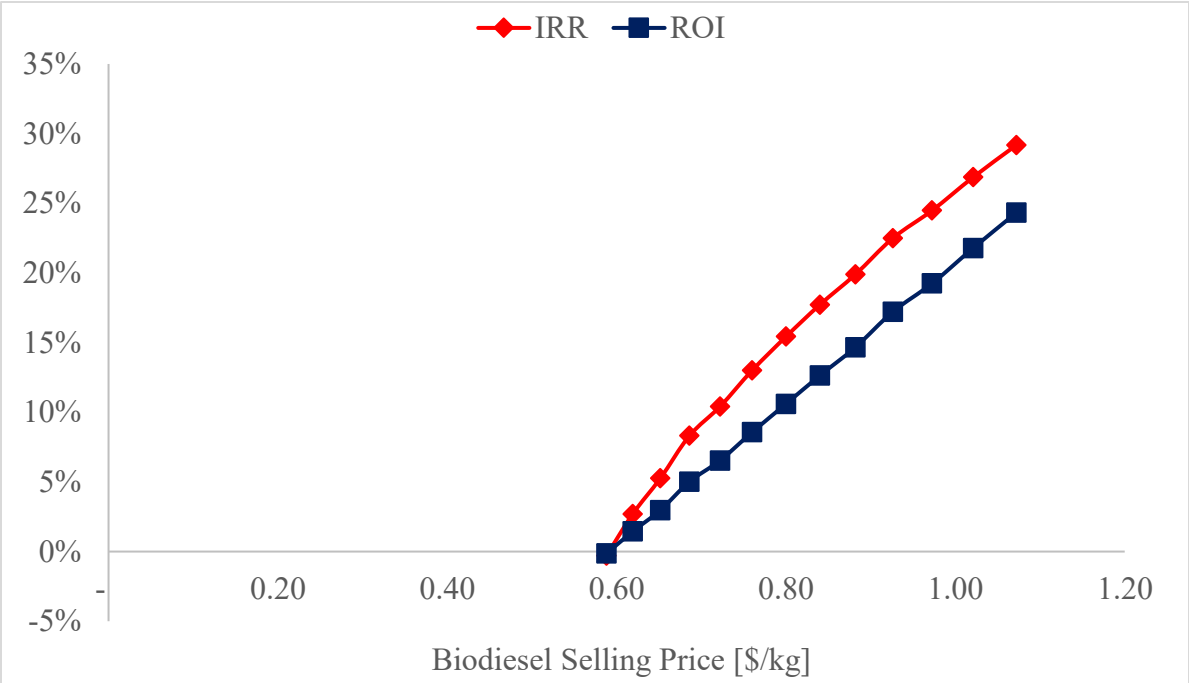

Figure 7.4: Effect of variation in selling price on IRR and ROI

Hence, biodiesel selling price below the basic selling price of 0.8 $/kg portrays a poor profitability index. For improve economic indices with a positive NPV, better PBP and PI, and at least 20% IRR and 15% ROI, the minimum biodiesel selling price must not go below 0.887 $/kg. Therefore, to attract investment in papaya oil-based biodiesel, the minimum selling price/kg must go beyond 0.887 $/kg (0.77 $/liter).

Similarly, the return on investment is an indication of how much profit can be made compared to the initial capital. A positive ROI is an indication that the returns made are higher than the capital cost. The results of the cost analysis as shown in Figure 7.4 indicate a positive return on investment of about 8% at the basic selling price of 0.8 $/kg. This implies that the returns are higher than the capital cost. These results will help to determine net present value which is an indication of profits that could be made if discounts are applied to the initial cost. Also, it will help to determine the payback period on the capital to make profits and reduce the risk of accruing high interests.

7.5 Chapter summary

The profitability analysis as well as sensitivity analysis were carried out to determine the price range of the produced biodiesel with considerable profits as well as measures of enhancing these profits if they are observed to be low or at a loss. The indices of profitability considered in this study included the net present value (NPV), the return on investment (ROI), the payback period (PBP), the internal rate of return (IRR). First, the total raw material cost was estimated to be over 80% of the production cost. An economic analysis carried out over a 15-year plant life cycle over an operation of 345 days/year revealed the following results NPV 2842, 444, IRR 15%, ROI 10.60%, PBP 7.25%, and a profitability index of 1.29.

In addition, the payback period was observed to be 7.25 years for a profitability index of 1.29 which is relatively low. This low profitability index could be attributed to the low unit selling price of biodiesel and the relatively high unit cost price of the raw materials. To enhance the profitability index, it is important that a price sensitivity analysis be carried out. The results obtained from the sensitivity analysis revealed that for the profitability index to be enhanced, the minimum selling price per kilogram of biodiesel must be above 0.887 $/kg, which is equivalent to 0.77 $/liter.

Chapter 8

Conclusions

8. Introduction

This chapter presents the key concerns raised and addressed in the previous chapters considering to what extent the laid-out objectives were actualized. The summary of the main findings and contributions made to the body of knowledge are also highlighted here. Also highlighted are likely directions and recommendations for further work.

8.1 Final conclusions

In chapter 1, two main objectives were defined to be achieved, and these have been carried out and evaluated in the results chapter 4 – chapter 7. The two objectives include: the provision of green catalysts to facilitate the conversion of waste seed oil to biodiesel and the provision of alternative and viable energy sources for achieving net zero carbon emissions. The main outcomes of this PhD study are presented below:

- ***Carica papaya* oil properties, fatty acid composition and optimization of reaction variables**

The results of the physicochemical characterization of the extracted *C. papaya* oil have been carried out and reported. The oil was observed to be predominated by unsaturated fatty acids with a value of 93.88 %. The dominance of unsaturated fatty acids implies that the oil is less prone to solidification which is highly desirable for this process. Also, this result was confirmed by the iodine value of 59.38 $gI_2/100g$ which is indicative of a high level of unsaturation. Among the different unsaturated fatty acids (UFAs), oleic acid was observed to be the predominant UFA in the oil.

Also, the oil showed high acidity values which suggests that it is inedible. It is important that the feedstock that would be employed for transesterification be unsuitable for consumption so that there will be no competition between its usage as a raw material for biodiesel production and its usage as a food ingredient. Besides, the low moisture content when compared to other reports in the literature is suggestive of a reduced possibility of soap formation which will result in improved yield of biodiesel. The cetane values, specific gravity and other physicochemical parameters were within the specified limits according to ASTM D6751 and EN 14214 standards which indicates compliance with regulations.

Statistical analysis of the effects of the parameters with respect to the oil yield indicates that all the studied parameters have some effects on the final yield of the oil. The quadratic model showed the highest correlation coefficient of 0.99 compared to the linear and the two factor interaction models. This suggests a multiple parametric effects on the oil yield rather than a single linear relationship between each parameter and the yield of oil.

- **The synthesis and properties of catalysts for biodiesel production**

In this section, the yield obtained from the preparation of the catalyst as well as the properties of the catalysts were assessed using different characterization techniques such as X-ray fluorescence spectroscopy and Energy dispersive x-ray spectroscopy for elemental analysis, powder x-ray diffraction for crystallinity, FTIR for surface functionalities, BET for surface area and porosity analysis, SEM for morphological assessment and TGA for thermal stability evaluation.

The yield of the catalysts was obtained as 11.95% after calcination at 700 °C but reduced to 7.28 % after treatment with methanol which is believed to have washed off organic impurities and a further decrease to 6.85 % after sieving. The elemental composition of the catalysts was carried out using both X-ray fluorescence spectroscopy and energy dispersive x-ray spectroscopy. Both

results indicated that the catalyst was rich in magnesium, potassium, calcium and oxygen when compared to the feedstock. However, XRF, Magnesium was not detected in the sample that was treated with methanol, but it was detected with EDX.

The results obtained from the scanning electron microscope, small pores with honeycomb-like structures were observed. This observation agreed with similar reports in the literature. The tiny pores were believed to be formed during the thermal cracking steps which is believed to be influenced by the presence of mineral oxides such as calcium oxide and potassium oxide. These were also confirmed by the BET results as the predominant pores that were observed within the mesoporous range of 2nm – 50 nm. In addition, the nitrogen adsorption isotherm showed a type IV physisorption isotherm according to IUPAC classifications which is characteristic of slit shaped pores and well-ordered materials. Moreover, the surface area of the catalysts was observed to range between 420-432.6 m^2/g, pore volume ranged between 0.25-0.26 cm^3/g and pore diameters were between 3.32-3.53 nm. Furthermore, the FTIR results indicated the presence of O-H and C-O groups with their characteristic stretching bands. The thermal stability of the catalyst was investigated from 30 °C to 900 °C. The loss in materials was observed in stages; the first stage was observed from 30 °C to 150 °C with a loss of 3.68 % representing the removal of moisture. The second stage was from 160 °C- 718 °C representing the degradation of organic matter giving a loss of 18.28 %. The breakdown of complex organic materials was believed to occur between 725 °C-890 °C resulting in a loss of 14.34%. After this stage, a loss of 43.78% was observed between 895 °C – 900 °C which could be attributed to phase transition or structural rearrangement as confirmed a change from the quartz phase to the calcite phase when assessed using powder x-ray diffraction spectroscopy.

- **Biodiesel synthesis using developed green heterogeneous catalysts**

In chapter 6, the yield of biodiesel as well as the effects of different process parameters such as temperature, methanol-oil molar ratio and the quantity of catalyst on biodiesel yield were carried out. The results showed that as the reaction temperature increased from 60 °C to 70 °C, there was a corresponding increase in the biodiesel yield from 77 wt.% to 83 wt.%. However, when the reaction temperature was further increased to 80 °C, the yield of biodiesel was observed to decrease significantly to 74 °C. This significant reduction in the yield of biodiesel could be attributed to the shift in the equilibrium of the reaction in which the reverse reaction is favoured culminating in the formation of side products (saponification). This has also been reported by other researchers at different reaction temperatures. However, a major limitation with the use of enzymes was the likelihood of denaturation, where the enzymes are deactivated because of the increased temperature of reaction culminating in reduced biodiesel yield.

In addition, the effect of the methanol-oil ratio on biodiesel yield was assessed in this study. The results indicate an increase in the biodiesel yield as the methanol-oil ratio was increased which suggests that the forward reaction was favoured. Other researchers, especially those with enzyme-based catalysts have reported a decline at some threshold, beyond which the reversible reaction predominates culminating in soap formation which significantly reduced the yield of biodiesel (Istiningrum *et al.,* 2017; Kasirajan *et al.,* 2021). Also, the effects of the quantity of catalyst on biodiesel yield was observed to be variable, which may be because of the influence of other contributing variables. This was confirmed by statistical analysis using linear, two-factor interactions and quadratic models. The coefficient of determination as derived from the plot of these models significantly favoured the quadratic model compared to the other models, suggesting the dependence of the yield of biodiesel on multiparameter rather than a single parameter. These

observations were also confirmed by the results of the one-way ANOVA which indicates an increase in the statistical significance values (p-values) as the models were changed from linear to quadratic.

- **AspenPlus biodiesel process design and simulation**

The profitability analysis as well as sensitivity analysis were carried out to determine the price range of the produced biodiesel with considerable profits as well as measures of enhancing these profits if they are observed to be low or at a loss. The indices of profitability considered in this study included the net present value (NPV), the return on investment (ROI), the payback period (PBP), the internal rate of return (IRR). First, the total raw material cost was estimated to be over 80% of the production cost. An economic analysis carried out over a 15-year plant life cycle over an operation of 345 days/year revealed the following results NPV 2842, 444, IRR 15%, ROI 10.60%, PBP 7.25%, and a profitability index of 1.29.

In addition, the payback period was observed to be 7.25 years for a profitability index of 1.29 which is relatively low. This low profitability index could be attributed to the low unit selling price of biodiesel and the relatively high unit cost price of the raw materials. To enhance the profitability index, it is important that a price sensitivity analysis be carried out. The results obtained from the sensitivity analysis revealed that for the profitability index to be enhanced, the minimum selling price per kilogram of biodiesel must be above 0.887 $/kg, which is equivalent to 0.77 $/liter.

References

Abbah, E. C., Nwandikom, G. I., Egwuonwu, C. C., and Nwakuba, N. R. (2016). Effect of reaction temperature on the yield of biodiesel from neem seed oil. *American Journal of Energy Science*, *3*(3), 16-20.

Abbaszaadeh, A., Ghobadian, B., Omidkhah, M. R., and Najafi, G. (2012). *Current biodiesel production technologies: A comparative review. Energy Conversion and Management, 63, 138–148.* doi:10.1016/j.enconman.2012.02.02

Abdulmalek, S. A., Li, K., Wang, J., Ghide, M. K., and Yan, Y. (2022). Enhanced performance of Rhizopus oryzae lipase immobilized onto a hybrid-nanocomposite matrix and its application for biodiesel production under the assistance of ultrasonic technique. *Fuel Processing Technology*, *232*, 107274.

Abdurakhman, Y. B., Putra, Z. A., Bilad, M. R., Nordin, N. A. H. M., and Wirzal, M. D. H. (2018). Techno-economic analysis of biodiesel production process from waste cooking oil using catalytic membrane reactor and realistic feed composition. *Chemical Engineering Research and Design*, *134*, 564-574.

Abrar, I., and Bhaskarwar, A. N. (2019). An overview of current trends and future scope for vegetable oil–based sustainable alternative fuels for compression ignition engines. *Second and third generation of feedstocks*, 531-556.

Abubakar, M. N., and Uthman, H. (2020). Manmasun Ndagi Abubakar; & Habibu Uthman (2020). Papaya Seed Oil as Potential for Bio–Fuel Production. African Scholar Publications & Research International, Vol. 19, No. 2, 325–336.7.

Abu-Ghazala, A. H., Abdelhady, H. H., Mazhar, A. A., and El-Deab, M. S. (2023). Exceptional room temperature catalytic transesterification of waste cooking oil to biodiesel using environmentally benign K2CO3/γ-Al2O3 nano-catalyst. *Chemical Engineering Journal*, *474*, 145784.

Adepoju, T.F., Olatunbosun, B.E., Olatunji, O.M., Ibeh M. A. Brette Pearl Spar Mable (BPSM): a potential recoverable catalyst as a renewable source of biodiesel from *Thevetia peruviana* seed oil for the benefit of sustainable development in West Africa. *Energ Sustain* 2018 https://doi.org/10.1186/s13705-018-0164-1

Adepoju, T. F. (2020). Optimization processes of biodiesel production from pig and neem (*Azadirachta indica a. Juss*) seeds blend oil using alternative catalysts from waste biomass. *Industrial crops and products*, *149*, 112334.

Adepoju, T. F., Ibeh, M. A., Babatunde, E. O., Asuquo, A. J., and Abegunde, G. S. (2020). Appraisal of CaO derived from waste fermented-unfermented kola nut pod for fatty acid

methylester (FAME) synthesis from *Butyrospermum parkii* (Shea butter) oil. *South African Journal of Chemical Engineering*, *33*, 160-171.

Adepoju, T. F., Ibeh, M. A., Udoetuk, E. N., and Babatunde, E. O. (2021). Quaternary blend of *Carica papaya-Citrus sinesis-Hibiscus sabdariffa*-Waste used oil for biodiesel synthesis using CaO-based catalyst derived from binary mix of Lattorina littorea and Mactra coralline shell. *Renewable Energy*, *171*, 22-33.

Adepoju, T. F., Olatunji, O. M., Ibeh, M. A., Salam, K. A., Olatunbosun, B. E., and Asuquo, A. J. (2020). *Heavea brasiliensis* (Rubber seed): An alternative source of renewable energy. *Scientific African*, *8*, e00339.

Adepoju, T. F., Rasheed, B., Olatunji, O. M., Ibeh, M. A., Ademiluyi, F. T., and Olatunbosun, B. E. (2018). Modeling and optimization of lucky nut biodiesel production from lucky nut seed by pearl spar catalysed transesterification. *Heliyon*, *4*(9).

Aderibigbe, F. A., Saka, H. B., Mustapha, S. I., Amosa, M. K., Shiru, S., Tijani, I. A., ... and Bello, B. T. (2023). Waste Cooking Oil Conversion to Biodiesel Using Solid Bifunctional Catalysts. *ChemBioEng Reviews*, *10* (3), 293-310.

Aderibigbe, F. A., Shiru, S., Saka, H. B., Amosa, M. K., Mustapha, S. I., Alhassan, M. I., ... and Owolabi, R. U. (2021). Heterogeneous catalysis of second generation oil for biodiesel production: A review. *ChemBioEng Reviews*, *8*(2), 78-89.

Agrawal, B. N., Sinha, S., Kuzmin, A. V., and Pinchuk, V. A. (2019). Effect of vegetable oil share on combustion characteristics and thermal efficiency of diesel engine fueled with different blends. *Thermal Science and Engineering Progress*, *14*, 100404.

Agu, O. S., Tabil, L. G., and Dumonceaux, T. (2021). Enzymatic saccharification of canola straw and oat hull subjected to microwave-assisted alkali pretreatment. *Alkaline Chemistry and Applications*, 29-44.

Agunbiade, F. O., and Adewole, T. A. (2014). Methanolysis of Carica Papaya Seed Oil for Production of Biodiesel. *Journal of Fuels, 2014*, 1-6. doi:10.1155/2014/904076

Ahmed, A., Ali, A., Mubashir, M., Lim, H. R., Khoo, K. S., and Show, P. L. (2023). Process optimization and simulation of biodiesel synthesis from waste cooking oil through supercritical transesterification reaction without catalyst. *Journal of Physics: Energy*, *5*(2), 024003.

Ahmed, M., Abdullah, A., Laskar, A., Patle, D. S., Vo, D. V. N., and Ahmad, Z. (2022). Process simulation and stochastic multiobjective optimisation of homogeneously acid-catalysed microalgal in-situ biodiesel production considering economic and environmental criteria. *Fuel*, *327*, 125165.

Alagu, R. M., and Sundaram, E. G. (2018). Preparation and characterization of pyrolytic oil through pyrolysis of neem seed and study of performance, combustion and emission characteristics in CI engine. *Journal of the Energy Institute*, *91*(1), 100-109.

Aleman-Ramirez, J. L., Moreira, J., Torres-Arellano, S., Longoria, A., Okoye, P. U., and Sebastian, P. J. (2021). Preparation of a heterogeneous catalyst from moringa leaves as a sustainable precursor for biodiesel production. *Fuel*, *284*, 118983.

Alvarez-Chavez, B. J., Godbout, S., Palacios-Rios, J. H., Le Roux, E., and Raghavan, V. (2019). Physical, chemical, thermal and biological pre-treatment technologies in fast pyrolysis to maximize bio-oil quality: A critical review. *Biomass and Bioenergy*, *128*, 105333.

Ambat, I., Srivastava, V., and Sillanpää, M. (2018). Recent advancement in biodiesel production methodologies using various feedstock: A review. *Renewable and sustainable energy reviews*, *90*, 356-369.

Amiruddin, M. I., Mashuri, S. I. S., Mutalib, A. A. A., Chayed, N. F., Rashid, U., and Ibrahim, M. L. (2021). Potential of advanced photocatalytic technology for biodiesel production from waste oil. In *Advanced Technology for the Conversion of Waste into Fuels and Chemicals* (pp. 49-76). Woodhead Publishing.

Anbarasan, P. M., Priyadharsini, C. I., Sathiyapriya, R., Hariharan, V., Parabakaran, K., and Aroulmoji, V. (2019). Development of TiO2 Nanomaterials and Dyes Selection (using DFT) for DSSC Applications–A Stepwise Review. *International journal of advanced Science and Engineering*, *6*(02), 1326-1350.

Anderson, J. and Fennell, A. (2013). Calculate Financial Indicators to Guide Investment. American Institute of Chemical Engineering (AIChE): 34 – 40. www.aiche.org.cep.

Andreo-Martínez, P., Ortiz-Martínez, V. M., García-Martínez, N., de los Ríos, A. P., Hernández-Fernández, F. J., and Quesada-Medina, J. (2020). Production of biodiesel under supercritical conditions: State of the art and bibliometric analysis. *Applied Energy*, *264*, 114753.

Anis, S., Alhakim, R., Khoiron, A. M., and Kusumastuti, A. (2021). Microwave-assisted pyrolysis and distillation of cooking oils for liquid bio-fuel production. *Journal of Analytical and Applied Pyrolysis*, *154*, 105014.

Aransiola, E. F., Ehinmitola, E. O., Adebimpe, A. I., Shittu, T. D., and Solomon, B. O. (2019). Prospects of biodiesel feedstock as an effective ecofuel source and their challenges. *Advances in Eco-Fuels for a Sustainable Environment*, 53-87.

Ariwaodo, J. O., Obidike-Ugwu, E. O., Ugwu, R. A., and Ezekwe, C. O. (2020). Checklist of Tree species of Humid Forest Research Station, Forestry Research Institute of Nigeria (FRIN), Umuahia, Abia State, Nigeria. *Ethiopian Journal of Environmental Studies and Management*, *13*(6), 707-718.

Arshad, S., Ahmad, M., Munir, M., Sultana, S., Zafar, M., Dawood, S., ... and Show, P. L. (2023). Assessing the potential of green CdO2 nano-catalyst for the synthesis of biodiesel using non-edible seed oil of Malabar Ebony. *Fuel*, *333*, 126492.

Asogwa, E. U., Otuonye, A. H., Oluyole, K. A., Ndubuaku, T.C.N., Uwagboe, E.U. (2012). Kolanut production, processing and marketing in the southeastern states of Nigeria. American-Eurasian J. Agric. & Environ. Sci., 12 (4): 463-468.

Asogwa, E. U., Anikwe, J. C., and Mokwunye, F. C. (2021). Kola production and utilization for economic development. *African Scientist*, *7*(4).

Ateş, F., and Yaşar, B. (2021). Utilization of date palm stones for bio-oil and char production using flash and fast pyrolysis. *Biomass Conversion and Biorefinery*, 1-13.

Athar, M., and Zaidi, S. (2020). A review of the feedstocks, catalysts, and intensification techniques for sustainable biodiesel production. *Journal of Environmental Chemical Engineering*, *8*(6), 104523.

Athar, M., Zaidi, S., and Hassan, S. Z. (2020). Intensification and optimization of biodiesel production using microwave-assisted acid-organo catalyzed transesterification process. *Scientific Reports*, *10*(1), 21239.

Avagyan, A. B., and Singh, B. (2019). Biodiesel: feedstocks, technologies, economics and barriers. *Assessment of Environmental Impact in Producing and Using Chains. Assessment of Environmental Impact in Producing and Using Chains*.

Awogbemi, O., Von Kallon, D. V., and Aigbodion, V. S. (2021). Trends in the development and utilization of agricultural wastes as heterogeneous catalyst for biodiesel production. *Journal of the Energy Institute*, *98*, 244-258.

Babadi, A. A., Rahmati, S., Fakhlaei, R., Barati, B., Wang, S., Doherty, W., and Ostrikov, K. K. (2022). Emerging technologies for biodiesel production: processes, challenges, and opportunities. *Biomass and Bioenergy*, *163*, 106521.

Babatunde, B.B. and R.A. Hamzat, (2005). Effects of feeding graded levels of kolanut husk meal on the performance of cockerels. Nigerian Journal of Animal Production. 32(1): 61-66.

Bahadi, M., Salimon, J., and Derawi, D. (2021). Synthesis of di-trimethylolpropane tetraester-based biolubricant from Elaeis guineensis kernel oil via homogeneous acid-catalyzed transesterification. *Renewable Energy*, *171*, 981-993.

Balajii, M., and Niju, S. (2019). A novel biobased heterogeneous catalyst derived from Musa acuminata peduncle for biodiesel production–Process optimization using central composite design. *Energy Conversion and Management*, *189*, 118-131.

Balajii, M., and Niju, S. (2020). Banana peduncle–A green and renewable heterogeneous base catalyst for biodiesel production from Ceiba pentandra oil. *Renewable Energy*, *146*, 2255-2269.

Barnwal, B. K., and Sharma, M. P. (2005). Prospects of biodiesel production from vegetable oils in India. *Renewable and sustainable energy reviews*, *9*(4), 363-378.

Beattie, G.B., 1970. soft drink flavors. Their history and characteristics. 1 cola or kola flavors. The flavor Industry. pp: 390-394.

Betiku, E., and Ishola, N. B. (2020). Optimization of sorrel oil biodiesel production by base heterogeneous catalyst from kola nut pod husk: Neural intelligence-genetic algorithm versus neuro-fuzzy-genetic algorithm. *Environmental Progress & Sustainable Energy*, *39*(4), e13393.

Betiku, E., Etim, A. O., Pereore, O., Ojumu, T. V. (2017). Two-step conversion of neem seed (Azadirachta indica) oil into fatty methyl esters using a bio-base catalyst: An example of cocoa pod husk. *Energy Fuel, 31*, 6182–6193.

Betiku, E., Okeleye, A. A., Ishola, N. B., Osunleke, A. S., and Ojumu, T. V. (2019). Development of a novel mesoporous biocatalyst derived from kola nut pod husk for conversion of kariya seed oil to methyl esters: A case of synthesis, modeling and optimization studies. *Catalysis Letters*, *149*, 1772-1787.

Bhowmik, D. (2020). Global Carbon di Oxide Emissions in Hamilton Filter Model. *International Journal of Environment, Agriculture and Biotechnology*, *5*(5).

Bi, X., Yao, N., Meng, X., Gou, M., and Zhao, P. (2021). MnCO 3-Catalyzed Transesterification of Alcohols with Dimethyl Carbonate Under Mild Conditions. *Catalysis Letters*, *151*, 454-462.

Bothon, F. T., Montcho, P. S., Nonviho, G., Agbangnan Dossa, C. P., Tchiakpe, L., Adomou, A. A., and Avlessi, F. (2020). Physicochemical variability and biodiesel potential of seed oils of two Hibiscus sabdariffa L. phenotypes. *ACS omega*, *5*(40), 25561-25567.

Brahma, S., Nath, B., Basumatary, B., Das, B., Saikia, P., Patir, K., and Basumatary, S. (2022). Biodiesel production from mixed oils: A sustainable approach towards industrial biofuel production. *Chemical Engineering Journal Advances*, *10*, 100284.

Brambila, C., Boyd, P., Keegan, A., Sharma, P., Vetter, C., Ponnusamy, E., and Patwardhan, S. V. (2022). A comparison of environmental impact of various silicas using a green chemistry evaluator. *ACS Sustainable Chemistry & Engineering*, *10*(16), 5288-5298.

Buasri, A., and Loryuenyong, V. (2017). *Application of waste materials as a heterogeneous catalyst for biodiesel production from Jatropha Curcas oil via microwave irradiation. Materials Today: Proceedings, 4(5), 6051–6059.* doi:10.1016/j.matpr.2017.06.093

Bukkarapu, K. R., and Krishnasamy, A. (2022). A critical review on available models to predict engine fuel properties of biodiesel. *Renewable and Sustainable Energy Reviews*, *155*, 111925.

Cardoso, B. J., Rodrigues, E., Gaspar, A. R., and Gomes, A. (2021). Energy performance factors in wastewater treatment plants: A review. *Journal of Cleaner Production*, *322*, 129107.

Carlucci, C. (2022). An overview on the production of biodiesel enabled by continuous flow methodologies. *Catalysts*, *12*(7), 717.

Cavalcante, F. T. T., Neto, F. S., de Aguiar Falcão, I. R., da Silva Souza, J. E., de Moura Junior, L. S., da Silva Sousa, P., ... and dos Santos, J. C. (2021). Opportunities for improving biodiesel production via lipase catalysis. *Fuel*, *288*, 119577.

Cavalheiro, L. F., Misutsu, M. Y., Rial, R. C., Viana, L. H., and Oliveira, L. C. S. (2020). Characterization of residues and evaluation of the physico chemical properties of soybean biodiesel and biodiesel: Diesel blends in different storage conditions. *Renewable Energy*, *151*, 454-462.

Chanakaewsomboon, I., Phoungthong, K., Palamanit, A., Seechamnanturakit, V., and Cheng, C. K. (2021). Biodiesel produced using potassium methoxide homogeneous alkaline catalyst: Effects of various factors on soap formation. *Biomass Conversion and Biorefinery*, 1-11.

Changmai, B., Vanlalveni, C., Ingle, A. P., Bhagat, R., and Rokhum, S. L. (2020). Widely used catalysts in biodiesel production: a review. *RSC advances*, *10*(68), 41625-41679.

Cheng, J., Mao, Y., Guo, H., Qian, L., Shao, Y., Yang, W., and Park, J. Y. (2022). Synergistic and efficient catalysis over Brønsted acidic ionic liquid [BSO3HMIm][HSO4]–modified metal–organic framework (IRMOF-3) for microalgal biodiesel production. *Fuel*, *322*, 124217.

Chin, L. H., Hameed, B. H., and Ahmad, A. L. (2009). Process optimization for biodiesel production from waste cooking palm oil (Elaeis guineensis) using response surface methodology. *Energy & Fuels*, *23*(2), 1040-1044.

Chinyere, B.E., Callistus, N.U., Okechuckwu, D.O. (2017). Optimization of the methanolysis of lard oil in the production of biodiesel with response surface methodology. *Egyptian Journal of Petroleum, 26*, 1001-1011.

Climate Action Tracker net zero target evaluations (2023). Net-zero Targets. Accessed on 12 October 2024 @ CAT net zero target evaluations | Climate Action Tracker

Chong, C. C., Aqsha, A., Ayoub, M., Sajid, M., Abdullah, A. Z., Yusup, S., and Abdullah, B. (2020). A review over the role of catalysts for selective short-chain polyglycerol production from biodiesel derived waste glycerol. *Environmental Technology & Innovation*, *19*, 100859.

Cieh, N. L., Mokhtar, M. N., Baharuddin, A. S., Mohammed, M. A. P., and Wakisaka, M. (2023). Progress on lipase immobilization technology in edible oil and fat modifications. *Food Reviews International*, 1-47.

Couper, J. R. (2003). *Process Engineering Economics*, Mercel Deker, Inc., New York, USA: 233 – 249. http://www.dekker.com

Danbaba, N., Nkama, I., and Badau, M. H. (2015). Application of response surface methodology (RSM) and central composite design (CCD) to optimize minerals composition of rice-cowpea composite blends during extrusion cooking. *International Journal of Food Science and Nutrition Engineering*, *5*(1), 40-52.

de Oliveira, A. S. K., Lopes, A. M. S., Barbosa, F. F., da Silva, F. I., de Sousa, J. A., Pontes, L. A. M., ... and Braga, T. P. (2022). Restraining deactivation of β-zeolite by modifying with MgAl2O4 spinel in gas-phase glycerol dehydration. *Molecular Catalysis*, *527*, 112414.

Dehghan, L., Golmakani, M. T., and Hosseini, S. M. H. (2019). Optimization of microwave-assisted accelerated transesterification of inedible olive oil for biodiesel production. *Renewable Energy*, *138*, 915-922.

Dehhaghi, M., Panahi, H. K. S., Aghbashlo, M., Lam, S. S., and Tabatabaei, M. (2021). The effects of nanoadditives on the performance and emission characteristics of spark-ignition gasoline engines: A critical review with a focus on health impacts. *Energy*, *225*, 120259.

Demirbas, A. (2005). Biodiesel production from vegetable oils via catalytic and non-catalytic supercritical methanol transesterification methods. *Progress in energy and combustion science*, *31*(5-6), 466-487.

Demirbas, A. (2009). Progress and Recent Trends in Biodiesel Fuels. *Energy Conversion and Management, 50* (1), 14-34.

Department for Energy Security and Net Zero (2025). 2023 UK Greenhouse Gas Emissions, Final Figures. https://assets.publishing.service.gov.uk/media/67a30e4f7da1f1ac64e5feb1/2023-final-greenhouse-gas-emissions-statistical-release.pdf. Accessed on 15 September 2025.

Department for Business, Energy and Industrial Strategy (2019). Contributions of each sector to the total greenhouse gas emissions in the UK. Accessed 15 September 2025 @ Greenhouse gas emissions: agriculture | AHDB

Devarajan, Y., Munuswamy, D. B., Subbiah, G., Vellaiyan, S., Nagappan, B., Varuvel, E. G., and Thangaraja, J. (2022). Inedible oil feedstocks for biodiesel production: A review of production technologies and physicochemical properties. *Sustainable Chemistry and Pharmacy*, *30*, 100840.

Dhinagaran, G., Vijayakumar, G., Prashanna Suvaitha, S., Harichandran, G., and Venkatachalam, K. (2023). Conversion of Neem Oil (Azadirachta indica) to Biodiesel over SBA-15 Supported Sulphated Zirconia Catalysts. *Catalysis Letters*, 1-16.

Dmitrienko, M. A., Nyashina, G. S., and Strizhak, P. A. (2017). Environmental indicators of the combustion of prospective coal water slurry containing petrochemicals. *Journal of Hazardous Materials*, *338*, 148-159.

Domingos, A. K., Saad, E. B., Wilhelm, H. M., and Ramos, L. P. (2008). Optimization of the ethanolysis of Raphanus sativus (L. Var.) crude oil applying the response surface methodology. *Bioresource Technology*, *99*(6), 1837-1845.

Dwivedi, S., Jaiswal, S., and Kushwaha, A. (2022). Renewable Biofuel Resources: Introduction, Production Technologies, Challenges, and Applications. *Bio-Clean Energy Technologies Volume 2*, 27-52.

Edgar, T. F., Himmelblau, D. M., and Lasdon, L. S. (2001). Optimization of chemical processes. 2nd ed. New York: McGraw-Hill Higher.

Eijnatten, C.L.M. Van. (1973). Kola: A review of the literature. Tropical Abstracts. 28(8): 1-10.

Eijnatten, C.L.M. Van. (1969). Kola. Its botany and cultivation. *Communication* No. 59. Roy. Trop. Inst. Amsterdam. pp:100.

Elavazhagan, E., Sowmiya, A., and Sivalingam, S. (2023). Comprehensive analysis and process simulation of biodiesel production from biomass sources. *Indian Journal of Chemical Technology (IJCT)*, *30*(5), 623-633.

Elgharbawy, A. A., Moniruzzaman, M., and Goto, M. (2020). Recent advances of enzymatic reactions in ionic liquids: Part II. *Biochemical Engineering Journal*, *154*, 107426.

Elgharbawy, A. S., Sadik, W., Sadek, O. M., and Kasaby, M. A. (2021). A review on biodiesel feedstocks and production technologies. *Journal of the Chilean Chemical Society*, *66*(1), 5098-5109.

Fallah, A., Kamran-Pirzaman, A., and Gholipour Zanjani, N. (2023). The sono-physical effect of cavitation bubbles on homogeneous catalyzed biodiesel production. *Biomass Conversion and Biorefinery*, *13*(6), 5339-5351.

Falowo, O. A., and Betiku, E. (2022). A novel heterogeneous catalyst synthesis from agrowastes mixture and application in transesterification of yellow oleander-rubber oil: Optimization by Taguchi approach. *Fuel*, *312*, 122999.

Falowo, O. A., Ojumu, T. V., Pereao, O., and Betiku, E. (2020). Sustainable biodiesel synthesis from honne-rubber-neem oil blend with a novel mesoporous base catalyst synthesized from a mixture of three agrowastes. *Catalysts*, *10*(2), 190.

Falowo, O. A., Oloko-Oba, M. I., and Betiku, E. (2019). Biodiesel production intensification via microwave irradiation-assisted transesterification of oil blend using nanoparticles from elephant-ear tree pod husk as a base heterogeneous catalyst. *Chemical Engineering and Processing-Process Intensification*, *140*, 157-170.

Faruque, M. O., Razzak, S. A., and Hossain, M. M. (2020). Application of heterogeneous catalysts for biodiesel production from microalgal oil-a review. *Catalysts*, *10*(9), 1025.

Faruque, M. O., Razzak, S. A., and Hossain, M. M. (2020). Application of heterogeneous catalysts for biodiesel production from microalgal oil—a review. *Catalysts*, *10*(9), 1025.

Fattah, I. R., Masjuki, H. H., Kalam, M. A., Wakil, M. A., Rashedul, H. K., and Abedin, M. J. (2014). Performance and emission characteristics of a CI engine fueled with Cocos nucifera and Jatropha curcas B20 blends accompanying antioxidants. *Industrial crops and products*, *57*, 132-140.

Fevzi Y. (2020). Comparison of fuel properties of biodiesel fuels produced from different oils to determine the most suitable feedstock type. Fuel 264, 116817.

Figueiredo, J.S.B., Alves, B.T.S., Freire, Alves, J.J.N., Barbosa, B.V.S. (2022*)* Preparation, characterization and evaluation of x-MoO_3/Al-SBA-15 catalysts for biodiesel production. *Mater Renew Sustain Energy* **11**, 17–31. https://doi.org/10.1007/s40243-021-00204-x

Folayan, A. J., Anawe, P. A. L., Aladejare, A. E., and Ayeni, A. O. (2019). Experimental investigation of the effect of fatty acids configuration, chain length, branching and degree of unsaturation on biodiesel fuel properties obtained from lauric oils, high-oleic and high-linoleic vegetable oil biomass. *Energy Reports*, *5*, 793-806.

Gao, C., Huang, D., Chang, X., and Xi, H. (2020). Meso-damage mechanism of strength and deformation characteristics of typical sandstone in Xinwen coalfield. *Symmetry*, *12*(11), 1815.

Garg, R., Sabouni, R., and Ahmadipour, M. (2023). From waste to fuel: Challenging aspects in sustainable biodiesel production from lignocellulosic biomass feedstocks and role of metal organic framework as innovative heterogeneous catalysts. *Industrial Crops and Products*, *206*, 117554.

Gbashi, S. M., Omenka, I. K., and Nwankwo, K. N. (2019). Effect of Extraction Method on the Functional Properties of Oils of Selected Oilseeds as Potential Feedstock for Biodiesel Production.

Ge, J. C., Kim, H. Y., Yoon, S. K., and Choi, N. J. (2020). Optimization of palm oil biodiesel blends and engine operating parameters to improve performance and PM morphology in a common rail direct injection diesel engine. *Fuel*, *260*, 116326.

Gebremariam, S. N. (2021). Technoeconomic Analysis of Biodiesel Production Using Different Feedstocks. *Nano-and Biocatalysts for Biodiesel Production*, 313-337.

Gebremariam, S. N., and Marchetti, J. M. (2018). Economics of biodiesel production. *Energy Conversion and Management*, *168*, 74-84.

Gebremariam, S. N., and Marchetti, J. M. (2021). Biodiesel production process using solid acid catalyst: influence of market variables on the process's economic feasibility. *Biofuels, Bioproducts and Biorefining*, *15*(3), 815-824.

Gebremariam, S.N and Marchetti, J.M. (2017). Biodiesel production technologies: review. *AIMS Energy, 5* (3), 425-457.

Ghedini, E., Taghavi, S., Menegazzo, F., and Signoretto, M. (2021). A review on the efficient catalysts for algae transesterification to biodiesel. *Sustainability*, *13*(18), 10479.

Ghesti, G. F., de Macedo, J. L., Parente, V. C. I., Dias, J. A., and Dias, S. C. L. (2009). Synthesis, characterization and reactivity of Lewis acid/surfactant cerium trisdodecylsulfate catalyst for transesterification and esterification reactions. *Applied Catalysis A: General*, *355*(1-2), 139-147.

Gholami, A., Pourfayaz, F., and Maleki, A. (2021). Techno-economic assessment of biodiesel production from canola oil through ultrasonic cavitation. *Energy Reports*, *7*, 266-277.

Ghosh, N., Rhithuparna, D., Rokhum, S. L., and Halder, G. (2023). Ethical issues pertaining to sustainable biodiesel synthesis over trans/esterification process. *Sustainable Chemistry and Pharmacy*, *33*, 101123.

Glisic, S. B., and Orlović, A. M. (2014). Review of biodiesel synthesis from waste oil under elevated pressure and temperature: Phase equilibrium, reaction kinetics, process design and techno-economic study. *Renewable and Sustainable Energy Reviews*, *31*, 708-725.

Gmehling, J., Kleiber, M., Kolbe, B., and Rarey, J. (2019). *Chemical thermodynamics for process simulation*. John Wiley & Sons.

Gogoaşă, C. I., Răducanu, C. E., Petraş, L. E., Cioroiu Tîrpan, D. R., Vasilievici, G., Mîrţ, A. L., ... and Pârvulescu, O. C. (2023). Bacterial Cellulose and Biodegradable Superbase for Heterogeneous Transesterification to Alkyl Esters. *Catalysts*, *13*(11), 1431.

Gohain, M., Devi, A., and Deka, D. (2017). Musa balbisiana Colla peel as highly effective renewable heterogeneous base catalyst for biodiesel production. *Industrial Crops and Products*, *109*, 8-18.

Gomez-Rodriguez, K. A., Chavarria-Hernandez, J. C., and Martinez-Tapia, G. E. (2021). Estimation of cold flow properties of biodiesel from fatty acid composition. *Energy & Fuels*, *35*(2), 1442-1448.

Gonçalves, P. C., Monteiro, L. P. C., and de Sousa Santos, L. (2020). Multi-objective optimization of a biodiesel production process using process simulation. *Journal of Cleaner Production*, *270*, 122322.

Günay, M. E., Türker, L., and Tapan, N. A. (2019). Significant parameters and technological advancements in biodiesel production systems. *Fuel*, *250*, 27-41.

Gupta, V., and Singh, K. P. (2023). The impact of heterogeneous catalyst on biodiesel production; a review. *Materials Today: Proceedings*, *78*, 364-371.

Hoekman, S. K., Broch, A., Robbins, C,m Ceniceros, E., Natarajan, M. (2012). Review of biodiesel composition, properties and specifications. Renewable and Sustainable Energy Reviews, 16(1): 143-169.

Hajek, M., Vavra, A., Skopal, F., Strakova, A. and Douda, M. (2020). The description of catalyst behaviour during transesterification of rapeseed oil-Formation of micellar emulsion. Renewable energy, 159:938-943.

Haghighat, M., Majidian, N., and Hallajisani, A. (2020). Production of bio-oil from sewage sludge: A review on the thermal and catalytic conversion by pyrolysis. *Sustainable Energy Technologies and Assessments*, *42*, 100870.

Haldar, S. K., Ghosh, B. B., and Nag, A. (2009). Utilization of unattended Putranjiva roxburghii non-edible oil as fuel in diesel engine. *Renewable energy*, *34*(1), 343-347.

Hasanah, M.G., Jalal deen, M.N., Bangun, P.N., Kamariah, L., and Noorzianna, A.Y. (2014). Physiochemical Characterization of Papaya (Carica Papaya L.) Seed Oil of the Hong Kong/ Sekaki Variety. *Journal of Oleo Science, 63* (9), 885- 892.

Hassan, T., Rahman, M. M., Rahman, M. A., and Nabi, M. N. (2022). Opportunities and challenges for the application of biodiesel as automotive fuel in the 21st century. *Biofuels, Bioproducts and Biorefining*, *16*(5), 1353-1387.

Hazrat, M. A., Rasul, M. G., Mofijur, M., Khan, M. M. K., Djavanroodi, F., Azad, A. K., ... and Silitonga, A. S. (2020). A mini review on the cold flow properties of biodiesel and its blends. *Frontiers in Energy Research*, *8*, 598651.

He, Y., Li, K., Wang, J., Xu, L., Yan, J., Yang, M., and Yan, Y. (2022). A novel strategy for biodiesel production by combination of liquid lipase, deep eutectic solvent and ultrasonic-assistance in scaled-up reactor: Optimization and kinetics. *Journal of Cleaner Production*, *372*, 133740.

Hoang, A. T., Ong, H. C., Fattah, I. R., Chong, C. T., Cheng, C. K., Sakthivel, R., and Ok, Y. S. (2021). Progress on the lignocellulosic biomass pyrolysis for biofuel production toward environmental sustainability. *Fuel Processing Technology*, *223*, 106997.

Hoang, A. T., Tabatabaei, M., and Aghbashlo, M. (2020). A review of the effect of biodiesel on the corrosion behavior of metals/alloys in diesel engines. *Energy Sources, Part A: Recovery, Utilization, and Environmental Effects*, *42*(23), 2923-2943.

Hobden, R. (2013). *Effectiveness of ultrafiltration on the recovery and reuse of liquid enzymes In: The production of biodiesel* (Doctoral dissertation, Master Thesis, Appalachian State University).

Hosseinzadeh-Bandbafha, H., Khalife, E., Tabatabaei, M., Aghbashlo, M., Khanali, M., Mohammadi, P., ... and Soltanian, S. (2019). Effects of aqueous carbon nanoparticles as a novel nanoadditive in water-emulsified diesel/biodiesel blends on performance and emissions parameters of a diesel engine. *Energy Conversion and Management*, *196*, 1153-1166.

Hosseinzadeh-Bandbafha, H., Kumar, D., Singh, B., Shahbeig, H., Lam, S. S., Aghbashlo, M., and Tabatabaei, M. (2022). Biodiesel antioxidants and their impact on the behavior of diesel engines: A comprehensive review. *Fuel Processing Technology*, *232*, 107264.

Hsiao, M. C., Kuo, J. Y., Hsieh, S. A., Hsieh, P. H., and Hou, S. S. (2020). Optimized conversion of waste cooking oil to biodiesel using modified calcium oxide as catalyst via a microwave heating system. *Fuel*, *266*, 117114.

Hsieh P.Y, Bruno T.J. (2015). A perspective on the origin of lubricity in petroleum distillate motor fuels. *Fuel Process Technol*; 129: 52–60

Huang, Y., Li, F., Bao, G., Li, M., and Wang, H. (2022). Qualitative and quantitative analysis of the influence of biodiesel fatty acid methyl esters on iodine value. *Environmental Science and Pollution Research*, *29*(2), 2432-2447.

Huang, Z., Zhang, J., Pan, M., Hao, Y., Hu, R., Xiao, W., ... and Lyu, T. (2022). Valorisation of microalgae residues after lipid extraction: Pyrolysis characteristics for biofuel production. *Biochemical Engineering Journal*, *179*, 108330.

Idowu, K. S., Abegunde, S. M., and Oyelade, W. A. (2023). A Sustainable Approach for Wastewater Remediation: Utilizing Biosorbents Derived from Kola Nut Pod to Adsorb Methylene Blue Dye. *Journal of Xidian University, 17*,6, 1438-1450

Ihoeghian, N. A., and Usman, M. A. (2020). Exergetic evaluation of biodiesel production from rice bran oil using heterogeneous catalyst. *Journal of King Saud University-Engineering Sciences*, *32*(2), 101-107.

Im-Orb, K., Arpornwichanop, A., and Simasatitkul, L. (2021). Process intensification approach for design and optimization of biodiesel production from palm fatty acid distillate. *Biotechnology Reports*, *30*, e00622.

Istiningrum, R. B., Aprianto, T. Pamungkas, F. L. U. (2017). Effect of reaction temperature on biodiesel production from waste cooking oil using lipase as biocatalyst. *AIP Conf. Proc.* 1911, 020031. https://doi.org/10.1063/1.5016024

Intasian, P., Prakinee, K., Phintha, A., Trisrivirat, D., Weeranoppanant, N., Wongnate, T., and Chaiyen, P. (2021). Enzymes, in vivo biocatalysis, and metabolic engineering for enabling a circular economy and sustainability. *Chemical Reviews*, *121*(17), 10367-10451.

Iqbal, M. S. (2021). Biodiesel Production Potential of Nigella sativa Oil. *Black cumin (Nigella sativa) seeds: Chemistry, Technology, Functionality, and Applications*, 389-405.

Ishak, S., and Kamari, A. (2019). A review of optimum conditions of transesterification process for biodiesel production from various feedstocks. *International journal of environmental science and technology*, *16*(5), 2481-2502.

Ismail, A. R., Kashtoh, H., and Baek, K. H. (2021). Temperature-resistant and solvent-tolerant lipases as industrial biocatalysts: Biotechnological approaches and applications. *International Journal of Biological Macromolecules*, *187*, 127-142.

Jambhulkar, D. K., Ugwekar, R. P., Bhanvase, B. A., and Barai, D. P. (2022). A review on solid base heterogeneous catalysts: preparation, characterization and applications. *Chemical Engineering Communications*, *209*(4), 433-484.

Jamil, S., Farooq, F., Khan, S. R., and Janjua, M. R. S. A. (2021). Synthesis of WSe 2 nanorods by selenium powder precursor for photocatalytic application and fuel additive. *Journal of Cluster Science*, *32*, 1061-1073.

Jiang, W., Lu, H. F., Qi, T., Yan, S. L., and Liang, B. (2010). Preparation, application, and optimization of Zn/Al complex oxides for biodiesel production under sub-critical conditions. *Biotechnology advances*, *28*(5), 620-627.

Johnson, J. U., Carpenter, M., Okeke, N. E., Nnabuife, S. G., and Mai, N. (2022). Investigation of Water Droplet Size Distribution in Conventional and Sustainable Aviation Turbine Fuels. *SAE International Journal of Fuels and Lubricants*, *15*(04-15-03-0016), 315-331.

Juera-Ong, P., Pongraktham, K., Oo, Y. M., and Somnuk, K. (2022). Reduction in Free Fatty Acid Concentration in Sludge Palm Oil Using Heterogeneous and Homogeneous Catalysis: Process Optimization, and Reusable Heterogeneous Catalysts. *Catalysts*, *12*(9), 1007.

Kalita, P., Basumatary, B., Saikia, P., Das, B., and Basumatary, S. (2022). Biodiesel as renewable biofuel produced via enzyme-based catalyzed transesterification. *Energy Nexus*, *6*, 100087.

Kalsoom, M., El Zerey-Belaskri, A., Nadeem, F., and Shehzad, M. R. (2017). Fatty acid chain length optimization for biodiesel production using different chemical and biochemical approaches–a comprehensive. *Int. J. Chem. Biochem. Sci*, *11*, 75-94.

Kamaruddin, M. R., Hassan, N., Sulaiman, S., and Norazmi, M. A. F. (2020). Analysis of the Exhaust Emission from Vehicle Fueled with Variance Research Octane Number Fuel. *Fuel, Mixture Formation and Combustion Process*, *2*(1).

Karayannis, D., Papanikolaou, S., Vatistas, C., Paris, C., and Chevalot, I. (2022). Yeast lipid produced through glycerol conversions and its use for enzymatic synthesis of amino acid-based biosurfactants. *International Journal of Molecular Sciences*, *24*(1), 714.

Kasani, A. A., Esmaeili, A., and Golzary, A. (2022). Software tools for microalgae biorefineries: Cultivation, separation, conversion process integration, modeling, and optimization. *Algal Research*, *61*, 102597.

Kasirajan, Ramachandran. (2021). Biodiesel Production by two step process from an Energy Source of Chrysophyllum albidum Oil using Homogeneous Catalyst. South African Journal of Chemical Engineering. 37. 10.1016/j.sajce.2021.05.011.

Kaushik, S., Sati, V., Kanojia, N., Mehra, K. S., Malkani, H., Pant, H., ... and Kumari, R. (2021). Biodiesel a Substitution for Conventional Diesel Fuel: A Comprehensive Review. *Advances in Mechanical Engineering: Select Proceedings of CAMSE 2020*, 113-122.

Khan, H. M., Iqbal, T., Mujtaba, M. A., Soudagar, M. E. M., Veza, I., and Fattah, I. R. (2021). Microwave assisted biodiesel production using heterogeneous catalysts. *Energies*, *14*(23), 8135.

Khedri, B., Mostafaei, M., and Safieddin Ardebili, S. M. (2019). A review on microwave-assisted biodiesel production. *Energy sources, part A: Recovery, utilization, and environmental effects*, *41*(19), 2377-2395.

Kianimanesh, H. R., Abbaspour-Aghdam, F., & Derakhshan, M. V. (2017). Biodiesel production from vegetable oil: Process design, evaluation and optimization. *Polish Journal of Chemical Technology*, *19*(3), 49-55.

Kibar, M. E., Hilal, L., Çapa, B. T., Bahçıvanlar, B., and Abdeljelil, B. B. (2023). Assessment of Homogeneous and Heterogeneous Catalysts in Transesterification Reaction: A Mini Review. *ChemBioEng Reviews*, *10*(4), 412-422.

Kiehbadroudinezhad, M., Merabet, A., and Hosseinzadeh-Bandbafha, H. (2023). A life cycle assessment perspective on biodiesel production from fish wastes for green microgrids in a circular bioeconomy. *Bioresource Technology Reports*, *21*, 101303.

Koh, M. Y., and Ghazi, T. I. M. (2011). A review of biodiesel production from Jatropha curcas L. oil. *Renewable and sustainable energy reviews*, *15*(5), 2240-2251.

Kolakoti, A., Setiyo, M., and Rochman, M. L. (2022). A Green Heterogeneous Catalyst Production and Characterization for Biodiesel Production using RSM and ANN Approach. *International Journal of Renewable Energy Development*, *11*(3).

Krishnan, S. G., Pua, F. L., and Fan, Z. (2023). Effect of Chemical Pre-Treatment on the Catalytic Performance of Oil Palm EFB Fibre Supported Magnetic Acid Catalyst. *Sustainability*, *15*(11), 8637.

Kukkohovi, M. (2020). Catalyst-free simultaneous esterification and transesterification of low-quality fats and oils to FAME under subcritical water conditions and their purification. A Master Thesis. Lappeenranta-Lahti University of Technology, Finland.

Kulkarni, S.J. (2019). Transesterification for biodiesel-a review. *International Journal of Advanced Trends in Computer Science and Engineering, 8*,1.6, 46-50.

Kumar, R., Ghosh, A. K., and Pal, P. (2020). Sustainable production of biofuels through membrane-integrated systems. *Separation & Purification Reviews*, *49*(3), 207-228.

Kumar, Y., Das, L., and Biswas, K. G. (2022). Biodiesel: Features, Potential Hurdles, and Future Direction. In *Status and Future Challenges for Non-conventional Energy Sources Volume 2* (pp. 99-122). Singapore: Springer Nature Singapore.

Kumbhar, V., Pandey, A., Sonawane, C. R., El-Shafay, A. S., Panchal, H., and Chamkha, A. J. (2022). Statistical analysis on prediction of biodiesel properties from its fatty acid composition. *Case Studies in Thermal Engineering*, *30*, 101775.

Kurzhals, P., Riewald, F., Bianchini, M., Sommer, H., Gasteiger, H. A., and Janek, J. (2021). The linio2 cathode active material: A comprehensive study of calcination conditions and their correlation with physicochemical properties. part i. structural chemistry. *Journal of The Electrochemical Society*, *168*(11), 110518.

Lateef, A. (2023). Cola nitida: Milestones in catalysis, biotechnology and nanotechnology for circular economy and sustainable development. *Biocatalysis and Agricultural Biotechnology*, 102856.

Lefebvre, A. H., & Ballal, D. R. (2010). *Gas turbine combustion: alternative fuels and emissions*. CRC press.

Leofanti, G., Padovan, M., Tozzola, G., Venturelli, B. (1998). Surface area and pore texture of catalysts, *Catalysis Today*, 41, 207-219. https://doi.org/10.1016/S0920-5861(98)00050-9.

Lei, Z., Chen, B., Koo, Y. M., and MacFarlane, D. R. (2017). Introduction: ionic liquids. *Chemical Reviews*, *117*(10), 6633-6635.

Lin, C. Y., and Lu, C. (2021). Development perspectives of promising lignocellulose feedstocks for production of advanced generation biofuels: A review. *Renewable and Sustainable Energy Reviews*, *136*, 110445.

Lin, C. Y., and Ma, L. (2020). Influences of water content in feedstock oil on burning characteristics of fatty acid methyl esters. *Processes*, *8*(9), 1130.

Liu, Y., Yang, X., Adamu, A., and Zhu, Z. (2021). Economic evaluation and production process simulation of biodiesel production from waste cooking oil. *Current Research in Green and Sustainable Chemistry*, *4*, 100091.

López, A., Aragón, J. A., Hernández-Cortez, J. G., Mosqueira, M. L., abd Martínez-Palou, R. (2019). Study of hydrotalcite-supported transition metals as catalysts for crude glycerol hydrogenolysis. *Molecular Catalysis*, *468*, 9-18.

Lv, Y., Sun, S., and Liu, J. (2019). Biodiesel production catalyzed by a methanol-tolerant lipase A from Candida antarctica in the presence of excess water. *ACS omega*, *4*(22), 20064-20071.

Ma, F., and Hanna, M. A. (1999). Biodiesel production: a review. *Bioresource technology*, *70*(1), 1-15.

Maheshwari, P., Haider, M. B., Yusuf, M., Klemeš, J. J., Bokhari, A., Beg, M., ... and Jaiswal, A. K. (2022). A review on latest trends in cleaner biodiesel production: Role of feedstock, production methods, and catalysts. *Journal of Cleaner Production*, *355*, 131588.

Mahmud, R., Moni, S. M., High, K., and Carbajales-Dale, M. (2021). Integration of techno-economic analysis and life cycle assessment for sustainable process design–A review. *Journal of Cleaner Production*, *317*, 128247.

Malode, S. J., Gaddi, S. A. M., Kamble, P. J., Nalwad, A. A., Muddapur, U. M., and Shetti, N. P. (2022). Recent evolutionary trends in the production of biofuels. *Materials Science for Energy Technologies*, *5*, 262-277.

Mandari, V., and Devarai, S. K. (2021). Biodiesel production using homogeneous, heterogeneous, and enzyme catalysts via transesterification and esterification reactions: A critical review. *BioEnergy Research*, 1-27.

Maroa, S., and Inambao, F. (2021). A review of sustainable biodiesel production using biomass derived heterogeneous catalysts. *Engineering in Life Sciences*, *21*(12), 790-824.

Martínez, A., Mijangos, G. E., Romero-Ibarra, I. C., Hernández-Altamirano, R., and Mena-Cervantes, V. Y. (2019). In-situ transesterification of Jatropha curcas L. seeds using homogeneous and heterogeneous basic catalysts. *Fuel*, *235*, 277-287.

Mathew, G. M., Raina, D., Narisetty, V., Kumar, V., Saran, S., Pugazhendi, A., ... and Binod, P. (2021). Recent advances in biodiesel production: Challenges and solutions. *Science of the Total Environment*, *794*, 148751.

Mathur, S., Waswani, H., Singh, D., and Ranjan, R. (2022). Alternative Fuels for Agriculture Sustainability: Carbon Footprint and Economic Feasibility. *AgriEngineering*, *4*(4), 993-1015.

Mazari, S. A., Ali, E., Abro, R., Khan, F. S. A., Ahmed, I., Ahmed, M., ... and Shah, A. (2021). Nanomaterials: Applications, waste-handling, environmental toxicities, and future challenges–A review. *Journal of Environmental Chemical Engineering*, *9*(2), 105028.

Mehmood, U., Muneer, F., Riaz, M., Sarfraz, S., and Nadeem, H. (2021). Biocatalytic processes for biodiesel production. *Biodiesel technology and applications*, 1-58.

Memudu, A. E., and Oluwole, T. J. (2021). The contraceptive potential of Carica papaya seed on oestrus cycle, progesterone, and histomorphology of the Utero-ovarian tissue of adult wistar rats. *JBRA Assisted Reproduction*, *25*(1), 34.

Meneghetti, S. M. P., Meneghetti, M. R., Wolf, C. R., Silva, E. C., Lima, G. E., de Lira Silva, L., ... and de Oliveira, L. G. (2006). Biodiesel from castor oil: a comparison of ethanolysis versus methanolysis. *Energy & Fuels*, *20*(5), 2262-2265.

Miceli, M., Frontera, P., Macario, A., and Malara, A. (2021). Recovery/reuse of heterogeneous supported spent catalysts. *Catalysts*, *11*(5), 591.

Micic, R. (2020). Storing, distribution and blending of biodiesel. *Agricultural Engineering International: CIGR Journal*, *22*(2), 105-111.

Mofijur, M., Siddiki, S. Y. A., Shuvho, M. B. A., Djavanroodi, F., Fattah, I. R., Ong, H. C., ... and Mahlia, T. M. I. (2021). Effect of nanocatalysts on the transesterification reaction of first, second and third generation biodiesel sources-A mini-review. *Chemosphere*, *270*, 128642.

Mohamad Aziz, N. A., Yunus, R., Kania, D., and Abd Hamid, H. (2021). Prospects and challenges of microwave-combined technology for biodiesel and biolubricant production through a transesterification: A review. *Molecules*, *26*(4), 788.

Muhammad, N., Elsheikh, Y. A., Mutalib, M. I. A., Bazmi, A. A., Khan, R. A., Khan, H., ... and Man, Z. (2015). An overview of the role of ionic liquids in biodiesel reactions. *Journal of Industrial and Engineering Chemistry*, *21*, 1-10.

Mukhtar, A., Saqib, S., Lin, H., Shah, M. U. H., Ullah, S., Younas, M., ... and Bokhari, A. (2022). Current status and challenges in the heterogeneous catalysis for biodiesel production. *Renewable and Sustainable Energy Reviews*, *157*, 112012.

Mulula, A., and Manoka, T. N. (2021). Physicochemical Properties of Biodiesel from Congolese Non Edible Oleaginous Plant Allanblackia floribunda Oliv. *Scholar International Journal of Chemistry and Material Sciences*, *4*, 304-309.

Mulyatun, M., Prameswari, J., Istadi, I., and Widayat, W. (2022). Production of non-food feedstock based biodiesel using acid-base bifunctional heterogeneous catalysts: A review. *Fuel*, *314*, 122749.

Mumtaz, M. W., Adnan, A., Mukhtar, H., Rashid, U., and Danish, M. (2017). Biodiesel production through chemical and biochemical transesterification: Trends, technicalities, and future perspectives. In *Clean energy for sustainable development* (pp. 465-485). Academic Press.

Najjar, A., Hassan, E. A., Zabermawi, N., Saber, S. H., Bajrai, L. H., Almuhayawi, M. S., ... and Harakeh, S. (2021). Optimizing the catalytic activities of methanol and thermotolerant Kocuria flava lipases for biodiesel production from cooking oil wastes. *Scientific Reports*, *11*(1), 13659.

Namitha, B., Sathish, A., Kumar, P. S., Nithya, K., and Sundar, S. (2021). Micro algal biodiesel synthesized from Monoraphidium sp., and Chlorella sorokiniana: feasibility and emission parameter studies. *Fuel*, *301*, 121063.

Nanthagopal, K., Kishna, R. S., Atabani, A. E., Ala'a, H., Kumar, G., and Ashok, B. (2020). A compressive review on the effects of alcohols and nanoparticles as an oxygenated enhancer in compression ignition engine. *Energy Conversion and Management*, *203*, 112244.

Nasir, N. F., Daud, W. R. W., Kamarudin, S. K., and Yaakob, Z. (2013). Process system engineering in biodiesel production: A review. *Renewable and Sustainable Energy Reviews*, *22*, 631-639.

Nayab, R., Imran, M., Ramzan, M., Tariq, M., Taj, M. B., Akhtar, M. N., and Iqbal, H. M. (2022). Sustainable biodiesel production via catalytic and non-catalytic transesterification of feedstock materials–A review. *Fuel*, *328*, 125254.

Neupane, D., Bhattarai, D., Ahmed, Z., Das, B., Pandey, S., Solomon, J. K., ... and Adhikari, P. (2021). Growing Jatropha (*Jatropha curcas L.)* as a potential second-generation biodiesel feedstock. *Inventions*, *6*(4), 60.

Nguyen, H. C., Nguyen, M. L., Su, C. H., Ong, H. C., Juan, H. Y., and Wu, S. J. (2021). Bio-derived catalysts: A current trend of catalysts used in biodiesel production. *Catalysts*, *11*(7), 812.

Ni, H., Huang, R. J., Cao, J., Guo, J., Deng, H., and Dusek, U. (2019). Sources and formation of carbonaceous aerosols in Xi'an, China: primary emissions and secondary formation constrained by radiocarbon. *Atmospheric Chemistry and Physics*, *19*(24), 15609-15628.

Nikolova, D., Ivanov, B., and Dzhelil, Y. (2020). An alternative strategy for the sustainable production of biodiesel from Dairy Waste Scum. *Scientific Works of UFT-Plovdiv*, *67*.

Nisar, S., Hanif, M. A., Rashid, U., Hanif, A., Akhtar, M. N., and Ngamcharussrivichai, C. (2021). Trends in widely used catalysts for fatty acid methyl esters (Fame) production: A review. *Catalysts*, *11*(9), 1085.

Niyas, M. M., and Shaija, A. (2022). Effect of repeated heating of coconut, sunflower, and palm oils on their fatty acid profiles, biodiesel properties and performance, combustion, and emission, characteristics of a diesel engine fueled with their biodiesel blends. *Fuel*, *328*, 125242.

Nkeiru, O. J., Osu, C. I., and Gordian, O. (2023). Green Synthesis and Chemically Enhanced Rhynchophorus Phoenicis Nano-Catalyst for Biodiesel Production from Carica papaya and Citrullus lanatus Oil. *American Journal of Applied Chemistry*, *11*(3), 81-85.

Nzekwe, O., (1961). Kola nut.Nig.Mag., 71:2298-305.

Ogunkunle, O., and Laseinde, O. T. (2023). Development of heterogeneous catalyst from assorted periwinkle snail shells for sustainable biodiesel synthesis. In *E3S Web of Conferences* (Vol. 430, p. 01230). EDP Sciences.

Ogutuga, D.B.A., (1975). Chemical composition and potential commercial uses of kola nuts, Cola nitida (vent) Schott and Endlicher. Ghana J. Agric. Sci., 8: 121-125.

Ogunsua, A. O., and Badifu, G. I. O. (1989). Stability of purified melon seed oil obtained by solvent extraction. *Journal of Food Science*, *54*(1), 71-73.

Oke, E. O., Adeyi, O., Okolo, B. I., Ude, C. J., Adeyi, J. A., Salam, K. K., ... and Nzeribe, I. (2021). Heterogeneously catalyzed biodiesel production from Azadiricha Indica oil: Predictive modelling with uncertainty quantification, experimental optimization and techno-economic analysis. *Bioresource Technology*, *332*, 125141.

Oke, E. O., Okolo, B. I., Adeyi, O., Adeyi, J. A., Ude, C. J., Osoh, K., ... and Oladunni, S. (2022). Process Design, Techno-Economic Modelling, and Uncertainty Analysis of Biodiesel Production from Palm Kernel Oil. *BioEnergy Research*, *15*(2), 1355-1369.

Okeniyi, J. A., Ogunlesi, T. A., Oyelami, O. A., and Adeyemi, L. A. (2007). Effectiveness of dried Carica papaya seeds against human intestinal parasitosis: a pilot study. *Journal of medicinal food*, *10*(1), 194-196.

Opeke, L.K., (1982). Tropical Tree Crops. John Wiley, Chi Chester.

Oladipo, B., and Betiku, E. (2020). Optimization and kinetic studies on conversion of rubber seed (Hevea brasiliensis) oil to methyl esters over a green biowaste catalyst. *Journal of environmental management*, *268*, 110705.

Oladokun, M.A.O., (1982). Morpho-physical aspect of germination, rooting and seedling growth in kola. PhD Thesis. University of Ibadan Nigeria pp:230

Oludemokun, A.A., (1983). Processing, storage and utilization of kolanuts, *Cola nitida* and *Cola acuminata*. Tropical Sci., 24: 111-117.

Oluokun, J.A. and E.A. Oladokun, (1999). The effects of graded levels of brewers spent grains and kolanut pod meal in the performance characteristics and carcass quality of rabbits. Nigerian J. Animal Production. 26: 71-77.

Oloyede, C. T., Jekayinfa, S. O., Alade, A. O., Ogunkunle, O., Otung, N. A. U., and Laseinde, O. T. (2023). Exploration of agricultural residue ash as a solid green heterogeneous base catalyst for biodiesel production. *Engineering Reports*, *5*(1), e12585.

Omotola, O. B. (2011). Optimisation of biodiesel production via different catalytic and process systems. A thesis submitted in fulfilment of the requirements for the degree of Doctor of Philosophy in the Department of Chemistry, University of the Western Cape, SA.

Ong, H. C., Tiong, Y. W., Goh, B. H. H., Gan, Y. Y., Mofijur, M., Fattah, I. R., ... and Mahlia, T. M. I. (2021). Recent advances in biodiesel production from agricultural products and microalgae using ionic liquids: Opportunities and challenges. *Energy Conversion and Management*, *228*, 113647.

Ooi, H. K., Koh, X. N., Ong, H. C., Lee, H. V., Mastuli, M. S., Taufiq-Yap, Y. H., ... and Asikin Mijan, N. (2021). Progress on modified calcium oxide derived waste-shell catalysts for biodiesel production. *Catalysts*, *11*(2), 194.

Osaba, E., Villar-Rodriguez, E., Del Ser, J., Nebro, A. J., Molina, D., LaTorre, A., ... and Herrera, F. (2021). A tutorial on the design, experimentation and application of metaheuristic algorithms to real-world optimization problems. *Swarm and Evolutionary Computation*, *64*, 100888.

Osakwe, E. U., Ani, I. J., Akpan, U. G., and Olutoye, M. A. (2018, July). Kolanut pod husk as a biobase catalyst for fatty acid methyl ester production using Thevetia peruviana (Yellow oleander) seed oil. In *IOP Conference Series: Earth and Environmental Science* (Vol. 173, No. 1, p. 012008). IOP Publishing.

Oshin, T. T., Kareem, R. A., Fadayini, O., and Momoh, J. O. (2021). Histological and cytotoxic evaluation of *Carica papaya* seed oil and its potential biodiesel feedstock. *Journal of Environmental Chemistry and Ecotoxicology*, *13*(2), 43-52.

Padmanabhan, S., Giridharan, K., Stalin, B., Kumaran, S., Kavimani, V., Nagaprasad, N., ... and Krishnaraj, R. (2022). Energy recovery of waste plastics into diesel fuel with ethanol and ethoxy ethyl acetate additives on circular economy strategy. *Scientific Reports*, *12*(1), 5330.

Pala, A.O., (1976). African women in rural development: Research trends and priorities. American Overseas Liaison Committee, Washington.

Panchal, B., Chang, T., Qin, S., Sun, Y., Wang, J., and Bian, K. (2020). Optimization of soybean oil transesterification using an ionic liquid and methanol for biodiesel synthesis. *Energy Reports*, *6*, 20-27.

Parangi, T., and Mishra, M. K. (2020). Solid acid catalysts for biodiesel production. *Comments on Inorganic Chemistry*, *40*(4), 176-216.

Pasha, M. K., Ahmad, I., Mustafa, J., and Kano, M. (2019). Modeling of a nickel-based fluidized bed membrane reactor for steam methane reforming process. *J Chem Soc Pakistan*, *41*, 219-229.

Pasha, M. K., Dai, L., Liu, D., Guo, M., and Du, W. (2021). An overview to process design, simulation and sustainability evaluation of biodiesel production. *Biotechnology for Biofuels*, *14*(1), 1-23.

Pathak, G., Das, D., Rajkumari, K., and Rokhum, L. (2018). Exploiting waste: towards a sustainable production of biodiesel using Musa acuminata peel ash as a heterogeneous catalyst. *Green Chemistry, 20* (10), 2365–2373. doi:10.1039/c8gc00071a

Paul, S., Bhagobaty, R. K., Nihalani, M. C., and Joshi, S. R. (2020). Characterization of oleaginous endophytic fungi of biodiesel plants as potential biofuel minifactories. *Biomass and Bioenergy*, *142*, 105750.

Petrovic, Z. S. (2008). Polyurethanes from vegetable oils, Polymer Reviews, 48 (1): 109-155.

Pinto, A. C., Guarieiro, L. L., Rezende, M. J., Ribeiro, N. M., Torres, E. A., Lopes, W. A., ... and Andrade, J. B. D. (2005). Biodiesel: an overview. *Journal of the Brazilian Chemical Society*, *16*, 1313-1330.

Pleşu, V., Puigcasas, J. S., Surroca, G. B., Bonet, J., Ruiz, A. E. B., Tuluc, A., and Llorens, J. (2015). Process intensification in biodiesel production with energy reduction by pinch analysis. *Energy*, *79*, 273-287.

Prabhahar, R. S. S., Benitha, V. S., and Nagarajan, J. (2021). Improved yield of palm oil biodiesel through nano catalytic transesterification. *Materials Today: Proceedings*, *46*, 8433-8437.

Pradhan, S., Malani, R. S., and Mishra, A. (2022). Microbial biodiesel: a comprehensive study toward sustainable biofuel production. In *Handbook of Biofuels* (pp. 353-375). Academic Press.

Pullagura, G., Vadapalli, S., Prasad, V. V., Bikkavolu, J., Chebattina, K. R., Chava, S. T., and Velisala, V. (2021). Effect of nano additives on fuel properties, engine performance, emission and combustion characteristics of CI engines fuelled with diesel and biodiesel blends: a comprehensive review. *Bulletin Monumental*, *21*(11), 39-50.

Qadeer, M. U., Ayoub, M., Komiyama, M., Daulatzai, M. U. K., Mukhtar, A., Saqib, S., ... and Bokhari, A. (2021). Review of biodiesel synthesis technologies, current trends, yield influencing factors and economical analysis of supercritical process. *Journal of Cleaner Production*, *309*, 127388.

Qasemi, Z., Jafari, D., Jafari, K., and Esmaeili, H. (2022). Heterogeneous aluminum oxide/calcium oxide catalyzed transesterification of Mespilus germanica triglyceride for biodiesel production. *Environmental Progress & Sustainable Energy*, *41*(2), e13738.

Qian, L. K., and Huey, S. J. (2023). Process simulation and economic assessments for biodiesel production catalyzed by green Nanocatalysts. *Asia-Pacific Journal of Chemical Engineering*, e2994.

Quarcoo, T., (1973). A handbook on kola. CRIN Ibadan pp: 99.

Quirino, M. R., Oliveira, M. J. C., Keyson, D., Lucena, G. L., Oliveira, J. B. L., and Gama, L. (2016). Synthesis of zinc aluminate with high surface area by microwave hydrothermal method applied in the transesterification of soybean oil (biodiesel). *Materials Research Bulletin*, *74*, 124-128.

Rahimi, V., Shafiei, M., and Karimi, K. (2020). Techno-economic study of castor oil crop biorefinery: production of biodiesel without fossil-based methanol and lignoethanol improved by alkali pretreatment. *Agronomy*, *10*(10), 1538.

Rakopoulos, C. D., Antonopoulos, K. A., Rakopoulos, D. C., Hountalas, D. T., and Giakoumis, E. G. (2006). Comparative performance and emissions study of a direct injection diesel engine using blends of diesel fuel with vegetable oils or bio-diesels of various origins. *Energy conversion and management*, *47*(18-19), 3272-3287.

Rasoulinezhad, E., Taghizadeh-Hesary, F., and Taghizadeh-Hesary, F. (2020). How is mortality affected by fossil fuel consumption, CO2 emissions and economic factors in CIS region?. *Energies*, *13*(9), 2255.

Ravi, A., Gurunathan, B., Rajendiran, N., Varjani, S., Gnansounou, E., Pandey, A., ... and Ramanujam, P. (2020). Contemporary approaches towards augmentation of distinctive heterogeneous catalyst for sustainable biodiesel production. *Environmental Technology & Innovation*, *19*, 100906.

Rezania, S., Mahdinia, S., Oryani, B., Cho, J., Kwon, E. E., Bozorgian, A., ... and Mehranzamir, K. (2022). Biodiesel production from wild mustard (Sinapis Arvensis) seed oil using a novel heterogeneous catalyst of $LaTiO_3$ nanoparticles. *Fuel*, *307*, 121759.

Rezania, S., Oryani, B., Park, J., Hashemi, B., Yadav, K. K., Kwon, E. E., ... and Cho, J. (2019). Review on transesterification of non-edible sources for biodiesel production with a focus on economic aspects, fuel properties and by-product applications. *Energy Conversion and Management*, *201*, 112155.

Rezende, M. J., Lima, A. L. D., Silva, B. V., Mota, C. J., Torres, E. A., Rocha, G. O. D., ... and Andrade, J. B. D. (2021). Biodiesel: an overview II. *Journal of the Brazilian Chemical Society*, *32*, 1301-1344.

Ridwan, I., Budiastuti, H., Indarti, R., Wahyuni, N. L. E., Safitri, H. M., and Ramadhan, R. L. (2023). The optimization of tetrahydrofuran as a co-solvent on biodiesel production from rubber seeds using response surface methodology. *Materials Science for Energy Technologies*, *6*, 15-20.

Rizwanul Fattah, I. M., Ong, H. C., Mahlia, T. M. I., Mofijur, M., Silitonga, A. S., Rahman, S. M., and Ahmad, A. (2020). State of the art of catalysts for biodiesel production. *Frontiers in Energy Research*, 101.

Rokni, E., Panahi, A., Ren, X., and Levendis, Y. A. (2016). Curtailing the generation of sulfur dioxide and nitrogen oxide emissions by blending and oxy-combustion of coals. *Fuel*, *181*, 772-784.

Roman, F. F., Ribeiro, A. E., Queiroz, A., Lenzi, G. G., Chaves, E. S., and Brito, P. (2019). Optimization and kinetic study of biodiesel production through esterification of oleic acid applying ionic liquids as catalysts. *Fuel*, *239*, 1231-1239.

Romero, R., Martínez, S. L., and Natividad, R. (2011). Biodiesel production by using heterogeneous catalysts. *Alternative fuel*, 3-20.

Roy, T., Sahani, S., and Sharma, Y. C. (2020). Green synthesis of biodiesel from Ricinus communis oil (castor seed oil) using potassium promoted lanthanum oxide catalyst: kinetic, thermodynamic and environmental studies. *Fuel*, *274*, 117644.

Ruatpuia, J. V., Changmai, B., Pathak, A., Alghamdi, L. A., Kress, T., Halder, G., ... and Rokhum, S. L. (2023). Green biodiesel production from Jatropha curcas oil using a carbon-based solid acid catalyst: A process optimization study. *Renewable Energy*, *206*, 597-608.

Saha, U and Jackson, D. (2018). Analysis of Moisture, Oil, and Fatty Acid Composition of Olives by Near-Infrared Spectroscopy: Development and Validation Calibration Models. *Journal of the Science of Food and Agriculture, 98* (5), 1821-1831.

Sahani, S., Upadhyay, S. N., and Sharma, Y. C. (2020). Critical review on production of glycerol carbonate from byproduct glycerol through transesterification. *Industrial & Engineering Chemistry Research*, *60*(1), 67-88.

Sahar, J., Farooq, M., Ramli, A., Naeem, A., Khattak, N. S., and Ghazi, Z. A. (2022). Highly efficient heteropoly acid decorated SnO2@ Co-ZIF nanocatalyst for sustainable biodiesel production from Nannorrhops ritchiana seeds oil. *Renewable Energy*, *198*, 306-318.

Sahu, O. (2021). Characterisation and utilization of heterogeneous catalyst from waste rice-straw for biodiesel conversion. *Fuel*, *287*, 119543.

Sakdasri, W., Sawangkeaw, R., and Ngamprasertsith, S. (2018). Techno-economic analysis of biodiesel production from palm oil with supercritical methanol at a low molar ratio. *Energy, 152, 144–153.* doi:10.1016/j.energy.2018.03.125

Sakthivel, R., Ramesh, K., Purnachandran, R., and Shameer, P. M. (2018). A review on the properties, performance and emission aspects of the third-generation biodiesels. *Renewable and Sustainable Energy Reviews*, *82*, 2970-2992.

Salaheldeen, M., Mariod, A. A., Aroua, M. K., Rahman, S. A., Soudagar, M. E. M., and Fattah, I. R. (2021). Current state and perspectives on transesterification of triglycerides for biodiesel production. *Catalysts*, *11*(9), 1121.

Salehi, A., Karbassi, A., Ghobadian, B., Ghasemi, A., and Doustgani, A. (2019). Simulation process of biodiesel production plant. *Environmental Progress & Sustainable Energy*, *38*(6), e13264.

Sanders, K. (2008). Sustainable trade in pre-colonial Asante.

Sankaranarayanan, T. M., Pandurangan, A., Banu, M., and Sivasanker, S. (2011). Transesterification of sunflower oil over MoO3 supported on alumina. *Applied Catalysis A: General*, *409*, 239-247.

Santana, I., Félix, M., Guerrero, A., and Bengoechea, C. (2022). Processing and characterization of bioplastics from the invasive seaweed rugulopteryx okamurae. *Polymers*, *14*(2), 355.

Santos, E. E., Amaro, R. C., Bustamante, C. C. C., Guerra, M. H. A., Soares, L. C., and Froes, R. E. S. (2020). Extraction of pectin from agroindustrial residue with an ecofriendly solvent: Use of FTIR and chemometrics to differentiate pectins according to degree of methyl esterification. *Food Hydrocolloids*, *107*, 105921.

Santos, S., Nobre, L., Gomes, J., Puna, J., Quinta-Ferreira, R., and Bordado, J. (2019). Soybean oil transesterification for biodiesel production with micro-structured calcium oxide (CaO) from natural waste materials as a heterogeneous catalyst. *Energies*, *12*(24), 4670.

Saputra, H., Husodo, D., Murti, S. S., and Senda, S. P. (2023). Preparation And Characterization of MCM-41 Membrane for Biogas Purification. *EVERGREEN Joint Journal of Novel Carbon Resource Sciences & Green Asia Strategy, 10* (03),1855-1861.

Sarianto, M., Rado, Kusuma, G. F., Asriza, R. O., Fabiani, V. A., and Kafillah, M. (2019). *Characterization of methyl ester compound of Carica papaya seed oil through Transesterification using CaO Catalyst from Strombus canarium shells. IOP Conference Series: Earth and Environmental Science, 353, 012008.* doi:10.1088/1755-1315/353/1/012008

Sarkar, A., Das, P., Laskar, I. B., Vadivel, S., Puzari, A., and Paul, B. (2023). Parkia speciosa: A basic heterogeneous catalyst for production of soybean oil-based biodiesel. *Fuel*, *348*, 128537.

Scarsella, M., de Caprariis, B., Damizia, M., and De Filippis, P. (2020). Heterogeneous catalysts for hydrothermal liquefaction of lignocellulosic biomass: A review. *Biomass and Bioenergy*, *140*, 105662.

Seal, S., Jeyaranjan, A., Neal, C. J., Kumar, U., Sakthivel, T. S., and Sayle, D. C. (2020). Engineered defects in cerium oxides: tuning chemical reactivity for biomedical, environmental, & energy applications. *Nanoscale*, *12*(13), 6879-6899.

Senrayan, J., and Venkatachalam, S. (2018). Solvent-assisted extraction of oil from papaya (Carica papaya L.) seeds: evaluation of its physiochemical properties and fatty-acid composition. *Separation Science and Technology*, *53*(17), 2852-2859.

Shaah, M. A. H., Hossain, M. S., Allafi, F. A. S., Alsaedi, A., Ismail, N., Ab Kadir, M. O., and Ahmad, M. I. (2021). A review on non-edible oil as a potential feedstock for biodiesel: physicochemical properties and production technologies. *RSC advances*, *11*(40), 25018-25037.

Sharma, S., and Maréchal, F. (2019). Carbon dioxide capture from internal combustion engine exhaust using temperature swing adsorption. *Frontiers in Energy Research*, *7*, 143.

Shi, K., Li, N., Qiao, Y., Jiang, Q., Xue, J., Wang, M., and Huang, G. (2022). Efficiently remove of diesel oil pollutants in the marine environment by a novel biological-C14H32O3Si-Enteromorpha: Preparation, mechanism, and application. *Journal of Environmental Chemical Engineering*, *10*(5), 108281.

Sia, C. B., Kansedo, J., Tan, Y. H., and Lee, K. T. (2020). Evaluation on biodiesel cold flow properties, oxidative stability and enhancement strategies: A review. *Biocatalysis and Agricultural Biotechnology*, *24*, 101514.

Silitonga, A. S., Shamsuddin, A. H., Mahlia, T. M. I., Milano, J., Kusumo, F., Siswantoro, J., ... and Ong, H. C. (2020). Biodiesel synthesis from Ceiba pentandra oil by microwave

irradiation-assisted transesterification: ELM modeling and optimization. *Renewable Energy*, *146*, 1278-1291.

Singh, C. S., Kumar, N., and Gautam, R. (2021). Supercritical transesterification route for biodiesel production: Effect of parameters on yield and future perspectives. *Environmental Progress & Sustainable Energy*, *40*(6), e13685.

Singh, D., Sharma, D., Soni, S. L., Inda, C. S., Sharma, S., Sharma, P. K., and Jhalani, A. (2021). A comprehensive review of physicochemical properties, production process, performance and emissions characteristics of 2nd generation biodiesel feedstock: *Jatropha curcas*. *Fuel*, *285*, 119110.

Singh, D., Sharma, D., Soni, S. L., Sharma, S., and Kumari, D. (2019). Chemical compositions, properties, and standards for different generation biodiesels: A review. *Fuel*, *253*, 60-71.

Singh, D., Sharma, D., Soni, S. L., Sharma, S., Sharma, P. K., and Jhalani, A. (2020). A review on feedstocks, production processes, and yield for different generations of biodiesel. *Fuel*, *262*, 116553.

Smith, R. (2005). *Chemical process: design and integration*. John Wiley & Sons.

Somvanshi, S. B., Jadhav, S. A., Khedkar, M. V., Kharat, P. B., More, S. D., and Jadhav, K. M. (2020). Structural, thermal, spectral, optical and surface analysis of rare earth metal ion ($Gd3^{+}$) doped mixed Zn–Mg nano-spinel ferrites. *Ceramics International*, *46*(9), 13170-13179.

Son, J., Kim, B., Park, J., Yang, J., and Lee, J. W. (2018). *Wet in situ transesterification of spent coffee grounds with supercritical methanol for the production of biodiesel. Bioresource Technology, 259, 465–468.* doi:10.1016/j.biortech.2018.03.067

Sotoft, L. F., Rong, B. G., Christensen, K. V., and Norddahl, B. (2010). Process simulation and economical evaluation of enzymatic biodiesel production plant. *Bioresource Technology*, *101*(14), 5266-5274.

Soumiya, S., and Baskar, G. (2017). Macroalgae: source for sustainable production of biodiesel. *Int J Ind Eng*, *1*, 1-7.

Stegen, S., and Kaparaju, P. (2020). Effect of temperature on oil quality obtained through pyrolysis of sugarcane bagasse. *Fuel*, *276*, 118112.

Sulaiman, N. F., Leong, Y. W., Lee, S. L., Toemen, S., and Bakar, W. A. W. A. (2023). Enhanced transesterification reaction using chromium-doped calcium oxide-based catalyst supported on alumina and its specification of biodiesel. *Energy Conversion and Management*, *293*, 117556.

Sultana, N., Hossain, S. M. Z., Taher, S., Khan, A., Razzak, S. A., and Haq, B. (2020). Modeling and optimization of non-edible papaya seed waste oil synthesis using data mining approaches. *South African Journal of Chemical Engineering*, *33*, 151-159.

Suprianto, F. D., Anggono, W., Sutrisno, T., Gunawan, D. W., and Gotama, G. J. (2019). The Effect of Biodiesel Blends Made from Carica papaya L. Seeds on the Performance of Diesel Engine. In *E3S Web of Conferences* (Vol. 130, No. 01009, pp. 1-11). EDP Sciences.

Suzihaque, M. U. H., Alwi, H., Ibrahim, U. K., Abdullah, S., and Haron, N. (2022). Biodiesel production from waste cooking oil: A brief review. *Materials Today: Proceedings*, *63*, S490-S495.

Tagarda, E. B. P., Deloso, L. E., Oclarit, L. J. Z., Lungay, G. S., Mabayo, V. I. F., and Arazo, R. O. (2023). Utilizing Carica papaya seeds as a promising source for bio-oil production: optimization and characterization. *Biomass Conversion and Biorefinery*, 1-10.

Takase, M., Zhang, M., Feng, W., Chen, Y., Zhao, T., Cobbina, S. J., ... and Wu, X. (2014). Application of zirconia modified with KOH as heterogeneous solid base catalyst to new non-edible oil for biodiesel. Energy Conversion and Management, 80, 117-125.

Tamjidi, S., Esmaeili, H., and Moghadas, B. K. (2021). Performance of functionalized magnetic nanocatalysts and feedstocks on biodiesel production: a review study. *Journal of Cleaner Production*, *305*, 127200.

Tan, S. X., Lim, S., Ong, H. C., and Pang, Y. L. (2019). State of the art review on development of ultrasound-assisted catalytic transesterification process for biodiesel production. *Fuel*, *235*, 886-907.

Thangaraj, B., Solomon, P. R., Muniyandi, B., Ranganathan, S., and Lin, L. (2019). Catalysis in biodiesel production—a review. *Clean Energy*, *3*(1), 2-23.

Thiruselvam, K., Murugapoopathi, S., Ramachandran, T., and Amesho, K. T. (2023). Hydrogen-enriched palm biodiesel as a potential alternative fuel for diesel engines: Investigating performance and emission characteristics and mitigation strategies for air pollutants. *International Journal of Hydrogen Energy*.

Tibesigwa, T., Olupot, P. W., and Kirabira, J. B. (2022). The critical techno-economic aspects for production of B10 biodiesel from second generation feedstocks: a review. *International Journal of Sustainable Energy*, *41*(7), 751-771.

Tobar, M., and Núñez, G. A. (2018). *Supercritical transesterification of microalgae triglycerides for biodiesel production: Effect of alcohol type and co-solvent. The Journal of Supercritical Fluids, 137, 50–56.* doi:10.1016/j.supflu.2018.03.008

Trirahayu, D. A., Abidin, A. Z., Putra, R. P., Hidayat, A. S., Safitri, E., and Perdana, M. I. (2022). Process Simulation and Design Considerations for Biodiesel Production from Rubber Seed Oil. *Fuels*, *3*(4), 563-579.

Troter, D. Z., Todorović, Z. B., Đokić-Stojanović, D. R., Stamenković, O. S., and Veljković, V. B. (2016). Application of ionic liquids and deep eutectic solvents in biodiesel production: A review. *Renewable and Sustainable Energy Reviews*, *61*, 473-500.

Udoetuk, E. N., Olatunbosun, B. E., Adepojua, T. F., Mayen, I. A., and Babalola, R. (2018). Evaluation of the effectiveness of the optimization procedure with methanolysis of waste oil as case study. *South African Journal of Chemical Engineering*, *25*(1), 169-177.

Usman, A., and Rufai, I. A. (2021). Effect of Oxidation Stability on the Fuel and Storage Properties of Balanites Aegyptiaca Biodiesel. *Jurnal Kejuruteraan*, *33*(4), 883-890.

Vahid, B. R., Haghighi, M., Alaei, S., and Toghiani, J. (2017). Reusability enhancement of combustion synthesized MgO/MgAl2O4 nanocatalyst in biodiesel production by glow discharge plasma treatment. *Energy Conversion and Management*, *143*, 23-32.

Varghese, G., Saeed, K., Lu, X., and Rutt, K. J. (2022). Effects of biodiesel degree of unsaturation, chain length and physical properties on tailpipe oxides of nitrogen (NOx). *Journal of the Energy Institute*, *105*, 355-366.

Vasaki, M., Sithan, M., Ravindran, G., Paramasivan, B., Ekambaram, G., and Karri, R. R. (2022). Biodiesel production from lignocellulosic biomass using Yarrowia lipolytica. *Energy Conversion and Management: X*, *13*, 100167.

Verma, P., and Sharma, M. P. (2016). Review of process parameters for biodiesel production from different feedstocks. *Renewable and sustainable energy reviews*, *62*, 1063-1071.

Vlnieska, V., Muniz, A. S., Oliveira, A. R., César-Oliveira, M. A., and Kunka, D. (2021). Synthesis and Chemical Functionalization of Pseudo-Homogeneous Catalysts for Biodiesel Production—Oligocat. *Polymers*, *14*(1), 19.

Wahab, R. A., Elias, N., Abdullah, F., and Ghoshal, S. K. (2020). On the taught new tricks of enzymes immobilization: An all-inclusive overview. *Reactive and Functional Polymers*, *152*, 104613.

Wang, L., Yang, D., Kang, Z., Zhao, J., and Meng, Q. (2022). Experimental study on the effects of steam temperature on the pore-fracture evolution of oil shale exposed to the convection heating. *Journal of Analytical and Applied Pyrolysis*, *164*, 105533.

Wang, W., Lemaire, R., Bensakhria, A., and Luart, D. (2022). Review on the catalytic effects of alkali and alkaline earth metals (AAEMs) including sodium, potassium, calcium and magnesium on the pyrolysis of lignocellulosic biomass and on the co-pyrolysis of coal with biomass. *Journal of Analytical and Applied Pyrolysis*, *163*, 105479.

Wang, X., Yang, K., Cai, R., ChenYang, Y., Huang, Z., and Han, B. (2022). Optimization and kinetics of biodiesel production from soybean oil using new tetraethylammonium ionic liquids with amino acid-based anions as catalysts. *Fuel*, *324*, 124510.

Wang, Z., Yu, C., Huang, H., Guo, W., Yu, J., and Qiu, J. (2021). Carbon-enabled microwave chemistry: From interaction mechanisms to nanomaterial manufacturing. *Nano Energy*, *85*, 106027.

Ward, T. J. (1994). Which Project Is Best? *Chemical Engineering*, 102 – 107.

Welton, T. (2018). Ionic liquids: a brief history. *Biophysical reviews*, *10*(3), 691-706.

Wen, Z., Yu, X., Tu, S. T., Yan, J., and Dahlquist, E. (2010). Synthesis of biodiesel from vegetable oil with methanol catalyzed by Li-doped magnesium oxide catalysts. *Applied Energy*, *87*(3), 743-748.

West, A. H., Posarac, D., and Ellis, N. (2008). Assessment of four biodiesel production processes using HYSYS. Plant. *Bioresource technology*, *99*(14), 6587-6601.

Winston, R. E. (1995). Rapid Method for Capital Investment Decisions. Cost Engineering, 37(4): 41 – 43. https://exoticfruits.co.uk/products/papaya-seeds?variant=43424938197208

Xiao, C., Lu, B. A., Xue, P., Tian, N., Zhou, Z. Y., Lin, X., ... and Sun, S. G. (2020). High-index-facet-and high-surface-energy nanocrystals of metals and metal oxides as highly efficient catalysts. *Joule*, *4*(12), 2562-2598.

Xie, W., and Wang, H. (2021). Grafting copolymerization of dual acidic ionic liquid on core-shell structured magnetic silica: A magnetically recyclable Brönsted acid catalyst for biodiesel production by one-pot transformation of low-quality oils. *Fuel*, *283*, 118893.

Xie, W., and Wang, T. (2013). Biodiesel production from soybean oil transesterification using tin oxide-supported WO3 catalysts. *Fuel processing technology*, *109*, 150-155.

Xu, L., Jiang, L., Zhang, H., Fang, Z., and Smith, R. L. (2020). Introduction to pyrolysis as a thermo-chemical conversion technology. *Production of biofuels and chemicals with pyrolysis*, 3-30.

Xu, P., Liang, S., Zong, M. H., and Lou, W. Y. (2021). Ionic liquids for regulating biocatalytic process: Achievements and perspectives. *Biotechnology advances*, *51*, 107702.

Xuan, T. S. (2019). *Ultrasound Assisted Biodiesel Synthesis from Jatropha Oilseeds Using In-Situ Reactive Extraction* (Doctoral dissertation, University of Malaya (Malaysia)).

Yang, X. X., Wang, Y. T., Yang, Y. T., Feng, E. Z., Luo, J., Zhang, F., ... and Bao, G. R. (2018). Catalytic transesterification to biodiesel at room temperature over several solid bases. *Energy Conversion and Management*, *164*, 112-121.

Yavir, K., Konieczna, K., Marcinkowski, Ł., and Kloskowski, A. (2020). Ionic liquids in the microextraction techniques: The influence of ILs structure and properties. *TrAC Trends in Analytical Chemistry*, *130*, 115994.

Yesilyurt, M. K. (2020). A detailed investigation on the performance, combustion, and exhaust emission characteristics of a diesel engine running on the blend of diesel fuel, biodiesel and 1-heptanol (C7 alcohol) as a next-generation higher alcohol. *Fuel*, *275*, 117893.

Yun, H., Wang, M., Feng, W., and Tan, T. (2013). Process simulation and energy optimization of the enzyme-catalyzed biodiesel production. *Energy*, *54*, 84-96.

Yusuf, N. N. A. N., Kamarudin, S. K., and Yaakub, Z. (2011). Overview on the current trends in biodiesel production. *Energy conversion and management*, *52* (7), 2741-2751.

Zabaruddin, N. H., Mohamed, N. H., Abdullah, L. C., Tamada, M., Ueki, Y., Seko, N., and Choong, T. S. Y. (2019). Palm oil-based biodiesel synthesis by radiation-induced kenaf catalyst packed in a continuous flow system. *Industrial Crops and Products*, *136*, 102-109.

Zahed, M. A., Revayati, M., Shahcheraghi, N., Maghsoudi, F., and Tabari, Y. (2021). Modeling and optimization of biodiesel synthesis using TiO2–ZnO nanocatalyst and characteristics of biodiesel made from waste sunflower oil. *Current Research in Green and Sustainable Chemistry*, *4*, 100223.

Zhang, Q., Hu, Y., Li, S., Zhang, M., Wang, Y., Wang, Z., ... and Pan, H. (2022). Recent advances in supported acid/base ionic liquids as catalysts for biodiesel production. *Frontiers in Chemistry*, *10*, 999607.

Zhang, W., Wang, C., Luo, B., He, P., Li, L., and Wu, G. (2023). Biodiesel production by transesterification of waste cooking oil in the presence of graphitic carbon nitride supported molybdenum catalyst. *Fuel*, *332*, 126309.

Zhang, Y. Q., Jin, L., Duan, J., Zhao, G. C., Xu, Y. Y., Liu, J. M., ... and Su, S. C. (2020). The assessment of two species of soapberry as resources for high-quality biodiesel production with an optimized method of ultrasound-assisted oil extraction. *Forests*, *11*(2), 212.

Zhang, Y., Zhong, Y., Lu, S., Zhang, Z., and Tan, D. (2022). A comprehensive review of the properties, performance, combustion, and emissions of the diesel engine fueled with different generations of biodiesel. *Processes*, *10*(6), 1178.

Zhu, Z., Liu, Y., Cong, W., Zhao, X., Janaun, J., Wei, T., and Fang, Z. (2021). Soybean biodiesel production using synergistic CaO/Ag nano catalyst: Process optimization, kinetic study, and economic evaluation. *Industrial Crops and Products*, *166*, 113479.

Zong, L., Ramanathan, S., and Chen, C. C. (2010). Predicting thermophysical properties of mono- and diglycerides with the chemical constituent fragment approach. *Industrial & Engineering Chemistry Research*, *49*(11), 5479-5484.

Babatunde, O., Oladimeji, A. O., and Oguntuase, B. J. (2019). Chemical composition and antioxidant properties of *Synsepalum dulcificum Daniell* and *Carica papaya L*. seeds oil. *Journal of Chemical Society of Nigeria*, *44*(7).

Khalaf, A., Desa, S., and Baharum, S. (2019). Agricultural waste biodiesel potential and physicochemical properties in extracted seeds oil. *Institute of Advanced Scientific Research*, *11*(Spe 4), 2202-2213.

Devi, V., and Khanam, S. (2019). Development of generalized and simplified models for supercritical fluid extraction: Case study of papaya (*Carica papaya*) seed oil. *Chemical Engineering Research and Design*, *150*, 341-358.

Agunbiade, F. O., and Adewole, T. A. (2014). Methanolysis of *Carica papaya* seed oil for production of biodiesel. *Journal of Fuels*, *2014*.

Hossain, S. M. Z., Taher, S., Khan, A., Sultana, N., Irfan, M. F., Haq, B., and Razzak, S. A. (2020). Experimental study and modeling approach of response surface methodology coupled with crow search algorithm for optimizing the extraction conditions of papaya seed waste oil. *Arabian Journal for Science and Engineering*, *45*, 7371-7383.

Balat, M. (2011). Potential alternatives to edible oils for biodiesel production–A review of current work. *Energy conversion and management*, *52*(2), 1479-1492.

Narvaez, P.C., Rincon, S.M. and Sanchez, F.J. (2007). "Kinetics of Palm Oil Methanolysis", *Journal of American Oil Chemical Society*, 84: 971 – 977.

Zong, L., Ramanathan, S. and Chen, C.-C. (2010). "Correction to Fragment-Based Approach for Estimating Thermophysical Properties of Fats and Vegetable Oils for Modeling Biodiesel Production Processes", *Industrial & Engineering Chemistry Research*, 49: 3022 – 3023.

Peters, M. S. and Timmerhau, K. D. (1991). Plant Design and Economics for Chemical Engineers, Fourth Edition, McGraw Hill Inc., Singapore. 192 – 211.

Tibesigwa, T., Olupot, P. W. and Kirabira, J. B. (2023). Assessment of the techno-economic viability of B10 synthesis from second-generation biodiesel feedstocks in Uganda, *International Journal of Sustainable Energy*, 42(1), 351 – 373. DOI:10.1080/14786451.2023.2191144.

Wood, C., Rosentrater, K. A. and Muthukumarappan, K. (2014). Techno-economic modeling of a corn-based ethanol plant in 2011/2012. *Industrial Crops and Products*, 56, 145 – 155.

APPENDICES

Appendix I: Process Modelling and Simulation

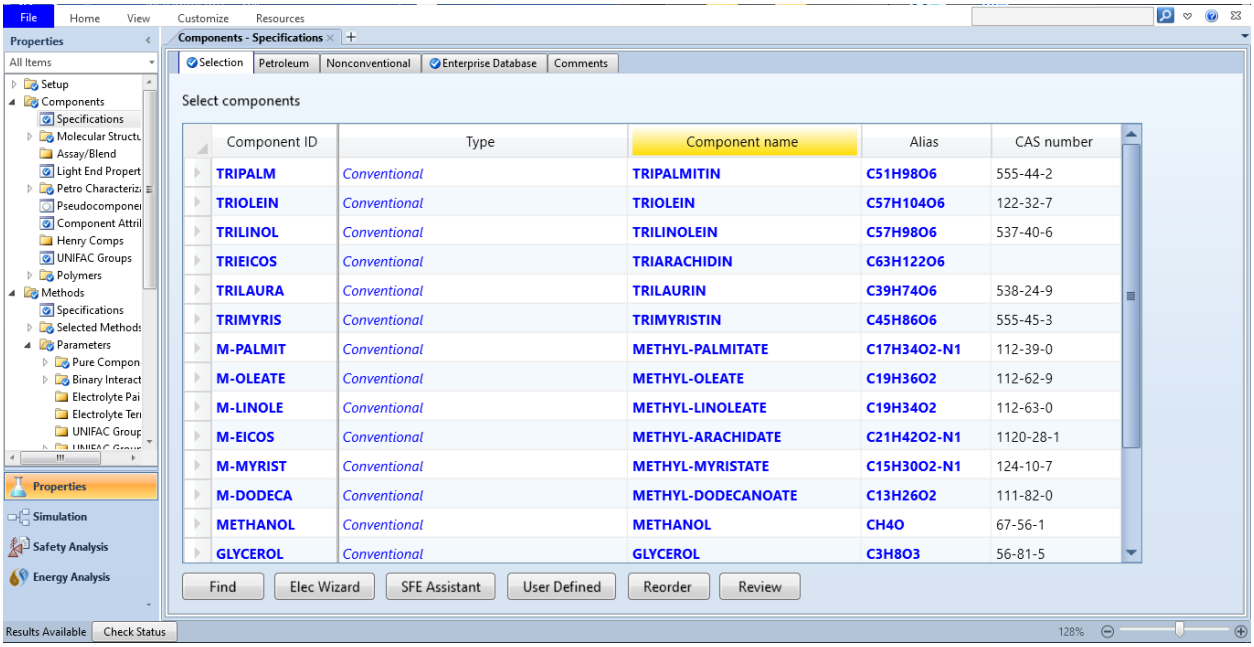

Plate 1: Component Selection

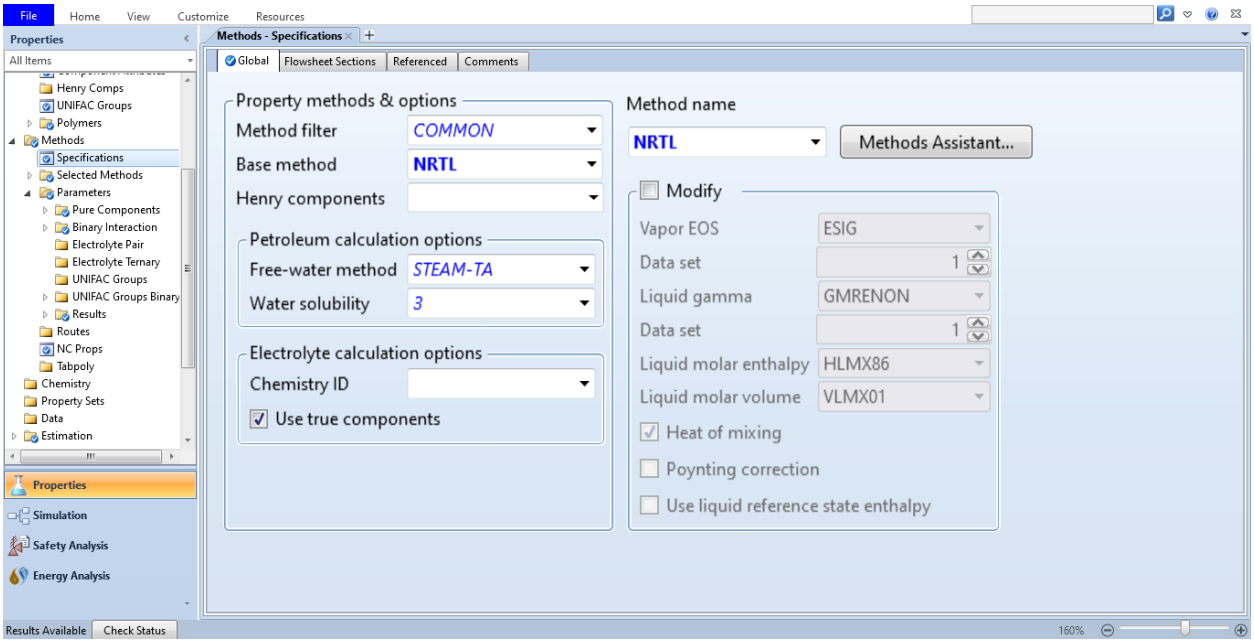

Plate 2: Property Method Selection

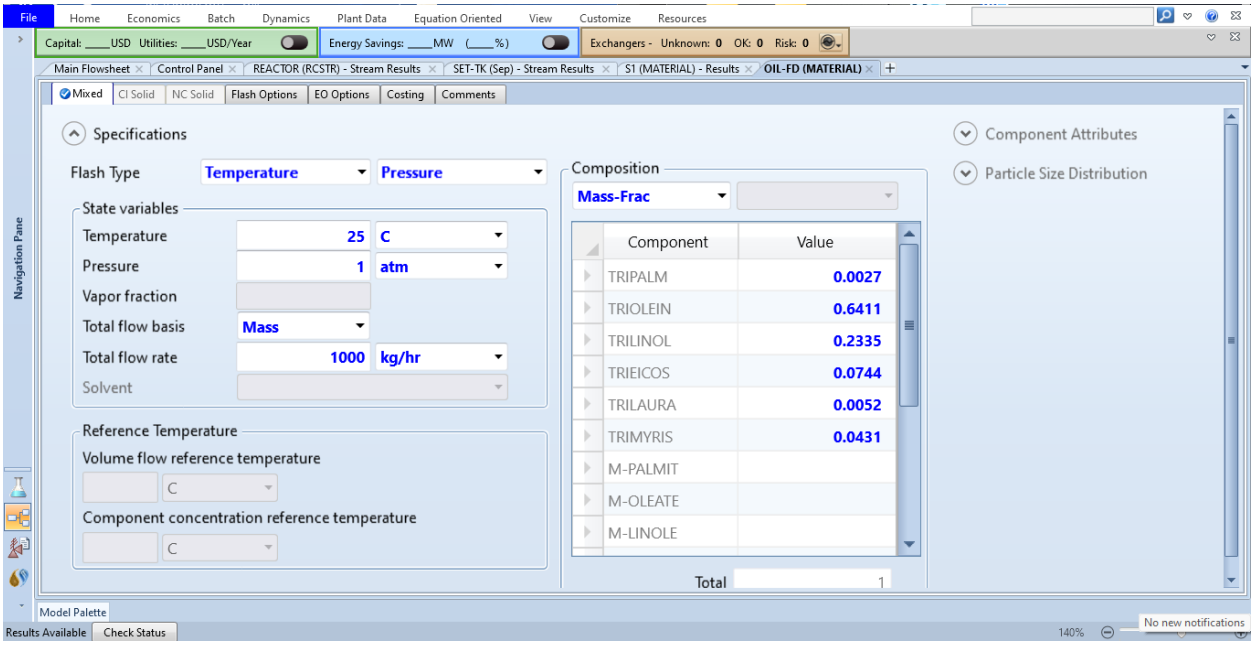

Plate 3: Feed Stream Definition

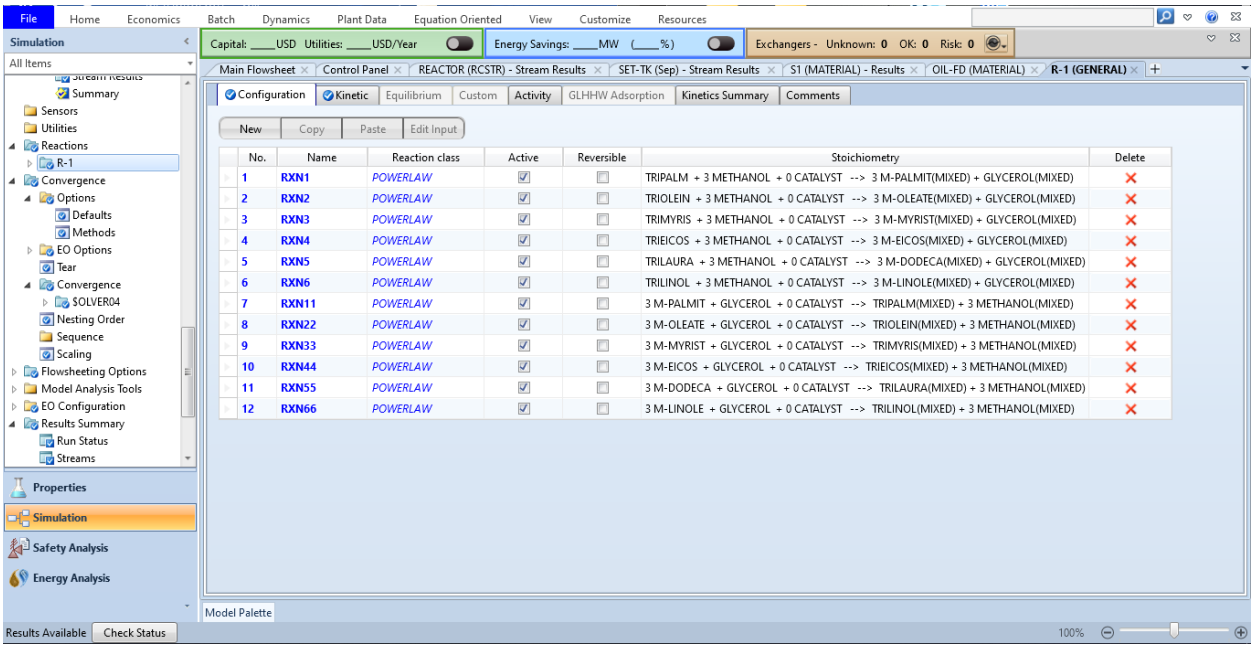

Plate 4: Kinetics Reaction Definition

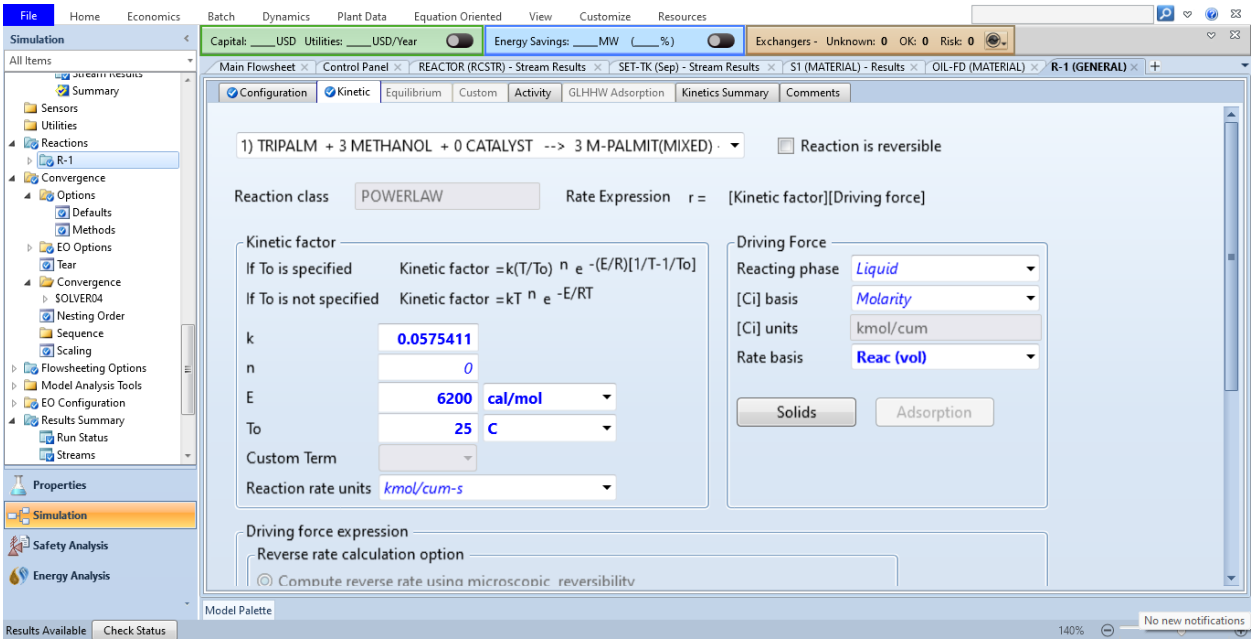

Plate 5: Definition of Kinetics Reaction Parameters

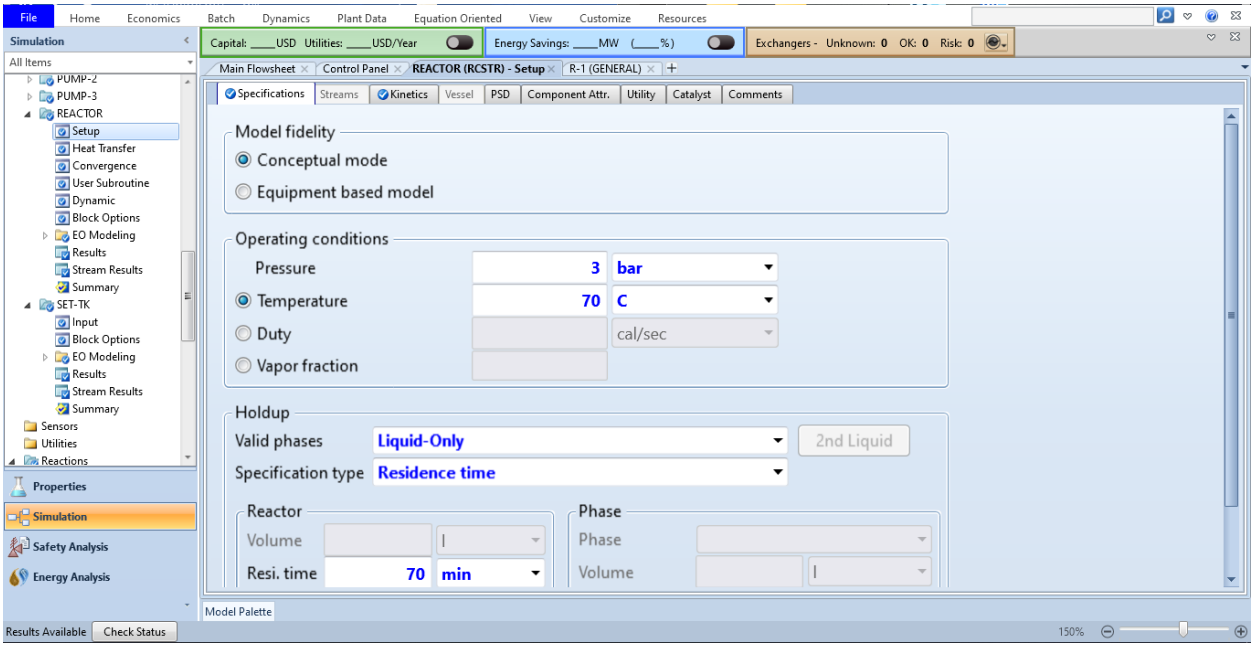

Plate 6: Definition of Reactor Operating Condition

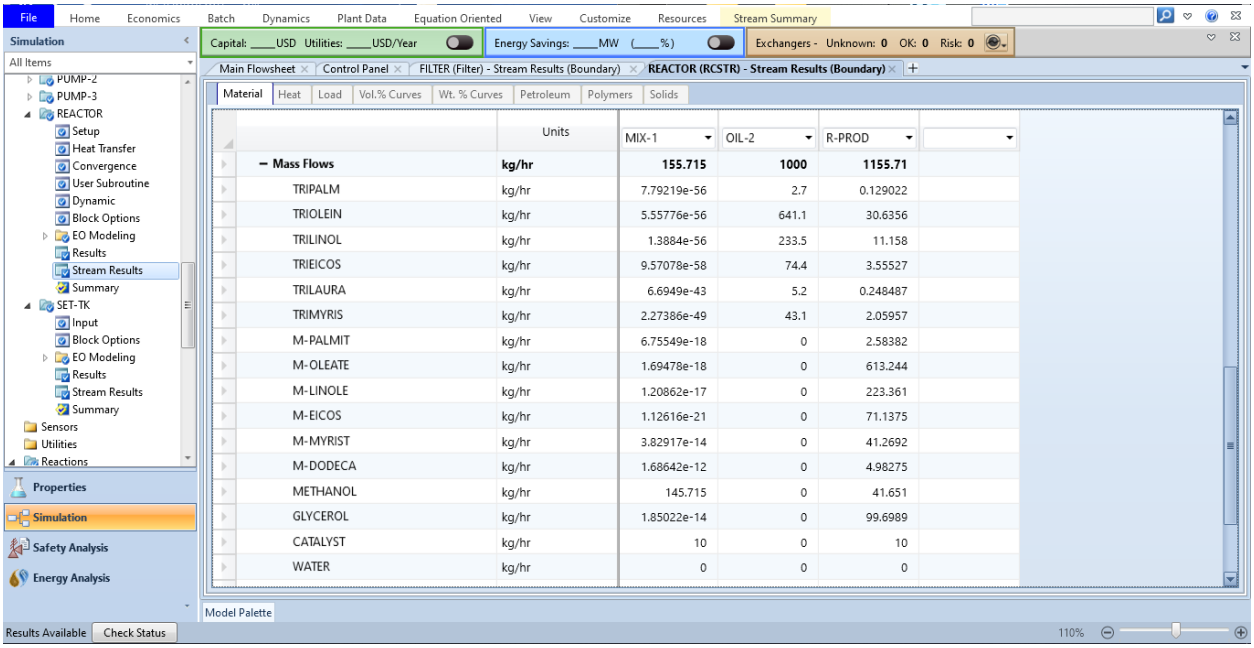

Plate 7: Reaction Outcome on mass basis

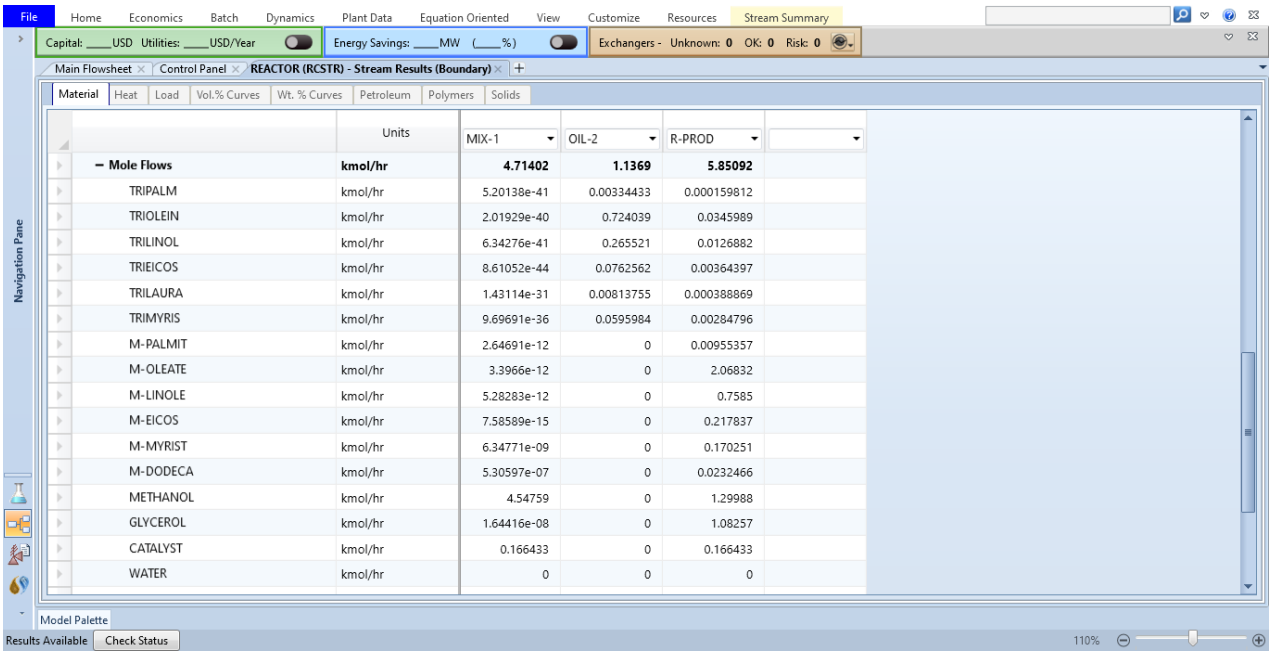

Plate 8: Reaction Outcome on molar basis

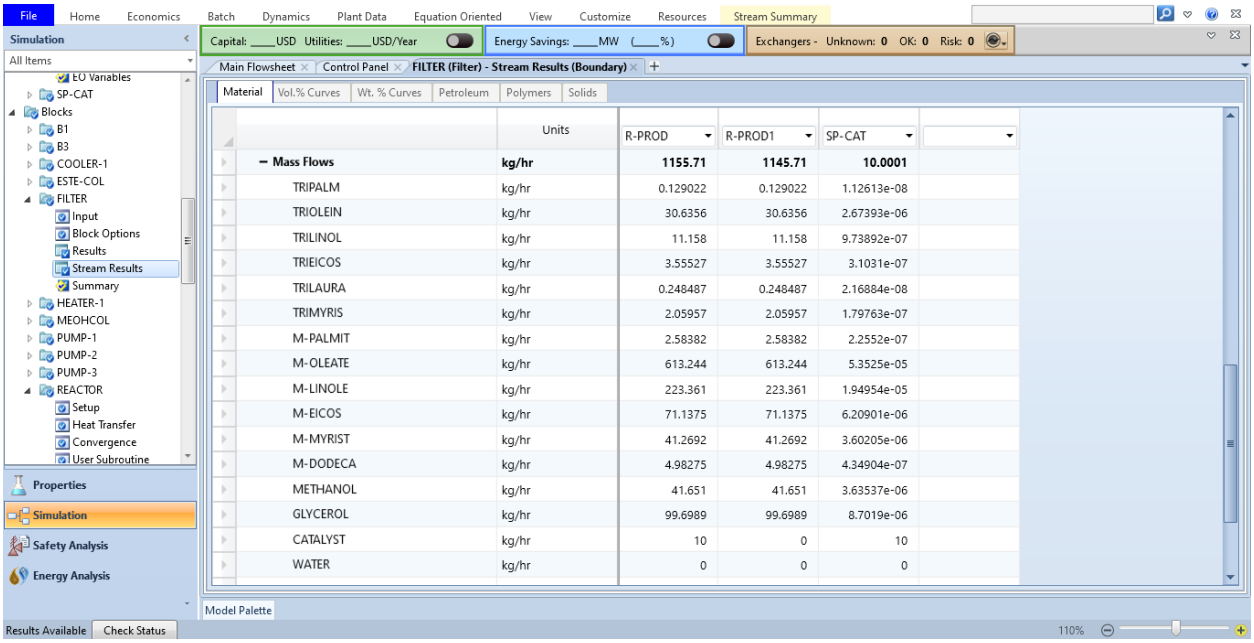

Plate 9: Filter Outcome

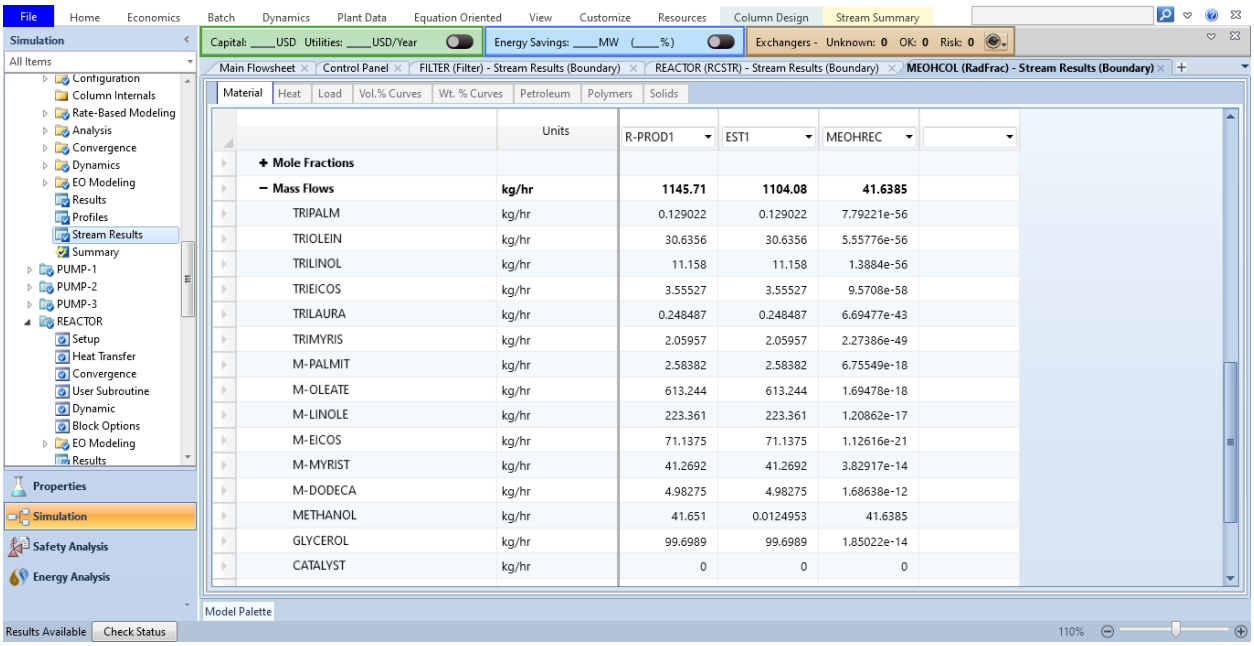

Plate 10: Excess Methanol Recovery Column Outcome

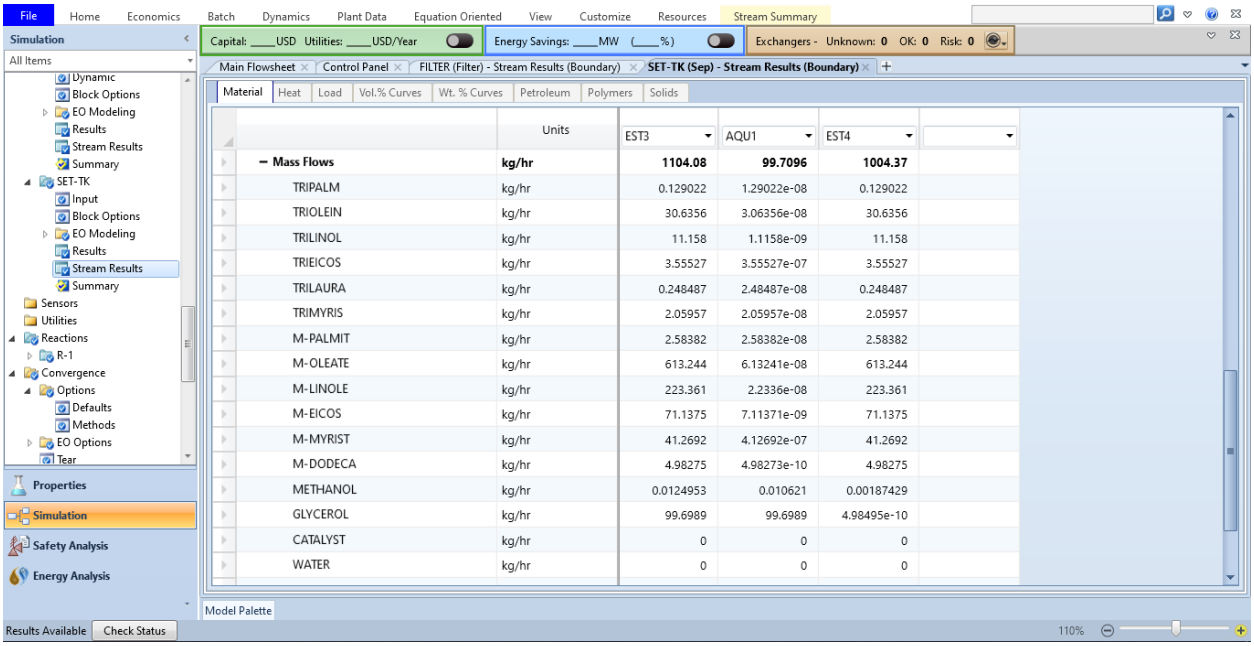

Plate 11: Biodiesel-Glycerol Settling Column Outcome

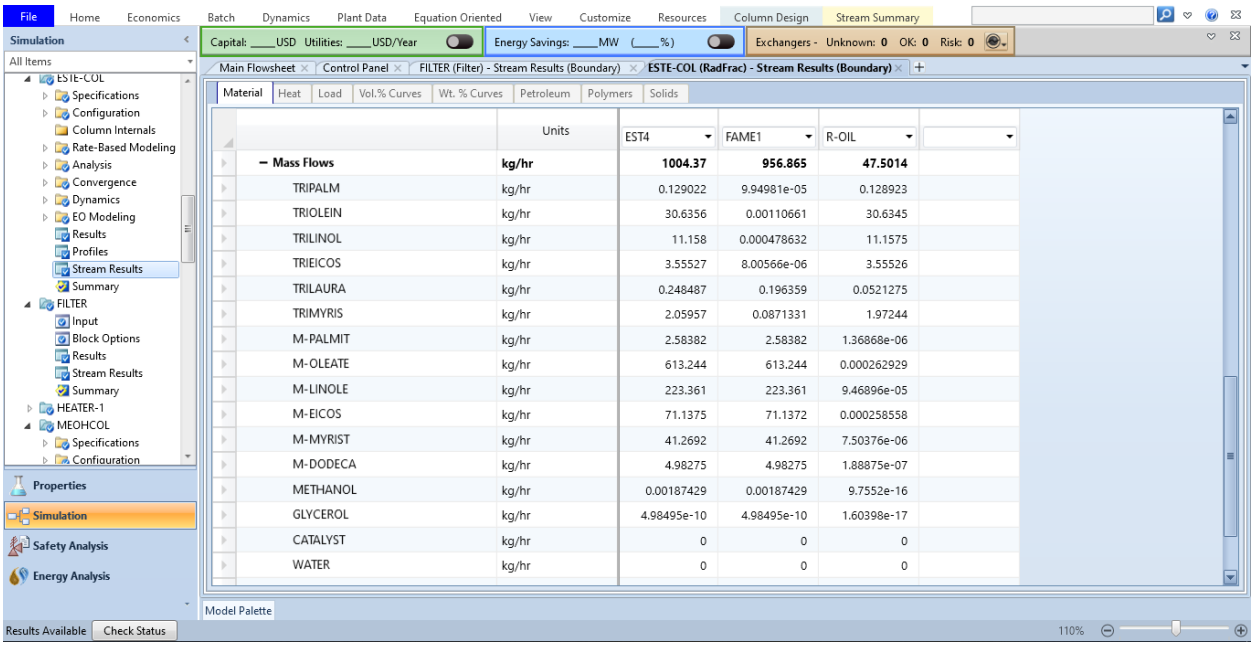

Plate 12: Biodiesel-Oil Separation Column Outcome

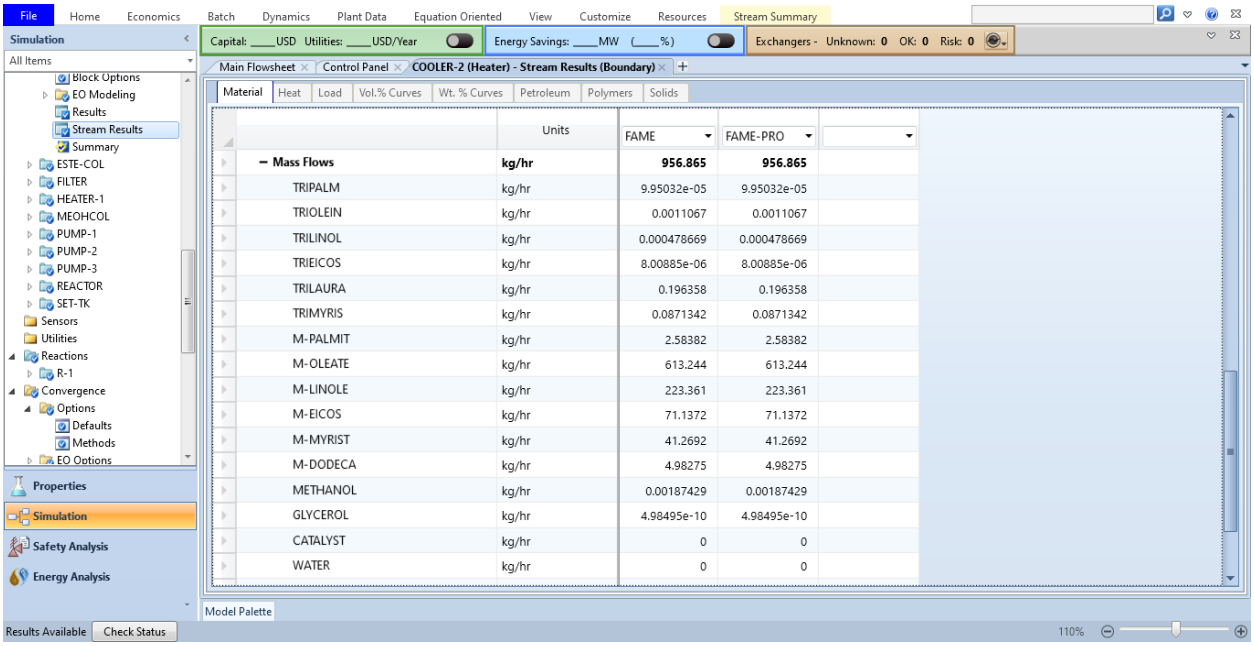

Plate 13: Biodiesel-Oil Separation Column Outcome

Appendix II: Techno-Economic Analysis

Purchase Equipment Cost and Capital Investment

Name	Installed Cost [USD]
MEOHCOL	451200
SET-TK	100300
COOLER-1	50700
HEATER-1	47600
PUMP-3	31300
ESTE-COL	636979
PUMP-2	28100
REACTOR	246300
FILTER	163800
PUMP-1	28000
COOLER-2	51900
Total Equipment Purchase Cost	**1,836,179**
Fixed Capital Investment	**9,308,613**
Working Capital Investment	**489,927**
TCI	**9,798,540**

Sensitivity Analysis Data

Selling Price	NPV	IRR	ROI	PBP [yr]	Profitability Index
0.59	- 4,175,915	-0.28%	-0.14%	15.27	0.57
0.62	- 3,117,632	2.70%	1.44%	12.74	0.68
0.65	- 2,118,340	5.26%	2.98%	11.08	0.78
0.69	- 795,464	8.31%	5.01%	9.56	0.92
0.72	196,692	10.40%	6.53%	8.73	1.02
0.76	1,519,568	13.00%	8.57%	7.88	1.16
0.80	2,842,444	15.43%	10.60%	7.23	1.29
0.84	4,165,319	17.72%	12.64%	6.72	1.43
0.88	5,488,195	19.90%	14.67%	6.31	1.56
0.93	7,141,789	22.49%	17.21%	5.89	1.73
0.97	8,464,665	24.48%	19.24%	5.62	1.86
1.02	10,118,260	26.87%	21.79%	5.33	2.03
1.07	11,771,854	29.18%	24.33%	5.09	2.20

Economics and Cash Flow Data

Items	**EPC Period**		**Production Period**												
Year	1	2	3	4	5	6	7	8	9	10	11	12	13	14	15
Production Volume [%]	0%	0%	70%	90%	100%	100%	100%	100%	100%	100%	100%	100%	100%	100%	100%
Product Unit Price															
Biodiesel Unit Selling Price [$/liter]			0.89	0.89	0.89	0.89	0.89	0.89	0.89	0.89	0.89	0.89	0.89	0.89	0.89
Glycerol Unit Selling Price [$/kg]			0.70	0.70	0.70	0.70	0.70	0.70	0.70	0.70	0.70	0.70	0.70	0.70	0.70
SP Unit Selling Price [$/kg]			0.10	0.10	0.10	0.10	0.10	0.10	0.10	0.10	0.10	0.10	0.10	0.10	0.10
Production Rate															
Biodiesel Production Rate [liter/yr]			6,386,384	8,211,065	9,123,406	9,123,406	9,123,406	9,123,406	9,123,406	9,123,406	9,123,406	9,123,406	9,123,406	9,123,406	9,123,406
Glycerol Production Rate [kg/yr]			577,850	742,950	825,500	825,500	825,500	825,500	825,500	825,500	825,500	825,500	825,500	825,500	825,500
SP Catalyst Production Rate [kg/yr]			138,018	177,452	197,169	197,169	197,169	197,169	197,169	197,169	197,169	197,169	197,169	197,169	197,169
Revenue [$/yr]			6,083,019	7,821,025	8,690,028	8,690,028	8,690,028	8,690,028	8,690,028	8,690,028	8,690,028	8,690,028	8,690,028	8,690,028	8,690,028
Raw Material Unit Price															
Papaya Oil Unit Selling Price [$/kg]			0.50	0.50	0.50	0.50	0.50	0.50	0.50	0.50	0.50	0.50	0.50	0.50	0.50
Methanol Unit Selling Price [$/kg]			0.51	0.51	0.51	0.51	0.51	0.51	0.51	0.51	0.51	0.51	0.51	0.51	0.51
Catalyst Unit Selling Price [$/kg]			0.20	0.20	0.20	0.20	0.20	0.20	0.20	0.20	0.20	0.20	0.20	0.20	0.20
Feed Rate															
Papaya Oil Feed Rate [liter/yr]			5,520,684	7,098,022	7,886,691	7,886,691	7,886,691	7,886,691	7,886,691	7,886,691	7,886,691	7,886,691	7,886,691	7,886,691	7,886,691
Methanol Feed Rate [kg/yr]			603,154	775,484	861,649	861,649	861,649	861,649	861,649	861,649	861,649	861,649	861,649	861,649	861,649

Catalyst Feed Rate [kg/yr]			138,017	177,451	197,167	197,167	197,167	197,167	197,167	197,167	197,167	197,167	197,167	197,167	197,167
Total Raw Material Cost [$/yr]			3,095,554	3,979,998	4,422,220	4,422,220	4,422,220	4,422,220	4,422,220	4,422,220	4,422,220	4,422,220	4,422,220	4,422,220	4,422,220
Utilities Cost [$/yr]			41,620	53,511	59,457	59,457	59,457	59,457	59,457	59,457	59,457	59,457	59,457	59,457	59,457
Other OpEx Cost [$/yr]			514,081	660,961	734,402	734,402	734,402	734,402	734,402	734,402	734,402	734,402	734,402	734,402	734,402
Total Production/Operating Cost [$/yr]			3,651,255	4,694,471	5,216,078	5,216,078	5,216,078	5,216,078	5,216,078	5,216,078	5,216,078	5,216,078	5,216,078	5,216,078	5,216,078
Capital Cost [$]	3,919,415	5,879,123													
Depreciation [$]			753,734	753,734	753,734	753,734	753,734	753,734	753,734	753,734	753,734	753,734	753,734	753,734	753,734
Profit Before Tax [$]			1,678,031	2,372,821	2,720,216	2,720,216	2,720,216	2,720,216	2,720,216	2,720,216	2,720,216	2,720,216	2,720,216	2,720,216	2,720,216
Tax @ 35% [$]			587,311	830,487	952,075	952,075	952,075	952,075	952,075	952,075	952,075	952,075	952,075	952,075	952,075
Net Income [$]			1,090,720	1,542,333	1,768,140	1,768,140	1,768,140	1,768,140	1,768,140	1,768,140	1,768,140	1,768,140	1,768,140	1,768,140	1,768,140
Cash Flow, CF [$]	-3,919,415	-5,879,123	1,844,454	2,296,067	2,521,874	2,521,874	2,521,874	2,521,874	2,521,874	2,521,874	2,521,874	2,521,874	2,521,874	2,521,874	2,521,874
Disconted Factor @ r=10%	0.9091	0.8264	0.7513	0.6830	0.6209	0.5645	0.5132	0.4665	0.4241	0.3855	0.3505	0.3186	0.2897	0.2633	0.2394
Discounted Cash Flow [$]	-3,563,105	-4,858,779	1,385,765	1,568,245	1,565,885	1,423,532	1,294,120	1,176,473	1,069,521	972,292	883,901	803,547	730,497	664,088	603,717
Acumulated CF [$]	-3,919,415	-9,798,538	-7,954,085	-5,658,018	-3,136,144	-614,270	1,907,604	4,429,478	6,951,352	9,473,226	11,995,099	14,516,973	17,038,847	19,560,721	22,082,595
Acumulated DCF [$]	-3,563,105	-8,421,884	-7,036,119	-5,467,874	-3,901,989	-2,478,457	-1,184,337	-7,864	1,061,657	2,033,948	2,917,850	3,721,396	4,451,893	5,115,982	5,719,698

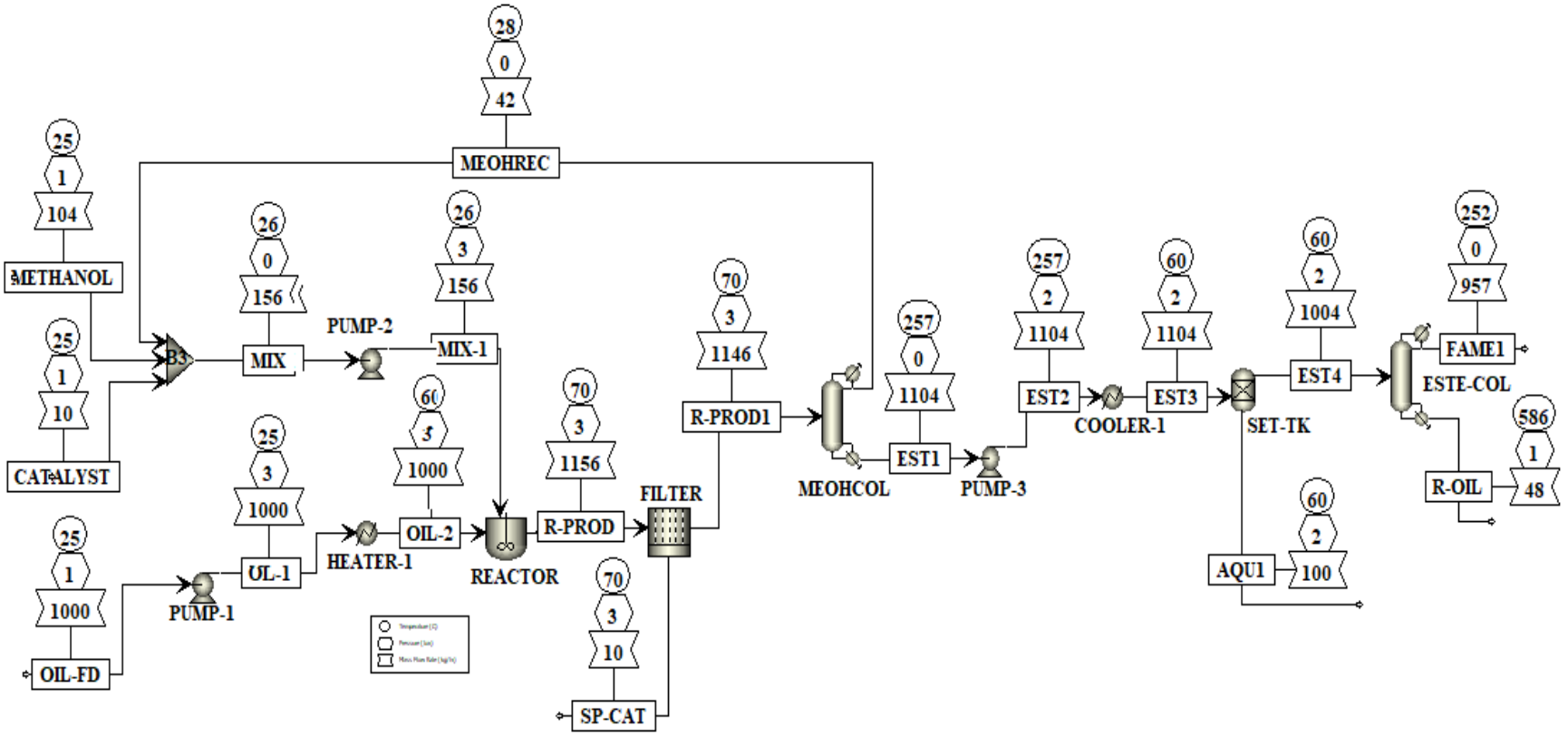
28
0
42
MEOHREC
25
1
104
METHANOL
25
1
10
CATALYST
25
1
1000
OIL-FD
PUMP-1
26
0
156
MIX
B3
PUMP-2
26
3
156
MIX-1
25
3
1000
UL-1
HEATER-1
60
3
1000
OIL-2
REACTOR
70
3
1156
R-PROD
70
3
10
SP-CAT
FILTER
70
3
1146
R-PROD1
MEOHCOL
257
0
1104
EST1
PUMP-3
257
2
1104
EST2
COOLER-1
60
2
1104
EST3
SET-TK
60
2
1004
EST4
60
2
100
AQU1
252
0
957
FAME1
ESTE-COL
586
1
48
R-OIL

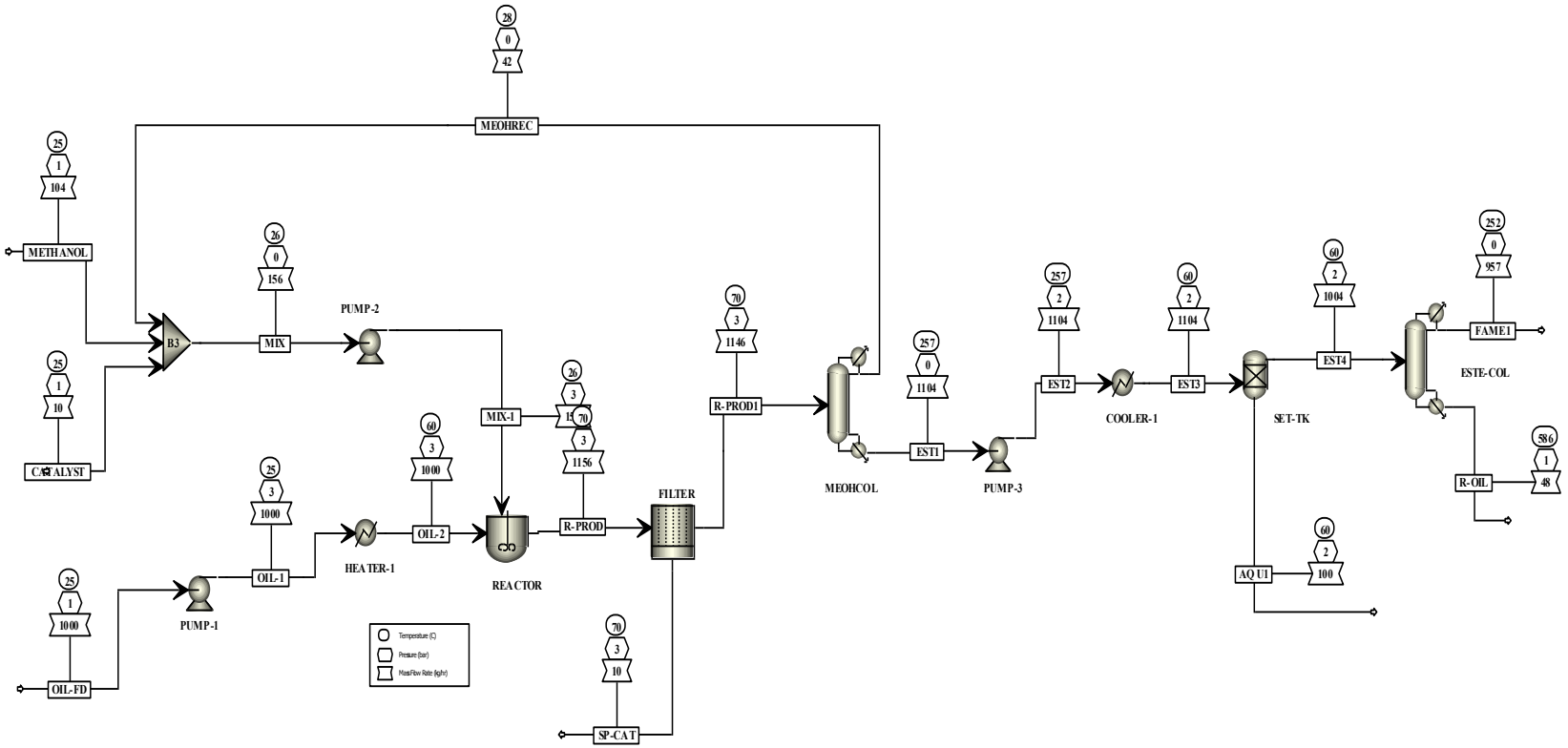
28
0
42
MEOHREC
25
1
104
METHANOL
25
1
10
CATALYST
B3
26
0
156
MIX
PUMP-2
MIX-1
26
3
15
70
3
1156
60
3
1000
25
3
1000
OIL-1
PUMP-1
25
1
1000
OIL-FD
HEATER-1
OIL-2
REACTOR
R-PROD
FILTER
70
3
1146
R-PROD1
MEOHCOL
257
0
1104
EST1
PUMP-3
257
2
1104
EST2
COOLER-1
60
2
1104
EST3
SET-TK
60
2
1004
EST4
ESTE-COL
252
0
957
FAME1
R-OIL
586
1
48
AQU1
60
2
100
70
3
10
SP-CAT
Temperature (C)
Pressure (bar)
Mass Flow Rate (kg/hr)